NONLINEAR GROUND RESPONSE ANALYSIS IN KOLKATA SOIL

THESIS SUBMITTED IN PARTIAL FULFILLMENT FOR THE AWARD OF THE DEGREE

of

MASTER OF CIVIL ENGINEERING

in

SOIL MECHANICS AND FOUNDATION ENGINEERING

By

SAMYARUP SENAPATI

UNIVERSITY REGD. NO. – **140638 of 2017-2018**

CLASS ROLL NO. – **001710402011**

EXAM ROLL NO. – **M4CIV19001**

Under The Guidance of

Dr. Ramendu Bikas Sahu
Professor

Dr. Narayan Roy
Assistant Professor

CIVIL ENGINEERING DEPARTMENT

JADAVPUR UNIVERSITY

MAY 2019

DECLARATION OF ORIGINALITY AND COMPLIANCE OF ACADEMIC ETHICS

I hereby declare that this thesis contains literature survey and original research work by the under signed candidate, as part of his **Master of Civil Engineering in Soil Mechanics & Foundation Engineering** studies.

All information in this document have been obtained and presented in accordance with academic rules and ethical conduct.

I also declare that, as required by these rules and conduct, I have fully cited and referenced all material and results that are not original to this work.

Name **:** SAMYARUP SENAPATI

University Regd. No. **:** 140638 of 2017-18

Class Roll No. **:** 001710402011

Exam Roll No. **:** M4CIV19001

THESIS TITLE **: NONLINEAR GROUND RESPONSE ANALYSIS IN KOLKATA SOIL**

……

(Signature with Date)

JADAVPUR UNIVERSITY

FACULTY OF ENGINEERING AND TECHNOLOGY

DEPARTMENT OF CIVIL ENGINEERING

CERTIFICATE OF RECOMMENDATION

We do hereby recommend that the thesis prepared under our supervision by **Samyarup Senapati** entitled "**Nonlinear Ground Response Analysis in Kolkata Soil**" be accepted in partial fulfilment of the requirements for the Degree of **Master of Civil Engineering** with specialization in **Soil Mechanics & Foundation Engineering** from Jadavpur University.

In-Charge of Thesis:

……...	……...……..
Dr. R. B. Sahu	Dr. N. Roy
Professor	Assistant Professor
Civil Engineering Department	Civil Engineering Department
Jadavpur Univeristy	Jadavpur University

Countersigned by:

……..	……..
(Head of the Department)	**(Dean)**
Civil Engineering Department	Faculty of Engineering and Technology
Jadavpur University	Jadavpur University

JADAVPUR UNIVERSITY

FACULTY OF ENGINEERING AND TECHNOLOGY

DEPARTMENT OF CIVIL ENGINEERING

CERTIFICATE OF APPROVAL*

The foregoing thesis entitled, "***Nonlinear Ground Response Analysis in Kolkata Soil***", is hereby approved as a creditable study of an engineering subject carried out and presented in a manner satisfactory to warrant its acceptance as a pre- requisite to the degree for which it has been submitted. It is implied that by this approval the undersigned do not necessarily endorse or approve any statement made, opinion expressed or conclusion drawn therein, but approved the thesis only for the purpose for which it is submitted.

FINAL EVALUATION FOR

EXAMINATION OF THESIS

1. _____

2. _____

3. _____

(Signature of Examiners)

* Only in case the thesis is approved

ACKNOWLEDGEMENT

I am extremely thankful and indebted to Dr. R. B. Sahu (Professor of Civil Engineering Department, Jadavpur University) and Dr. N. Roy (Assistant Professor of Civil Engineering Department, Jadavpur University) for their valuable guidance, constant support and encouragement throughout my thesis work. This thesis would never have been completed without their blessings, guidance, constant vigil, careful supervision and inspiration at all stages of the work.

I am sincerely thankful and obliged to other professors of Soil Mechanics Division, Prof. S. P. Mukherjee, Prof. P. Aitch, Prof. G. Bhandari and Prof. S. K. Biswas for their constant encouragement and continuous valuable suggestions throughout my thesis work.

I would like to mention the contribution of various Research Scholars of Soil Mechanics Specialization in successful completion of this thesis.

I sincerely acknowledge the help of Mr. Rabin Pal, Mr. Apurba Banerjee and Mr. Ranjit Kushari, Technical staffs of Soil Mechanics Laboratory. Thanks to all other professors and staff of Civil Engineering Department for their kind co-operation.

Last but not the least, I express my sincere gratitude to all of my colleagues of Soil Mechanics and Foundation Engineering section, Civil Engineering Department, for being with me.

Place: Kolkata

Dated: ____/____/_____

SAMYARUP SENAPATI

EXAMINATION ROLL NO.: M4CIV19001

CLASS ROLL NO. – 001710402011

REGD. NO.: 140638 of 2017-2018

DEPARTMENT OF CIVIL ENGINEERING

FACULTY OF ENGINEERING & TECHNOLOGY

JADAVPUR UNIVERSITY

KOLKATA - 700032

CONTENTS

LIST OF TABLES

LIST OF FIGURES

ABSTRACT

After the Bhuj earthquake (2001) ground response analysis in India has become need of the hour for analysis and design of various important structures, like, nuclear power plants, dams, bridges, tall structures etc. For this purpose, different parameters such as, peak ground acceleration (PGA), PGA amplification/ attenuation, surface displacement, shear strains, excess pore pressure generation and dissipation etc are evaluated for spectrum compatible expected future earthquake. With respect to dimensionality, ground response can be of 1D, 2D or 3D with respect to ground shaking. Generally, 2D and 3D ground response analyses are extensions of 1D ground response analysis. In terms of calculation, ground response can be divided into three types, namely, linear, equivalent linear and nonlinear analysis. Linear analysis is performed with view that soil remains in elastic state throughout the analysis. Equivalent linear is an iterative approach in which soil nonlinearity is approximated assuming equivalent shear modulus as secant shear modulus and equivalent damping ratio as that damping ratio which produces the same energy loss in a single cycle as the actual hysteresis loop. Although equivalent linear is convenient in terms of calculations, it is still an approximation. Soil always behaves nonlinearly when load reversal takes place. Thus, nonlinear approach is suitable to analyse ground response. Also, the pore pressure variation in soil during strong motion shaking can be predicted by nonlinear analysis coupled with effective stress approach.

Kolkata, the only metro city in eastern India, is lying on the alluvial Gangetic deposit. It has two distinct soil formations, i.e., normal Kolkata deposit and river channel deposit. The former one consists of mainly clayey deposit up to a depth of 40-50m with intermediate sand layers. The latter one consists of sandy deposit down to considerable depth. In the present study, nonlinear ground response analysis of normal Kolkata soil deposit and river channel soil deposit with effective stress approach has been performed with the software DEEPSOIL using various SPT value and shear wave velocity correlations provided by various researchers. Due to lack of recording of past strong motions, spectral compatible synthetic acceleration time histories have been generated from two earthquakes, namely, San Fernando earthquake (1971) and Northridge earthquake (1994). The results are presented in terms of variation of PGA with depth, variation of PGA amplification with depth, relative displacement of the soil profiles, variation of maximum shear strain with depth and variation of maximum pore pressure ratio with depth. Along with these, Fourier amplification ratio and Spectral acceleration of surface layer have been predicted. Lastly, liquefaction potential for river channel deposit has been estimated along with post liquefaction settlement due to the spectrum compatible strong motion shakings.

In the study, it has been observed that PGA calculated from equivalent linear analysis is more than that from nonlinear analysis and also a motion with low peak bedrock acceleration amplifies more than a

motion with higher peak bedrock acceleration does. Equivalent linear analysis predicts less maximum shear strain generated in the soil than nonlinear analysis does. Due to high shear strain is associated with top 5m depth in river channel deposit, the excess pore pressure ratio almost become unity in that region. Nonlinear analysis performed with OPENSEES also predicts the similar result. The simplified liquefaction evaluation procedure also verifies this fact. The post-liquefaction settlement has been calculated for the river channel deposit which predicts a range of 20-120cm settlement in case a spectrum compatible strong motion with peak bed rock acceleration of around 0.22g occurs in the region.

CHAPTER 1

INTRODUCTION

1.1. BACKGROUND

Present practice for the design of structures, foundations, dams, embankments, excavations etc. is to follow the recommendation of IS code of practice for estimation of the magnitude of lateral forces due to a given earthquake intensity. For this, the value of Sa/g is calculated from the response spectra specified for a particular soil condition (Stiff, medium and soft) and the particular zone where the proposed site falls. However, for important structures like a nuclear power plant, dams, bridges, tall structures, etc. very often this methodology fails to predict the response that the structure may exhibit as aground motion, in general, is substantially modified due to local soil condition. This was first noticed in India during Bhuj earthquake in 2001. It was observed that different structures situated in Ahmedabad region, about 250km away from earthquake epicenter, suffered substantial damages as the ground motion amplified due to local soil condition (Sitharam et. al., 2004). So mainly after the Bhuj earthquake researchers started working in this direction.

General practice for estimation of site specific ground response is to use the linear method and equivalent linear method of analysis. For various cities in India, several studies have been performed to assess the local site effects using various commercially available software based on 1D equivalent linear ground response analysis (Hanumantharao and Gunturi, 2009; Anbazhagan and Sitharam, 2008; Roy and Sahu, 2012; Satyam et. al., 2012; Bhattacharya and Govindaraju, 2012; Choudhury and Chatterjee, 2015; Desai and Choudhury, 2015). In most of these cases bed rock was at shallow depth unlike Kolkata city where 10 to 12 km of huge sediment thickness lies over the bed rock. So in such type of scenarios, equivalent engineering bedrock is assumed at shallow depth with shear wave velocity more than 700m/s. For Kolkata city, site response analysis has been carried out assuming an engineering bed rock at 30m depth. The studies so far performed for Kolkata region are mainly based on equivalent linear analysis, but for strong ground motion, this kind of analysis fails to assess the actual behavior as the soil behave non-linearly under strong ground motions. To overcome these shortcomings, researchers have started to conduct non-linear ground response analysis where non-linear stress-strain behavior is considered for estimation of shear modulus and damping behavior of soil for the induced shear strain due to earthquake motion (Maheswari et al., 2008; Jishnu et. al., 2013; Dammala et. al, 2019). The non-linear analysis was found to predict more realistic site response analysis, whereas, equivalent linear sometimes overestimate the soil response, specifically for strong ground motion. In addition to that, for sandy deposit, variation of pore water pressure can be predicted in nonlinear analysis which may indicate the initiation of liquefaction and an approximate ground deformation can be evaluated.

Kolkata city covers an area of about 185 sq. km. In most part of the city, buildings, schools, business centers have come up haphazardly. Kolkata, in the past, has suffered enormous damages due to notable earthquakes such as 1897 Great Assam Earthquake, 1906 and 1964 Kolkata Earthquake. The 1964 Kolkata Earthquake epicenter was located over the Eocene Hinge Zone (SEISSAT 2000). IS: 1893 (Part 1)-2002 designates Kolkata on the boundary of Zone III and Zone IV. However, the seismic macrozonation is not enough to forecast the damage scenario in the event of an earthquake. The damage pattern depends on the local geology, vicinity to active faults, geotechnical and geophysical properties of surface and subsurface strata and topography. Mohanty and Walling (2008) presented the microzonation of Kolkata on the basis of PGA variation using a quasi-probabilistic approach considering attenuation relationship of Toro et. al. (1997). But, they did not consider the local site effects. In this context, it may be noted that Kolkata lying on the alluvial Gangetic deposit has two distinct soil formations, i.e., normal Kolkata deposit and river channel deposit. Normal Kolkata deposit consists of a thick soft compressible silty clay/clayey silt down to a depth of about 14.0 m below the existing ground surface followed by stiff/ very stiff/ hard/ very hard clayey deposit with intermediate sand layers down to considerable depth of 40-50 m. The river channel deposit existing along the old Adiganga channel consists of medium/ dense/ very dense sandy deposit down to considerable depth. These local soil conditions with increasing urbanization and industrialization in Kolkata and adjoining areas makes it necessary to consider microzonation in order to prevent huge loss in terms of life and economy due to future earthquakes. Also liquefaction potential needs to be evaluated for river channel deposit using the site specific PGAs.

In the proposed study, an attempt has been made to evaluate the equivalent linear and non-linear ground response analysis at two specific sites in Kolkata city for two specific soil formations, namely, normal Kolkata deposit and river channel deposit. For this purpose DEEPSOIL and OPENSEES software were used along with a number of proposed correlations for SPT value - shear wave velocity suggested by various researchers (Jafari et. al., 2002; Hanumantharao and Ramana, 2008; Maheswari et. al., 2010; Anbazhagan et. al., 2012; Choudhury and Chatterjee, 2013; Nath et. al., 2016).

1.2. OBJECTIVES AND SCOPE OF WORK

The objectives of the present study are summarized as follows:

1. To perform an equivalent linear and nonlinear site response analysis for the two soil sites with regard to the different V_S-N correlations in two soil sites (Normal Kolkata Deposit and River Channel Deposit) using DEEPSOIL software. The results will be presented in the form of Fourier Amplification Ratio (FAR), Spectral Acceleration (SA), Peak Ground Acceleration (PGA), strain variation for equivalent linear and nonlinear and variation of pore water pressure ratio (excess pore water pressure normalised by initial vertical effective stress) in case of nonlinear analysis.

2. To perform nonlinear site response analysis for two soil sites (Normal Kolkata and River Channel deposit) with OPENSEES software using Choudhury and Chatterjee (2013) uncorrected SPT-Vs correlation and compare the results obtained from DEEPSOIL analysis.
3. To carry out liquefaction potential analysis using simplified method of analysis (Idriss and Boulanger, 2014) in case of river channel deposit using the PGA values obtained from equivalent linear and nonlinear analysis and make a comparative analysis with that obtained from nonlinear analysis.
4. To predict post liquefaction settlement of river channel deposit.

The scopes of the present investigation are given below:

- Choosing two representative soil profiles:
    1. Normal Kolkata Deposit.
    2. River Channel Deposit.

  These typical soil profiles are taken from Roy and Sahu (2012).
- Using two following acceleration time histories:
    1. San Fernando Earthquake (1971)
    2. Northridge Earthquake (1994)

  These time histories are taken from PEER NGA Database.
- Generating spectrum compatible time histories of the above two earthquakes generated for zone-III and zone-IV.
- Performing equivalent linear and nonlinear site response analysis in DEEPSOIL with different SPT-N and V_s relationships given by:
    1. Jafari et. al. (2002)
    2. Hanumantharao and Ramana (2008)
    3. Maheswari et. al. (2010)
    4. Anbazhagan et. al. (2012)
    5. Choudhury and Chatterjee (2013) (with uncorrected N values)
    6. Choudhury and Chatterjee (2013) (with $[(N_1)_{60}]$)
    7. Nath et. al. (2016)
- Performing nonlinear site response analysis in OPENSEES with a specific SPT-N and Vs correlation prescribed by Choudhury and Chatterjee (2013) (Uncorrected SPT).
- Performing liquefaction potential analysis in the River Channel Deposit.
- Evaluation of post-liquefaction settlement in the River Channel Deposit.

1.3. OUTLINE OF THE THESIS

- Chapter 2 deals with the review of the concerned literature that have been used in this study.
- Chapter 3 deals with the methodologies for conducting the above mentioned objectives.
- Chapter 4 deals with the results obtained through the analysis performed and discussions and inferences drawn from the results.
- Chapter 5 deals with the final conclusions on this study.

CHAPTER 2

LITERATURE REVIEW

2.1. GENERAL

Ground response analyses are used to predict ground surface motions for development of design response spectra, to evaluate dynamic stresses and strains for evaluation of liquefaction hazards, and to determine the earthquake-induced forces that can lead to instability of earth and earth-retaining structures

The chapter reviews relevant topics concerning various aspects of ground response analyses along with liquefaction potential and post liquefaction settlement. The pre-requisite of any ground response analysis is the site characterisation of the relevant site, site-specific SPT value and shear wave velocity and initial shear modulus selection, selection or synthesis of proper ground motion and selection of dynamic soil properties (i.e. modulus reduction and damping characteristics). The output of the ground response analyses then can be used to predict liquefaction susceptibility during cyclic loading. The end result of the whole assessment can then be used to mitigate the severe consequences of the earthquake. The steps to be followed along with input and output for each step during ground response analysis is presented as follows:

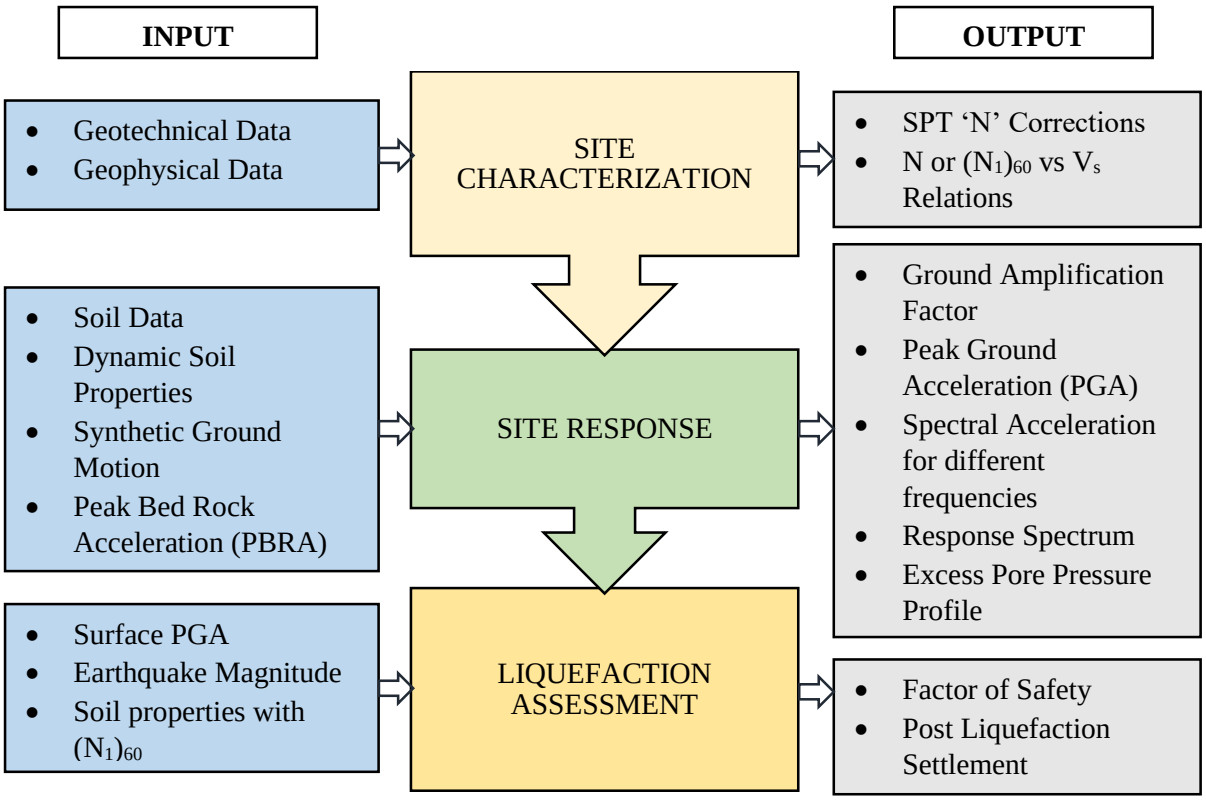

Figure 2.1: Flow Chart of Ground Response Analysis and Liquefaction Assessment

2.2. GROUND REPONSE ANALYSIS IN INDIA

Anbazhagan and Sitharam (2008) evaluated the seismic hazard considering local site effects by carrying out detailed geotechnical and geophysical site characterization in Bangalore to develop microzonation maps. Seismic hazard analysis and microzonation of Bangalore were addressed in three parts: 1) Estimation of seismic hazard was done using seismotectonic and geological information. 2) The site characterization of Bangalore was attempted using measured shear wave velocity from Multichannel Analysis of Surface Wave (MASW). As per NEHRP and IBC, Bangalore was classified as 'Site class D'. 3) Assessment of local site effects by carrying out 1D ground response analysis (using SHAKE2000) using both SPT data and shear wave velocity data from MASW. Theoretical 1-D site response study showed that the amplification factor was in the range of 1 to 4.7 and predominant frequency varied from 3 to 12Hz. Further, the Seed and Idriss (1971) simplified approach had been adopted to evaluate the soil liquefaction susceptibility and liquefaction resistance assessment. Expected PGA at rock level using DSHA for Bangalore was about 0.15 g. Liquefaction study showed that Bangalore was safe against liquefaction except at few locations where the overburden was sandy silt with presence of shallow water table.

Maheswari et. al. (2008) performed nonlinear ground response analysis considering the different sites in Chennai city USING FLAC3D. The evaluation of seismic hazard at bed rock level using deterministic approach was described in the first part of the study. Next, the site characterization was carried out by conducting MASW tests. The equivalent linear analysis was also carried out using SHAKE to compare with nonlinear ground response analysis. Based on the ground response analyses carried out for the selected sites at Chennai by the nonlinear approach using FLAC3D and by the equivalent linear approach using SHAKE, the following they concluded that: The significant amplification can occur for sandy and clayey sites subjected to relatively low intensity of ground motion. Both the site response analysis indicates the similar period corresponds to peak spectral acceleration for the sites considered. The nonlinear and equivalent linear approaches estimate similar PGA value for sandy site of about 20 m thick overburden. But the equivalent linear approach estimates two times higher PGA than that for nonlinear approach for the clayey site of Chennai. Hence, it is important to carry out nonlinear ground response analysis for deep clayey sites with low stiffness.

Hanumantharao and Gunturi (2009) conducted equivalent linear ground response analyses at four representative sites at Delhi, India to compare the free field acceleration spectra with local code of practice. Possible ground motions at rock outcrop were generated using stochastic finite source model (Boore, 2003) and specific barrier model (Papageorgiou, 2003) for earthquakes that are likely to occur from central seismic gap (Khattri, 1999) and local sources. To take into account the uncertainty in ground motion parameters, 10 random rupture scenarios were considered for each case. Spectral Analysis of Surface Waves (SASW) technique was adopted to measure the in-situ shear wave velocity profile at the representative sites. Experimentally evaluated strain dependent modulus reduction and

damping curves for local soils were adopted in the ground response analysis. As per IBC, 2003, most of the sites in Delhi fall under class *D* and *C* categories though there are locations where rock outcrop is seen or where the thickness of soil deposit is small, that falls under site classes *A* and *B*. Hence, to cover the entire spectrum of soil profiles encountered in Delhi, ground response analyses were conducted for all the four site classes. The shear wave velocities measured at four typical soil sites using the SASW method was used for soil profiles. It was observed that the peaks in the response spectrum were to the left of *IS 1893* provisions. This may due to the following two reasons: (i) They contain high frequency components and (ii) Since the amplitude of earthquake is large, the strains induced in the ground are high and thus there is significant modulus reduction. For long distance sources, the free field acceleration response spectra were found to be in conformity with the codal provisions. A comparison of computed response with the standard code of practice being used in India for seismic zone of Delhi indicated that the design spectra is not able to capture site amplification due to local sources.

Roy and Sahu (2012) estimated the spatial variation of ground motion in Kolkata Metropolitan District (KMD) by generating synthetic ground motion considering the point source model coupled with site response analysis. The rock level acceleration time histories in Kolkata due to maximum credible earthquake (MCE) moment magnitude (M_w) 6.2 were generated by synthetic ground motion model. 1D ground response analysis was performed using SHAKE2000 software. The results were presented in the form of PGA at rock level and ground surface, amplification factor, and the response spectra at the ground for 5% damping ratio. Site response study showed maximum amplification in some portion in KMD area was found to be as high as 3.0 times compared to rock level. On the basis the present analysis following conclusions were drawn: From synthetic ground motion model Eocene Hinge Zone was identified as the most vulnerable source with maximum credible earthquake of 6.2 M_w for Kolkata. PGA at two typical soil deposits, namely, Normal Kolkata Deposit and River Channel Deposit of Kolkata amplified from 0.141 g to 0.278 g and 0.136 g to 0.223 g due to the presence of soft compressible silty clay/loose sandy silt deposit. PGA at bedrock level of KMD varied from 0.169 g to 0.414 g, however, in major portion of the study area it ranged from 0.23 g to 0.35 g. Maximum amplification factor was observed in the northern part of Kolkata which ranged from 2.2-3. Spectral acceleration of the major portion of study area for 1.5, 3, 5 and 10 Hz were found to range from 0.7 g to 1.26 g, 0.56 g to 0.84 g, 0.44 g to 0.65 g and 0.32 g to 0.5 g respectively.

Akhila, Ghosh and Satyam (2012) carried out ground response analysis at the Park hotel located in Kolkata city, India. The PGA of the city ranged from 0.1g to 0.34g. For the site specific ground response analysis at the hotel site, borehole logs were collected at different test locations. The shear wave velocity and other soil characteristics were found out using SPT and DCPT tests. The shear wave velocity, damping, dry density, soil layer depth etc were used in DEEPSOIL. The PGA values were varying from 0.30g to 0.73g and the amplification factors from 1.5-3.8. Almost all the test sites had amplification factors of nearly 1.5.

Bhattacharya and Govindaraju (2012) assessed the seismic hazard assessment study on Kolkata and speculated that the deep alluvial deposit in the city may increase the seismic hazard probability due to the amplification of the seismic energies. For that purpose, they performed site specific 1D ground response analysis using SHAKE2000 software. Due to lack of strong motion data in the city, they used wavelet-based spectrum compatibility approach to generate synthetic earthquake motions using the spectrum matching technique with the software WAVGEN. IS:1893 (Part 1)-2002 classifies Kolkata as moderate seismic zone Zone III and IV with a zone factor of 0.16 and 0.24 respectively. But the study had been carried out based on GSHAP (Global Seismic Hazard Assessment Programme) which specified PGA value of 0.163g for Kolkata. The results of the analysis indicated the amplification of the ground motion in the range of 4.46-4.82 with the fundamental period ranging from 0.81-1.17s. Furthermore, the maximum spectral accelerations varied in the range of 0.78-0.95g. From the results of the detailed study, it was shown that the alluvial deposits of Kolkata have tendency to increase the amplification of acceleration from 1.34 to 1.73 and amplification of ground motion parameters in the range of 4.46-4.82. The maximum spectral acceleration at four locations in Kolkata varied in the range of 0.777-0.947g. Further the response spectrum obtained for four different locations was quite different from that recommended by the current IS codes of practice.

Jishnu et. al. (2013) performed 1D and 2D ground response analysis and liquefaction analysis of alluvial soil deposits from Kanpur region along Indo-Gangetic plains using SHAKE and OPENSEES software respectively. They conducted SPT and seismic downhole tests at four locations namely IITK, Nankari village, Mandhana and Bithoor at 1.5 m interval upto a depth of 30 m below the ground surface to calculate SPT-N values and the shear wave velocity along the depth. From the selected sites undisturbed as well as representative soil samples have been collected for detailed soil classification. Three Himalayan earthquakes namely Chamba earthquake (M_w—5.1), Chamoli earthquake (M_w—6.4) and Uttarkashi earthquake (M_w—6.5) were used as input strong motions. An average value of PGA obtained from 1D and 2D analysis was considered for liquefaction analysis and post-liquefaction settlement. Based on the results obtained from the above study the following conclusions were drawn: The excess pore water pressure ratio was greater than 0.8 at a depth of 24 m from ground surface indicating Kanpur soil will undergo severe liquefaction damage due to the rise in excess pore water pressure under large earthquake shaking. The soil layers at deeper depths (21–30 m) were prone to liquefaction. Large value of peak ground displacement was observed under high intensity of earthquakes which could be ascertained as an indicative of lateral spreading or cyclic softening in cohesive deposits. Post liquefaction settlement contributed by the deeper layers (21–30 m) was more than 50% of total liquefaction settlement. This was due to the presence of loose to moderate dense soil in deeper layer (21–30m).

Choudhury and Chatterjee (2015) studied the effects of local site conditions on ground motions by performing 1D equivalent linear ground response analyses for 16 typical soil sites in Kolkata city of

India using SHAKE2000 taking five different input motions (i.e. 1989 Loma Gilroy, 1994 Northridge, 1995 Kobe, 2001 Bhuj and 2011 Sikkim) having a wide variation in ground motion parameters. It was observed that the maximum PGA at the ground surface is amplified by 4.1 times for 2001 Bhuj motion while the Fourier amplification factor and spectral acceleration at 5 % damping was observed to be 10.15 and 3.84 g, respectively at Rajarhat area due to 2011 Sikkim motion. The natural frequency of the soil sites calculated using the empirical relation and that obtained from SHAKE2000 computer program were found to be in close agreement. From the study, it was concluded that local soil sites play a significant role in modifying the ground response.

Desai and Choudhury (2015) performed site-specific seismic hazard and 1D equivalent linear ground response analysis of important sites in Mumbai [Jawaharlal Nehru Port (JNPT), Mumbai Port, Bhabha Atomic Research Center (BARC), and Tarapur Atomic Power Station (TAPS)]. The seismicity of the concerned region was modelled through delineation of 31 fault sources with an earthquake database of the past 418 years (years 1594–2012). The probabilistic seismic hazard analysis (PSHA) at each site provided the design uniform hazard response spectra (UHRS) for 5% damping for three different levels of ground shaking. Using the recorded acceleration-time history of the 2001 Bhuj earthquake as a seed acceleogram, synthetic time histories were generated to match the design UHRSs obtained from PSHA for three different levels of bedrock motion. Site-specific ground response analyses performed by using the equivalent-linear method showed the tendency of amplification of bedrock motions at all research sites except the TAPS. The JNPT and Mumbai Port sites on reclaimed land showed the significant amplification of bedrock motion, within a range of 3.87–4.14 for a frequency range of 1.75–2.25 Hz, and 2.53–2.89 for a frequency range of 2.88–3.5 Hz, respectively. The BARC site showed peak amplification at higher frequencies, whereas for the TAPS site, no amplification was observed. In addition, the bedrock and freefield surface levels response spectrum obtained for the four sites were different from that recommended by BIS 1893 (2002).

Puri et. al. (2017) carried out earthquake response analysis for various locations in the State of Haryana adopting the equivalent linear approach. Based on the provisions of NEHRP, all the sites were classified using the average N-value (N_{30}) for the soil profile. The initial shear modulus (G_{max}) values of the layers in a soil profile were estimated using standard correlations. Cyclic response was accounted for using the standard shear modulus degradation and damping curves. Time histories from Himalayan Thrust System (e.g. Uttarkashi Earthquake (1991), Chamoli Earthquake (1999) and Sikkim Earthquake (2011)) was used as an input and soil amplification was estimated at the surface using DEEPSOIL software. The results of the study were formulated in terms of soil amplification map, response spectra, PGA along depth, surface time histories and strain along depth. It was observed that sites in Haryana can significantly amplify ground motions and hence a site-specific design approach must be adopted for important structures. High strain amplitudes were observed at various sites for deep soil layers. This

shows that during an earthquake, soil at deeper depths can also undergo settlements or earthquake induced liquefaction if conditions are favorable.

Dammala et. al. (2019) presented a comprehensive study of dynamic soil properties [i.e. Initial shear modulus-G_{max}; normalized shear modulus reduction (G/G_{max}); and damping ratio (D) variation curves] and pore water pressure parameters of a river bed sand (Brahmaputra Sand (BS)), sampled from a highly active seismic region in northeast India. Resonant column-RC and cyclic triaxial-CTX) were adopted in the study. RC apparatus was used to obtain the small strain properties (0.001-0.1%) while CTX equipment was adopted to obtain the high strain properties (0.1-5%) along with the pore water pressure parameters. The results obtained from both the equipment were combined to provide a comprehensive data of dynamic soil properties over wide range of strains. Based on the CTX results, a pore water pressure generation model with appropriate curve fitting parameters was presented. Furthermore, a nonlinear effective stress ground response study incorporating the pore water pressure generation, was performed using the recorded earthquake motions of varying peak bed rock acceleration (PBRA) in the region, to demonstrate the applicability of proposed dynamic soil properties and pore pressure parameters. High amplification for low PBRA ground motions (< 0.10 g) was observed and attenuation of seismic waves was witnessed beyond a PBRA of 0.10 g near the surficial stratum due to the induced high strains and the resulting high hysteretic damping of the soil. Also, increased excess pore pressure generation with increased PBRA of the input motion was observed and the considered soil stratum was expected to liquefy beyond a PBRA of 0.1 g.

OBSERVATIONS FROM THE ABOVE STUDIES

Non-linear site response analysis response is yet to be performed in Kolkata region. Except for Bangalore and Kanpur region, liquefaction potential analysis coupled with equivalent linear and non-linear site response analysis is yet to be performed. Lack of recorded acceleration data in Kolkata during earthquake is another limitation which can be overcome with synthetic wavelet-based response spectrum matching time history generation method though fundamental properties of seed earthquake change with this technique. Due to difficulty in performing MASW or SASW tests, regression analysis between SPT value and shear wave velocity is performed in each case except for Bangalore and Chennai. So, a lot variability is expected in terms of shear wave velocity if regression analysis is performed which may lead to unrealistic ground response. Only in Kanpur region, post liquefaction settlement is calculated. River channel deposit in Kolkata mainly consists of sandy or silty-sand deposit. During strong earthquake, the sandy deposit may undergo liquefaction which can cause seismic compaction.

2.3. THEORY OF GROUND RESPONSE ANALYSIS (KRAMER, 1996)

Ground response analyses are used to predict ground surface motions for development of design response spectra, to evaluate dynamic stresses and strains for evaluation of liquefaction hazards, and to determine the earthquake-induced forces that can lead to instability of earth and earth-retaining structures.

ONE DIMENSIONAL GROUND RESPONSE ANALYSIS

One dimensional ground response analyses are based on the assumption that all boundaries are horizontal and that the response of a soil deposit is predominantly caused by shear waves propagating vertically from the underlying bedrock. For one-dimensional ground response analysis, the soil and bedrock surface are assumed to extend infinitely in the horizontal direction.

LINEAR APPROACH

For the linear ground response problem, transfer functions can be used to express various response parameters, such as displacement, velocity, acceleration, shear stress, and shear strain, to an input motion parameter such as bedrock acceleration. Because it relies on the principle of superposition, this approach is limited to the analysis of linear systems.

$$Bedrock\ (Input)Motion \xrightarrow{FFT} Fourier\ Series\ of\ Input\ Motion * Transfer\ Function$$
$$= Fourier\ Series\ of\ Output\ Motion \xrightarrow{Inverse\ FFT} Ground\ Surface\ (Output)Motion$$

Commonly Used Transfer Functions:

Uniform undamped soil on rigid rock

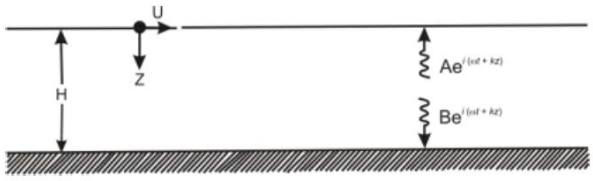

Figure 2.2: Linear elastic soil deposit of thickness *H* underlain by rigid bedrock

In this case, the modulus of the transfer function is given by:

$$|F(\omega)| = \frac{1}{\left|cos\left(\frac{\omega H}{V_s}\right)\right|} \tag{2.1}$$

Here $|F(\omega)|$ is the ratio of the free surface motion amplitude to the bedrock motion amplitude. As $\left(\frac{\omega H}{V_s}\right)$ approaches $\left(n\pi + \frac{\pi}{2}\right)$, the denominator of equation (2.1) approaches zero, which implies that infinite amplification, or *resonance,* will occur. Even this very simple model illustrates that the response of a soil deposit is highly dependent upon the frequency of the base motion, and that the frequencies at which strong amplification occurs depend on the geometry (thickness) and material properties (shear wave velocity) of the soil layer.

Uniform, damped soil on rigid rock

In this case, the modulus of the transfer function is given by:

$$|F(\omega)| = \frac{1}{\left|\sqrt{\cos^2\left(\frac{\omega H}{V_s}\right) + \left[\xi\left(\frac{\omega H}{V_s}\right)\right]^2}\right|} \tag{2.2}$$

For small damping ratios, equation (2.2) indicates that amplification by a damped soil layer also varies with frequency. The amplification will reach a local maximum whenever but will never reach a value of infinity since (for $\xi > 0$) the denominator will always be greater than zero. The frequencies that correspond to the local maxima are the *natural frequencies* of the soil deposit.

Uniform, damped soil on elastic rock

If the bedrock is rigid, its motion will be unaffected by motions in, or even the presence of, the overlying soil. Any downward-traveling waves in the soil will be completely reflected back toward the ground surface by the rigid layer, thereby trapping all of the elastic wave energy within the soil layer. If the rock is elastic, however, downward-traveling stress waves that reach the soil rock boundary will be reflected only partially; part of their energy will be transmitted through the boundary to continue traveling downward through the rock. If the rock extends to great depth, the elastic energy of these waves will effectively by removed from the soil layer. This is a form of radiation damping, and it causes the free surface motion amplitude to be smaller than those for the case of rigid bedrock.

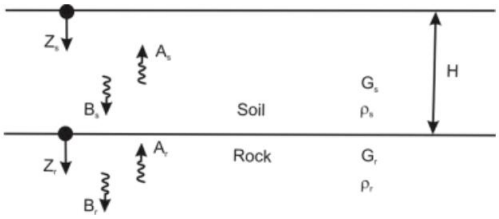

Figure 2.3: Nomenclature for the case of a soil layer overlying a half space of elastic rock

The modulus of the transfer function $|F(\omega)|$ for zero damping can be written as,

$$|F(\omega, \xi = 0)| = \frac{1}{\left|\sqrt{\cos^2\left(\frac{\omega H}{V_s}\right) + \left[\alpha_z sin\left(\frac{\omega H}{V_s}\right)\right]^2}\right|} \tag{2.3}$$

Resonance cannot occur as the denominator is always greater than zero, even when the soil is undamped. The effect of the bedrock stiffness, as reflected by the impedance ratio (α_z) on amplification behavior is illustrated in figure (2.4). The elasticity of the rock affects amplification similarly to the damping ratio of the soil-both prevent the denominator from reaching zero.

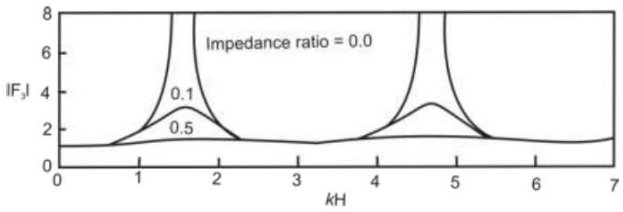

Figure 2.4: Effect of impedance ratio on amplification factor for case of undamped soil

EQUIVALENT LINEAR APPROACH

The actual nonlinear hysteretic stress-strain behavior of cyclically loaded soils can be approximately by equivalent linear soil properties. The equivalent linear shear modulus, *G*, is generally taken as a secant shear modulus and the equivalent linear damping ratio, as the damping ratio that produces the same energy loss in a single cycle as the actual hysteresis loop. Since the linear approach requires that G and ξ be constant for each soil layer, the problem becomes one of determining the values of effective strain that is consistent with the level of strain induced in each layer. The laboratory tests from which modulus reduction and damping ratio curves have been developed used simple harmonic loading and characterized the strain level by the peak shear strain amplitude. The time history of shear strain for a typical earthquake motion, however, is highly irregular with peak amplitude that may only be approached by a few spikes in the record. Figure (2.5) shows both harmonic (as in a typical laboratory

test) and transient (as in a typical earthquake) shear strain time histories that have the same peak cyclic shear strain. It is common to characterise the strain level of the transient record in terms of an effective shear strain which is often taken as 65% of the peak strain.

Figure 2.5: Two shear strain time histories with identical peak shear strains. For the transient motion of an actual earthquake, the effective shear strain is usually taken as 65% of the peak strain

Since the computed strain level depends on the values of the equivalent linear properties, an iterative procedure is required to ensure that the properties used in the analysis are compatible with the computed strain levels is all layers (Figure 2.6).

The iterative procedure operates as follows:

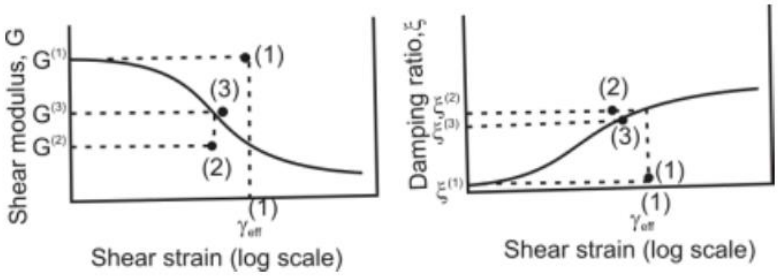

Figure 2.6: Iteration toward strain compatible shear modulus and damping ratio in equivalent linear analysis. Using initial estimates, $G^{(1)}$and $\xi^{(1)}$the equivalent linear analysis predicts of an effective shear strain, $\gamma_{eff}^{(1)}$. Because this strain is greater than those corresponding to $G^{(1)}$and $\xi^{(1)}$ an iteration is required. The next iteration uses parameters $G^{(2)}$and $\xi^{(2)}$ that are compatible with $\gamma_{eff}^{(1)}$. The equivalent linear analysis is repeated and the parameters checked until strain compatible values of G and ξ are obtained

1. Initial estimates of G and ξ are made for each layer. The initially estimated values usually correspond to the same strain level: low-strain values are often used for the initial estimate.
2. The estimated G and ξ values are used to compute the ground response, including time histories of shear strain for each layer.
3. The effective shear strain in each layer is determined from the maximum shear strain in the computed shear strain time history.

$$\gamma_{eff_j}^{(i)} = R_\gamma \gamma_{max_i}^{(i)}$$

(2.4)

For layer *j* where the superscript refers to the iteration number and R_γ is the ratio of the effective shear strain to maximum shear strain, R_γ depends on earthquake magnitude (Idriss and Sun, 1992) and can be estimated from:

$$R_\gamma = \frac{M-1}{10}$$

(2.5)

4. From this effective shear strain, new equivalent values, $G^{(i+1)}$ and $\xi^{(i+1)}$ are chosen for the next iteration.
5. Steps 2 to 4 are repeated until differences between the computed shear modulus and damping ratio values in two successive iterations fall below some predetermined value in all layers. Although convergence is not absolutely guaranteed, differences of less than 5 to 10% are usually achieved in three to five iterations (Schnabel et al., 1972).

Even though the process of iteration toward strain-compatible soil properties allows nonlinear soil behavior to be approximated, it is important to remember that the complex response method is still a linear method of analysis. The strain-compatible soil properties are constant throughout the duration of the earthquake, regardless of whether the strains at a particular time are small or large. The method is incapable of representing the changes in soil stiffness that actually occurs during the earthquake.

NON LINEAR APPROACH

Equivalent linear approach remains an approximation to the actual nonlinear process of seismic ground response. An alternative approach is to analyze the actual nonlinear response of a soil deposit using direct numerical integration in the time domain. By integrating the equation of motion in small time steps, any linear or nonlinear stress-strain model or advanced constitutive model can be used. At the beginning of each time step, the stress-strain relationship is referred to obtain the appropriate soil properties to be used in that time step. By this method, a nonlinear inelastic stress-strain relationship can be followed in a set of small incrementally linear steps.

Consider the soil deposit of infinite lateral extent shown in figure (2.7.a).

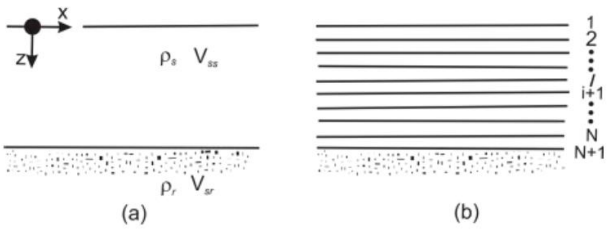

Figure 2.7: (a) Nomenclature for uniform soil deposit of infinite lateral extent overlying bedrock; **(b)** Discretization of soil deposit into N sublayers

If the layer is subjected to horizontal motion at the bedrock level, the response will be governed by the equation of motion:

$$\frac{\partial \tau}{\partial z} = \rho \frac{\partial^2 u}{\partial t^2} = \rho \frac{\partial \dot{u}}{\partial t} \tag{2.6}$$

Dividing the soil layer into *N* sublayers of thickness *Δz*, figure (2.7.b) and proceeding through time in small time increments of length, *Δt*, the notation $u_{i,t} = u(z = i\Delta z, t)$ can be used to write finite difference approximation to the derivatives

$$\frac{\partial \tau}{\partial z} = \frac{\tau_{i+1,t} - \tau_{i,t}}{\Delta z} \tag{2.7}$$

$$\frac{\partial \dot{u}}{\partial t} = \frac{\dot{u}_{i,t+\Delta t} - \dot{u}_{i,t}}{\Delta t} \tag{2.8}$$

From equations (2.7) and (2.8), equation (2.6) becomes by the explicit finite difference equation,

$$\left(\frac{\tau_{i+1,t} - \tau_{i,t}}{\Delta z}\right) = \rho \left(\frac{\dot{u}_{i,t+\Delta t} - \dot{u}_{i,t}}{\Delta t}\right) \tag{2.9}$$

Solving for $\dot{u}_{i,t+\Delta t}$ gives,

$$\dot{u}_{i,t+\Delta t} = \dot{u}_{i,t} + \frac{\Delta t}{\rho \Delta z}(\tau_{i+1,t} - \tau_{i,t}) \tag{2.10}$$

Equation (2.10) simply shows how the conditions at time, *t*, can be used to determine the conditions at time, *t+Δt*. Using equation (2.10), for all *i*, the velocity profile can be determined at time *t+Δt*. Using the computed velocities at the end of each time steps as the initial velocities for the next time step, the repeated application of equation (2.10) allows the equation of motion to be integrated in a series of small time steps.

Since the ground surface is a free surface, $\tau_1 = 0$, so

$$\dot{u}_{1,t+\Delta t} = \dot{u}_{1,t} + \frac{\Delta t}{\rho \Delta z}\tau_{2,t}$$

(2.11)

The boundary condition at the bottom of the soil deposit depends on the nature of the underlying bedrock. If the bedrock is rigid, its particle velocity, $\dot{u}_b(t) = \dot{u}_{N+1}(t)$, can be specified directly as the input motion. If the bedrock is elastic, continuity of stresses requires that the shear stress at the bottom of the soil layer, $\tau_{N+1,t}$, be equal to the shear stress at the top of the rock layer, $\tau_{r,t}$. Thus

$$\dot{u}_{N+1,t+\Delta t} = \dot{u}_{N+1,t} + \frac{\Delta t}{\rho \Delta z}(\tau_{r,t} - \tau_{N,t})$$

(2.12)

If an incident wave traveling upward through the rock has a particle velocity $\dot{u}_r(t)$ at the soil-rock boundary, the shear stress at the boundary is approximated (Joyner and Chen, 1975) by

$$\tau_{r,t} \approx \rho_r v_{sr}[2\dot{u}_r(t + \Delta t) - \dot{u}_{N+1,t+\Delta t}]$$

(2.13)

Substituting equation (2.13) into equation (2.12) and solving $\dot{u}_{N+1,t+\Delta t}$ for gives

$$\dot{u}_{N+1,t+\Delta t} = \frac{\dot{u}_{N+1,t} + \frac{\Delta t}{\rho \Delta z}[2\rho_r v_{sr}\dot{u}_r(t + \Delta t) - \tau_{N,t}]}{1 + \left(\frac{\Delta t}{\rho \Delta z}\right)\rho_r v_{sr}}$$

(2.14)

Once the boundary conditions have been established, the integration calculations proceed from the bottom *(i=N+1)* to the top *(i=1)* of the soil deposit in each time step, and step by step in time. Computation of the velocity at the end of each time step, however, requires knowledge of the shear stress in that time step. If the soil deposit is initially at rest, then $\dot{u}_{i,t=0} = 0$ and $\tau_{i,t=0} = 0$ for all *i*. When the input motion, in the form of $\dot{u}_b(t)$ (rigid bedrock) or $\dot{u}_r(t)$ (elastic bedrock), imparts some velocity to the base of the soil deposit, $\dot{u}_{N+1}$ will take on a nonzero value. In subsequent time steps, $\dot{u}_N, \dot{u}_{N-1}, \dot{u}_{N-2}, \ldots$ will all take on nonzero values as the soil deposit moves in response to the input motion.

The incremental displacement in each time step is given by,

$$\Delta u_{i,t} = \dot{u}_{i,t}\Delta t$$

(2.15)

Summing the incremental displacement allows the total displacement, $u_{i,t}$ to be determined at the beginning of each time step. The shear strain in each sublayer is given by,

$$\gamma_{i,t} = \frac{\partial u_{i,t}}{\partial z} = \frac{u_{i+1,t} - u_{i,t}}{\Delta z} \tag{2.16}$$

If the soil is assumed to be linear elastic, the shear stress depends only on the current shear strain, (i.e., $\tau_{i,t} = G_i \gamma_{i,t}$). If he soil is nonlinear and inelastic, however the shear stress will depend on the current shear strain and the stress-strain history. In such cases the computed shear strain, $\gamma_{i,t}$ and the cyclic stress-strain relationship (or advanced constitutive model) are used to determine the corresponding shear stress, $\tau_{i,t}$.

The integration process can then be summarized as follows:

1. At the beginning of each time step, the particle velocity, $\dot{u}_{i,t}$, and total displacement, $u_{i,t}$ are known as each layer boundary.
2. The particle displacement profile is used to determine the shear strain, $\gamma_{i,t}$ within each layer.
3. The stress-strain relationship is used to determine the shear stress, $\tau_{i,t}$ in each layer. The stress-strain curve may be linear or nonlinear. If nonlinear inelastic soil behavior is assumed, stress reversals are checked and accounted for (e.g., by application of the Masing criteria) in each layer.
4. The input motion is used to determine the motion of the base of the soil layer at time $t + \Delta t$.
5. The motion of each layer boundary at time $t + \Delta t$ is calculated, working from bottom to top. The process is then repeated from step 1 to compute the response in the next time step.

CRITICAL OBSERVATIONS FROM THE THEORY

EL analyses can lead to spurious resonances at certain frequencies. These resonances do not occur in NL analyses. EL analyses requires use of γ_{eff} to ensure compatibility between field and laboratory results, while NL directly computes the shear strain for each time step. EL is computationally much more efficient than NL. Usually it requires solution at significant frequencies. However, NL requires solution at all-time steps. NL can be formulated in terms of effective stresses if it incorporates a pore water pressure generation model. EL can only deal with total stress and cannot account for pore water pressure generation. NL can account for the site response effects of liquefied soil if it incorporates a good pore water pressure generation model. EL should not be used when liquefied soils exist. NL has the capability of modelling dynamic behaviour of soils with very large strains if it uses a good constitutive model. Strains greater than about 1% in EL are usually frowned upon. NL requires a good 'universal' constitutive model for the soil which is usually not available. Differences in the results of EL and NL analyses depend upon the degree of nonlinearity. For low strains (stiff profiles and/or weak input motions), results are nearly identical. EL should be chosen when low strains, stiff soils and

negligible pore pressure generation is expected. NL should be chosen when high strain, soft soils and considerable pore pressure generation is expected.

2.4. SITE CLASSIFICATION AND CHARACTERISATION

Site classification is done in order to characterize soil type for a site. It is based on the average N values for the top 30m soil profile (N_{30}) or average shear wave velocity for the top 30m soil profile $(V_{s,30})$. Based on the site classification, soil softness/ hardness can be judged through which an idea about the site response and liquefaction susceptibility can be ascertained. Three site classification procedures are provided in the tabular form:

INDIAN STANDARD CLASSIFICATION (IS:1893-2002)

Table 2.1. IS-1993 (Part 1)-2002 Soil Classification

Soil Description	N_{30}
Very dense soil and soft rock	>30
Dense to medium soil	All the soil 10-30 or sand with little fines >15
Medium to soft soil	<10

where $N_{30} = \frac{30}{\sum_{i=0}^{30}\left(\frac{d_i}{N_i}\right)}$ and $V_{s,30} = \frac{30}{\sum_{i=0}^{30}\left(\frac{d_i}{V_{s_i}}\right)}$.

Time period of the site is given by, $T = 4 * \sum_{i=0}^{30}\left(\frac{d_i}{V_{s_i}}\right)$

where $d_i, N_i \; and \; V_{s_i}$ is the thickness, N-value and shear wave velocity respectively of the i^{th} layer.

NATIONAL EARTHQUAKE HAZARDS REDUCTION PROGRAM (2003)

Table 2.2. NEHRP (2003) Soil Classification

Site Class	$\bar{V}_s$	$\bar{N}$	$\bar{S}_u^a$
E	< 600 fps (<180 m/s)	<15	<1000 psf (<50 kPa)
D	600-1200 fps (180-360 m/s)	15-50	1000-2000 psf (50-100 kPa)
C	1200-2500 fps (360-760 m/s)	>50	>2000 psf (>100 kPa)

[a] If the $\bar{S}_u$ method is used and the $\bar{N}$ and $\bar{S}_u$ criteria differ, select the category with the softer soils.

- Assignment of Site Class B shall be based on the shear wave velocity for rock. For competent rock with moderate fracturing and weathering, estimation of this shear wave velocity shall be permitted. For more highly fractured and weathered rock, the shear wave velocity shall be directly measured or the site shall be assigned to Site Class C.
- Assignment of Site Class A shall be supported by either shear wave velocity measurements on site or shear wave velocity measurements on profiles of the same rock type in the same formation with an equal or greater degree of weathering and Fracturing. Where hard rock conditions are known to be continuous to a depth of 100 ft (30 m), surficial shear wave velocity measurements may be extrapolated to assess$\overline{V_s}$.
- Site Classes A and B shall not be used where there is more than 10 ft (3 m) of soil between the rock surface and the bottom of the spread footing or mat foundation.

INTERNATIONAL BUILDING CODE (2009)

Table 2.3. IBC (2009) Soil Classification

Site Classification	Description	Average Properties in Top 30m		
		Shear wave velocity (m/s)	SPT N (blows/300mm)	Undrained Shear Strength (S_u) (kPa)
A	Hard Rock	>1500	NA	NA
B	Rock	750-1500	NA	NA
C	Very dense soil and soft rock	360-750	>50	>100
D	Stiff soil	180-360	15-50	50-100
E	Soft soil	<180	<15	<50
		Plus any profile with more than 3m of soil having the following characteristics: Plasticity Index (PI) > 20% Moisture Content (w) ≥ 40% Undrained Shear Strength (S_u) < 25kPa		

F	Any profile containing soils with one or more of the following characteristics: Soil vulnerable to potential collapse under seismic loading e.g. liquefiable soils, quick and highly sensitive clay, collapsible weakly cemented soils. Peats and/or highly organic clays (H>8m of peat and/or highly organic clay) Very high plasticity clays (H>8m with PI>75%) Very thick soft/medium stiff clays (H>36m)

Where the soil properties are not known in sufficient detail to determine the site class in accordance with above, it shall be permitted to assume Site class D unless the authority having jurisdiction determines that site class E or F could apply at the site or in the event that Site Class E or F is established by geotechnical data.

2.5. SPT VALUE – SHEAR WAVE VELOCITY RELATIONSHIP

Shear wave velocity is an important parameter for site classification as well as site response analysis. The in-situ determination of shear wave velocity is necessary in case of site response studies. But due to time and cost constraint and also specialised manpower constraint, the shear wave velocity is correlated worldwide from SPT-N number. There are many correlations available worldwide given by many researchers. But only, site specific correlations can depict the picture as close as possible. Here are few correlations that are soil type specific and lithology specific and may be used for uncertainty analysis is site response. A brief review of the work performed on SPT-N and shear wave velocity correlations by various researchers are given in Table 2.4 (a).

Table 2.4. (a) SPT N-Vs Correlations by Different Researchers

Author(s)	Site	Remarks
Jafari et. al. (2002)	Tehran, Iran	• Correlations were developed from simple linear regression analysis. • Correlations provided for fine grained soils. • For N>30, difference is observed for existing and proposed relationships.
Hanumantharao and Ramana (2008)	Delhi, India	• SASW tests were conducted. • Correlations were developed for sand and silty sand profiles based on N values alone without considering other parameters such as

		soil type, geological age, depth, effective stress etc. • Applicable upto N=40.
Maheswari et. al. (2010)	Chennai, India	• MASW and seismic crosshole tests were performed. • Correlations for all types of soils in Chennai were presented.
Anbazhagan et. al. (2012)	Lucknow, India	• MASW and SPT were conducted. • Correlations for all types of soils were presented. • Site classification based on N_{30} and $V_{s,30}$ as per NEHRP (2003) was contradictory.
Choudhury and Chatterjee (2013)	Kolkata, India	• Correlations for all kinds of soil were given based on regression and sensitivity analysis. • Correlations were based on both uncorrected and corrected SPT-N value. • Site Classification of Kolkata based on $V_{s,30}$ according to NEHRP were 'D' and 'E'.
Nath et. al. (2016)	Kolkata, India	• Seismic downhole, MASW and Microtremor survey were conducted. • Site specific, depth and lithology dependent correlations were provided.

CORRELATIONS PRESCRIBED BY SELECTED AUTHORS FOR DIFFERENT SOIL TYPES

Table 2.4. (b) SPT N-Vs Correlations by Different Researchers

Author(s)	Soil Type	N-Vs correlations
Jafari et. al. (2002)	Clay	$V_s = 27 * N^{0.73}$ (m/s)
	Silt	$V_s = 22 * N^{0.77}$ (m/s)
	Fine Grained Soil	$V_s = 19 * N^{0.85}$ (m/s)

Hanumantharao and Ramana (2008)	Sand	$V_s = 79 * N^{0.434}$ (m/s)	
	Silty sand/ sandy silt	$V_s = 86 * N^{0.42}$ (m/s)	
	All soils	$V_s = 82.6 * N^{0.43}$ (m/s)	
Maheswari et. al. (2010)	All soils	$V_s = 95.64 * N^{0.301}$ (m/s)	
	Clay	$V_s = 89.31 * N^{0.358}$ (m/s)	
	Sand	$V_s = 100.53 * N^{0.265}$ (m/s)	
Anbazhagan et. al. (2012)	All soils	$V_s = 68.96 * N^{0.51}$ (m/s)	
	Clay	$V_s = 106.63 * N^{0.39}$ (m/s)	
	Sand	$V_s = 60.17 * N^{0.56}$ (m/s)	
Choudhury and Chatterjee (2013)		**Correlations for Uncorrected SPT (N)**	**Correlations for Corrected SPT [($N_{1,60}$)]**
	All soils	$V_s = 78.21\ N^{0.38}$	$V_s = 78.63\ (N_{1,60})^{0.37}$
	Clay	$V_s = 77.11\ N^{0.39}$	$V_s = 78.03\ (N_{1,60})^{0.38}$
	Silt	$V_s = 58.02\ N^{0.46}$	$V_s = 58.62\ (N_{1,60})^{0.45}$
	Silty sand	$V_s = 54.82\ N^{0.53}$	$V_s = 56.44\ (N_{1,60})^{0.51}$
Nath et. al. (2016)	All soils	$V_S = 87.54\ N^{0.345}$	
	Sand	$V_S = 82.59\ N^{0.358}$	
	Silt	$V_S = 60.47\ N^{0.473}$	
	Clay	$V_S = 97.86\ N^{0.308}$	

DEPTH AND LITHOLOGY SPECIFIC CORRELATIONS PRESCRIBED BY NATH ET. AL. (2016) FOR KOLKATA CITY

Table 2.5. Depth and lithology specific SPT N-Vs Correlations by Nath et. al. (2016)

Depth Range (m)	Lithology	Relation
0-1.95	Top Fill	$V_S = 74.98(\pm4.79)*N^{0.2679(\pm0.0449)}$
1.5-4.95	Silty Clay with Mica, Sand and Kankar	$V_S = 78.55(\pm8.01)*N^{0.3116(\pm0.0559)}$
1.5-9.96	Silty Clay with Decomposed Wood	$V_S = 85.18(\pm6.32)*N^{0.3196(\pm0.0599)}$
1.5-4.97	Fine Sand with Silt and Clay	$V_S = 81.14(\pm4.74)*N^{0.2448(\pm0.0498)}$
4.5-10.1	Clay with Decomposed Wood	$V_S = 102.2(\pm10.13)*N^{0.286(\pm0.0417)}$
4.5-10.95	Silty Clay with Mica, Sand and Kankar	$V_S = 71.52(\pm11.05)*N^{0.3894(\pm0.0619)}$
6-15.5	Silty Sand with Mica and Kankar	$V_S = 68.18(\pm10.9)*N^{0.39929(\pm0.0598)}$
10.5-18.45	Silty Clay with Decomposed Wood	$V_S = 85.63(\pm6.23)*N^{0.2149(\pm0.0336)}$
12-18.95	Silty Clay with Kankar and Silty Spots	$V_S = 115.0(\pm11.0)*N^{0.2914(\pm0.0367)}$
14.9-17.2	Bluish Grey/ Light Yellowish Grey Silt	$V_S = 117.3(\pm10.3)*N^{0.246(\pm0.0295)}$
18.25-26.95	Silty Sand with Mica and Clay	$V_S = 57.57(\pm7.57)*N^{0.4568(\pm0.0384)}$
16.5-22.5	Silty Clay/Clayey Silt with Micaceous Sand	$V_S = 72.13(\pm13.37)*N^{0.4802(\pm0.0572)}$
23.95-34.45	Silty Clay with Mica, Sand and Kankar	$V_S = 63.33(\pm9.82)*N^{0.4497(\pm0.0416)}$
24.6-34.6	Fine Sand with Gravel	$V_S = 69.73(\pm9.43)*N^{0.4053(\pm0.0406)}$
34.45-45.45	Silty Clay/ Clayey Silt with Micaceous Fine Sand	$V_S = 67.47(\pm5.88)*N^{0.5101(\pm0.0236)}$
45.5-54.5	Silty Clay/ Clayey Silt with Micaceous	$V_S = 138.2(\pm18.1)*N^{0.3182(\pm0.0357)}$

	Fine Sand	
40.5-54.5	Silty Clay/Clayey Silt with Mica	$V_S = 87.68(\pm 11.02)*N^{0.4772(\pm 0.0339)}$

2.6. SPECTRUM COMPATIBLE TIME HISTORY GENERATION

Mukherjee and Gupta (2002) presented the way to generate spectrum-compatible synthetic accelerograms for the linear and non-linear time-history analyses of structural systems. A wavelet-based procedure was used to decompose a recorded accelerogram into a desired number of time-histories with non-overlapping frequency contents, and then each of the time-histories was suitably scaled for matching of the response spectrum of the revised accelerogram with a specified design spectrum. The key idea behind this iterative procedure was to modify a recorded accelerogram such that the temporal variations in its frequency content were retained in the synthesized accelerogram.

The reason for using spectrum compatible synthetic accelerogram is because strong motion recorded at some site will be affected by the local site conditions. In many places around the world, earthquake recording stations are absent. Thus, using a non-local strong motion will show a lot of variations with the site specific response spectrum which might yield unhelpful results. Thus in such cases, site specific spectrum compatible strong motion will be helpful. The advantage of spectrum matching technique is that the compatible time history shows less variability with the target response spectrum. But the limitations of this are:

1. It can result in unrealistic ground motions.
2. Certain valuable aspects in an original time history can be neglected (e.g. Directivity pulse).

2.7. SELECTION OF MODULUS REDUCTION AND DAMPING CURVES

Modulus reduction and damping curves are generated from the laboratory tests such as, resonant column test, cyclic triaxial test etc. But in case of non-availability of such facilities, empirical correlations can be used to generate such curves. Ishibashi and Zhang (1993) presented an empirical method to produce such curves. Alternatively, DEEPSOIL has several sets of correlations to produce modulus reduction and damping curves, namely, Seed and Idriss (1991). One advantage of using Ishibashi and Zhang (1993) method is that the modulus reduction and damping curves are confining pressure and plasticity dependent. Thus, this method presents more accurate prediction than other methods.

ISHIBASHI AND ZHANG (1993)

They collected experimental data on dynamic shear moduli and damping ratios of various soils including non-plastic sands to highly plastic clays and analysed and brought into simple unified

formulas. The unified formulas express the dynamic shear moduli and the damping ratios in terms of maximum dynamic shear modulus, cyclic shear strain amplitude, mean effective confining pressure and soil's plasticity index.

General Equations for Sandy Soils

Equivalent shear modulus, G, is generally expressed in the form:

$$G = K(\gamma) f(e) {\sigma'_0}^{m(\gamma)} \tag{2.17}$$

where, $K(\gamma)$ is a decreasing function of the cyclic shear strain amplitude γ; $K(\gamma)$ = 1 at very small γ ($\leq 10^{-6}$); $f(e)$ is a function of void ratio e; σ'_0 is the mean effective confining pressure and power $m(\gamma)$ is an increasing function of γ.

G_{max}, the maximum shear dynamic shear modulus is the maximum value of *G* and is usually obtained at $\Upsilon = 10^{-6}$ or less. Hence G_{max} is:

$$G_{max} = K_0 f(e) {\sigma'_0}^{m_0} \tag{2.18}$$

where, $K_0 = K\ (\Upsilon \leq 10^{-6}) = 1$ and $m_0 = m\ (\Upsilon \leq 10^{-6})$.

From equations (2.17) and (2.18), equation (2.19) is obtained:

$$\frac{G}{G_{max}} = K(\gamma) {\sigma'_0}^{m(\gamma) - m_0} \tag{2.19}$$

The following equations were proposed to best fit data points:

$$K(\gamma) = 0.5 \left[1 + \tanh \left\{ ln \left(\frac{0.000102}{\gamma} \right)^{0.492} \right\} \right] \tag{2.20}$$

$$m(\gamma) - m_0 = 0.272 \left[1 - \tanh \left\{ ln \left(\frac{0.000556}{\gamma} \right)^{0.4} \right\} \right] \tag{2.21}$$

where γ is expressed as raw strain; σ'_0 is expressed in kPa.

Hardin and Drnevich (1972) and Tatsuoka et. al. (1978) proposed that the damping ratio, D is expressed as a function of $\frac{G}{G_{max}}$:

$$D_{sand} = 0.333\left\{0.586\left(\frac{G}{G_{max}}\right)^2 - 1.547\left(\frac{G}{G_{max}}\right) + 1\right\}$$

(2.22)

D = 0.333 is the maximum damping ratio at very high shear strain levels γ ($\geq 10^{-2}$), where G/G_{max} is nearly equal to zero. $D_{sand,max}$ = 33.3% is a representative value from previous researchers (Hardin and Drnevich, 1972; Sherif et. al., 1977; Tatsuoka et al., 1978) for sands.

General Equations for Plastic Soils (Silts and Clays)

The availability of comprehensive data on dynamic properties of silts and clays is limited. Researchers (Kokusho et al., 1982; Dobry and Vucetic, 1987) reported that the modulus and damping ratios are significantly affected by soil's plasticity index (I_P). General observations for plastic soils are that: (1) $K(\gamma)$ versus Υ curve moves upward and right side when I_P increases, (2) for highly plastic clays, the effect of σ_0' on G value becomes negligible i.e. $m(\gamma) - m_0$ function approaches to zero for high I_P values regardless of Υ and (3) the damping ratio D decreases with increasing I_P values. Based on those observations, $K(\gamma)$, $m(\gamma) - m_0$ and D equations are modified to include I_P:

$$\frac{G}{G_{max}} = K(\gamma, I_P){\sigma'_0}^{m(\gamma, I_P) - m_0}$$

(2.23)

$$D_{sand} = 0.333\left\{0.586\left(\frac{G}{G_{max}}\right)^2 - 1.547\left(\frac{G}{G_{max}}\right) + 1\right\}A(I_P)$$

(2.24)

where, $A(I_P)$ is a modification function for damping ratio applied to Eq. (2.7.6) of sands.

$$m(\gamma, I_P) - m_0 = 0.272\left[1 - \tanh\left\{ln\left(\frac{0.000556}{\gamma}\right)^{0.4}\right\}\right]e^{-0.0145{I_P}^{1.3}}$$

(2.25)

where, $m(\gamma, I_P) - m_0$ function decreases with increasing I_P and approaches to zero at high I_P ($\geq$70) regardless of Υ.

$$K(\gamma, I_P) = 0.5\left[1 + \tanh\left\{ln\left(\frac{0.000102 + n(I_P)}{\gamma}\right)^{0.492}\right\}\right]$$

(2.26)

$$\text{where, } n(I_P) = \begin{cases} 0 \; for \; I_P = 0 \\ 3.37X10^{-6} {I_P}^{1.404} \; for \; 0 < I_P \leq 15 \\ 7.0X10^{-7} {I_P}^{1.976} \; for \; 15 < I_P \leq 70 \\ 2.7X10^{-5} {I_P}^{1.115} \; for \; I_P > 70 \end{cases}$$

(2.27)

Proposed Equation for damping ratio D is:

$$D_{plastic\ soil} = 0.333 \left\{ 0.586 \left(\frac{G}{G_{max}} \right)^2 - 1.547 \left(\frac{G}{G_{max}} \right) + 1 \right\} \frac{1 + e^{-0.0145 {I_P}^{1.3}}}{2}$$

(2.28)

2.8. SOIL CONSTITUTIVE MODEL

Soil constitutive model provides the backbone curve which represents the loading-unloading reloading behaviour of soil under cyclic loading. The Modified Kondner Zelasko (MKZ) Model is provided in the DEEPSOIL software to perform site response analysis. The Multi Yield Plasticity Models (Pressure Dependent and Pressure Independent) are incorporated in the OpenSees software.

MODIFIED KONDNER ZELASKO MODEL (KONDNER AND ZELASKO, 1963; MATASOVIC, 1993; HASHASH AND PARK, 2001)

The shear stiffness and damping of the soil are related to the developed shear strains in the soil sample with the aid of a soil constitutive model. The pressure dependent hyperbolic model used in DEEPSOIL defines the inter-relationship between the stresses and strains developed in soil subjected to a cyclic loading-unloading phenomenon. Generally, the development of cyclic shear stress due to cyclic strains in governed by Masing rules (Masing, 1926) and extended Masing rules (Pyke, 1979). The hyperbolic model can be described by using two sets of equations; the first equation – known as the backbone curve - defines the stress-strain relationship for loading:

$$\tau = \frac{\gamma G_0}{1 + \beta \left(\frac{\gamma}{\gamma_r} \right)^s}$$

(2.29)

The second equation defines the stress-strain relationship for unloading-reloading conditions:

$$\tau = \frac{2G_0 \left(\frac{\gamma - \gamma_{rev}}{2} \right)}{1 + \beta \left(\frac{\gamma - \gamma_{rev}}{2\gamma_r} \right)^s} + \tau_{rev}$$

(2.30)

whereby, γ is the given shear strain, γ_r is the reference shear strain, β is a dimensionless factor, G_0 is the maximum shear modulus and s is a dimensionless exponent.

Hashash and Park (2001) modified the non-linear model proposed by Matasovic (1993) to include the effect of confining pressure on the secant shear modulus of the soil. In the modified model, a new formulation is introduced in which the reference strain, γ_r is no longer a constant for a soil type but a variable that depends on the effective stress following the expression shown in Equation (2.31):

$$\gamma_r = a\left(\frac{\sigma_v'}{\sigma_{ref}}\right)^b \tag{2.31}$$

where a and b are curve fitting parameters, σ_v' is the vertical (overburden) effective stress to the midpoint of the soil layer and σ_{ref} is a reference confining pressure of 0.18 MPa. To take into account the reduction of the small strain damping with the increase of confining pressure Hashash and Park (2001) proposed the relationship presented in Equation (2.32):

$$\xi = \frac{c}{(\sigma_v')^d} \tag{2.32}$$

where c and d are curve fitting parameters and σ_v' is the vertical effective stress.

PRESSURE DEPENDENT MULTI YIELD MATERIAL (YANG ET. AL., 2003)

PressureDependMultiYield material is an elastic-plastic material for simulating the essential response characteristics of pressure sensitive soil materials under general loading conditions. Such characteristics include dilatancy (shear-induced volume contraction or dilation) and cyclic mobility, typically exhibited in sands or silts during monotonic or cyclic loading.

During the application of gravity load (and static loads if any), material behavior is linear elastic. In the subsequent dynamic (fast) loading phase(s), the stress-strain response is elastic-plastic. Plasticity is formulated based on the multi-surface (nested surfaces) concept, with a non-associative flow rule to reproduce dilatancy effect. The yield surfaces are of the Drucker-Prager type.

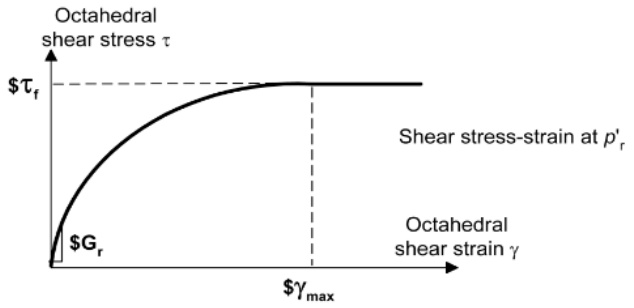

Figure 2.8: Backbone curve at p_r' for Pressure Dependent Multi-Yield Plasticity Model

The friction angle Φ defines the variation of peak (octahedral) shear strength τ_f as a function of current effective confinement *p*':

$$\tau_f = \frac{2\sqrt{2}\, sin\varphi}{3 - sin\varphi} p'$$

(2.33)

Octahedral shear stress is defined as:

$$\tau = \frac{1}{3}\left[\left(\sigma_{xx} - \sigma_{yy}\right)^2 + \left(\sigma_{yy} - \sigma_{zz}\right)^2 + (\sigma_{xx} - \sigma_{zz})^2 + 6{\sigma_{xy}}^2 + 6{\sigma_{yz}}^2 + 6{\sigma_{xz}}^2\right]^{1/2}$$

(2.34)

At a constant confinement *p*', the shear stress τ (octahedral) - shear strain γ (octahedral) nonlinearity is defined by a hyperbolic curve (backbone curve):

$$\tau = \frac{G\gamma}{1 + \frac{\gamma}{\gamma_r}\left(\frac{p'_r}{p'}\right)^d}$$

(2.35)

where γ_r satisfies the following equation at p'_r:

$$\tau_f = \frac{2\sqrt{2}\, sin\varphi}{3 - sin\varphi} p'_r = \frac{G_r \gamma_{max}}{1 + \gamma_{max}/\gamma_r}$$

(2.36)

The user specified friction angle Φ is ignored. Instead, Φ is defined as follows:

$$sin\varphi = \frac{3\sqrt{3}\, \sigma_m/p'_r}{6 + \sqrt{3}\, \sigma_m/p'_r}$$

(2.37)

where σ_m is the product of the last modulus and strain pair in the modulus reduction curve. Therefore, it is important to adjust the backbone curve so as to render an appropriate Φ. If the resulting Φ is smaller than the phase transformation angle Φ_{PT}, Φ_{PT} is set equal to Φ.

Table 2.6. Pressure Dependent Multi Yield Model Soil Parameters

Dr (%)	30	40	50	60	75
Density (t/m^3)	1.7	1.8	1.9	2.0	2.1
G_{max} (kPa) (at p'$_r$ = 80 kPa)	60000	90000	100000	110000	130000

B_{max} (kPa) (at p'_r = 80 kPa)	160000	220000	233000	240000	260000
K_0	0.5	0.47	0.45	0.43	0.4
Φ	31	32	33.5	35	36.5
Φ_{PT}	31	26	25.5	26	26
γ_{max} (at p'_r = 101 kPa)	0.1				
Reference Pressure (p'_r) (kPa)	101				
Pressure Dependent Coefficient	0.5				
Contrac1	0.087	0.067	0.045	0.028	0.013
Contrac3	0.18	0.23	0.15	0.05	0
Dilat1	0	0.06	0.06	0.1	0.3
Dilat3	0	0.27	0.15	0.05	0
e	0.85	0.77	0.7	0.65	0.55

PRESSURE INDEPENDENT MULTI YIELD MATERIAL (YANG ET. AL., 2003)

Pressure Independent Multi Yield material is an elastic-plastic material in which plasticity exhibits only in the deviatoric stress-strain response. The volumetric stress-strain response is linear-elastic and is independent of the deviatoric response. This material is implemented to simulate monotonic or cyclic response of materials whose shear behavior is insensitive to the confinement change. Such materials include, for example, organic soils or clay under fast (undrained) loading conditions.

During the application of gravity load (and static loads if any), material behavior is linear elastic. In the subsequent dynamic (fast) loading phase(s), the stress-strain response is elastic-plastic. Plasticity is formulated based on the multi-surface (nested surfaces) concept, with an associative flow rule. The yield surfaces are of the Von Mises type.

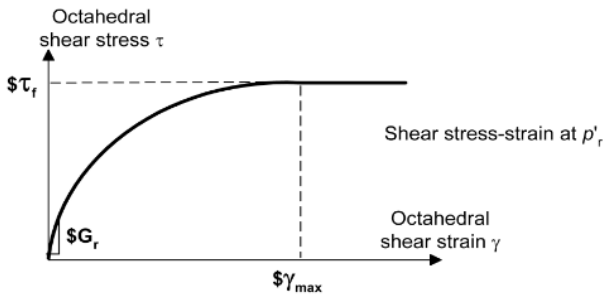

Figure 2.9: Backbone curve at p_r' for Pressure Independent Multi-Yield Plasticity Model

The friction angle Φ and cohesion c define the variation of peak (octahedral) shear strength τ_f as a function of initial effective confinement p'_r:

$$\tau_f = \frac{2\sqrt{2}\,sin\varphi}{3 - sin\varphi} p_r' + \frac{2\sqrt{2}}{3} c$$

(2.38)

At a constant confinement p', the shear stress τ (octahedral) - shear strain γ (octahedral) nonlinearity is defined by a hyperbolic curve (backbone curve):

$$\tau = \frac{G\gamma}{1 + \frac{\gamma}{\gamma_r}\left(\frac{p_r'}{p'}\right)^d}$$

(2.39)

where γ_r satisfies the following equation at p'_r:

$$\tau_f = \frac{2\sqrt{2}\,sin\varphi}{3 - sin\varphi} p_r' + \frac{2\sqrt{2}}{3} c = \frac{G_r \gamma_{max}}{1 + \gamma_{max}/\gamma_r}$$

(2.40)

where C is defined by c=sqrt(3)* σ_m/2, where σ_m is the product of the last modulus and strain pair in the modulus reduction curve. Therefore, it is important to adjust the backbone curve so as to render an appropriate c.

If the user specifies Φ >0, this Φ will be ignored. Instead, Φ is defined as follows:

$$sin\varphi = \frac{3\left(\sqrt{3}\,\sigma_m - 2c\right)/p_r'}{6 + \left(\sqrt{3}\,\sigma_m - 2c\right)/p_r'}$$

(2.41)

If the resulting Φ <0, we set Φ =0 and c=sqrt(3)* σ_m/2.

Also remember that improper modulus reduction curves can result in strain softening response (negative tangent shear modulus), which is not allowed in the current model formulation. Finally, note that the

backbone curve varies with confinement, although the variation is small within commonly interested confinement ranges.

Table 2.7. Pressure Independent Multi Yield Model Soil Parameters

	Soft Clay	Medium Clay	Stiff Clay
Density (t/m^3)	1.3	1.5	1.8
G_{max} (kPa)	13000	60000	150000
B_{max} (kPa)	65000	300000	750000
Cohesion (kPa)	18	37	75
γ_{max}	0.1		
Φ	0		
Pressure Dependent Coefficient	0		

2.9. STRAIN-BASED PORE PRESSURE GENERATION MODEL

Nonlinear ground response analysis with effective stress approach is a very useful method to predict pore pressure generation and dissipation in soil. The pore pressure generation model can be based on stress based (Seed et. al., 1975), strain based (Dobry et. al., 1982), energy based (Green et. al., 2000) etc. DEEPSOIL uses strain based pore pressure generation model proposed by Vucetic and Dobry (1986) for sands and Matasovic and Vucetic (1995) for clays.

FOR SANDS - DOBRY ET. AL. (1982), VUCETIC & DOBRY (1986), CARLTON (2014) & MEI ET. AL. (2018)

Dobry et al. (1985a) presented a pore pressure generation model for saturated sands which was based on undrained testing, theoretical effective stress considerations, and a curve-fitting procedure. Vucetic and Dobry (1988) presented a modified version of the Dobry et al (1982) model in order to include the effects of 2-D shaking, which was established as shown in Equation (2.42):

$$r_u = \frac{p * f * F * N * \left(\gamma_c - \gamma_{tvp}\right)^s}{1 + f * F * N * \left(\gamma_c - \gamma_{tvp}\right)^s} \tag{2.42}$$

where r_u is the excess cyclic porewater pressure ratio after cycle N. The primary factors controlling the generation of pore water pressure were identified as the amplitude of the cyclic shear strain, γ_c, the number of shear straining cycles, N, and the magnitude of the volumetric threshold shear strain, γ_{tvp}. The f parameter is used in simulating 2-D effects (i.e. f = 1 and 2 for 1D and 2D shaking respectively), while p, F, and s are curve-fitting parameters.

Mei et al. (2018) proposed empirical correlations for the three curve fitting parameters (p, F, and s) to avoid the need of performing laboratory cyclic testing to calibrate the model. Mei et al. suggested setting p = 1 and s = 1 based on the analysis of data from laboratory cyclic tests that they performed and from others (Dobry et al.; Vucetic and Dobry; and Matasovic). Additionally, Mei et al. developed a correlation relating F, D_r, and C_u. They noted that F reflects the rate of Δu generation and should be inversely related to D_r and directly related to C_u. Figure. (2.10) shows their proposed correlation for clean, subangular to subrounded silica sands.

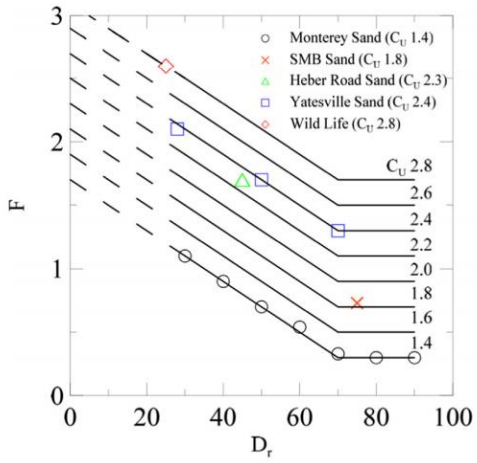

Figure 2.10: Proposed correlation to estimate curve-fitting parameter F for the Vucetic and Dobry model

The following relationship presented by Idriss and Boulanger (2008) for sands was used to obtain D_r from corrected SPT N-value (i.e., $N_{1,60}$):

$$D_r = \sqrt{\frac{N_{1,60}}{46}} \tag{2.43}$$

Alternatively, F can be estimated using the correlation proposed by Carlton (2014), which related F to V_s:

$$F = 3810 * V_s^{-1.55}$$

(2.44)

Carlton (2014) also gave a relationship between fines content (FC %) and s:

$$s = (1 + FC)^{0.1252}$$

(2.45)

γ_{tvp} is the limiting value of γ_c, below which no excess pore pressure develops, regardless of the number of applied load cycles (N). Mei et al. refer to Dobry et al, stating that γ_{tvp} is usually between 0.01% and 0.02% for most sands.

N can be correlated to peak ground acceleration (a_{max}) and moment magnitude of earthquake (M_w) in the following way (Lasley et. al., 2017):

$$\ln(N) = 0.4605 - 0.4082 * \ln(a_{\max}) + 0.2332 * M_w$$

(2.46)

where a_{max} is the same as defined previously and has units of g. This correlation shows a negative correlation between N and a_{max}.

FOR CLAYS - MATASOVIC AND VUCETIC (1995) & CARLTON (2014)

Matasovic and Vucetic (1995) proposed the following equation for the excess pore water pressure generation in clays:

$$r_u = AN^{-3s(\gamma_c - \gamma_{tvp})^r} + BN^{-2s(\gamma_c - \gamma_{tvp})^r} + CN^{-s(\gamma_c - \gamma_{tvp})^r} + D$$

(2.47)

where r_u is the excess pore pressure ratio (=$\Delta u/\sigma'_{vo}$); N is the equivalent numbers of cycles calculated for the most recent strain reversal. For uniform strain cycles, the equivalent number of cycle is the same as number of loading cycles. For irregular strain cycles, since the cycle number does not increase uniformly, N is calculated using the r_u obtained from previous step and then increased by 0.5 for the current step; γ_c is the most recent reversal shear strain; γ_{tvp} is the threshold shear strain value below which reversals will not generate excess pore pressure (generally taken as 0.1% for clays); r and s are the curve fitting parameters; A, B, C and D are the curve fitting coefficients.

Carlton (2014) presented empirical correlations for curve fitting parameters s, r, A, B, C and D:

$$s = 1.6374 * (PI)^{-0.802} * (OCR)^{-0.417}$$

(2.48)

$$r = 0.7911 * (PI)^{-0.113} * (OCR)^{-0.147}$$

(2.49)

$$A = \begin{cases} 7.6451, & OCR < 1.1 \\ 15.641 * (OCR)^{-0.242}, & OCR \geq 1.1 \end{cases}$$

(2.50)

$$B = \begin{cases} -14.714, & OCR < 1.1 \\ -33.691 * (OCR)^{-0.33}, & OCR \geq 1.1 \end{cases}$$

(2.51)

$$C = \begin{cases} 6.38, & OCR < 1.1 \\ 21.45 * (OCR)^{-0.468}, & OCR \geq 1.1 \end{cases}$$

(2.52)

$$D = \begin{cases} 0.6922, & OCR < 1.1 \\ -3.4708 * (OCR)^{-0.857}, & OCR \geq 1.1 \end{cases}$$

(2.53)

where OCR is the overconsolidation ratio and PI is the plasticity index.

2.10. LIQUEFACTION POTENTIAL ANALYSIS

IDRISS & BOULANGER (2014)

The semi empirical procedure to evaluate liquefaction potential during earthquakes was introduced by Seed and Idriss (1971) and later was updated by Idriss and Boulanger (2014). It consisted of evaluation of Factor of Safety (FS) in terms of Cyclic Resistance Ratio (CRR) (i.e. capacity of soil to resist liquefaction) and Cyclic Stress Ratio (CSR) (i.e. demand of liquefaction induced by earthquake):

$$FS = \frac{CRR}{CSR}$$

(2.54)

CYCLIC RESISTANCE RATIO (CRR)

CRR for earthquake magnitude of 7.5 was determined in terms of equivalent clean sand SPT value corrected for overburden and 60% hammer efficiency $\left[(N_1)_{60,CS}\right]$:

$$CRR = exp\left[\frac{(N_1)_{60,CS}}{14.1} + \left\{\frac{(N_1)_{60,CS}}{126}\right\}^2 - \left\{\frac{(N_1)_{60,CS}}{23.6}\right\}^3 + \left\{\frac{(N_1)_{60,CS}}{25.4}\right\}^4 - 2.8\right]$$

(2.55)

$(N_1)_{60,CS}$ was calculated as:

$$(N_1)_{60,CS} = (N_1)_{60} + \Delta(N_1)_{60}$$

(2.56)

where

$$\Delta(N_1)_{60} = exp\left[1.63 + \frac{9.7}{FC} - \left(\frac{15.7}{FC}\right)^2\right]$$

(2.57)

where FC =Fines content. It was seen that CRR increases with increasing fines content and relative density and effective overburden pressure.

$(N_1)_{60}$ was calculated as:

$$(N_1)_{60} = C_N * C_E * C_B * C_R * C_S * N_m$$

(2.58)

where N_m is the in-situ SPT value, C_N is the correction factor for overburden, C_E is correction factor for hammer energy, C_B is the correction factor for nonstandard borehole diameter, C_R is the correction factor for nonstandard rod lengths and C_S is the correction factor that depends on sampler.

C_N was calculated as (Liao and Whitman, 1986):

$$C_N = \left(\frac{P_a}{\sigma_0'}\right)^{0.5}$$

(2.59)

where P_a is the atmospheric pressure (= 100 kPa); and σ_0' is the effective overburden pressure.

Correction Factors to be applied for the conversion of Raw SPT-N values to Corrected $(N_1)_{60}$ values (after Nath, 2011; Skempton, 1986; Robertson and Wride, 1998; Youd et al., 2001):

Table 2.8. Corrections for SPT values

Factor	Size/Criteria	Correction Factor
Hammer Energy Correction Factor (C_E)		
Donut Hammer	--	0.5-1.0
Safety Hammer	--	0.7-1.2
Automatic-trip Donut Hammer	--	0.8-1.3

Correction Factor for Borehole Diameter (C_E)		
Borehole Diameter	65-115 mm	1
	150 mm	1.05
	200 mm	1.15
Correction for Rod Length (C_R)		
Rod Length	< 3 m	0.75
	3-4 m	0.8
	4-6 m	0.85
	6-10 m	0.95
	10-30 m	1
Correction for Sampler based on method (C_S)		
Sampling Method	Standard Samplers	1
	Samplers without Liners	1.1-1.3

CYCLIC STRESS RATIO (CSR)

CSR for earthquake magnitude of 7.5 and normalized for effective overburden pressure was determined from:

$$CSR_{M=7.5|\sigma'_{v0}=1\ atm} = 0.65 * \left(\frac{a_{max}}{g}\right) * \left(\frac{\sigma_{v0}}{\sigma'_{v0}}\right) * \left(\frac{r_d}{MSF * K_\sigma}\right) \quad (2.60)$$

where a_{max} is the peak horizontal acceleration at ground surface in terms of g; σ_{v0} and σ'_{v0} are the total and effective initial vertical stresses respectively; r_d, MSF and K_σ are the stress reduction factor dependent on depth in the soil profile, Magnitude Scaling Factor and overburden correction factor respectively.

r_d was calculated as (Idriss, 1999):

$$r_d = exp\left[-1.012 - 1.126 * sin\left(\frac{z}{11.73} + 5.133\right) + 0.106 + 0.118 * sin\left(\frac{z}{11.26} + 5.142\right) * M_w\right]$$

(2.61)

where z is the depth below the ground surface, in meters and M_w is the moment magnitude of the earthquake.

Since all correlations in literature were based on earthquakes of magnitude of 7.5, a magnitude scaling factor *MSF* was used to adjust the induced CSR during an earthquake of magnitude M_w.

MSF was calculated as:

$$MSF = min\begin{cases} 6.9 * exp\left(\frac{-M_w}{4}\right) - 0.058 \\ 1.8 \end{cases}$$

(2.62)

The overburden correction factor (K_σ) accounts for the non-linearity of the overburden pressure. K_σ allows to scale the CSR for a reference effective stress of 1 atm (100 kPa). K_σ was calculated as (Boulanger, Brandenberg, Singh and Chang (2003)):

$$K_\sigma = 1 - C_\sigma * ln\left(\frac{\sigma'_{v0}}{P_a}\right) \leq 1.1$$

(2.63)

where C_σ was expressed in terms of $(N_1)_{60,CS}$ (Idriss and Boulanger (2008)):

$$C_\sigma = \frac{1}{18.9 - 2.55 * \sqrt{(N_1)_{60,CS}}} \leq 0.3$$

(2.64)

2.11. POST-LIQUEFACTION SETTLEMENT

Due to liquefaction, saturated sands densify and thus settlement occurs. The calculation for settlement was presented by various researchers namely, Tokimatsu and Seed, 1987; Ishihara and Yoshimine, 1992; Shamoto et al., 1998; and Wu and Seed, 2004 etc. Two methods, namely, Tokimatsu and Seed (1987) and Ishihara and Yoshemine (1992) is being discussed. The two methods were then modified by Cetin et. al. (2009).

TOKIMATSU AND SEED (1987)

Simplified methods of analysis were proposed for estimating probable settlements in either saturated or unsaturated sand deposits subjected to earthquake shaking. It was suggested that the primary factors controlling induced settlement are the cyclic stress ratio and maximum shear strain induced in saturated

sands by the earthquake shaking and the cyclic strains induced in dry or partially saturated sands, together with the SPT N-value of the sand and the magnitude of the earthquake.

A chart was presented which correlates volumetric strain ($\varepsilon_v\%$) with CSR and $N_{1,60}$ in Figure. (2.11).

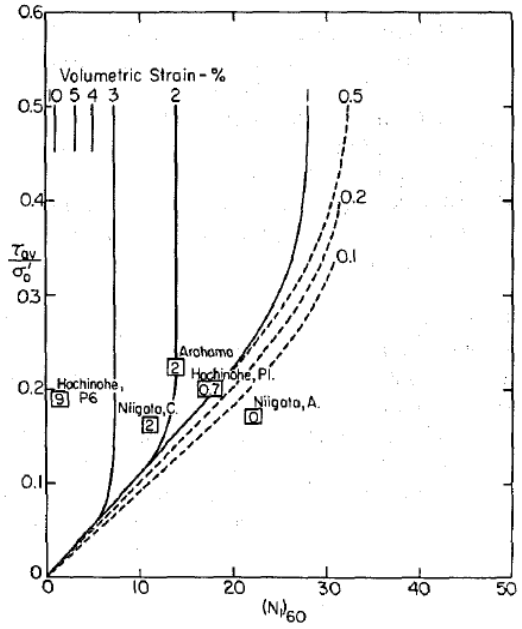

Figure 2.11: Proposed tentative relationship between CSR, $N_{1,60}$ and volumetric strain for saturated clean sands

It should be noted that volumetric strains after liquefaction may be as high as 2-3% for loose to medium sands and even higher for very loose sands. It should be recognized that, even under static loading conditions, the error associated with the estimation of settlements in sands is on the order of 25-50%.

ISHIHARA AND YOSHEMINE (1992)

A bulk of laboratory test data were examined on sands by using a simple shear apparatus and a family of curves was established in which the volumetric strain resulting from dissipation of pore pressure was correlated with the density of sand and conventionally used factor of safety against liquefaction. Thus, given the factor of safety and the density in each layer of a sand deposit at a given site, the volumetric strain could be calculated and by integrating the volume changes throughout the depth, it became possible to estimate the amount of settlements on the ground surface produced by shaking during earthquakes.

The chart which correlates the volumetric strain with factor of safety against liquefaction and relative density or SPT or CPT value was given in the following figure (2.12):

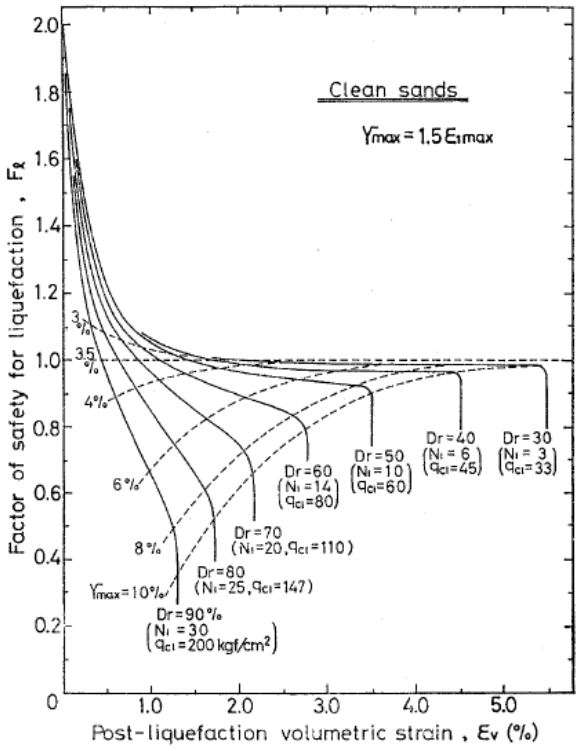

Figure 2.12: Chart for determining volumetric strain as functions of factor of safety

Idriss and Boulanger (2008) recommended the following functions of $(N_1)_{60,CS}$ and factor of safety against liquefaction (FS_{liq}) to approximate the Ishihara and Yoshemine (1992) volumetric strains:

$$(\varepsilon_v)_i = 1.5 * \exp\left(-0.369 * \sqrt{(N_1)_{60,CS}}\right) * Min\begin{Bmatrix}0.08\\ \gamma_{max}\end{Bmatrix} \tag{2.65}$$

where γ_{max} is the maximum shear strain the undrained loading.

To compute γ_{max}, we need a few intermediate values:

$$F_\alpha = 0.032 + 0.69 * \sqrt{(N_1)_{60,CS}} - 0.13 * (N_1)_{60,CS} \tag{2.66}$$

and limiting shear strain, $\gamma_{lim} = 1.859 * \left(1.1 - \sqrt{\frac{(N_1)_{60,CS}}{46}}\right)^3 \geq 0$ (2.67)

and γ_{max} is given by:

$$\gamma_{max} = \begin{cases} 0 \quad for\ FS_{liq} \geq 2 \\ Min\begin{cases} \gamma_{lim} \\ 0.035 * (2 - FS_{liq} * \left(\frac{1 - FS_{liq}}{FS_{liq} - F_\alpha}\right) \quad for\ 2 > FS_{liq} > F_\alpha \\ \gamma_{lim} \quad for\ FS_{liq} \leq F_\alpha \end{cases} \end{cases}$$

(2.68)

CETIN ET. AL. (2009)

They described a maximum likelihood framework for the probabilistic assessment of cyclically induced reconsolidation settlements of saturated cohesionless soil sites. For this purpose, over 200 case history sites were carefully studied. After screening for data quality and completeness, the resulting database was composed of 49 high-quality, cyclically induced ground settlement case histories from seven different earthquakes. For these case history sites, settlement predictions by currently available methods of Tokimatsu and Seed 1984, Ishihara and Yoshimine 1992, Shamoto et al. 1998, and Wu and Seed 2004 were presented comparatively, along with the predictions of the proposed probabilistic model. The analyses results revealed that

a) The predictions of Shamoto et al. and Tokimatsu and Seed were smaller than the actual settlements and needed to be calibrated by a factor of 1.93 and 1.45, respectively.
b) Ishihara and Yoshimine, and Wu and Seed predictions were higher than the actual settlements and needed to be calibrated by a factor of 0.90 and 0.98, respectively.

It was assumed that the contribution of layers to surface settlement diminishes as the depth of layer increases, and beyond a certain depth, settlement of an individual layer cannot be traced at the ground surface. After statistical assessments, the optimum value of this threshold depth was found to be 18 m.

The depth weighting factor (DF_i) is defined as:

$$DF_i = 1 - \frac{d_i}{18\ m}$$

(2.69)

where d_i is the middepth of each saturated cohesionless soil layer from the ground surface.

Equivalent volumetric strain, $\varepsilon_{v,equ}$, of the soil profile was estimated by:

$$\varepsilon_{v,equ} = \frac{\sum \varepsilon_{v,i} * t_i * DF_i}{\sum t_i * DF_i}$$

(2.70)

and the estimated settlement, $s_{estimated}$ of the profile was simply calculated as:

$$s_{estimated} = \varepsilon_{v,equ} * \sum t_i$$

(2.71)

where t_i is the thickness of the ith layer in soil profile and $\varepsilon_{v,i}$ is the volumetric strain in the ith layer.

The reason behind the use of a depth weighting factor was based on the following:

a) Upward seepage, triggering void ratio redistribution, and resulting in unfavorably higher void ratios for the shallower sublayers of soil layers;
b) Reduced induced shear stresses and number of shear stress cycles transmitted to deeper soil layers due to initial liquefaction of surficial layers;
c) Possible arching effects due to nonliquefied soil layers.

All these may significantly reduce the contribution of volumetric settlement of deeper soil layers to the overall ground surface settlement.

2.12. SUMMARY OF THE LITERATURE REVIEW

Prerequisite of any sound ground response analysis is the site characterization for which geotechnical data of the soil (particle size distribution, consistency limits, permeability values etc.) and geophysical data of the site (i.e. SPT, CPT values etc.) are required.

Shear wave velocity is one of the main criteria for site classification. But in-situ measurement of shear wave velocity requires time, cost and expertise. On absence of it, shear wave velocity can be correlated to site specific SPT value. But caution is needed when applying existing SPT-Vs correlations as any wrong correlation can lead to incorrect measurement of site response. Thus, uncertainty analysis must be performed with as many as possible site specific, confinement specific and lithology specific SPT-Vs correlations for better judgement.

Previous ground response studies on Kolkata (Roy and Sahu (2012), Akhila et. al. (2012), Bhattacharya and Govindaraju (2012) and Choudhury and Chatterjee (2015)) have been conducted using equivalent linear method. Roy and Sahu (2012) stated vulnerable source for Kolkata is Eocene Hinge Zone with maximum credible earthquake (MCE) moment magnitude as 6.2. Kolkata lies in Zone III and IV (IS:1893-2002). Akhila et. al. (2012) mentioned that Peak Bed Rock Acceleration (PBRA) for Kolkata ranges from 0.1g to 0.34g. Bhattacharya and Govindaraju (2012) used GSHAP map which specified PBRA as 0.163g for Kolkata and they used synthetic earthquake motion as input strong motion due to lack of recording stations in the city. Choudhury and Chatterjee (2015) used five different motions (i.e. 1989 Loma Gilroy, 1994 Northridge, 1995 Kobe, 2001 Bhuj and 2011 Sikkim) having a wide variation in ground motion parameters. All of them predicted PGA amplification about 3-4.8 times at surface.

Ground response analysis can be divided on the basis of dimensionality of shear wave propagation. Also, on the basis of complexity and realistic analysis, it can be divided into three groups, namely, linear, equivalent linear and non-linear. In linear method, shear modulus and damping ratio are assumed to be constant. It is limited to analysis of linear systems. In equivalent linear analysis, nonlinearity of soil is approximated by taking equivalent linear shear modulus as secant shear modulus and equivalent linear damping ratio as the damping ratio that produces the same energy loss in a single cycle as the actual hysteresis loop. This method is incapable of representing the changes in soil stiffness that actually occurs during the strong motion. Nonlinear approach is used to analyse the actual nonlinear response of a soil deposit using direct numerical integration in the time domain. In this method, nonlinear inelastic stress-strain relationship can be followed in a set of small incrementally time steps. Site classification according to IS:1893-2002 implies that Kolkata falls in the category of soft to medium dense soil. According to NEHRP (2003) and IBC (2009), Kolkata falls in the category of site class 'D' and 'E'. This implies the severity of earthquake damage due to even small scale earthquakes.

In absence of site specific recorded bedrock accelerations due to earthquake, synthetic earthquake can be generated using wavelet based computer program called WAVGEN (Mukherjee and Gupta, 2002) from any given earthquake with the help of target response spectrum matching.

Ishibashi and Zhang (1993) presented the modulus reduction and damping curves in case of absence of laboratory data for both non-plastic and plastic soils. One advantage of this method is that the modulus reduction and damping curves varies accordingly with confinement levels and plasticity index (for plastic soils).

Strain based pore pressure generation models [Dobry et. al. (1982) and Matasovic and Vucetic (1995)] are incorporated in the software DEEPSOIL which performs pore pressure generation for sands and clays respectively. In absence of laboratory data, Carlton (2014) equations can be used to predict the values of pore pressure calibration parameters.

Simplified procedure of liquefaction potential analysis (Seed and Idriss, 1971; Idriss and Boulanger, 2014) can be used to judge the liquefaction potential with PGA values obtained from ground response analysis and moment magnitude of the earthquake shaking. Since, this is a stress based procedure and pore pressure generation depends on strains rather than stresses thus this method cannot capture the pore pressure generated in the soil profile during earthquake shaking.

Post liquefaction settlement for dry/saturated sandy deposit can be assessed from two methods namely, Tokimatsu and Seed (1987) and Ishihara and Yoshemine (1992). Cetin et. al. (2009) found that the former method underestimates the settlement while the latter overestimates the same. Hence they incorporated a factor of 1.45 and 0.9 to the respective methods. They also found out a cutoff depth of 18m in the sandy deposit below which any volumetric strain will not cause any surficial settlement.

CHAPTER 3

METHODOLOGY

3.1.LINEAR GROUND RESPONSE ANALYSIS FOR A UNIFORM SOIL LAYER USING DEEPSOIL

An analysis has been done in DEEPSOIL considering a 20m deep soil column as a single layer with a uniform shear wave velocity of 200 m/s as shown in figure 3.1. So, the natural frequency of the soil column is observed to be $f_n = \frac{V_s}{4H} = \frac{200}{4*20} = 2.5$ Hz. The following cases are now performed:

1. Soil is undamped ($\xi = 0$) with rigid bedrock
2. Soil is damped ($\xi = 5\%, 10\%$ &20%) with rigid bedrock
3. Soil is undamped with elastic bedrock (Impedance ratio = 0.1 & 0.5)

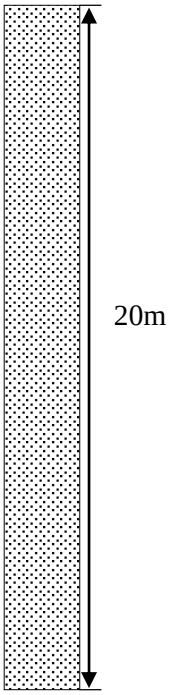

Figure 3.1: Homogeneous, uniform sand column

To introduce impedance in the model, elastic bedrock should be chosen with proper shear wave velocity and unit weight. DEEPSOIL states damping in bedrock has no effect on transfer function.

Impedance ratio is defined as $(\alpha_z) = \frac{\gamma_s V_s}{\gamma_r V_r}$ where γ_s and γ_r are the unit weights of soil and bedrock respectively and V_s and V_r are the soil and bedrock shear wave velocities respectively. If γ_r = 25 kN/m^3, then for α_z = 0.1 and 0.5, V_r should be chosen as 1600 m/s and 320 m/s respectively.

The results as obtained from DEEPSOIL analysis are presented in figures 3.2 (a)-(c) as Fourier Amplitude Ratio (FAR) vs frequency. Manual calculation has also been done for the transfer function using equations 2.1 to 2.3 and the variation with frequency are presented in figures 3.3 (a)-(c).

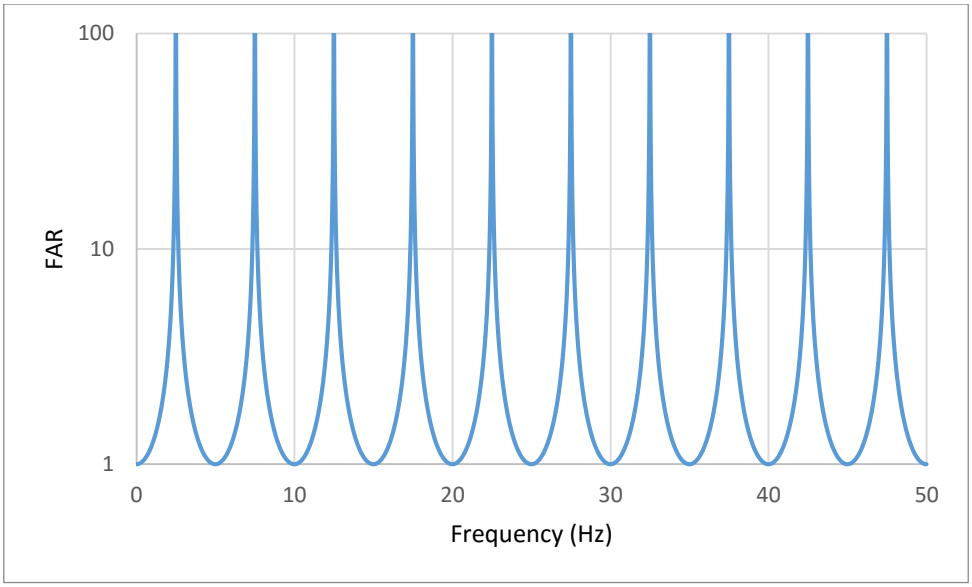

Figure 3.2 (a): FAR for Undamped Soil Underlain by Rigid Bedrock from DEEPSOIL software

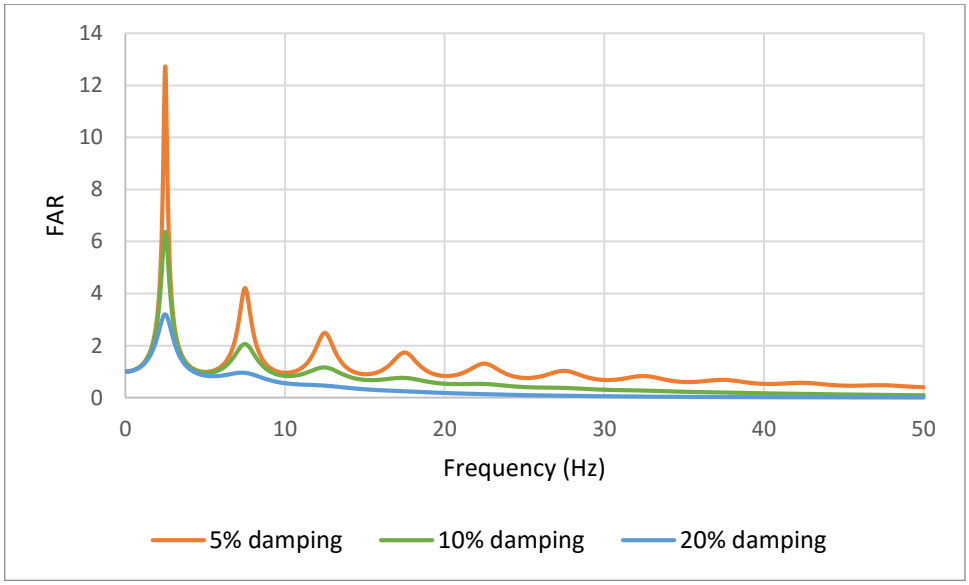

Figure 3.2 (b): FAR for Damped Soil Underlain by Rigid Bedrock

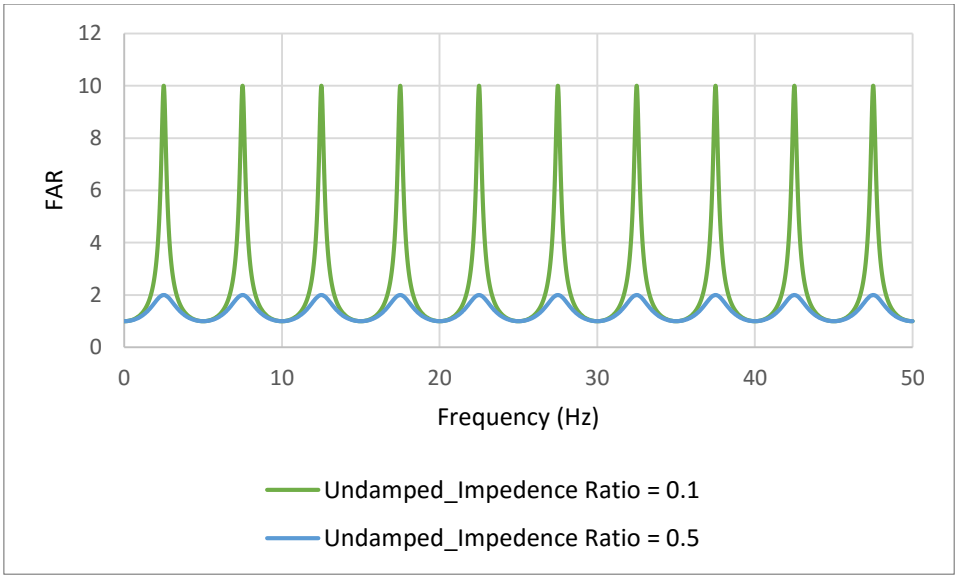

Figure 3.2 (c): FAR for Undamped Soil Underlain by Elastic Bedrock

The results obtained from equations 2.1 to 2.3 are presented as follows:

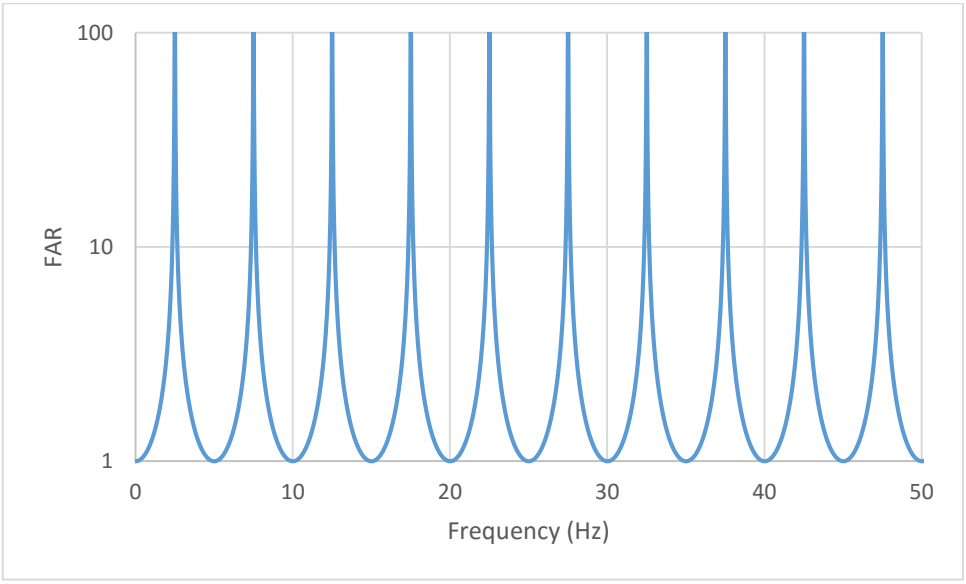

Figure 3.3 (a): FAR for Undamped Soil Underlain by Rigid Bedrock from equation (2.1)

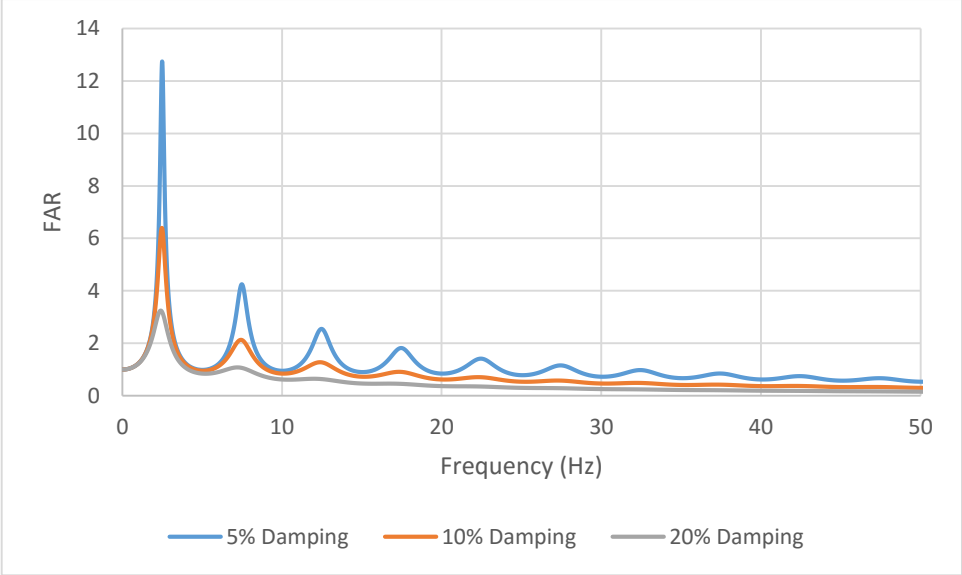

Figure 3.3 (b): FAR for Damped Soil Underlain by Rigid Bedrock from equation (2.2)

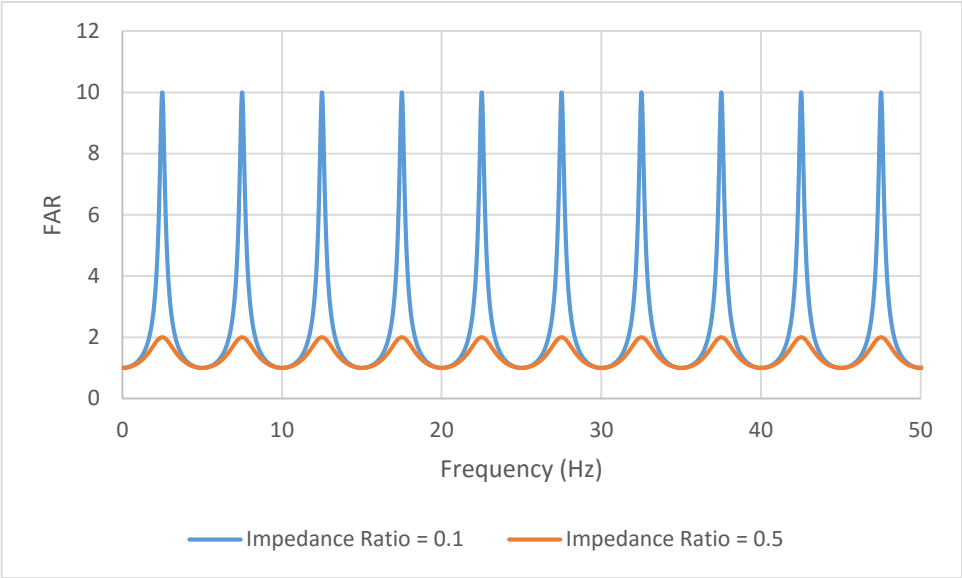

Figure 3.3 (c): FAR for Undamped Soil Underlain by Elastic Bedrock from equation (2.3)

From these figures it may be observed that variation of FAR with the frequency for both the cases are same. Thus, the software DEEPSOIL can be used with confidence for ground response analysis problems.

3.2. ANALYSIS USING DEEPSOIL FOR NORMAL KOLKATA SOIL DEPOSIT

3.2.1. SOIL PROFILE

The subsoil profile at the site at CIT Road, Kolkata as reported by Roy and Sahu (2012) has been used in the present study. The stratification and properties of different layers are presented in Table 3.1.

Table 3.1. Soil Profile and Properties for Normal Kolkata Deposit

Depth (m)	Soil description	Unit weight (kN/m^3)	$\bar{N}$ value	LL (%)	PL (%)
1.5	Fill	17	2	53	25
3	Soft brownish clayey silt	18.5	5	53	25
12.5	Soft dark grey/ grey silty clay with decayed vegetation & organic matter	17.5	3	56	20
16.5	Stiff bluish grey silty clay with kankar	20.9	12	62	18
18.5	Stiff to very stiff molted brown clayey silt with sand	20.8	16	35	18
25.5	Dense to very dense yellowish/ brownish silty sand	20	47		
30	Very stiff to hard molted grey clayey silt to silty clay with sand	20.5	29	50	29

It may be noted that for analysis in DEEPSOIL software the soil column has been divided into 26 sublayers so that shear wave of maximum frequency can be maintained. The SPT-N values have been varied gradually from the $\bar{N}$ values for each layers. Then N-values have been corrected to $(N_1)_{60}$ by

applying overburden correction factor (C_N), hammer energy correction factor (C_E), borehole diameter correction factor (C_B), rod length correction factor (C_R) and correction factor for sampler (C_S).

$$(N_1)_{60} = C_N * C_E * C_B * C_R * C_S * N \tag{3.1}$$

The values for C_E, C_B, C_R and C_s are taken as 1, 1.05, 0.95 and 1 respectively (Nath, 2011; Skempton, 1986; Robertson and Wride, 1998; Youd et al., 2001). C_N can be calculated as (Liao and Whitman, 1986):

$$C_N = \left(\frac{P_a}{\sigma_0'}\right)^{0.5} \tag{3.2}$$

where P_a is the atmospheric pressure (= 100 kPa); and σ_0' is the effective overburden pressure.
The uncorrected SPT profile and corrected SPT $[(N_1)_{60}]$ profiles have been shown in the figure 3.4:

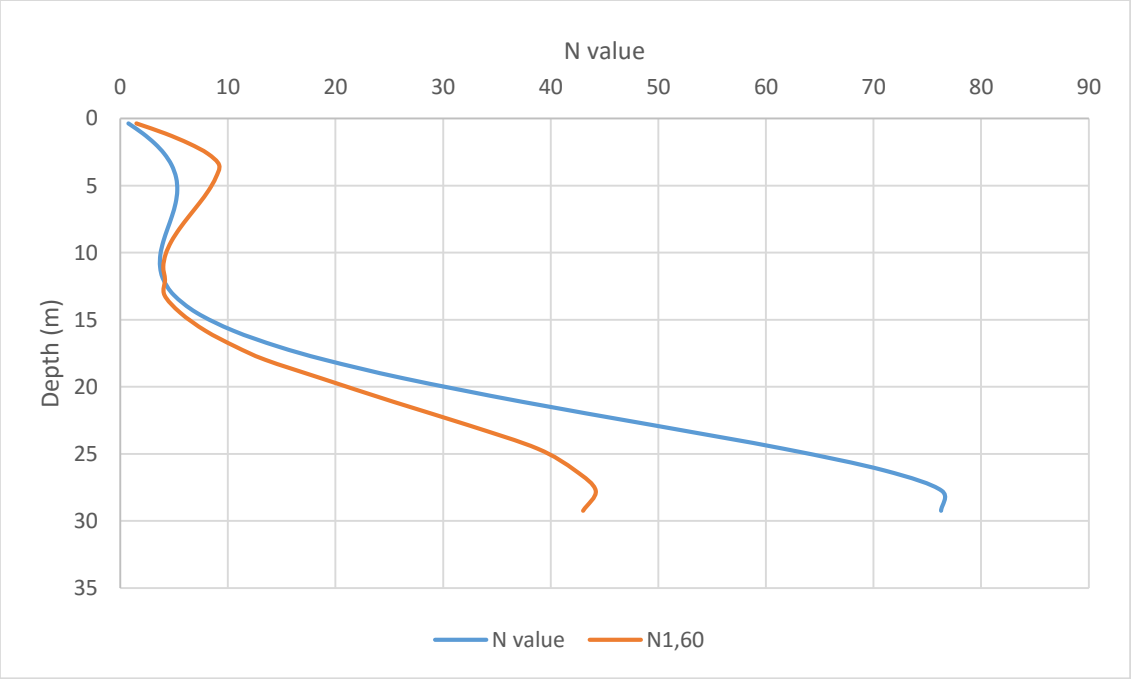

Figure 3.4: SPT Profile for Normal Kolkata Soil Deposit

3.2.2.PREDICTION OF SHEAR WAVE VELOCITIES FROM SPT-N VALUES

The shear wave velocities (Vs) for different layers have been predicted from uncorrected N values and corrected N values i.e. $[(N_1)_{60}]$ with different correlations given by various researchers. The correlations are given in section 2.5 of Chapter 2. These are presented in Table 3.2 (a)-(b).

Table 3.2. (a) Various SPT-Shear wave relationships

Layer No.	Depth (m)	N value	$[(N_1)_{60}]$	Maheswari et. al. (2010)	Anbazhagan et. al. (2012)	Choudhury and Chatterjee (2013) (Uncorrected SPT value)	Choudhury and Chatterjee (2013) (Corrected SPT value)
1	0.375	0.750803	1.497852	80.60062643	95.35304598	68.95501618	90.9787174
2	1.125	2.09272	4.174977	116.3361534	142.2187241	102.8461579	134.3105619
3	1.875	3.203128	6.39024	135.4863886	167.9010308	121.4184421	157.8912706
4	2.625	4.070745	8.121136	147.6261657	184.3538553	133.3163817	172.9481756
5	3.475	4.761366	9.187638	156.1449632	195.9723085	141.7183223	181.2504428
6	4.425	5.18592	8.867861	160.9932701	202.6102754	146.5186002	178.8268734
7	5.375	5.288065	8.204597	162.1213926	204.1574072	147.637416	173.6214432
8	6.325	5.132853	7.34139	160.4015475	201.7991611	145.932039	166.4398686
9	7.275	4.801466	6.403347	156.6144814	196.6143441	142.1826134	158.0142622
10	8.225	4.387495	5.502986	151.6399547	189.8208432	137.2698604	149.1725818
11	9.175	3.993234	4.742108	146.613628	182.9768099	132.3205647	140.9713139
12	10.125	3.725958	4.212018	143.0221469	178.0993066	128.7933746	134.7621371
13	11.075	3.694217	3.993008	142.5847557	177.5060384	128.3643498	132.0552571
14	12.025	4.004113	4.153493	146.7564975	183.1710603	132.4610378	134.0475026
15	13.165	4.967021	4.100461	158.5267099	199.2309643	144.074835	133.3945299
16	14.495	7.096306	5.583035	180.1232016	228.971807	165.5820692	149.9934637
17	15.83	10.50395	7.907864	207.2737429	266.8129411	192.9470683	171.2080177
18	17	14.63122	10.67751	233.3837012	303.6259034	219.5685399	191.9023351
19	18	19.02168	13.49046	256.3723506	336.3461563	243.230349	209.7354026
20	19.375	26.30078	18.67126	239.1042953	375.4589507	310.1147492	251.1224562
21	21.125	37.3262	25.37706	262.3489592	456.7807068	373.3415767	293.6649101
22	22.875	49.54463	32.36993	282.7937274	535.2763899	433.7976656	332.4752615
23	24.625	61.61815	38.80131	299.6183987	604.8070758	486.9502838	364.6688329
24	26.25	71.01415	42.28675	410.8483539	562.2169138	406.5698792	323.7570447
25	27.75	76.3108	44.19555	421.566303	578.2131469	418.1376325	329.2346012
26	29.25	76.26183	43.01979	421.4694241	578.0683937	418.0329536	325.8783994

Table 3.2. (b) Various SPT-Shear wave relationships

Layer No.	Depth (m)	N value	$[(N_1)_{60}]$	Nath et. al. (2016) (Simplified)	Nath et. al. (2016) (Depth and lithology specific)
1	0.375	0.750803	1.497852	110.8280392	83.5513688
2	1.125	2.09272	4.174977	151.9730834	109.9559336
3	1.875	3.203128	6.39024	173.2624655	140.0055751
4	2.625	4.070745	8.121136	186.537942	150.8630138
5	3.475	4.761366	9.187638	193.7635142	192.720184
6	4.425	5.18592	8.867861	191.6608581	190.7774753
7	5.375	5.288065	8.204597	187.126306	186.5826553
8	6.325	5.132853	7.34139	180.8276884	180.7438347
9	7.275	4.801466	6.403347	173.3718504	173.8134234
10	8.225	4.387495	5.502986	165.4662881	166.441662
11	9.175	3.993234	4.742108	158.0536063	159.5066238
12	10.125	3.725958	4.212018	152.3870979	154.1896057
13	11.075	3.694217	3.993008	149.9013979	151.8527853
14	12.025	4.004113	4.153493	151.7317831	153.5738067
15	13.165	4.967021	4.100461	151.1324328	173.4911317
16	14.495	7.096306	5.583035	166.2039246	189.8173281
17	15.83	10.50395	7.907864	185.0152137	210.0836664
18	17	14.63122	10.67751	202.942971	224.8988799
19	18	19.02168	13.49046	218.0988763	251.625553
20	19.375	26.30078	18.67126	235.5090614	219.2140261
21	21.125	37.3262	25.37706	262.8557266	252.1999548
22	22.875	49.54463	32.36993	286.7861936	281.8571236
23	24.625	61.61815	38.80131	306.0091848	306.1831208
24	26.25	71.01415	42.28675	310.0816916	341.1249974
25	27.75	76.3108	44.19555	314.327094	347.965543
26	29.25	76.26183	43.01979	311.7274585	343.7717133

Variation of shear wave velocity with depth as obtained using various correlations are provided in figure 3.5.

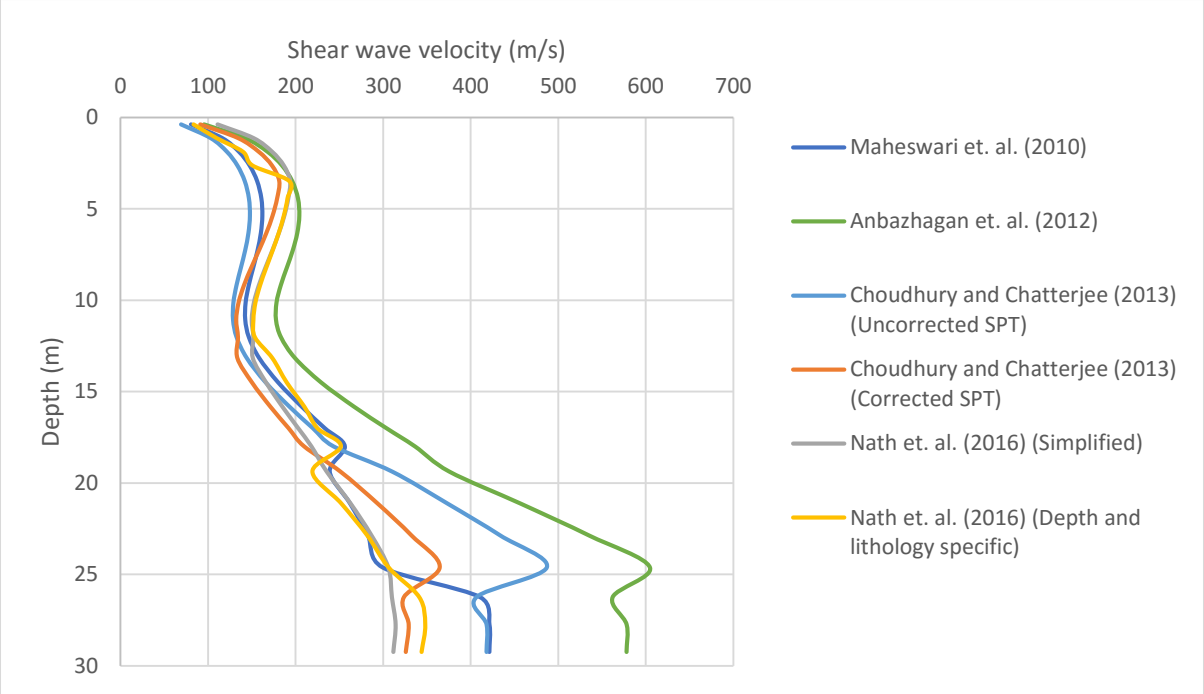

Figure 3.5: Shear wave velocity profile given by different researchers

The shear wave velocities from various correlations are observed to be around 150-200 m/s above 15m depth. After that depth, these increase and around 30m depth, they range from 300 m/s to 600 m/s.

3.2.3.SITE CLASSIFICATION USING IS:1893-2002, NEHRP (2003) AND IBC (2009):

The 30m average uncorrected SPT value $(N)_{30}$ and corrected SPT value $[(N_1)_{60}]_{30}$ are coming out to be 6.165 and 7.843 respectively and the 30m average shear wave velocity $V_{s,30}$ measured with different correlations is coming out to be in the range of 186.88m/s to 254.76m/s. Site classification according to NEHRP (2003) and IBC (2009) are presented in Table 3.3

Table 3.3. Site Classification of Normal Kolkata Deposit according to NEHRP (2003) and IBC (2009)

N-Vs correlations	$(N)_{30}$	$[(N_1)_{60}]_{30}$	Site Classification		$V_{s,30}$	Site Classification	
			NEHRP (2003)	IBC (2009)		NEHRP (2003)	IBC (2009)
Maheswari et. al. (2010)	6.165	7.842	E	E	192.4	D	D
Anbazhagan et. al. (2012)	6.165	7.842	E	E	254.8	D	D

Choudhury and Chatterjee (2013) (Uncorrected SPT value)	6.165	7.842	E	E	186.9	D	D
Choudhury and Chatterjee (2013) (Corrected SPT value)	6.165	7.842	E	E	189.3	D	D
Nath et. al. (2016) (Simplified)	6.165	7.842	E	E	199.7	D	D
Nath et. al. (2016) (Depth and lithology specific)	6.165	7.842	E	E	198	D	D

According to NEHRP (2003) and IBC (2009), the Normal Kolkata Deposit is classified as site class 'E' with respect to $[(N_1)_{60}]_{30}$ and site class 'D' with respect to $V_{s,30}$ prescribed by all the above researchers. Hence NEHRP (2003) and IBC (2009) classification becomes unreliable in this case. According to IS:1893 (Part 1) - 2002, Kolkata is divided among earthquake Zone 3 and Zone 4. The place CIT road which is selected for Normal Kolkata Deposit site is assumed to be situated in **Zone 3**. The soil type is **Soft soil** with respect to $[(N_1)_{60}]_{30}$ according to IS Code of practice.

3.2.4.SELECTION OF MODULUS REDUCTION AND DAMPING CURVES

The modulus reduction and damping curves are generated for each layer from the methods prescribed by Ishibashi and Zhang (1993). These curves are sensitive to confinement and plasticity of the soil. The curves are then fitted with MRDF-UIUC method implemented in DEEPSOIL (Hashash and Phillips, 2008). The fitted curves are shown in figures 3.6 (a) and (b).

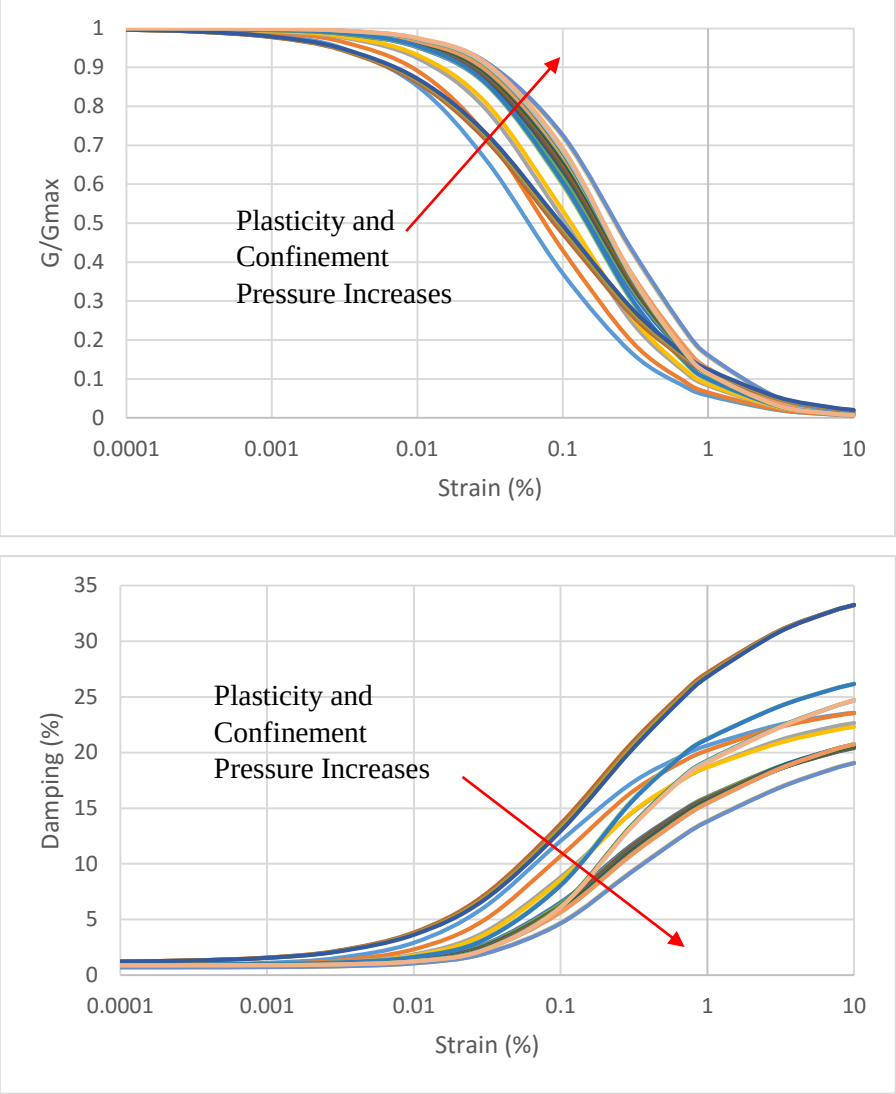

Figure 3.6 (a), (b): Modulus Reduction and Damping Curves for each Layer

3.2.5.SELECTION OF INPUT GROUND MOTION

Table 3.4. Selected Earthquake Strong Motion

Earthquake	San Fernando	Northridge-01
Year	1971	1994
Recording Station	LA - Hollywood Stor FF	Hollywood - Willoughby Ave
Moment Magnitude	6.61	6.69
PGA (g)	0.225	0.136
Significant Duration (s)	13.14	15.45
Distance to rupture (km)	22.77	23.07
Mechanism	Reverse	Reverse

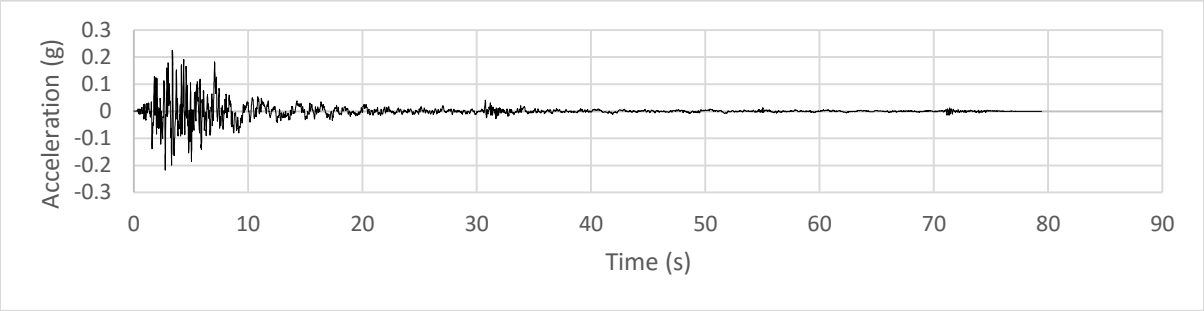

Figure 3.7: Original San Fernando Earthquake Acceleration Time History

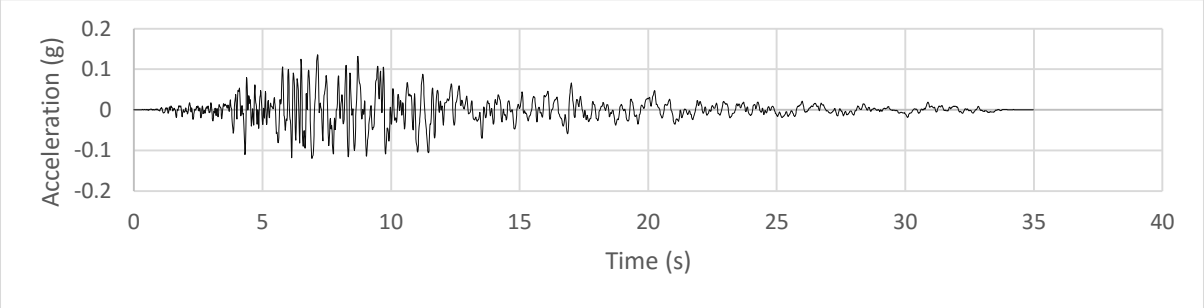

Figure 3.8: Original Northridge Earthquake Acceleration Time History

The selected earthquakes are used as seed earthquakes to synthesize new earthquakes which are spectrally compatible with IS:1893-Zone 3, Soft Soil Response Spectra using wavelet-based target spectra matching software named WAVGEN (Mukherjee and Gupta, 2002).

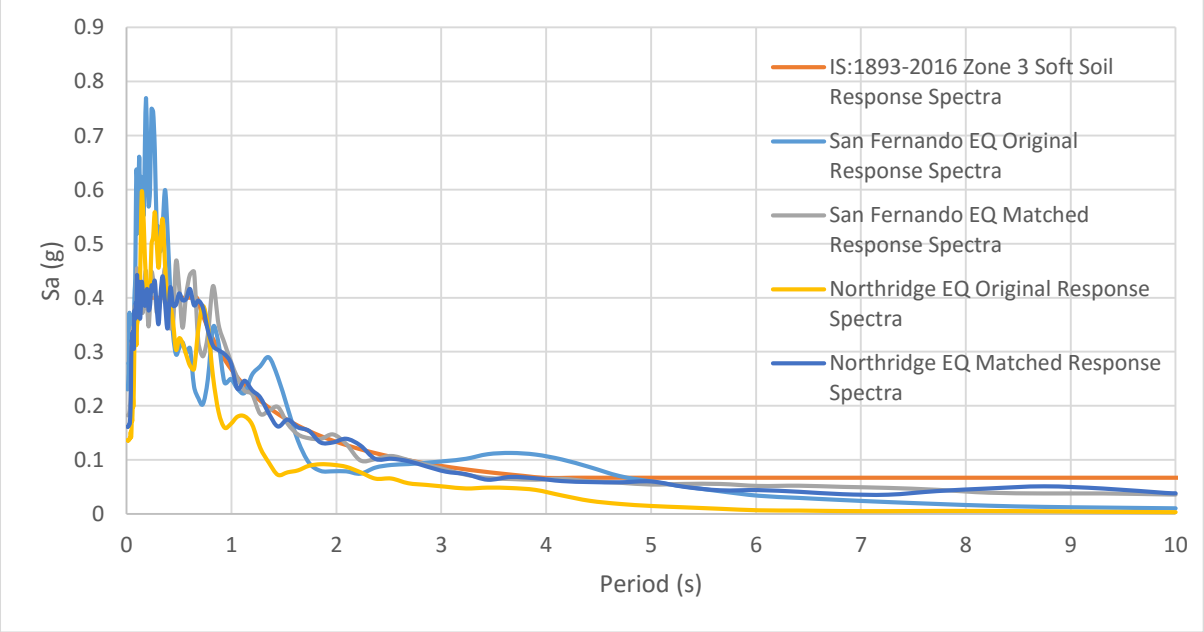

Figure 3.9: Spectrum Compatibility of Selected Earthquakes with IS: 1893 (Part 1) - 2016 Zone 3 Soft Soil Response Spectrum

The synthesized earthquakes are thus shown below in terms of acceleration time history in figures 3.10 and 3.11.

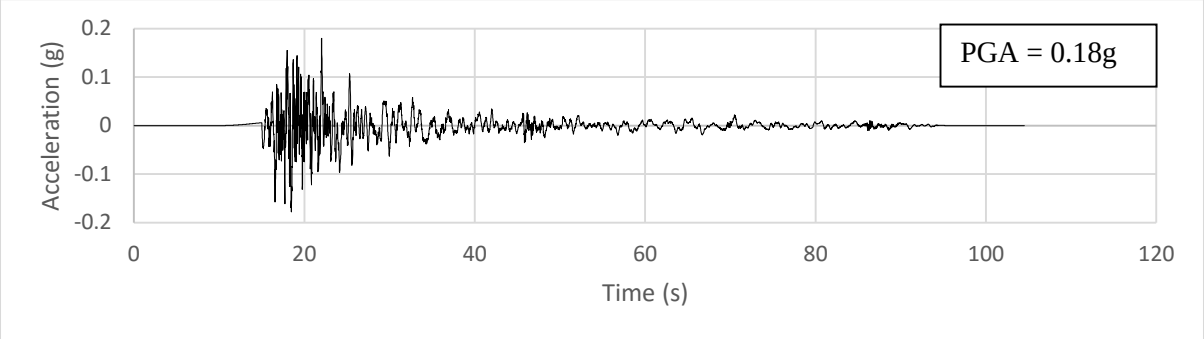

Figure 3.10: Matched San Fernando Earthquake Acceleration Time History

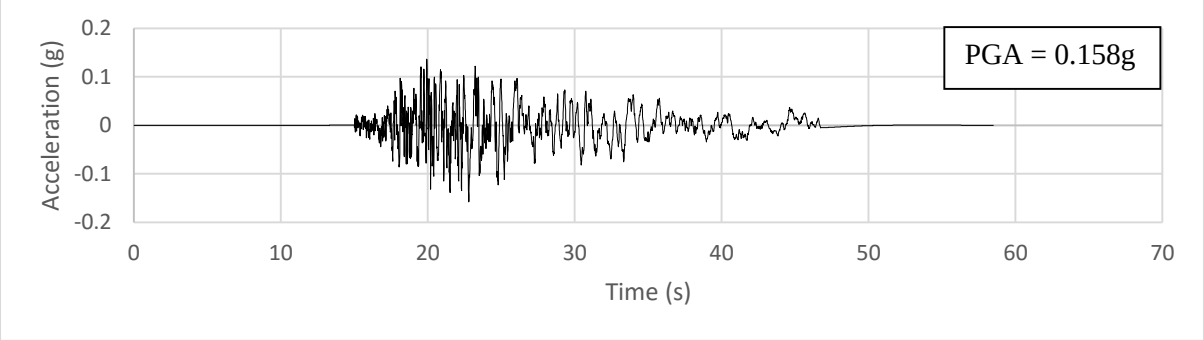

Figure 3.11: Matched Northridge Earthquake Acceleration Time History

3.2.6.ANALYSIS

The inputs for various N-Vs correlations given by Maheswari et. al. (2010), Anbazhagan et. al. (2012), Choudhury and Chatterjee (2013) (Uncorrected SPT values), Choudhury and Chatterjee (2013) (corrected SPT values), Nath et. al. (2016) (simplified) and Nath et. al. (2016) (depth and lithology specific) are given as input in the software DEEPSOIL. Elastic Bedrock with unit weight 25 kN/m^3 and shear wave velocity 2000 m/s are given as input. Full Rayleigh Damping is formulated by targeting two frequencies (PEER Report, 2008). The 1st target frequency is the natural frequency of soil. The 2nd target frequency is the 5 times the natural frequency of the soil.

3.3. ANALYSIS USING DEEPSOIL FOR RIVER CHANNEL SOIL DEPOSIT

3.3.1. SOIL PROFILE

The subsoil profile at the site at Alipore Road, Kolkata as reported by Roy and Sahu (2012) has been used in the present study. The stratification and properties of different layers are presented in Table 3.5.

Table 3.5. Soil Profile for River Channel Deposit

Depth (m)	Soil description	Unit weight (kN/m^3)	$\bar{N}$ value	LL (%)	PL (%)
2	Fill	17	5		
6	Loose brownish grey sandy silt	18	11		
27	Dense to very dense bluish grey silty sand	19.5	42		
30	Very dense grey fine to medium sand	20	50		

It may be noted that for analysis in DEEPSOIL software the soil layers have been divided into 17 sublayers so that shear wave of maximum frequency can be maintained. The SPT-N values have been varied gradually from the $\bar{N}$ values for each layers. The N-values have been corrected to $(N_1)_{60}$ by applying overburden correction factor (C_N), hammer energy correction factor (C_E), borehole diameter correction factor (C_B), rod length correction factor (C_R) and correction factor for sampler (C_S).

$$(N_1)_{60} = C_N * C_E * C_B * C_R * C_S * N \tag{3.3}$$

The values for C_E, C_B, C_R and C_s are taken as 1, 1.05, 0.95 and 1 respectively (Nath, 2011; Skempton, 1986; Robertson and Wride, 1998; Youd et al., 2001). C_N can be calculated as (Liao and Whitman, 1986):

$$C_N = \left(\frac{P_a}{\sigma_0'}\right)^{0.5} \tag{3.4}$$

where P_a is the atmospheric pressure (= 100 kPa); and σ_0' is the effective overburden pressure.

The uncorrected SPT profile and corrected SPT $[(N_1)_{60}]$ profiles have been shown in the figure 3.12:

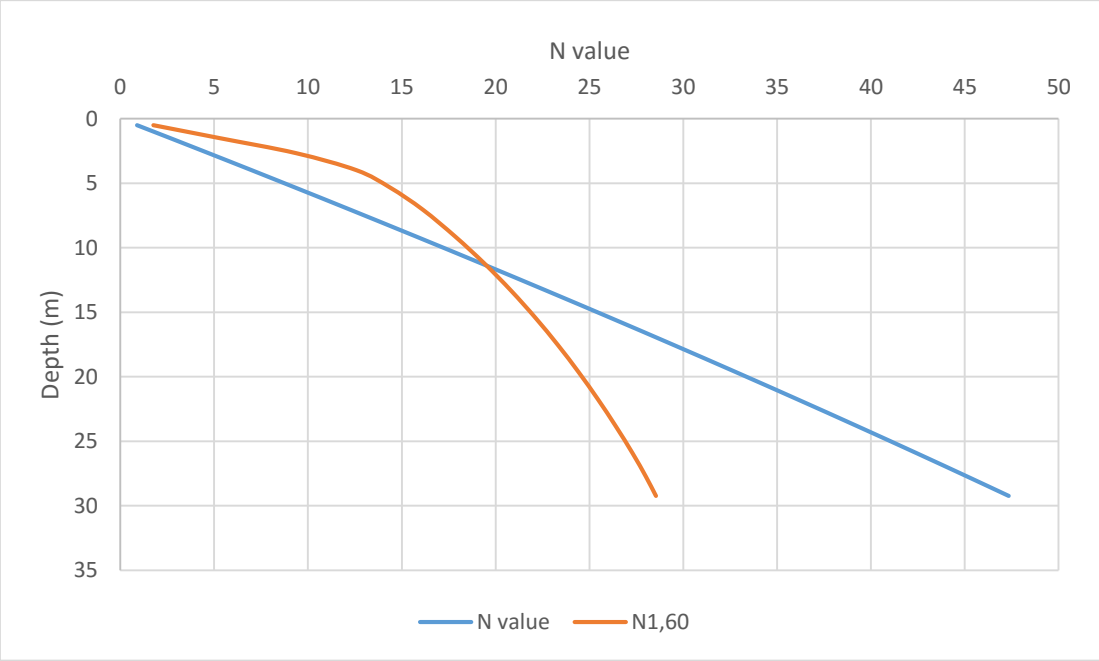

Figure 3.12: SPT Profile for River Channel Soil Deposit

3.3.2. PREDICTION OF SHEAR WAVE VELOCITIES FROM SPT-N VALUES

The shear wave velocities (Vs) for different layers have been predicted from uncorrected N values and corrected N values i.e. $[(N_1)_{60}]$ with different correlations given by various researchers. The correlations are given in section 2.5 of Chapter 2. These are presented in Table 3.6 (a)-(b).

Table 3.6 (a). Various SPT-Shear wave relationships

Layer No.	Depth (m)	N value	$[(N_1)_{60}]$	Jafari et. al. (2002)	Hanumantharao and Ramana (2008)	Maheswari et. al. (2010)	Anbazhagan et. al. (2012)	Choudhury and Chatterjee (2013) (Uncorrected SPT value)
1	0.5	0.885375	1.766323	20.03137065	81.71313977	97.33844524	56.20452401	51.39447999
2	1.5	2.648175	5.283109	46.56843311	129.4601355	130.1297373	103.8078397	91.85457082
3	2.6650411	4.688541	9.353639	72.29724111	164.5637947	151.3981883	142.9424213	124.3337471
4	3.9951234	7.000359	12.59198	98.43857082	194.7372221	168.3652881	178.9152546	153.7633322
5	5.3300823	9.301796	14.36911	122.5234252	219.4302581	181.5373071	209.7864474	178.7637448

6	7.0499848	12.23902	16.11798	151.3518106	246.2362876	195.2308978	244.6347509	206.7496433
7	9.1499543	15.7828	17.8559	184.0875801	273.9906868	208.8403857	282.0740568	236.5792438
8	11.249924	19.27984	19.41662	214.7594907	298.0176018	220.2156129	315.5280431	263.0533755
9	13.349893	22.73014	20.83108	243.7845941	319.3532285	230.0356916	346.0008437	287.0371545
10	15.449863	26.13369	22.124	271.435843	338.6278958	238.7007918	374.1212578	309.0689562
11	17.549832	29.49049	23.31424	297.9050186	356.2582174	246.4684944	400.3150617	329.5114349
12	19.649802	32.80055	24.41634	323.3338361	372.5362409	253.515305	424.8870036	348.6229976
13	21.749771	36.06387	25.44148	347.8310419	387.6759051	259.9679665	448.0644514	366.5956779
14	23.849741	39.28044	26.39871	371.4825675	401.8393854	265.9208586	470.0226041	383.5769264
15	25.94971	42.45026	27.29523	394.3579286	415.1530307	271.4463363	490.8999939	399.6829617
16	27.749619	45.12996	27.99954	413.3906557	425.964798	275.885504	508.0194696	412.8624918
17	29.249467	47.33669	28.53649	428.8693812	434.5918292	279.3978876	521.7840736	423.4419711

Table 3.6 (b). Various SPT-Shear wave relationships

Layer No.	Depth (m)	N value	$[(N_1)_{60}]$	Choudhury and Chatterjee (2013) (Corrected SPT value)	Nath et. al. (2016) (Simplified)	Nath et. al. (2016) (Depth and lithology specific)
1	0.5	0.885375	1.766323	75.43845477	101.2461649	87.32438396
2	1.5	2.648175	5.283109	131.9048279	149.8724946	117.1136603
3	2.6650411	4.688541	9.353639	176.517237	183.8817075	140.2591036
4	3.9951234	7.000359	12.59198	205.4163005	204.531917	150.8474575
5	5.3300823	9.301796	14.36911	219.7233262	214.43087	155.8022768
6	7.0499848	12.23902	16.11798	232.9782679	223.431634	206.8826389
7	9.1499543	15.7828	17.8559	245.4684788	231.7743417	215.5167147
8	11.249924	19.27984	19.41662	256.1860994	238.8326124	222.8495952
9	13.349893	22.73014	20.83108	265.5400138	244.9211307	229.1951339
10	15.449863	26.13369	22.124	273.8214704	250.2584066	234.7727183
11	17.549832	29.49049	23.31424	281.2379318	254.9974931	242.619478
12	19.649802	32.80055	24.41634	287.9413621	259.2489949	247.7927966
13	21.749771	36.06387	25.44148	294.0448954	263.0944315	252.4922263
14	23.849741	39.28044	26.39871	299.6361397	266.5962772	256.7882909
15	25.94971	42.45026	27.29523	304.7833854	269.8028615	260.7358169
16	27.749619	45.12996	27.99954	308.7691974	272.2748276	269.1224506

17	29.249467	47.33669	28.53649	311.7750224	274.1327271	271.2024039

Variation of shear wave velocity with depth as obtained using various correlations are provided in figure 3.13.

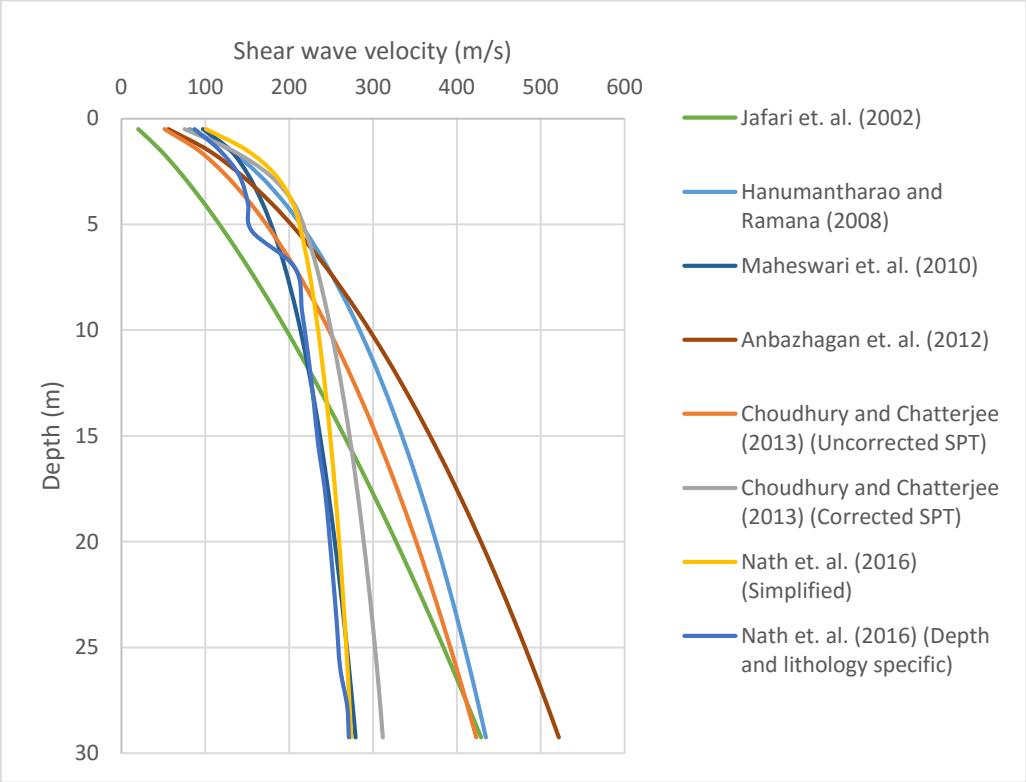

Figure 3.13: Shear wave velocity profile given by different researchers

The shear wave velocity varies from 100 m/s at just below the surface to 300-500m/s at around 30m depth.

3.3.3.SITE CLASSIFICATION USING IS:1893-2002, NEHRP (2003) AND IBC (2009)

The 30m average uncorrected SPT value $(N)_{30}$ and corrected SPT value $[(N_1)_{60}]_{30}$ are coming out to be 9.764 and 13.83 respectively and the 30m average shear wave velocity $V_{s,30}$ measured with different correlations is coming out to be in the range of 203.943m/s to 269.78m/s except for the case of correlation given Jafari et. al. (2002) where $V_{s,30}$ is coming out to be 147.538m/s. Site classification according to NEHRP (2003) and IBC (2009) are presented in Table 3.7

Table 3.7. Site Classification of River Channel Deposit according to NEHRP (2003) and IBC (2009)

N-Vs correlations	$(N)_{30}$	$[(N_1)_{60}]_{30}$	Site Classification		$V_{s,30}$	Site Classification	
			NEHRP (2003)	IBC (2009)		NEHRP (2003)	IBC (2009)
Jafari et. al. (2002)	9.764	13.83	E	E	147.54	E	E
Hanumantharao and Ramana (2008)	9.764	13.83	E	E	269.78	D	D
Maheswari et. al. (2010)	9.764	13.83	E	E	211.84	D	D
Anbazhagan et. al. (2012)	9.764	13.83	E	E	262.32	D	D
Choudhury and Chatterjee (2013) (Uncorrected SPT value)	9.764	13.83	E	E	223.31	D	D
Choudhury and Chatterjee (2013) (Corrected SPT value)	9.764	13.83	E	E	234.82	D	D
Nath et. al. (2016) (Simplified)	9.764	13.83	E	E	227.77	D	D
Nath et. al. (2016) (Depth and lithology specific)	9.764	13.83	E	E	203.94	D	D

According to NEHRP (2003) and IBC (2009), the River Channel Deposit is classified as site class 'E' with respect to $[(N_1)_{60}]_{30}$ and site class 'D' with respect to $V_{s,30}$ prescribed by all the above researchers except Jafari et. al. (2002). Hence NEHRP (2003) and IBC (2009) classification becomes unreliable in

this case. According to IS:1893 (Part 1)-2002, Kolkata is divided among earthquake Zone 3 and Zone 4. The place Alipore Road which is selected for River Channel Deposit site is assumed to be situated in Zone 4. The soil type is Medium to dense soil with respect to $[(N_1)_{60}]_{30}$ according to IS Code of practice.

3.3.4.SELECTION OF MODULUS REDUCTION AND DAMPING CURVES

The modulus reduction and damping curves are generated for each layer from the methods prescribed by Ishibashi and Zhang (1993). These curves are sensitive to confinement and plasticity of the soil. The curves are then fitted with MRDF-UIUC method implemented in DEEPSOIL (Hashash and Phillips, 2008). The fitted curves are shown below:

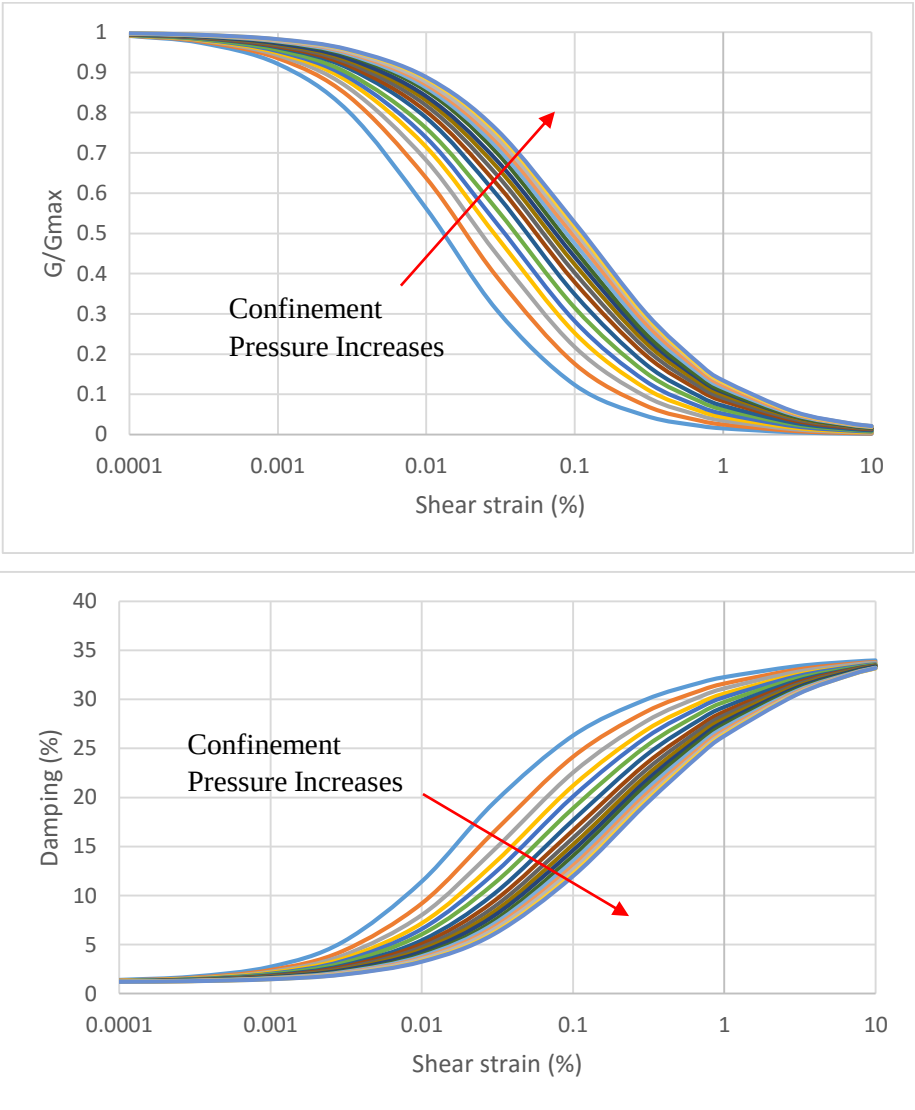

Figure 3.14 (a), (b): Modulus Reduction Damping Curves for each Layer

3.3.5.SELECTION OF INPUT GROUND MOTION

Table 3.8. Selected Earthquake Strong Motion

Earthquake	San Fernando	Northridge-01
Year	1971	1994
Recording Station	LA - Hollywood Stor FF	Hollywood - Willoughby Ave
Moment Magnitude	6.61	6.69
PGA (g)	0.225	0.136
Significant Duration (s)	13.14	15.45
Distance to rupture (km)	22.77	23.07
Mechanism	Reverse	Reverse

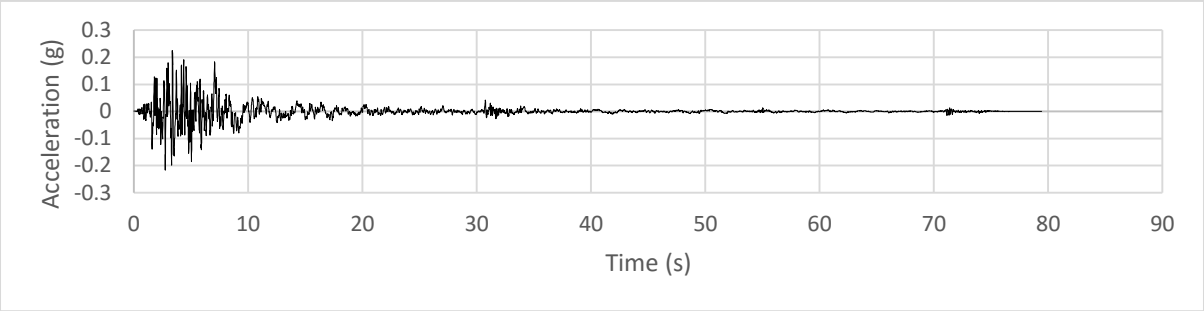

Figure 3.15: Original San Fernando Earthquake Acceleration Time History

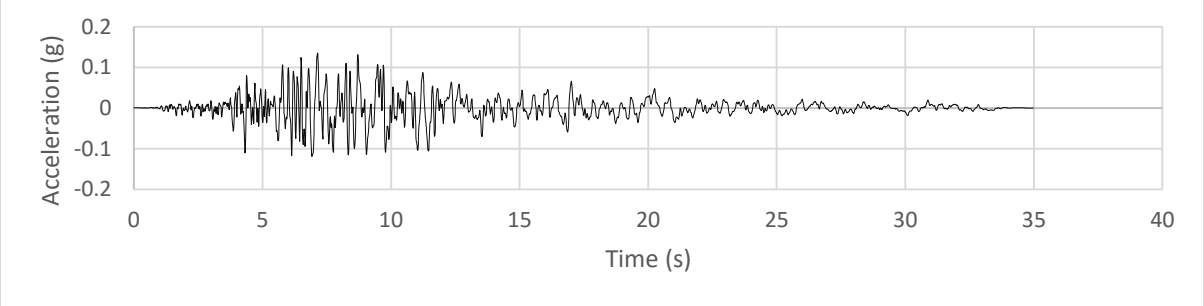

Figure 3.16: Original Northridge Earthquake Acceleration Time History

The selected earthquakes are used as seed earthquakes to synthesize new earthquakes which are spectrally compatible with IS:1893-Zone 4, Medium Dense Soil Response Spectra using wavelet-based target spectra matching software named WAVGEN (Mukherjee and Gupta, 2002).

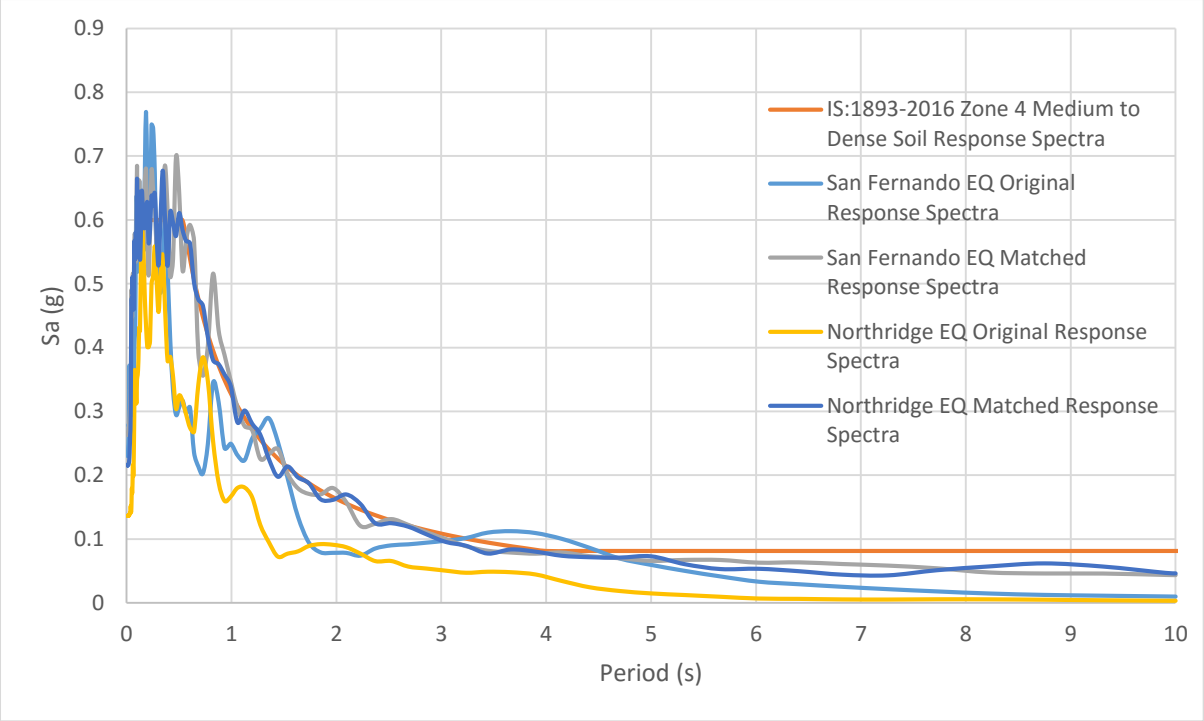

Figure 3.17: Spectrum Compatibility of Selected Earthquakes with IS: 1893 (Part 1)-2016 Zone 4 Medium Dense Soil Response Spectrum

The synthesized earthquakes are thus shown below in terms of acceleration time history:

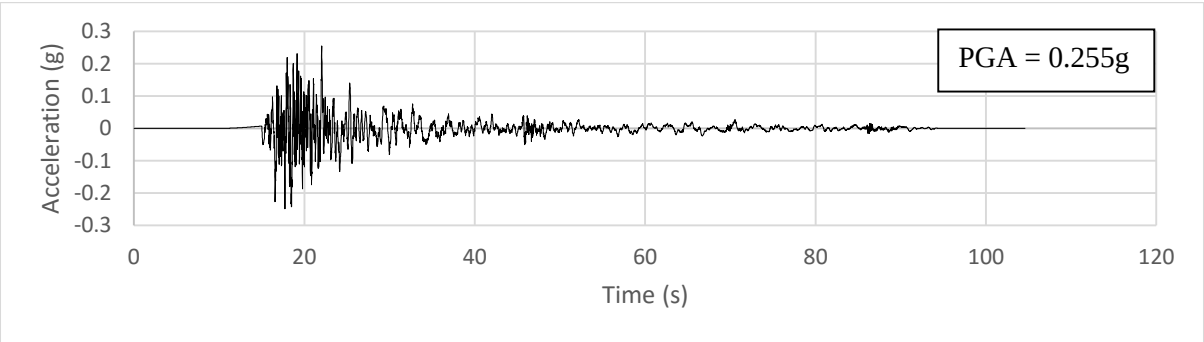

Figure 3.18: Matched San Fernando Earthquake Acceleration Time History

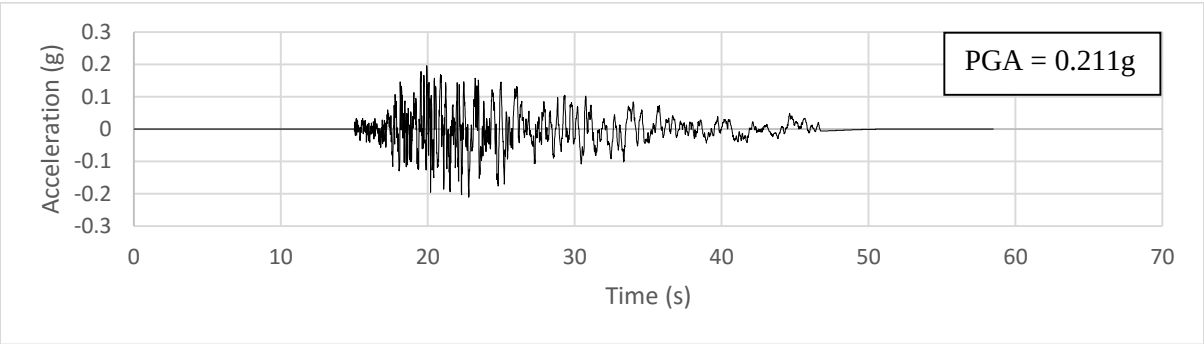

Figure 3.19: Matched Northridge Earthquake Acceleration Time History

3.3.6.ANALYSIS

The inputs for various N-Vs correlations given by Jafari et. al. (2002), Hanumanthrao and Ramana (2008), Maheswari et. al. (2010), Anbazhagan et. al. (2012), Choudhury and Chatterjee (2013) (Uncorrected SPT values), Choudhury and Chatterjee (2013) (corrected SPT values), Nath et. al. (2016) (simplified) and Nath et. al. (2016) (depth and lithology specific) are given as input in the software DEEPSOIL. Elastic Bedrock with unit weight 25 kN/m^3 and shear wave velocity 2000 m/s are given as input. Full Rayleigh Damping is formulated by targeting two frequencies (PEER Report, 2008). The 1st target frequency is the natural frequency of soil. The 2nd target frequency is the 5 times the natural frequency of the soil.

3.4.ANALYSIS USING OPENSEES FOR NORMAL KOLKATA SOIL DEPOSIT

Soil model in OPENSEES includes a 3D soil column which is 30m tall and a square base of 1m by 1m. The column has been discretised into a number of elements for each layer. Figure 3.20 shows the 3D soil column modelled in OPENSEES.

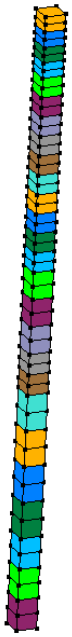

Figure 3.20: Soil Column Modelled in OPENSEES

The maximum dimension of any element is taken as one-fifth (Kuhlemeyer and Lysmer, 1973) of the shortest wavelength considered in the analysis. But since number of elements in that case would be too high to cause numerical instability, number of elements in each layer is considered as 2. Thus the total number of elements comes out to be 52. All the required input data for Normal Kolkata Deposit has been estimated and implemented into the model as given in Table 3.7 as per Pressure Independent Multi Yield Soil Model & Pressure Dependent Multi Yield Soil Model (section 2.8, Chapter 2). The input

parameters correspond to Choudhury and Chatterjee (2013) Uncorrected SPT-N and Vs correlation. The spectral matched time histories are given as input motion at the base of the soil column as shown in Figures (3.10) and (3.11). Boundary conditions that have been used for this model include a shear beam type boundary condition. The bedrock is elastic with unit weight of 2.5 t/m^3 and shear wave velocity of 2000 m/s. Type of element used in this analysis is 8-node Brick soil element. Rayleigh damping used in this analysis is full Rayleigh damping with two target frequencies. The 1st one is the natural frequency of the soil and the 2nd one is the five times the natural frequency of the soil. The maximum shear modulus has been calculated from the equation 3.5.

$$G_{max} = \rho V_s^2 \tag{3.5}$$

The other parameters such as B_{max}, C, ϕ, Dr, ϕPT, c1, c3, d1 and d3 have been estimated from Table 2.6 and 2.7 of Chapter 2. An arbitrary value of void ratio (e) has been assumed to be 0.67 for clay while for sand, it has been estimated from Table 2.6. Combined bulk modulus is estimated from Bulk modulus of water (2.2x10^6 kPa) normalised by porosity (OPENSEES Manual).

The soil parameters are provided in Table 3.9 (a)-(b).

Table 3.9 (a). Input Parameters of Normal Kolkata Soil in OPENSEES

Layer #	Layer Name	Thickness (m)	Density (t/m3)	ϕ (deg)	C (kPa)	Dr (%)	Gmax (kPa)	Bmax (kPa)
1	Clay	0.75	1.73	0	16.07		8225.794	41128.97
2	Clay	0.75	1.73	0	20.142		148298.78	91493.9
3	Clay	0.75	1.89	0	24		27863.21	139316.1
4	Clay	0.75	1.89	0	26.32		33591.46	167957.3
5	Clay	0.95	1.78	0	27.2		35749.67	178748.4
6	Clay	0.95	1.78	0	28.2		38212.51	191062.6
7	Clay	0.95	1.78	0	28.43		38798.32	193991.6
8	Clay	0.95	1.78	0	28.07		37907.16	189535.8
9	Clay	0.95	1.78	0	27.29		35984.29	179921.5
10	Clay	0.95	1.78	0	26.3		33540.57	167702.9
11	Clay	0.95	1.78	0	25.34		31165.54	155827.7
12	Clay	0.95	1.78	0	24.68		29526.17	147630.9
13	Clay	0.95	1.78	0	24.6		29329.78	146648.9
14	Clay	0.95	1.78	0	25.37		31231.75	156158.8

15	Clay	1.33	2.13	0	30.62		44213.6	221068
16	Clay	1.33	2.13	0	36.35		58399.11	291995.6
17	Clay	1.34	2.13	0	45.15		79296.86	396484.3
18	Clay	1	2.12	0	54.82		102205.9	511029.5
19	Clay	1	2.12	0	64.62		125421.3	627106.5
20	Sand	1.75	2.04	35.4	0	63.71004	168294.4	683377.26
21	Sand	1.75	2.04	36.5	0	74.27484	243920	990463.03
22	Sand	1.75	2.04	37.4	0	83.88649	329319.3	1337235.95
23	Sand	1.75	2.04	38	0	91.84262	414960.5	1684991.24
24	Clay	1.5	2.09	0	157.5		345475	1727375
25	Clay	1.5	2.09	0	165.95		365413.7	1827069
26	Clay	1.5	2.09	0	165.88		365230.7	1826154

Table 3.9 (b). Input Parameters of Normal Kolkata Soil in OPENSEES

Layer #	ϕPT (deg)	c1	c3	d1	d3	e	Combined Bulk Modulus (kPa)
1						0.67	5483582.09
2						0.67	5483582.09
3						0.67	5483582.09
4						0.67	5483582.09
5						0.67	5483582.09
6						0.67	5483582.09
7						0.67	5483582.09
8						0.67	5483582.09
9						0.67	5483582.09
10						0.67	5483582.09
11						0.67	5483582.09
12						0.67	5483582.09
13						0.67	5483582.09
14						0.67	5483582.09
15						0.67	5483582.09
16						0.67	5483582.09
17						0.67	5483582.09
18						0.67	5483582.09
19						0.67	5483582.09

20	26	0.024	0.037	0.153	0.037	0.62	5748387.097
21	26	0.013	0	0.3	0	0.55	6200000
22	26	0.004	0	0.42	0	0.49	6689795.918
23	26	0	0	0.5	0	0.45	7088888.889
24						0.67	5483582.09
25						0.67	5483582.09
26						0.67	5483582.09

3.5.ANALYSIS USING OPENSEES FOR RIVER CHANNEL SOIL DEPOSIT:

Soil model in OPENSEES includes a 3D soil column which is 30m tall and a square base of 1m by 1m. The column has been discretised into a number of elements for each layer. Figure 3.21 shows the 3D soil column modelled in OPENSEES.

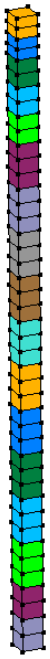

Figure 3.21: Soil Column Modelled in OPENSEES

The total number of elements considered in the soil profile is 44. All the required input data for River Channel Deposit has been estimated and implemented into the model as given in Table 3.8 as per Pressure Dependent Multi Yield Soil Model (Section 2.8, Chapter 2). The input parameters correspond to Choudhury and Chatterjee (2013) Uncorrected SPT-N and Vs correlation. The spectral compatible time histories are given as input motion at the base of the soil column as shown in figures (3.18) and (3.19). Boundary conditions that have been used for this model include a shear beam type boundary condition. The bedrock is elastic with unit weight of 2.5 t/m^3 and shear wave velocity of 2000 m/s.

Type of element used in this analysis is 8-node Brick soil element. Rayleigh damping used in this analysis is full Rayleigh damping with two target frequencies. The 1st one is the natural frequency of the soil and the 2nd one is the five times the natural frequency of the soil. The maximum shear modulus has been calculated from the equation 3.6.

$$G_{max} = \rho V_s^2 \tag{3.6}$$

The other parameters such as B_{max}, C, ϕ, Dr, ϕPT, c1, c3, d1, d3 and e have been estimated from Table 2.6 of Chapter 2. Combined bulk modulus is estimated from Bulk modulus of water (2.2×10^6 kPa) normalised by porosity (OPENSEES Manual).

The soil parameters are provided in Table 3.10 (a)-(b):

Table 3.10 (a). Input Parameters of River Channel Soil in OPENSEES

Layer #	Layer Name	Thickness (m)	Density (t/m3)	ϕ (deg)	C (kPa)	Dr (%)	Gmax (kPa)	Bmax (kPa)
1	Sand	1	1.73	30	0	20	4569.61	12185.6
2	Sand	1	1.73	31.4	0	34	14596.46	36570.5
3	Sand	1.33	1.83	32.75	0	45	28289.75	66863.5
4	Sand	1.33	1.83	33.8	0	52	43266.99	97947.3
5	Sand	1.34	1.83	34.4	0	56	58480.35	129036.3
6	Sand	2.1	1.99	34.85	0	59	85063.38	184527.4
7	Sand	2.1	1.99	35.2	0	62	111379.78	238229
8	Sand	2.1	1.99	35.5	0	65	137702.19	290414.9
9	Sand	2.1	1.99	35.7	0	67	163956.75	342886.7
10	Sand	2.1	1.99	35.9	0	69	190092.00	395322.2
11	Sand	2.1	1.99	36.1	0	71	216069.79	445590.5
12	Sand	2.1	1.99	36.3	0	73	241860.61	494615.8
13	Sand	2.1	1.99	36.4	0	74	267440.86	545405
14	Sand	2.1	1.99	36.6	0	76	292791.20	592132.5
15	Sand	2.1	1.99	36.7	0	77	317895.48	639334.9
16	Sand	1.5	2.04	36.8	0	78	347729.09	697393.2
17	Sand	1.5	2.04	36.9	0	79	365778.33	731556.7

Table 3.10 (b). Input Parameters of River Channel Soil in OPENSEES

Table 3.8 (b). Input Parameters of Normal Kolkata Soil in OPENSEES							
Layer #	**ϕPT (deg)**	**c1**	**c3**	**d1**	**d3**	**e**	**Combined Bulk Modulus (kPa)**
1	30	0.107	0.13	0	0	0.93	4565591.4
2	29	0.079	0.2	0.024	0.108	0.818	4889486.6
3	25.75	0.056	0.19	0.06	0.21	0.735	5193197.3
4	25.6	0.042	0.13	0.068	0.13	0.69	5388405.8
5	25.8	0.035	0.09	0.084	0.09	0.67	5483582.1
6	25.95	0.03	0.06	0.096	0.06	0.655	5558778.6
7	26	0.026	0.043	0.127	0.043	0.64	5637500
8	26	0.023	0.033	0.167	0.033	0.62	5748387.1
9	26	0.021	0.027	0.193	0.027	0.6	5866666.7
10	26	0.019	0.02	0.22	0.02	0.59	5928813.6
11	26	0.017	0.013	0.25	0.013	0.58	5993103.4
12	26	0.015	0.01	0.27	0.01	0.56	6128571.4
13	26	0.014	0	0.29	0	0.56	6128571.4
14	26	0.012	0	0.31	0	0.54	6274074.1
15	26	0.011	0	0.33	0	0.54	6274074.1
16	26	0.01	0	0.34	0	0.53	6350943.4
17	26	0.009	0	0.35	0	0.52	6430769.2

3.6. SIMPLIFIED PROCEDURE OF LIQUEFACTION ANALYSIS IN RIVER CHANNEL DEPOSIT

Liquefaction potential has been calculated in terms of CRR, CSR and Factor of Safety against liquefaction for two spectrum compatible strong motions with the semi empirical method prescribed by Idriss and Boulanger (2014). The magnitude of the earthquake has been considered as 6.2 for the most vulnerable source of Eocene Hinge Zone (Roy and Sahu, 2012). The surface PGA is considered as the average of surface PGA obtained from DEEPSOIL equivalent linear analysis, DEEPSOIL nonlinear analysis and OPENSEES nonlinear analysis. For spectrum compatible San Fernando and Northridge Earthquake, surface PGAs considered are 0.22g and 0.172g.

3.6.1. CALCULATION OF CRR

CRR for earthquake magnitude of 7.5 can be determined in terms of equivalent clean sand SPT value corrected for overburden and 60% hammer efficiency $[(N_1)_{60,CS}]$:

$$CRR = \exp\left[\frac{(N_1)_{60,CS}}{14.1} + \left\{\frac{(N_1)_{60,CS}}{126}\right\}^2 - \left\{\frac{(N_1)_{60,CS}}{23.6}\right\}^3 + \left\{\frac{(N_1)_{60,CS}}{25.4}\right\}^4 - 2.8\right]$$

(3.7)

$(N_1)_{60,CS}$ can be calculated as:

$$(N_1)_{60,CS} = (N_1)_{60} + \Delta(N_1)_{60}$$

(3.8)

$\Delta(N_1)_{60}$ can be calculated as:

$$\Delta(N_1)_{60} = exp\left[1.63 + \frac{9.7}{FC} - \left(\frac{15.7}{FC}\right)^2\right]$$

(3.9)

3.6.2. CALCULATION OF CSR

CSR for earthquake magnitude of 7.5 and normalized for effective overburden pressure can be determined from:

$$CSR_{M=7.5|\sigma'_{v0}=1\ atm} = 0.65 * \left(\frac{a_{max}}{g}\right) * \left(\frac{\sigma_{v0}}{\sigma'_{v0}}\right) * \left(\frac{r_d}{MSF * K_\sigma}\right)$$

(3.10)

where a_{max} is the peak horizontal acceleration at ground surface in terms of g; σ_{v0} and σ'_{v0} are the total and effective initial vertical stresses respectively; r_d, MSF and K_σ are the stress reduction factor dependent on depth in the soil profile, Magnitude Scaling Factor and overburden correction factor respectively.

r_d can be calculated as (Idriss, 1999):

$$r_d = exp\left[-1.012 - 1.126 * sin\left(\frac{z}{11.73} + 5.133\right) + 0.106 + 0.118 * sin\left(\frac{z}{11.26} + 5.142\right) * M_w\right]$$

(3.11)

where *z* is the depth below the ground surface, in meters and M_w is the moment magnitude of the earthquake.

Since all correlations in literature are based on earthquakes of magnitude of 7.5, a magnitude scaling factor *MSF* has to be used to adjust the induced CSR during an earthquake of magnitude M_w.

MSF can be calculated as:

$$MSF = min\begin{cases}6.9 * exp\left(\frac{-M_w}{4}\right) - 0.058 \\ 1.8\end{cases}$$

(3.12)

The overburden correction factor (K_σ) accounts for the non-linearity of the overburden pressure. K_σ allows to scale the CSR for a reference effective stress of 1 atm (100 kPa). K_σ can be calculated as (Boulanger, Brandenberg, Singh and Chang (2003)):

$$K_\sigma = 1 - C_\sigma * ln\left(\frac{\sigma'_{v0}}{P_a}\right) \leq 1.1$$

(3.13)

where C_σ is expressed in terms of $(N_1)_{60,CS}$ (Idriss and Boulanger (2008)):

$$C_\sigma = \frac{1}{18.9 - 2.55 * \sqrt{(N_1)_{60,CS}}} \leq 0.3$$

(3.14)

Factor of Safety (FS) is determined by:

$$FS = \frac{CRR}{CSR}$$

(3.15)

Liquefaction potential analysis for the two earthquakes considered are presented in Table 3.11 and 3.12.

Table 3.11. Liquefaction Potential Parameters for San Fernando Earthquake

Layer #	Depth (m)	N value	N1,60	Fines Content (%) (<)	ΔN1,60	N1,60,cs	CRR	CSR	FS, liq
1	0.5	0.885375	1.766323	40	5.575844	7.342167	0.15527	0.33843	0.458795
2	1.5	2.648175	5.283109	40	5.575844	10.85895	0.192046	0.333619	0.575643
3	2.665041	4.688541	9.353639	30	5.362636	14.71627	0.237874	0.32091	0.741247
4	3.995123	7.000359	12.59198	30	5.362636	17.95461	0.283493	0.307104	0.923117
5	5.330082	9.301796	14.36911	30	5.362636	19.73174	0.313512	0.295731	1.060125
6	7.049985	12.23902	16.11798	20	4.476202	20.59418	0.323165	0.277645	1.16395
7	9.149954	15.7828	17.8559	20	4.476202	22.33211	0.34788	0.256446	1.356541
8	11.24992	19.27984	19.41662	20	4.476202	23.89282	0.375826	0.237955	1.579401
9	13.34989	22.73014	20.83108	20	4.476202	25.30728	0.407401	0.221112	1.842507

10	15.44986	26.13369	22.124	20	4.476202	26.60021	0.443167	0.205686	2.15458
11	17.54983	29.49049	23.31424	20	4.476202	27.79045	0.483735	0.191685	2.523593
12	19.6498	32.80055	24.41634	20	4.476202	28.89254	0.529744	0.179177	2.956536
13	21.74977	36.06387	25.44148	20	4.476202	29.91769	0.581837	0.168224	3.45871
14	23.84974	39.28044	26.39871	20	4.476202	30.87491	0.640671	0.158862	4.032863
15	25.94971	42.45026	27.29523	20	4.476202	31.77144	0.706885	0.151106	4.678074
16	27.74962	45.12996	27.99954	20	4.476202	32.47574	0.767314	0.145623	5.26919
17	29.24947	47.33669	28.53649	20	4.476202	33.0127	0.818677	0.141844	5.771652

Table 3.12. Liquefaction Potential Parameters for Northridge Earthquake

Layer #	Depth (m)	N value	N1,60	Fines Content (%) (<)	ΔN1,60	N1,60,cs	CRR	CSR	FS, liq
1	0.5	0.885375	1.766323	40	5.575844	7.342167	0.15527	0.264591	0.58683
2	1.5	2.648175	5.283109	40	5.575844	10.85895	0.192046	0.26083	0.736288
3	2.665041	4.688541	9.353639	30	5.362636	14.71627	0.237874	0.250893	0.948107
4	3.995123	7.000359	12.59198	30	5.362636	17.95461	0.283493	0.2401	1.180731
5	5.330082	9.301796	14.36911	30	5.362636	19.73174	0.313512	0.231208	1.355974
6	7.049985	12.23902	16.11798	20	4.476202	20.59418	0.323165	0.217068	1.488773
7	9.149954	15.7828	17.8559	20	4.476202	22.33211	0.34788	0.200494	1.73511
8	11.24992	19.27984	19.41662	20	4.476202	23.89282	0.375826	0.186038	2.020165
9	13.34989	22.73014	20.83108	20	4.476202	25.30728	0.407401	0.17287	2.356695
10	15.44986	26.13369	22.124	20	4.476202	26.60021	0.443167	0.160809	2.755858
11	17.54983	29.49049	23.31424	20	4.476202	27.79045	0.483735	0.149863	3.227852
12	19.6498	32.80055	24.41634	20	4.476202	28.89254	0.529744	0.140084	3.781616
13	21.74977	36.06387	25.44148	20	4.476202	29.91769	0.581837	0.13152	4.423931
14	23.84974	39.28044	26.39871	20	4.476202	30.87491	0.640671	0.124202	5.158313
15	25.94971	42.45026	27.29523	20	4.476202	31.77144	0.706885	0.118137	5.983583

16	27.74962	45.12996	27.99954	20	4.476202	32.47574	0.767314	0.113851	6.739662
17	29.24947	47.33669	28.53649	20	4.476202	33.0127	0.818677	0.110897	7.382346

3.7.POST LIQUEFACTION SETTLEMENT CALCULATION IN RIVER CHANNEL DEPOSIT

3.7.1.BY TOKIMATSU AND SEED (1987) APPROACH

Volumetric strain ($\varepsilon_v\%$) for each layer is calculated from the following chart by means of CSR and $N_{1,60}$:

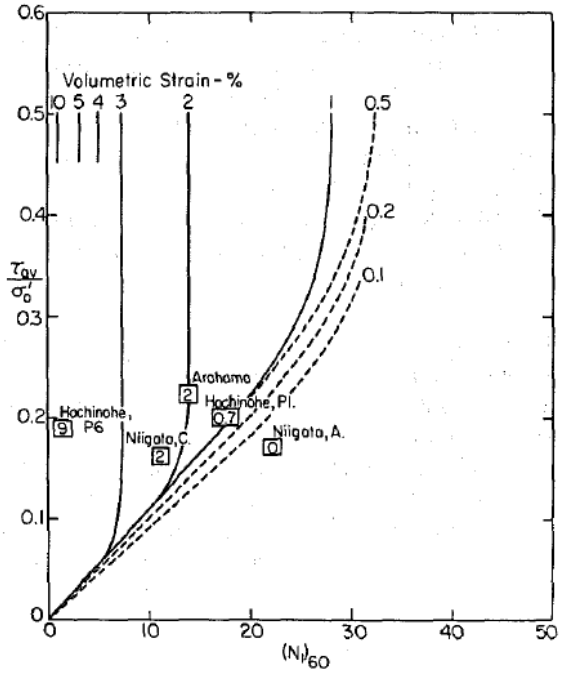

Figure 3.22: Relationship between CSR, $N_{1,60}$ and Volumetric Strain for Saturated Clean Sands

A depth weighting factor (DF_i) is given by (Cetin et. al., 2009):

$$DF_i = 1 - \frac{d_i}{18\,m} \tag{3.16}$$

DF_i is multiplied by volumetric strain for each layer and the modified volumetric strain is multiplied by the thickness of the corresponding layer which gives the settlement of that particular layer. The total settlement, summation of settlements of all layers, is multiplied with 1.45 to give modified total settlement.

3.7.2.BY ISHIHARA AND YOSHEMINE (1992) APPROACH

Volumetric strain $(\varepsilon_v\%)$ for each layer is calculated from the following chart by means of Factor of Safety against liquefaction (FS_{liq}) and relative density or SPT or CPT value :

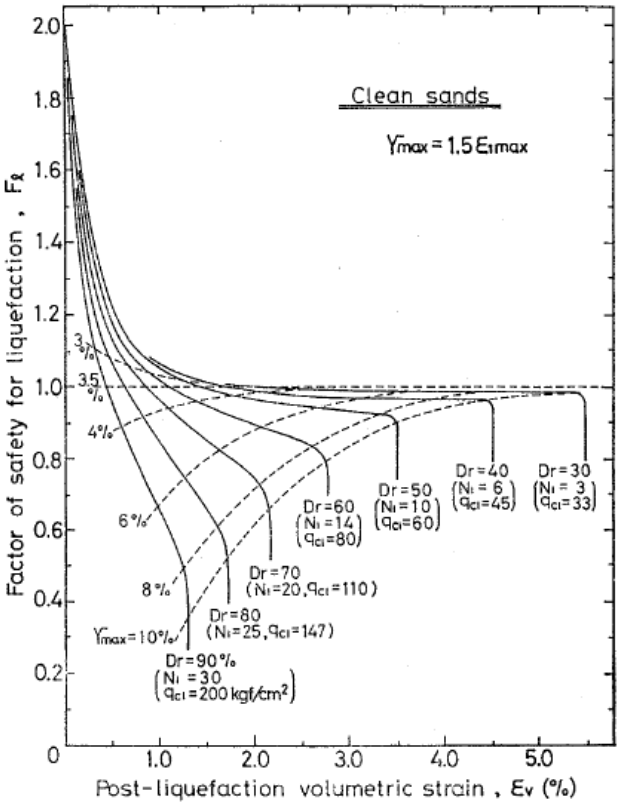

Figure 3.23: Chart for Determining Volumetric Strain as Functions of Factor of Safety against Liquefaction

Idriss and Boulanger (2008) recommended the following functions of $(N_1)_{60,CS}$ and factor of safety against liquefaction (FS_{liq}) to approximate the Ishihara and Yoshemine (1992) volumetric strains:

$$(\varepsilon_v)_i = 1.5 * \exp\left(-0.369 * \sqrt{(N_1)_{60,CS}}\right) * Min\begin{Bmatrix}0.08\\ \gamma_{max}\end{Bmatrix}$$

(3.17)

where γ_{max} is the maximum shear strain the undrained loading.

To compute γ_{max}, we need a few intermediate values:

$$F_\alpha = 0.032 + 0.69 * \sqrt{(N_1)_{60,CS}} - 0.13 * (N_1)_{60,CS}$$

(3.18)

and limiting shear strain,

$$\gamma_{lim} = 1.859 * \left(1.1 - \sqrt{\frac{(N_1)_{60,CS}}{46}}\right)^3 \geq 0$$

(3.19)

γ_{max} is given by:

$$\gamma_{max} = \begin{cases} 0 & for\ FS_{liq} \geq 2 \\ Min\begin{cases} \gamma_{lim} \\ 0.035 * (2 - FS_{liq} * \left(\frac{1 - FS_{liq}}{FS_{liq} - F_\alpha}\right) & for\ 2 > FS_{liq} > F_\alpha \\ \gamma_{lim} & for\ FS_{liq} \leq F_\alpha \end{cases} \end{cases}$$

(3.20)

The volumetric strain of each layer $(\varepsilon_v)_i$ is then multiplied with the thickness of the corresponding layer to give settlement of that layer. A depth weighting factor (DF_i) is given by (Cetin et. al., 2009):

$$DF_i = 1 - \frac{d_i}{18\ m}$$

(3.21)

DF_i is multiplied by volumetric strain for each layer and the modified volumetric strain is multiplied by the thickness of the corresponding layer which gives the settlement of that particular layer. The total settlement, summation of settlements of all layers, is multiplied with 0.9 to give modified total settlement.

CHAPTER 4

RESULTS & DISCUSSIONS

4.1. GENERAL

Ground responses for two types of soil profiles in Kolkata i.e. 1) Normal Kolkata Deposit and 2) River Channel Deposit are analysed by DEEPSOIL and OPENSEES software. Using various SPT-N and shear wave velocity relationships in DEEPSOIL software, variation of various parameters, such as, peak ground acceleration (PGA), amplification factor, relative displacement, maximum strain, maximum stress ratio, maximum pore pressure ratio with depth are evaluated. In addition, Fourier amplification ratio and spectral acceleration response at the ground surface are predicted. For this purpose, two input motions, namely, San Fernando earthquake (1971, California) and Northridge earthquake (1994, California), spectrum compatible with corresponding soil profiles and soil zones as specified in IS:1893 (Part 1)-2002 have been used in order to incorporate local site effect in the analysis. For analysis using OPENSEES software, only one specific SPT-N and shear wave velocity relationship (Chowdhury and Chatterjee, 2013, Uncorrected SPT) has been used. Then liquefaction potential has also been evaluated for river channel deposit along with post liquefaction settlement. The results of the analyses are presented in the subsequent sections.

4.2. EQUIVALENT LINEAR AND NONLINEAR ANALYSES FOR NORMAL KOLKATA DEPOSIT USING DEEPSOIL

The two input motions spectrum compatible with the response spectra of IS:1893 (Part 1)-2002 Zone 3 soft soil as mentioned in Chapter 3 are presented in figures 4.1 and 4.2. PGA of these two input motions are 0.18g and 0.158g respectively. In this context, it is worthwhile to mention that Peak Bed Rock Acceleration of Kolkata region as reported by various researchers are in the range of 0.1g to 0.34g (average ~0.22g) (Roy and Sahu, 2012; Akhila et. al., 2012; Govindaraju and Bhattacharya, 2012).

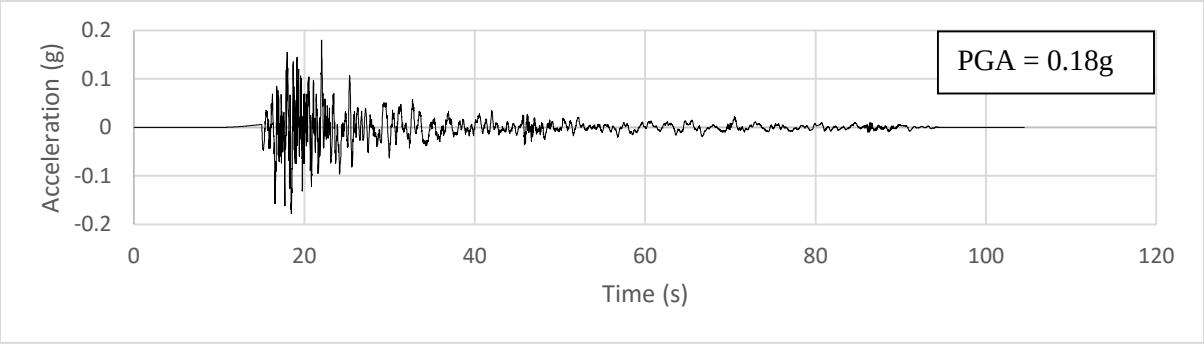

Figure 4.1: Spectrally compatible San Fernando Earthquake Acceleration Time History

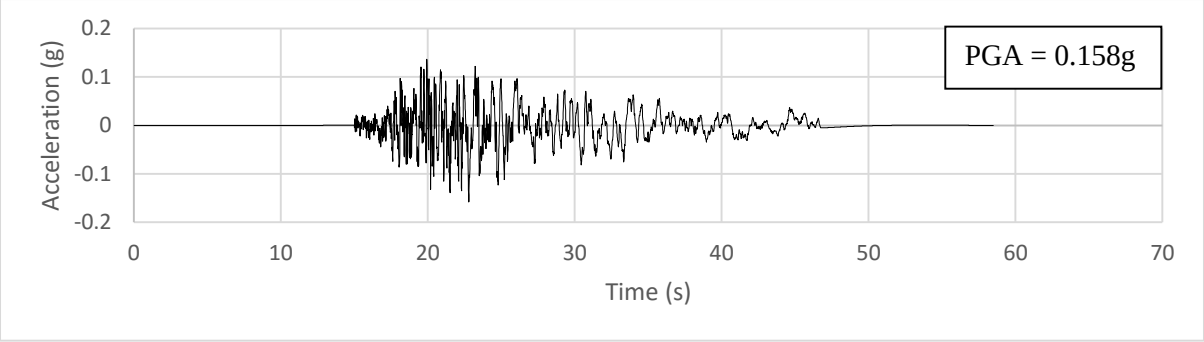

Figure 4.2: Spectrally compatible Northridge Earthquake Acceleration Time History

4.2.1.Peak Ground Acceleration (PGA)

The variation of PGA with depth for different N-Vs correlations for equivalent linear and nonlinear analyses are separately presented in figures 4.3 to 4.8 for comparison. In figures 4.9 to 4.12, PGA for different N-Vs correlations as obtained from equivalent linear and nonlinear analyses are presented separately.

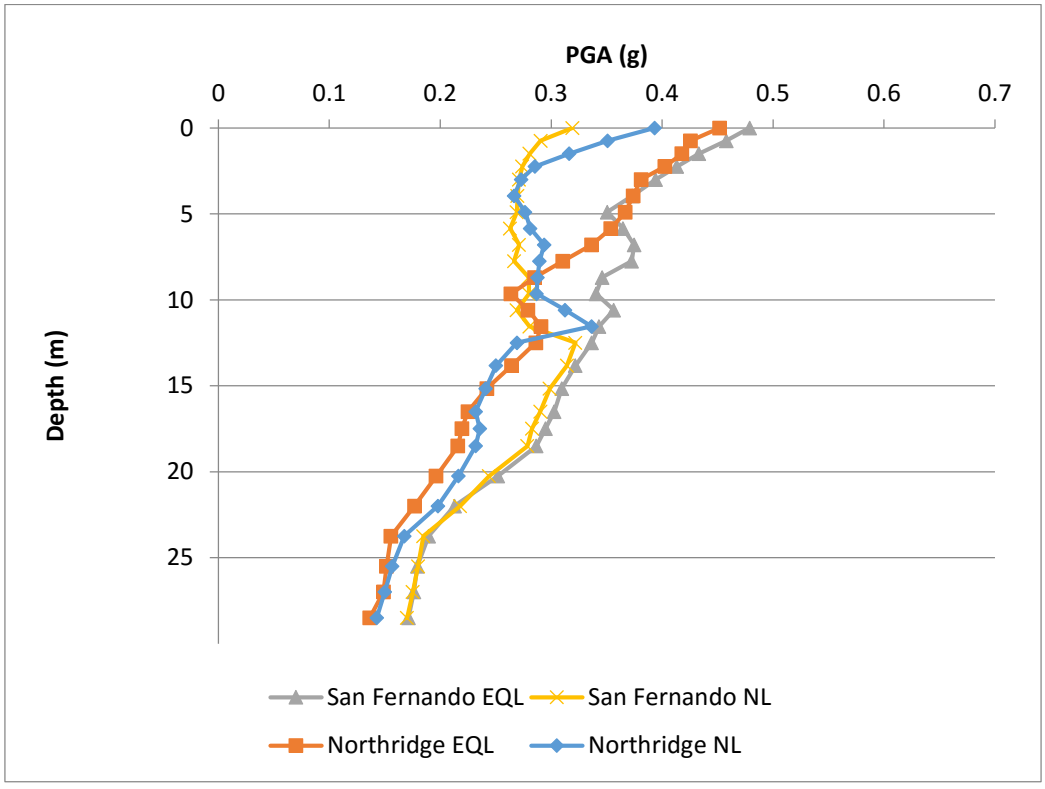

Figure 4.3: PGA Profiles for Equivalent Linear and Nonlinear Analysis using N-Vs correlations given by Maheswari et. al. (2010)

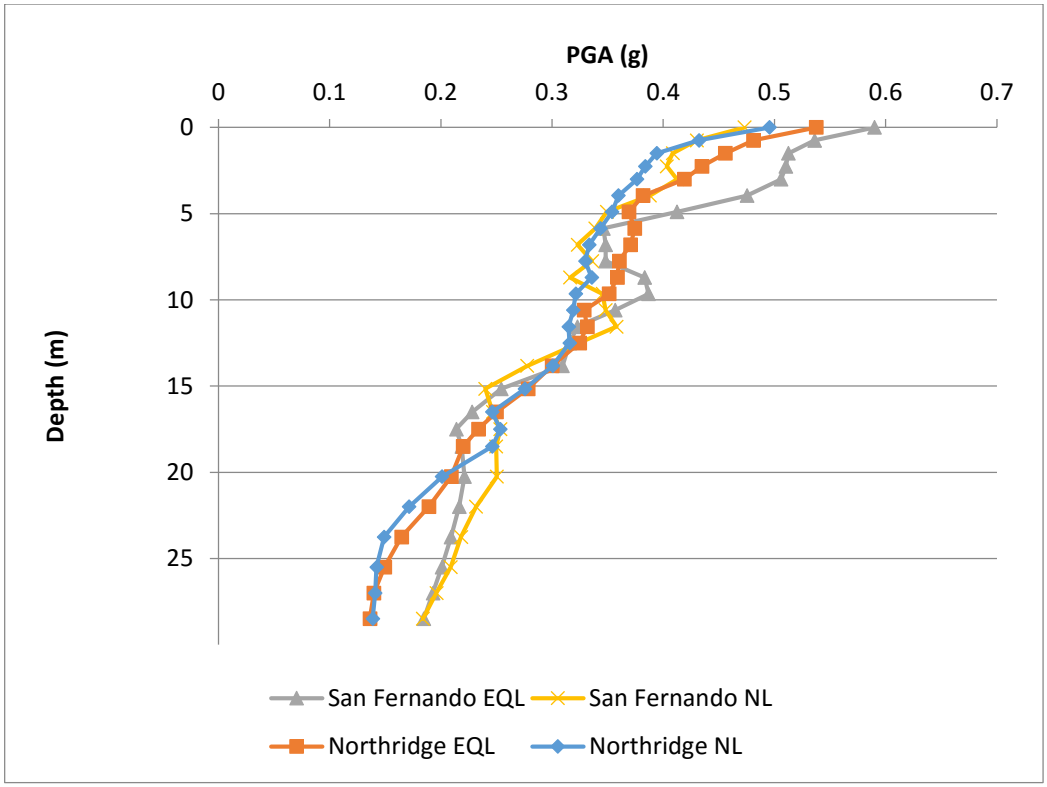

Figure 4.4: PGA Profiles for Equivalent Linear and Nonlinear Analysis using N-Vs correlations given by Anbazhagan et. al. (2012)

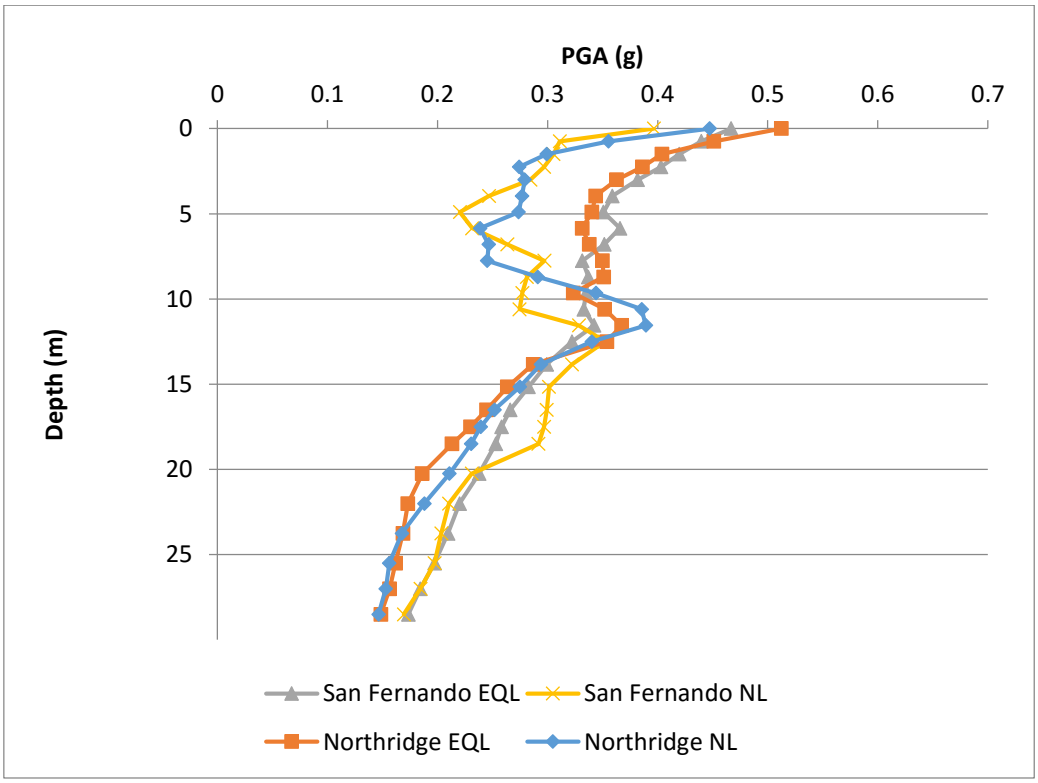

Figure 4.5: PGA Profiles for Equivalent Linear and Nonlinear Analysis using N-Vs correlations given by Choudhury and Chatterjee (Uncorrected SPT) (2013)

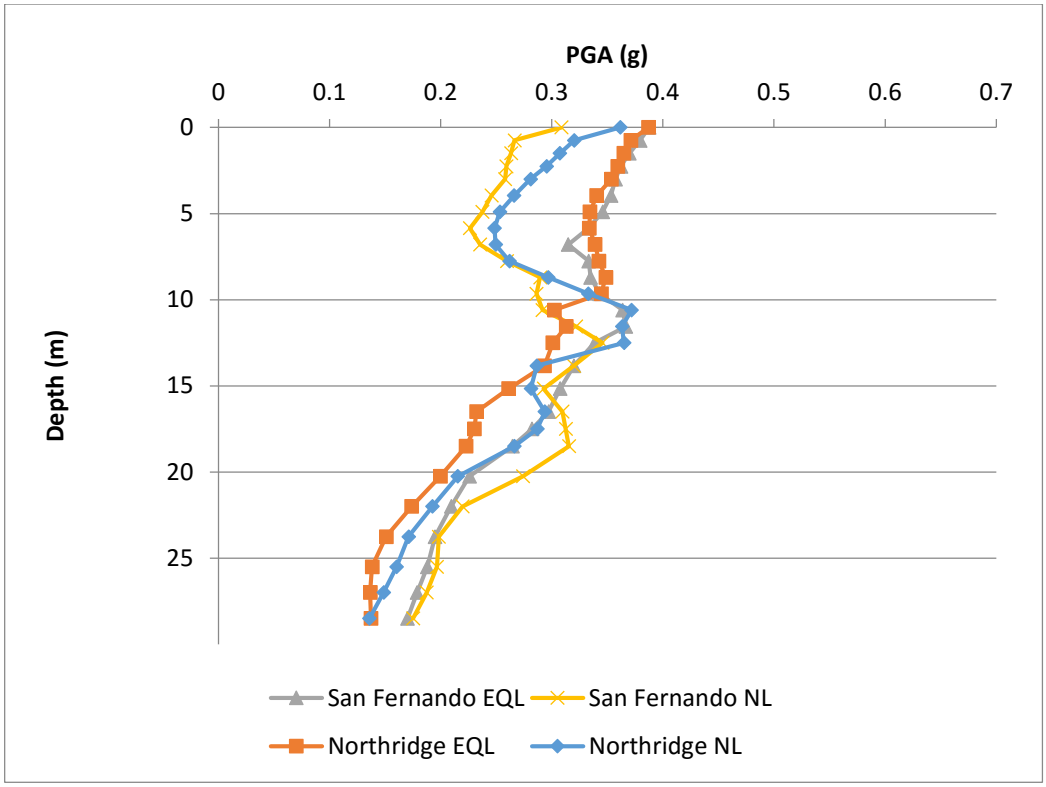

Figure 4.6: PGA Profiles for Equivalent Linear and Nonlinear Analysis using N-Vs correlations given by Choudhury and Chatterjee (Corrected SPT) (2013)

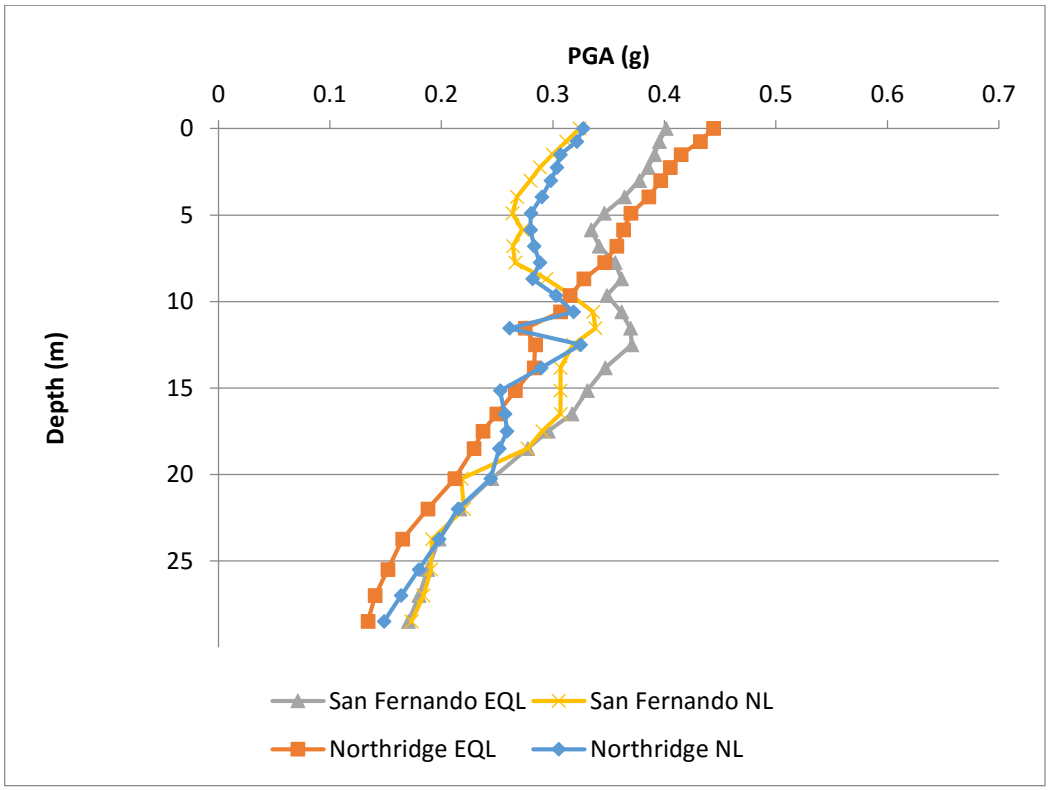

Figure 4.7: PGA Profiles for Equivalent Linear and Nonlinear Analysis using N-Vs correlations given by Nath et. al. (2016) (Simplified)

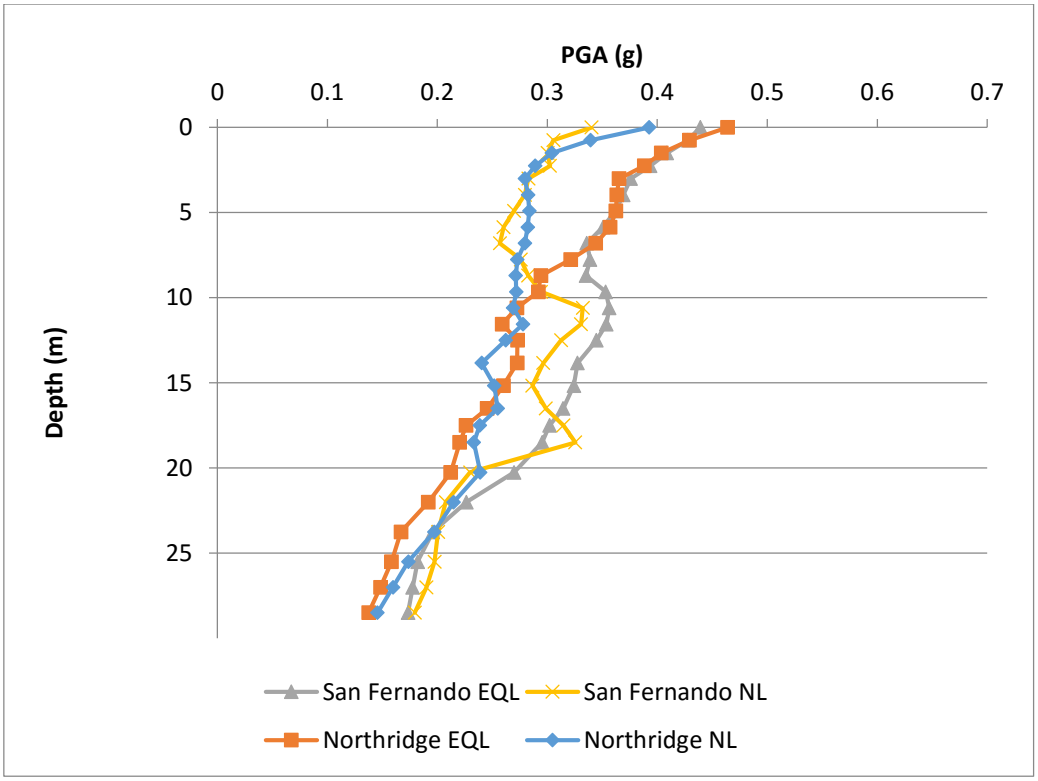

Figure 4.8: PGA Profiles for Equivalent Linear and Nonlinear Analysis using N-Vs correlations given by Nath et. al. (2016) (Depth and Lithology Specific)

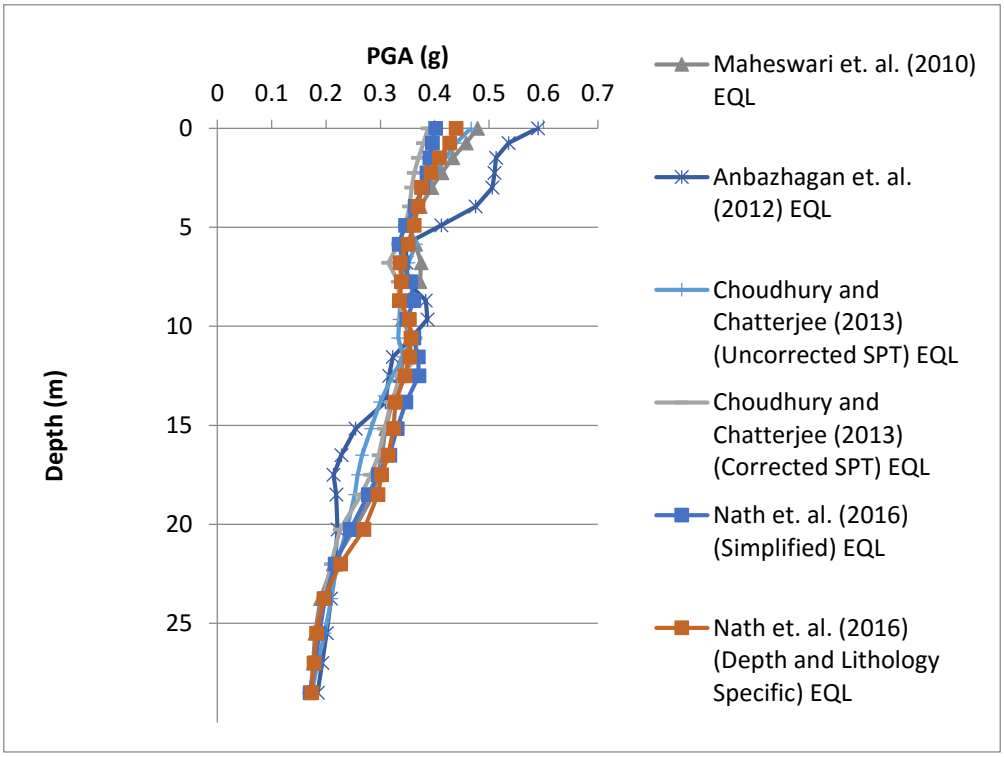

Figure 4.9: PGA Profiles for Equivalent Linear Analysis for Normal Kolkata Soil Deposit using Spectrally Matched San Fernando Earthquake and Various N-Vs correlations

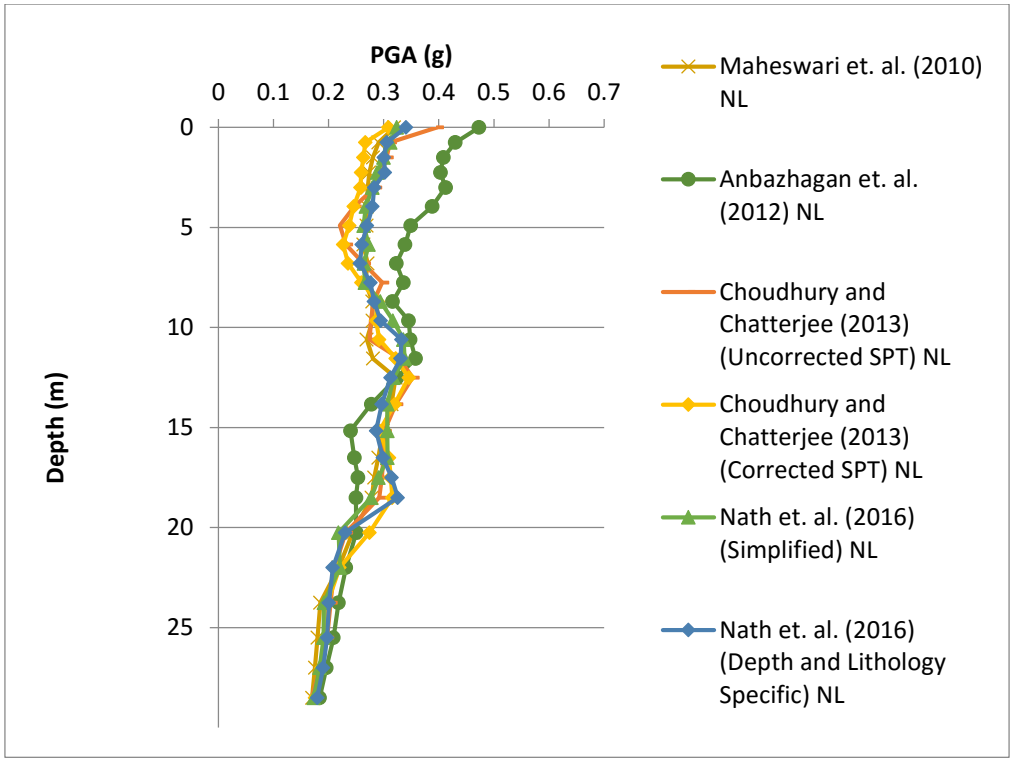

Figure 4.10: PGA Profiles for Nonlinear Analysis for Normal Kolkata Soil Deposit using Spectrally Matched San Fernando Earthquake and Various N-Vs correlations

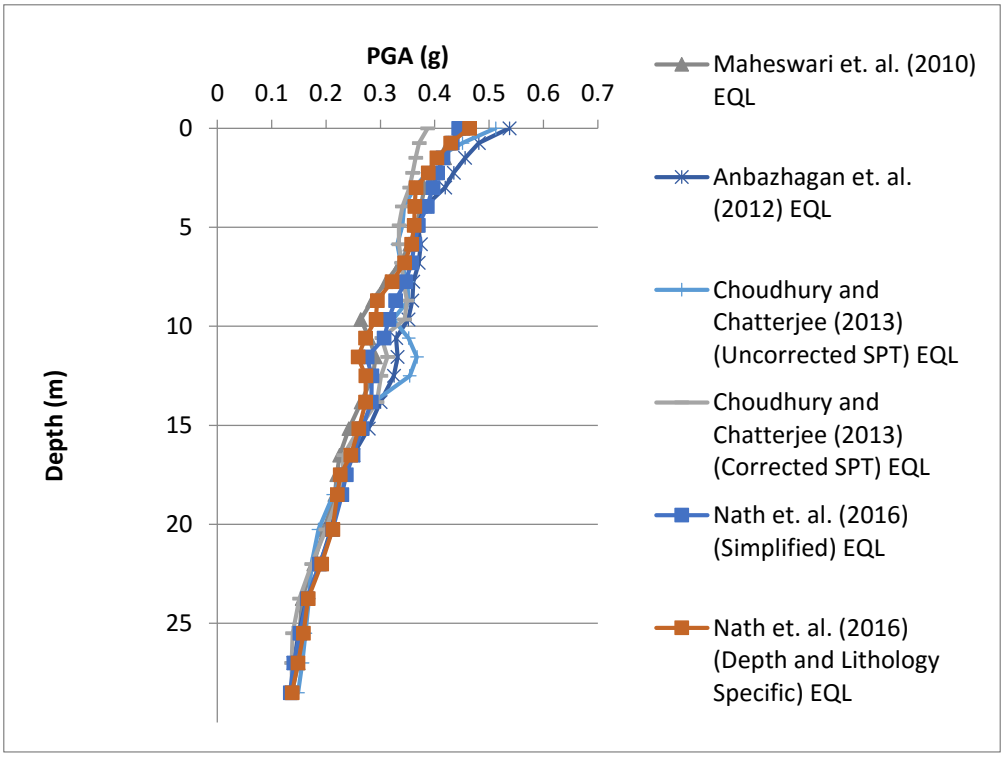

Figure 4.11: PGA Profiles for Equivalent Linear Analysis for Normal Kolkata Soil Deposit using Spectrally Matched Northridge Earthquake and Various N-Vs correlations

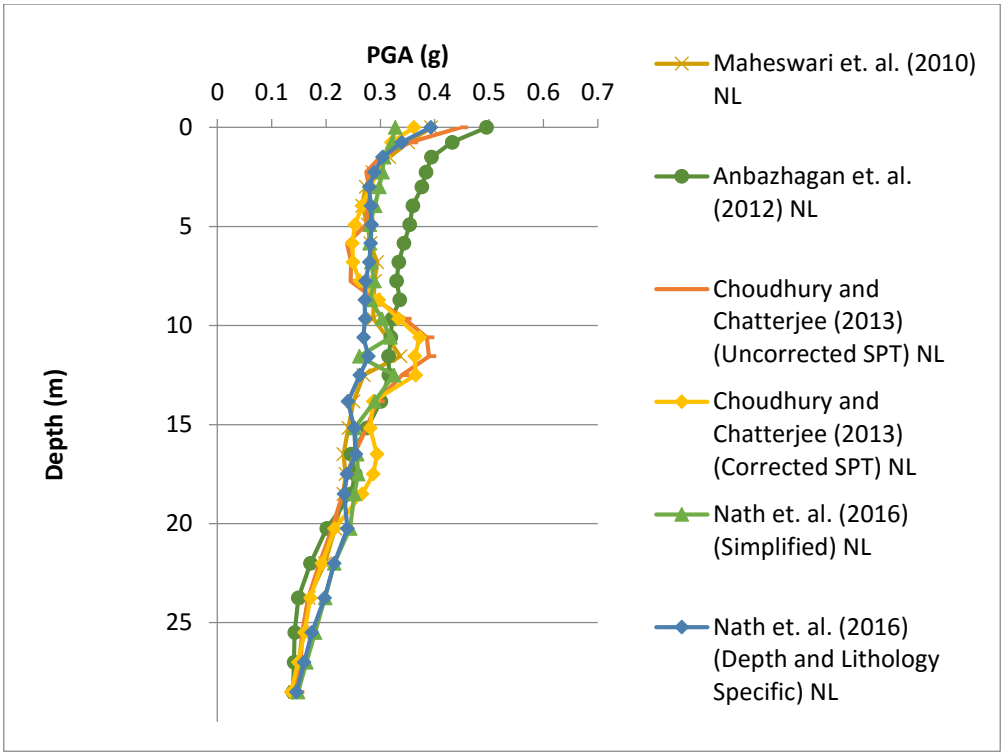

Figure 4.12: PGA Profiles for Nonlinear Analysis for Normal Kolkata Soil Deposit using Spectrally Matched Northridge Earthquake and Various N-Vs correlations

From the figures (4.3) to 4.12), it may be observed that below 12m depth, practically there is no variation in PGA profiles calculated from equivalent linear and nonlinear analysis for different N-Vs correlations. However, for depth above 12m, PGA profiles calculated from nonlinear analysis are found to be less than that from equivalent linear analysis. Surface PGAs calculated from nonlinear analysis are found to be about 0.35g while that of equivalent linear analysis is about 0.45g. This reduction in PGA values above 12m may be due to low consistency (SPT - N value) which induces comparatively larger deformation and results in higher damping in the top soft clay layer.

4.2.2.PGA Amplification Ratio

PGA amplification ratio at any depth is the PGA at that corresponding depth normalised by peak bedrock amplification **(PBRA)**. PGA amplification ratio depicts the amount of amplification or attenuation of ground motion at any depth. The PGA amplification ratio calculated with equivalent linear and nonlinear analysis with two different spectrum compatible strong motions are shown in figures (4.13) to (4.16).

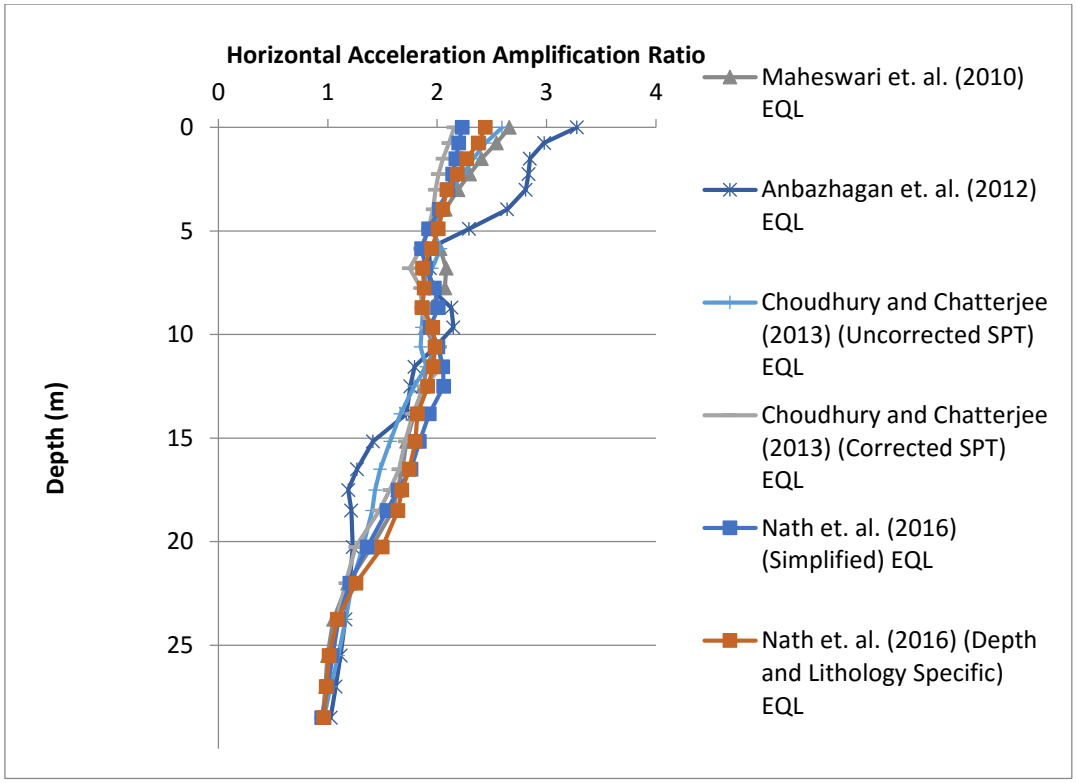

Figure 4.13: PGA Amplification Ratio Profiles for Equivalent Linear Analysis for Normal Kolkata Soil Deposit using Spectrally Matched San Fernando Earthquake and various N-Vs correlations

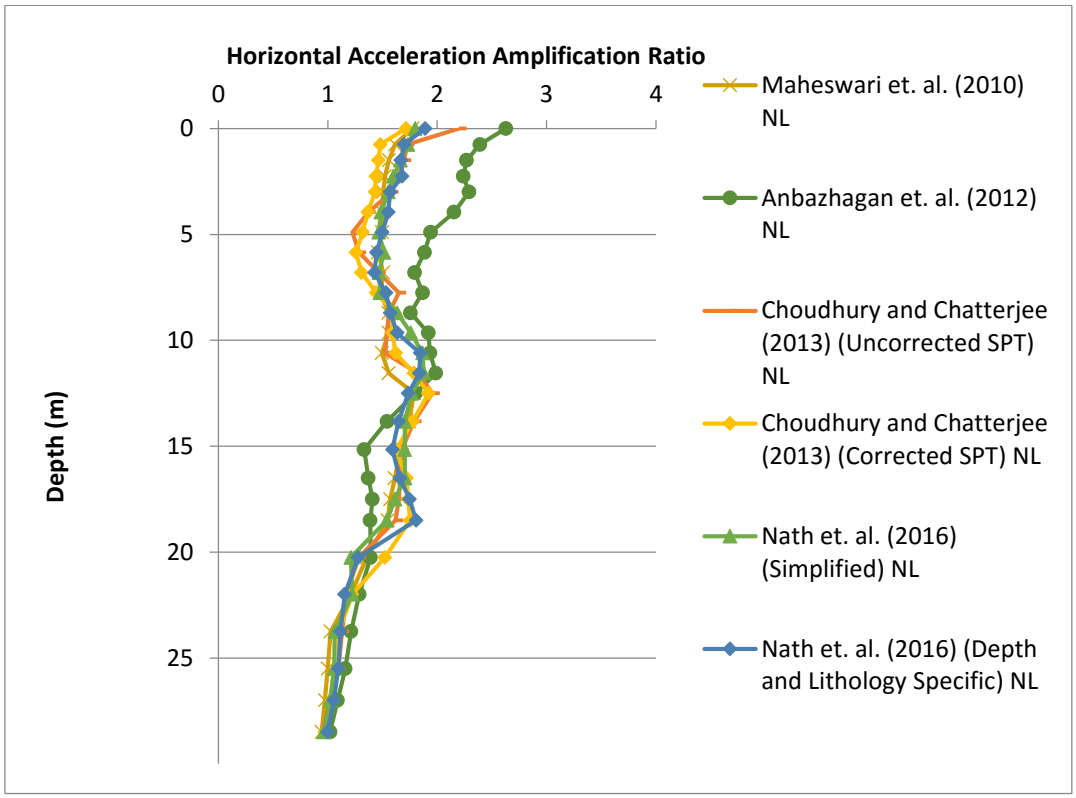

Figure 4.14: PGA Amplification Ratio Profiles for Nonlinear Analysis for Normal Kolkata Soil Deposit using Spectrally Matched San Fernando Earthquake and various N-Vs correlations

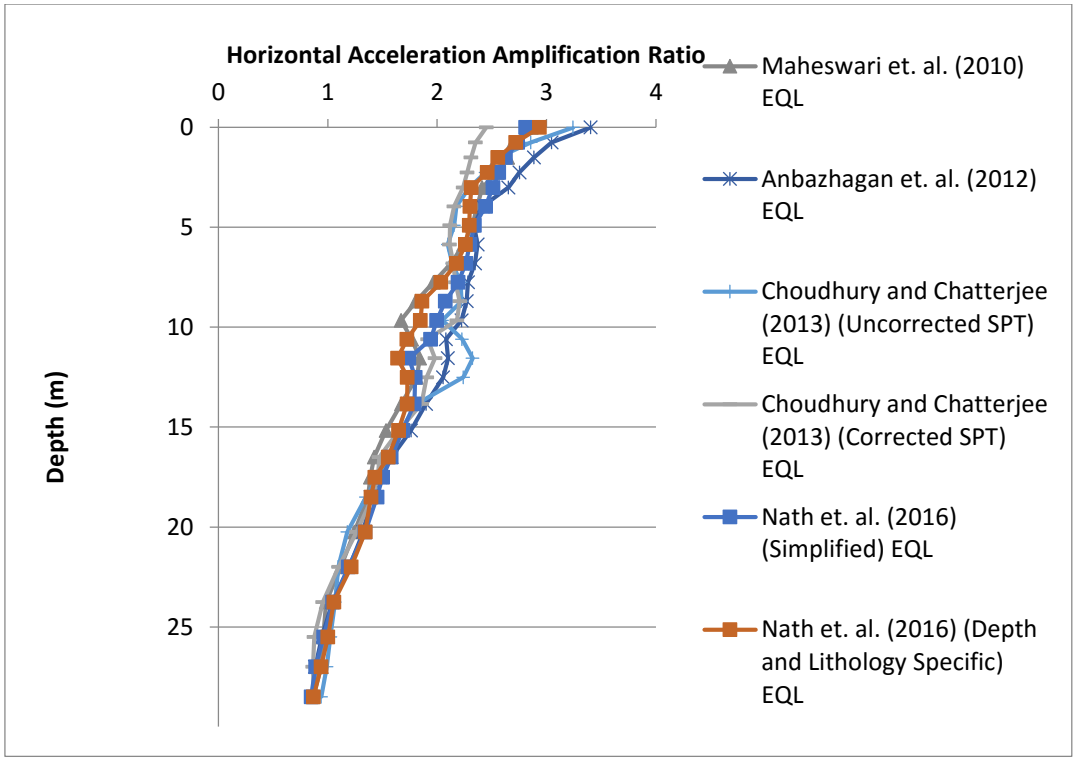

Figure 4.15: PGA Amplification Ratio Profiles for Equivalent Linear Analysis for Normal Kolkata Soil Deposit using Spectrally Matched Northridge Earthquake and various N-Vs correlations

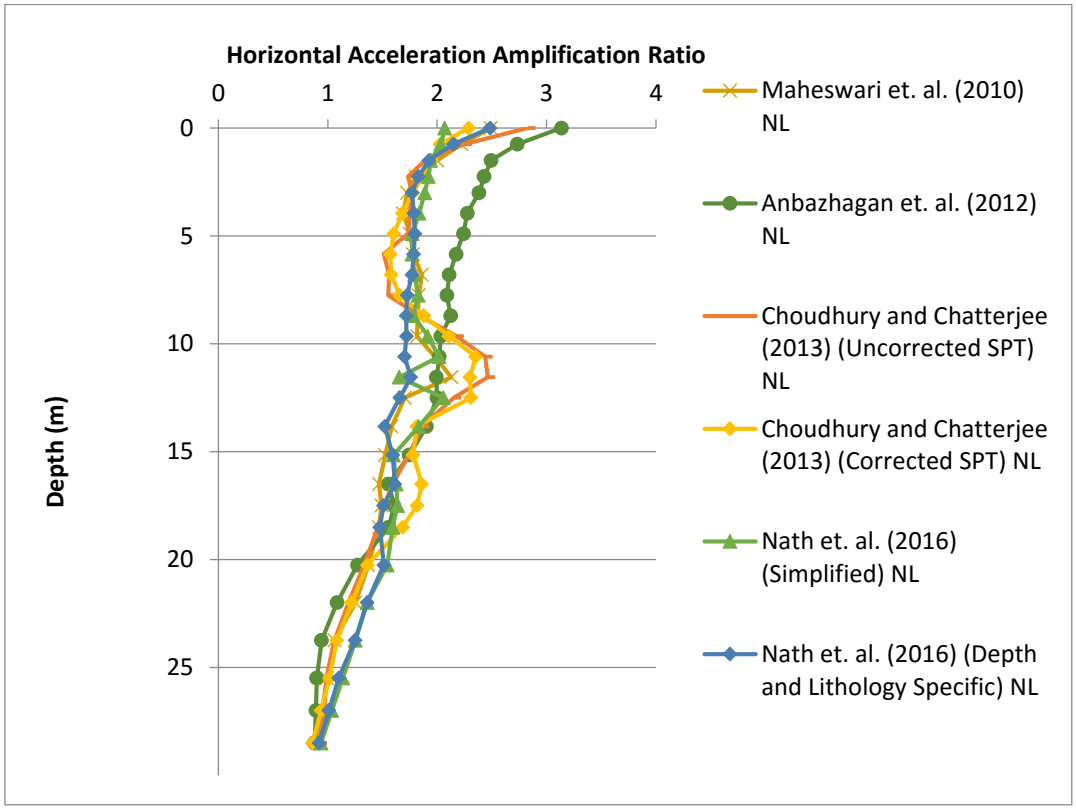

Figure 4.16: PGA Amplification Ratio Profiles for Nonlinear Analysis for Normal Kolkata Soil Deposit using Spectrally Matched Northridge Earthquake and various N-Vs correlations

From the figures (4.13) to 4.16), it is observed that PGA amplification at the ground surface in normal Kolkata deposit ranges between 2.0-3.0 and 2.5-3.5 in equivalent linear analysis for spectrum compatible San Fernando Earthquake (PBRA = 0.18g) and Northridge Earthquake (PBRA = 0.158g) respectively. PGA amplification ranges between 1.8-2.2 and 2.0-3.0 for nonlinear analysis for the above mentioned motions respectively. Thus PGA amplification is less in nonlinear analysis than that in the equivalent linear analysis due to higher induced strain in soil in nonlinear analysis than that in equivalent linear analysis. Higher strain induces higher damping which attenuates the PGA. PGA amplification increases from bedrock to surface in the equivalent linear analysis. In the nonlinear analysis, the PGA amplification increases from bedrock to a depth of approximately 12m. Above this it decreases down to a depth of 5m and then almost remains constant. Ground motion amplification / attenuation is function of both dynamic soil properties and magnitude of ground motions. The ground motion amplification occurs in the stiffer soils and attenuation occurs in the softer soils. Further higher PBRA motion induces higher hysteretic damping than that for lower PBRA motion. So, Northridge motion with lower PBRA amplifies more than higher PBRA motion (San Fernando).

4.2.3.Relative Displacement

The relative displacement of each layers calculated with equivalent linear and nonlinear analysis with two different spectrum compatible strong motions are shown in Figures (4.17) to (4.20).

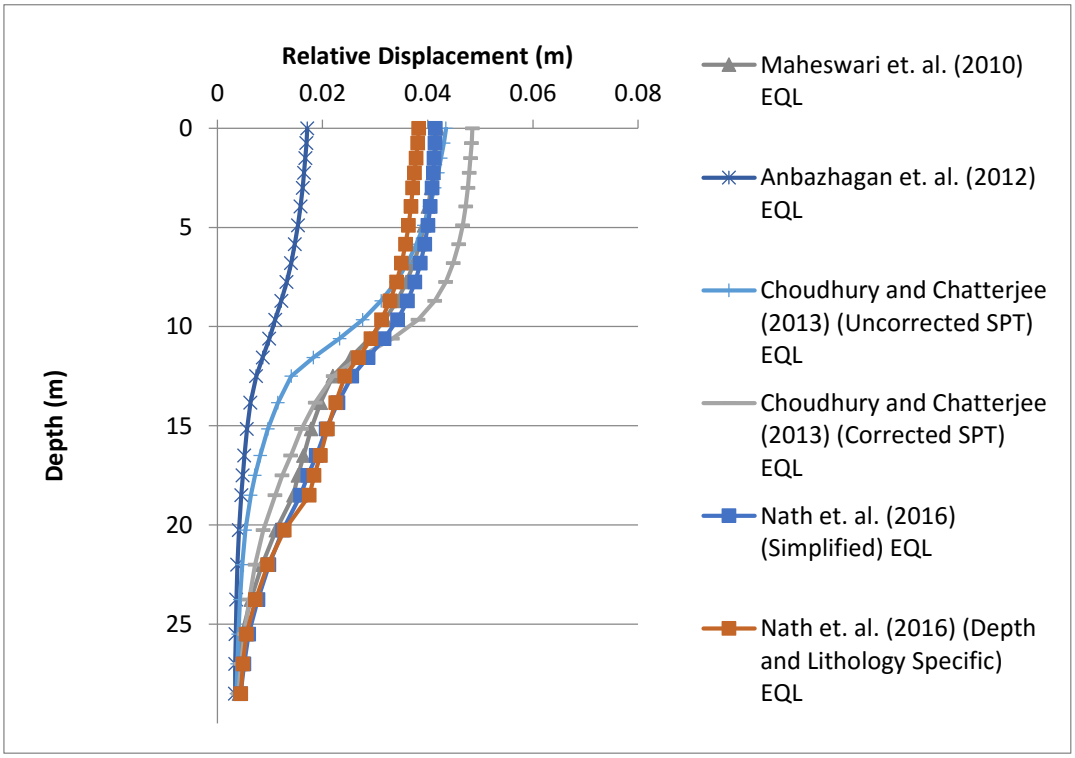

Figure 4.17: Relative Displacement Profiles for Equivalent Linear Analysis for Normal Kolkata Soil Deposit using Spectrally Matched San Fernando Earthquake and various N-Vs correlations

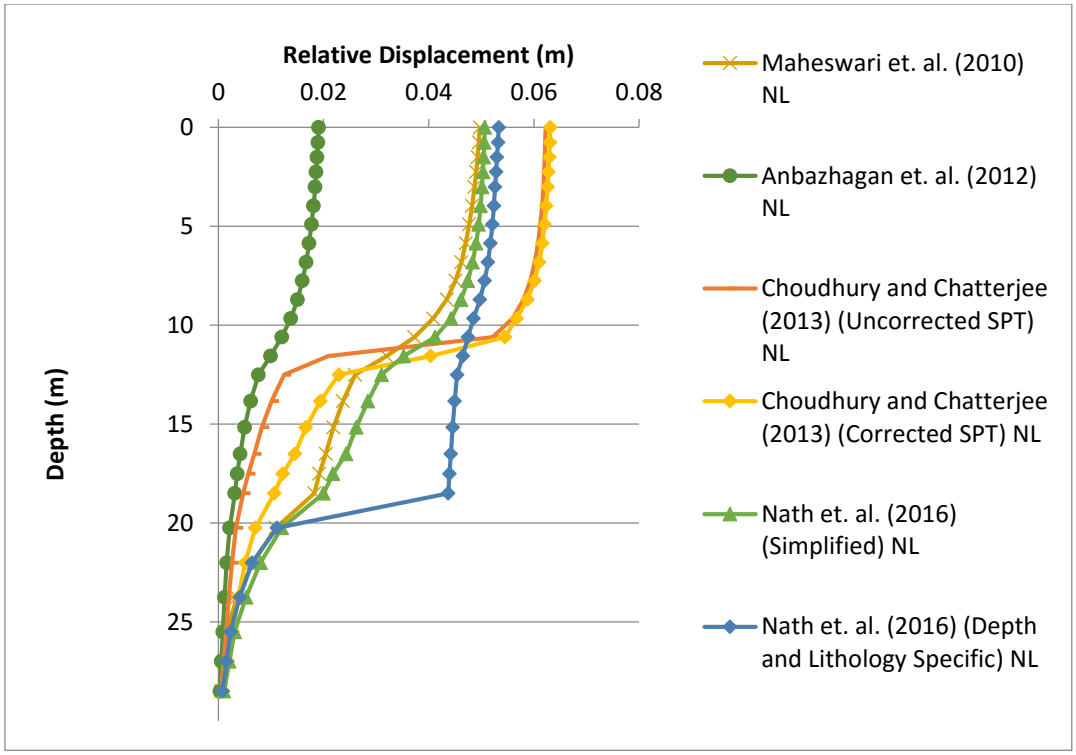

Figure 4.18: Relative Displacement Profiles for Nonlinear Analysis for Normal Kolkata Soil Deposit using Spectrally Matched San Fernando Earthquake and various N-Vs correlations

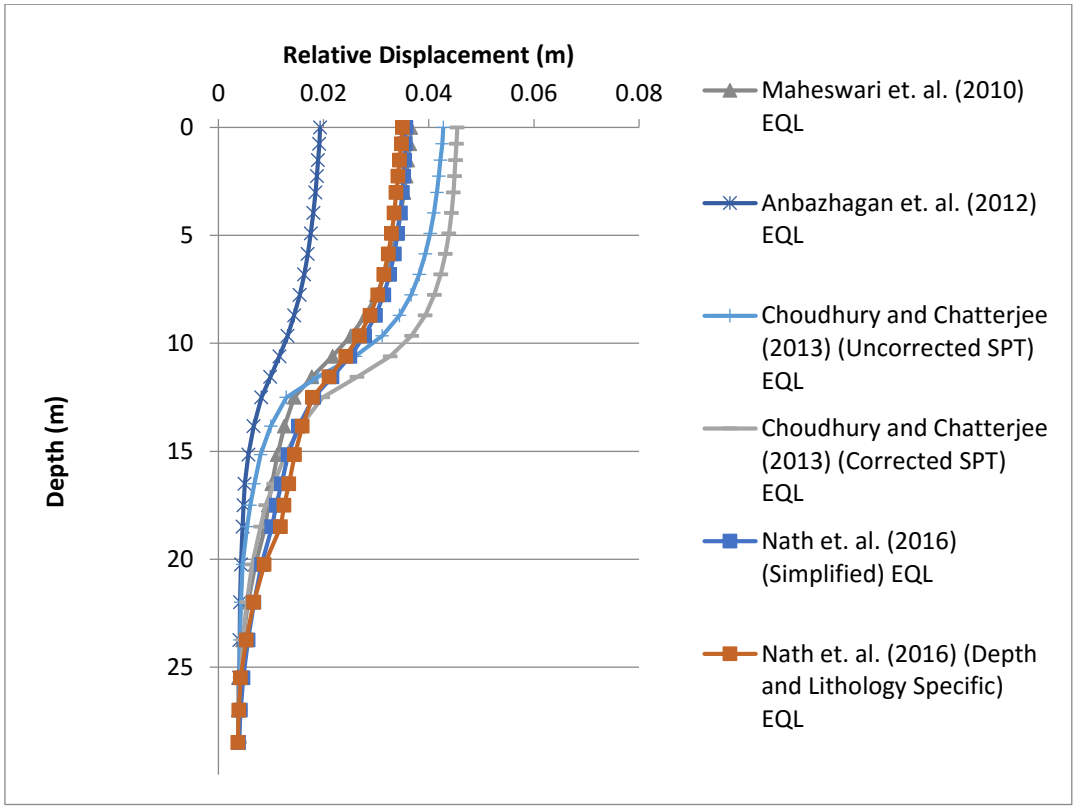

Figure 4.19: Relative Displacement Profiles for Equivalent Linear Analysis for Normal Kolkata Soil Deposit using Spectrally Matched Northridge Earthquake and various N-Vs correlations

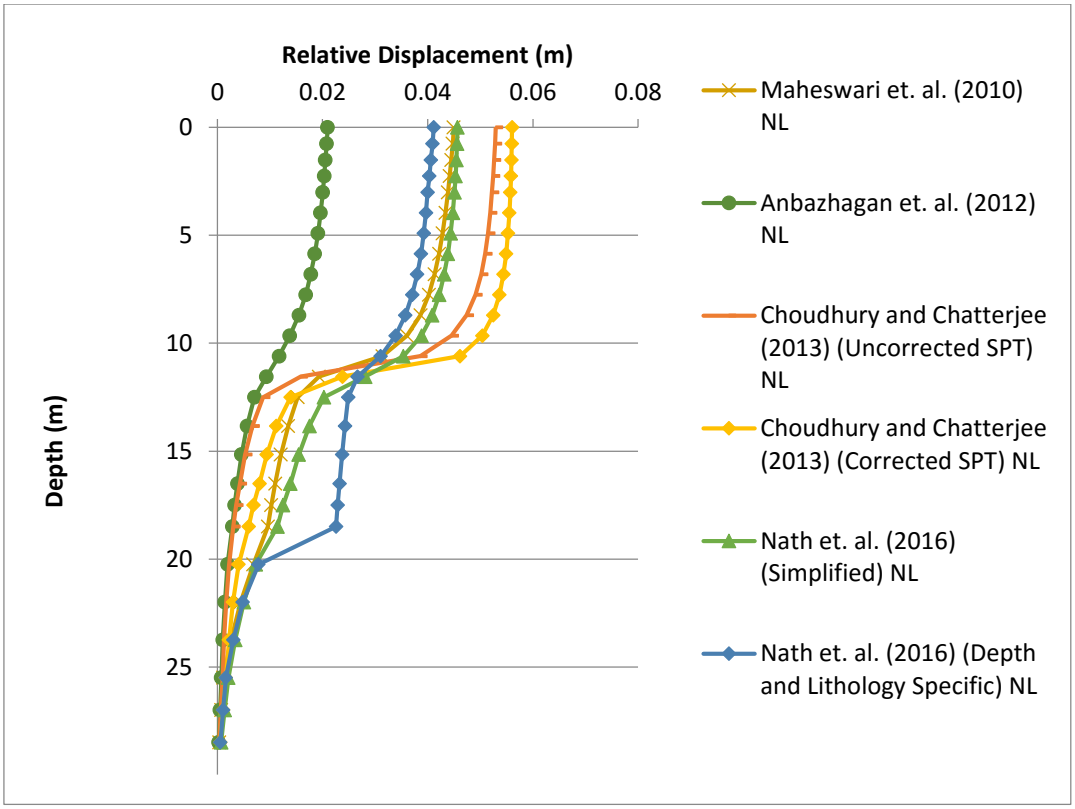

Figure 4.20: Relative Displacement Profiles for Nonlinear Analysis for Normal Kolkata Soil Deposit using Spectrally Matched Northridge Earthquake and various N-Vs correlations

From the figures 4.17 – 4.20, it may be observed that the variation of relative displacement is more or less uniform down to a depth of about 10m from surface in both equivalent linear and nonlinear analyses. Again, this may be due to soft consistency of the top 10m soil deposit. Below 10m depth, the relative displacement is gradual and becomes more or less negligible at about 25m depth. It is to be noted that higher PBRA motion results in more ground displacement. Also ground displacement is more in nonlinear analysis than that in equivalent linear analysis. The range of relative displacement at surface for different cases are given in Table 4.1. In this context it may be mentioned that the displacement obtained using the SPT N-Vs correlation given by Anbazhagan et. al. (2012) is substantially less and has not been provided in Table 4.1.

Table 4.1. Surface Displacement (m) for Various Correlations

N-Vs correlation	San Fernando Earthquake		Northridge Earthquake	
	Equivalent Linear	Nonlinear	Equivalent Linear	Nonlinear
Maheswari et. al. (2010)	0.04	0.05	0.037	0.045
Choudhury and Chatterjee (2013) (Uncorrected SPT)	0.043	0.062	0.043	0.053
Choudhury and Chatterjee (2013) (Corrected SPT)	0.048	0.063	0.045	0.056
Nath et. al. (2016) (Simplified)	0.041	0.05	0.036	0.046
Nath et. al. (2016) (Depth and Lithology Specific)	0.038	0.053	0.035	0.041

4.2.4.Maximum Shear Strain

Variation of maximum shear strain is obtained from equivalent linear and nonlinear analysis for a typical N-Vs correlation (Choudhury and Chatterjee, 2013 (Uncorrected SPT)) has been presented in figure 4.21. Further comparative presentations of maximum shear strains are shown in figures 4.22 to 4.25.

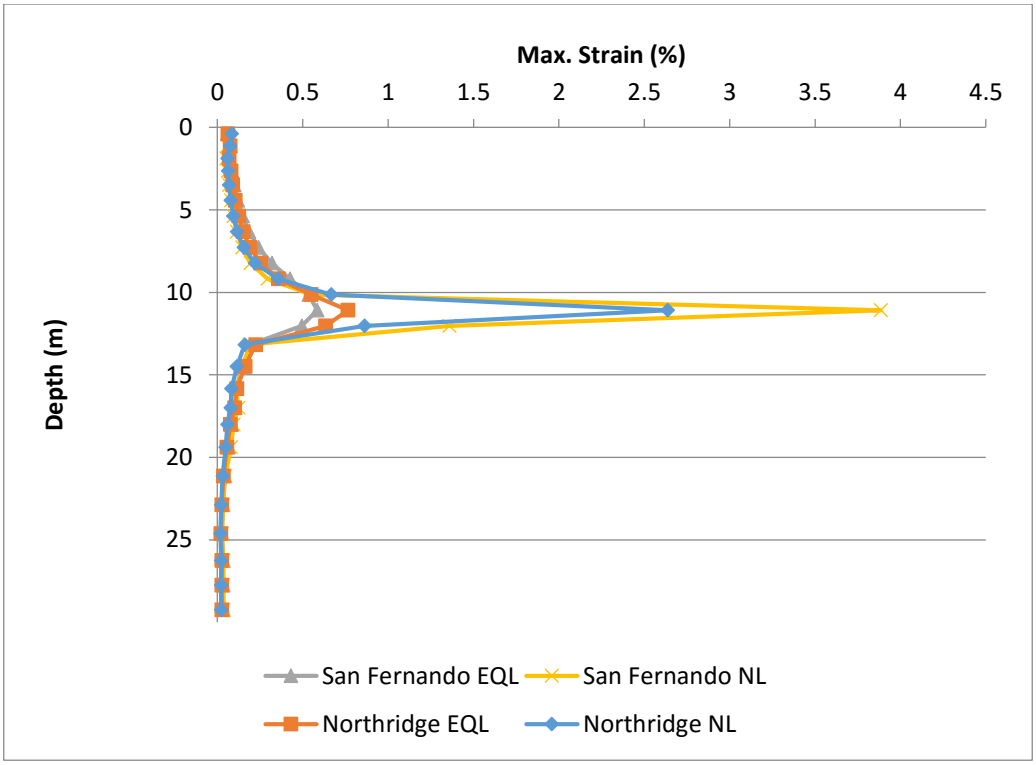

Figure 4.21: Maximum Shear Strain Profiles for Equivalent Linear and Nonlinear Analyses using Choudhury and Chatterjee (2013) (Uncorrected SPT)

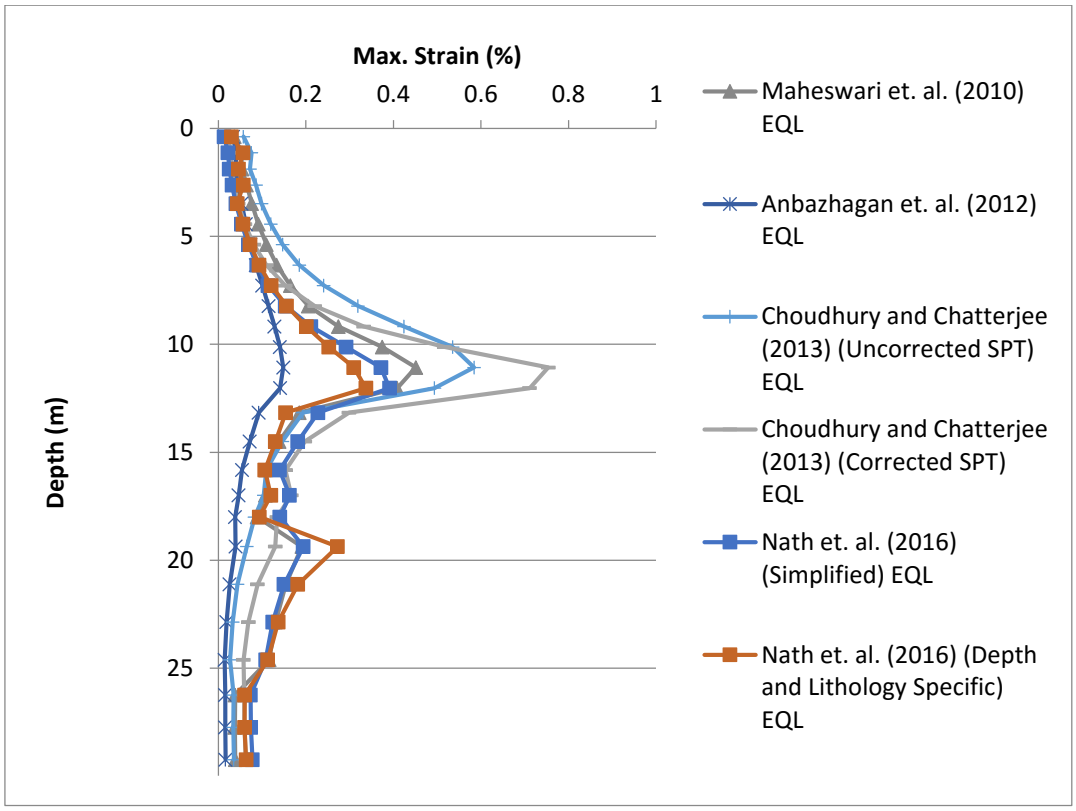

Figure 4.22: Maximum Shear Strain Profiles for Equivalent Linear Analysis for Normal Kolkata Soil Deposit using Spectrally Matched San Fernando Earthquake and various N-Vs correlations

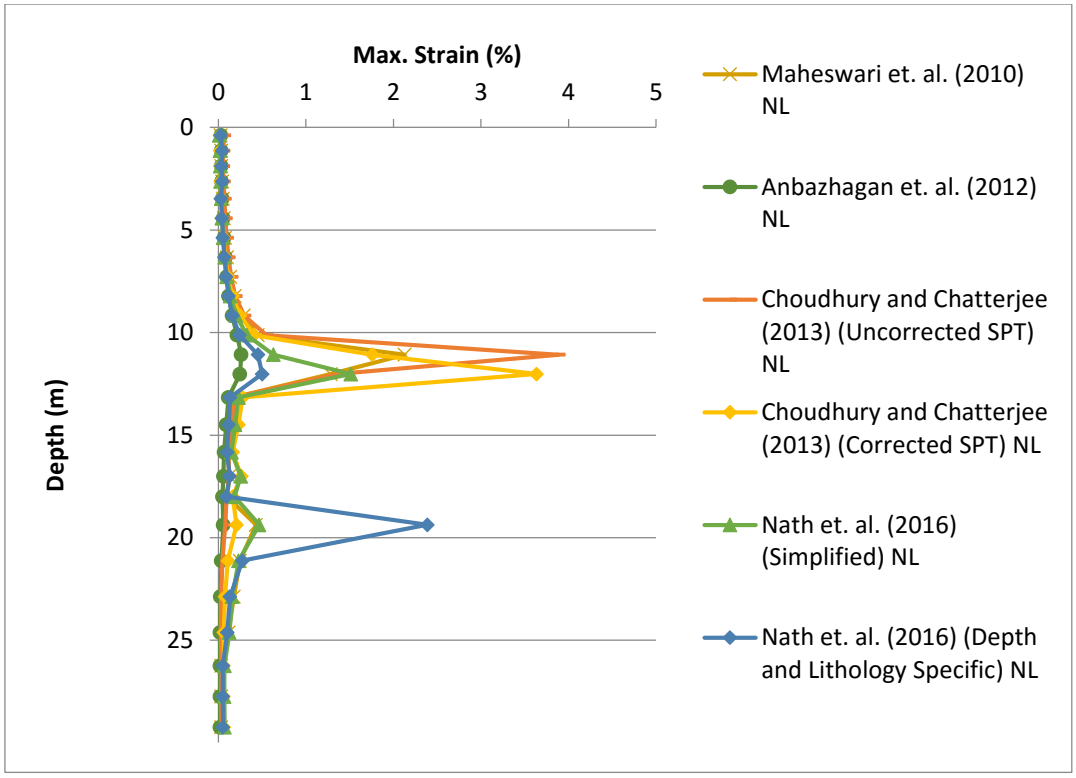

Figure 4.23: Maximum Shear Strain Profiles for Nonlinear Analysis for Normal Kolkata Soil Deposit using Spectrally Matched San Fernando Earthquake and various N-Vs correlations

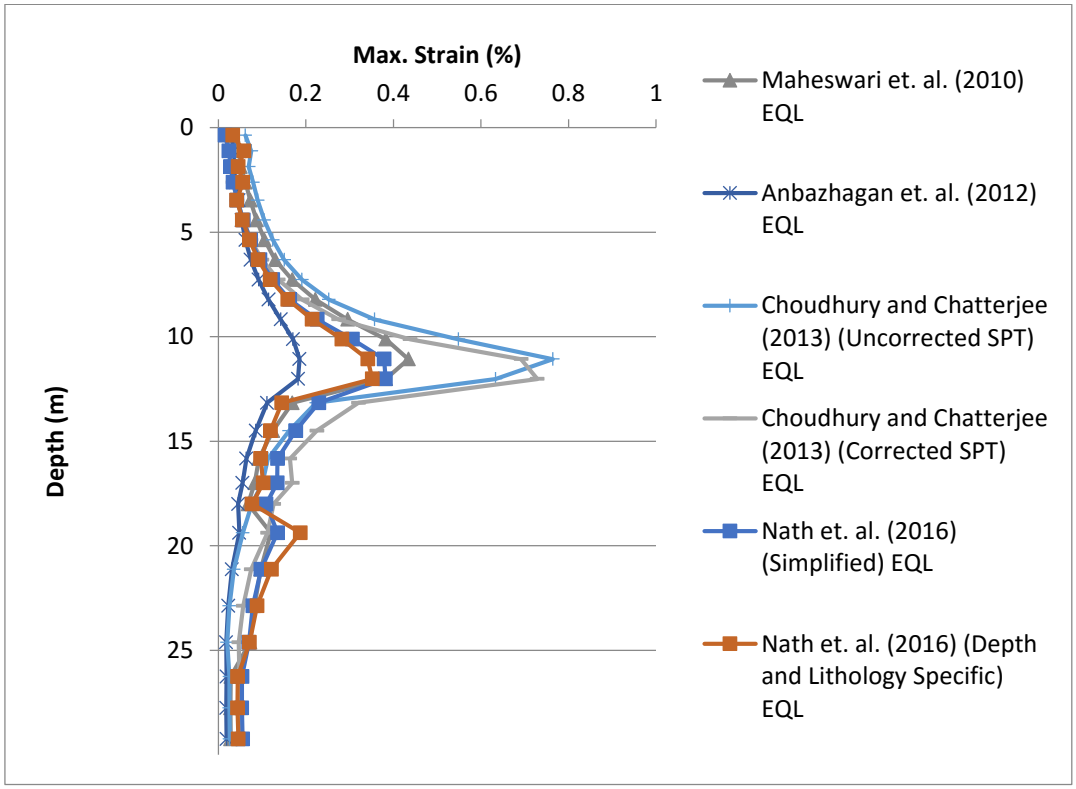

Figure 4.24: Maximum Shear Strain Profiles for Equivalent Linear Analysis for Normal Kolkata Soil Deposit using Spectrally Matched Northridge Earthquake and various N-Vs correlations

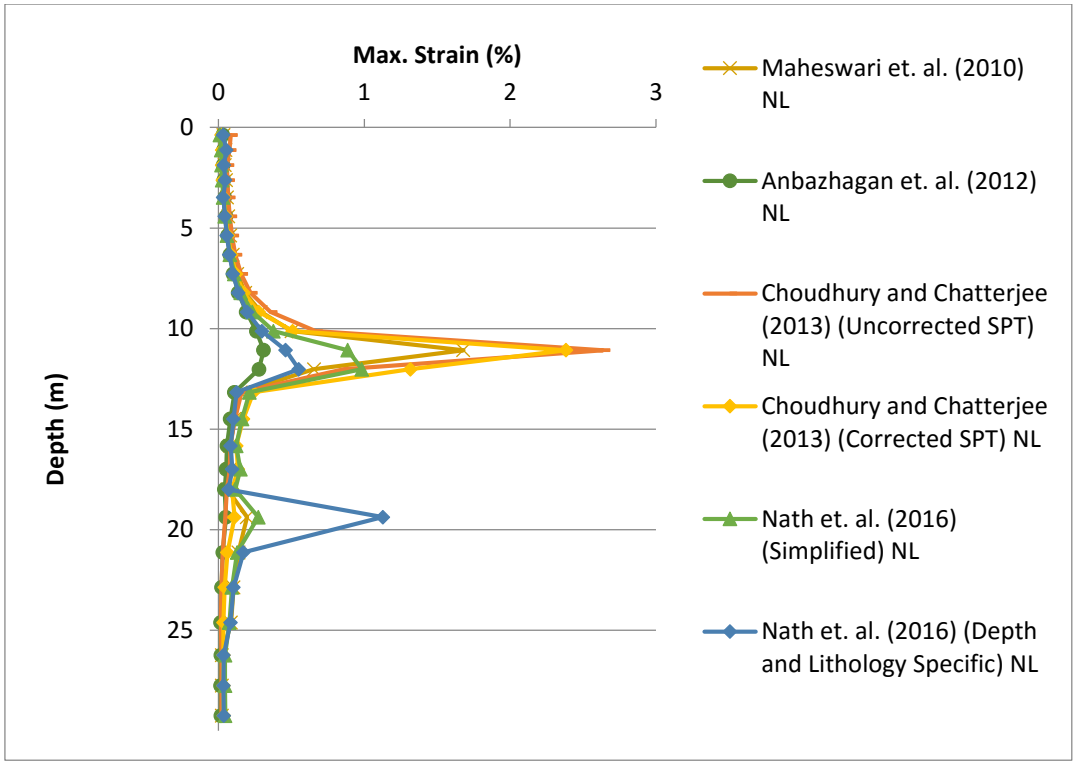

Figure 4.25: Maximum Shear Strain Profiles for Nonlinear Analysis for Normal Kolkata Soil Deposit using Spectrally Matched Northridge Earthquake and various N-Vs correlations

From these figures it may be noted that initially the shear strain is very low with depth and becomes maximum at 10 – 13 m depth below ground surface. Beyond this it reduces and at a depth of about 20m below ground surface it again increases. This is because relative displacement is more or less uniform down to a depth of about 10 m and then it reduces substantially, thus induces a larger strain at a depth of 10 -12 m. Further, the shear strain induced in nonlinear analysis is more than that of equivalent linear analysis and are in the range of 0.2 – 0.8% for equivalent linear and 1 – 4% for nonlinear with higher strain for San Fernando earthquake with higher PGA. The shear strain around 20m depth may be due the presence of sand layer. Shear strain induced in the sand layer by the N-Vs correlation given by Nath et. al. (2016) (Depth and Lithology Specific) is around 1% which may be due to generation of high excess pore pressure in that layer. However, for other cases it is comparatively lesser.

4.2.5.Maximum Stress Ratio

Maximum stress ratio is defined as induced shear stress normalised by effective vertical stress in soil. The comparative representation of maximum stress ratio profiles in equivalent linear and nonlinear analyses for various SPT-Vs correlations are shown in figures (4.26) to (4.29)

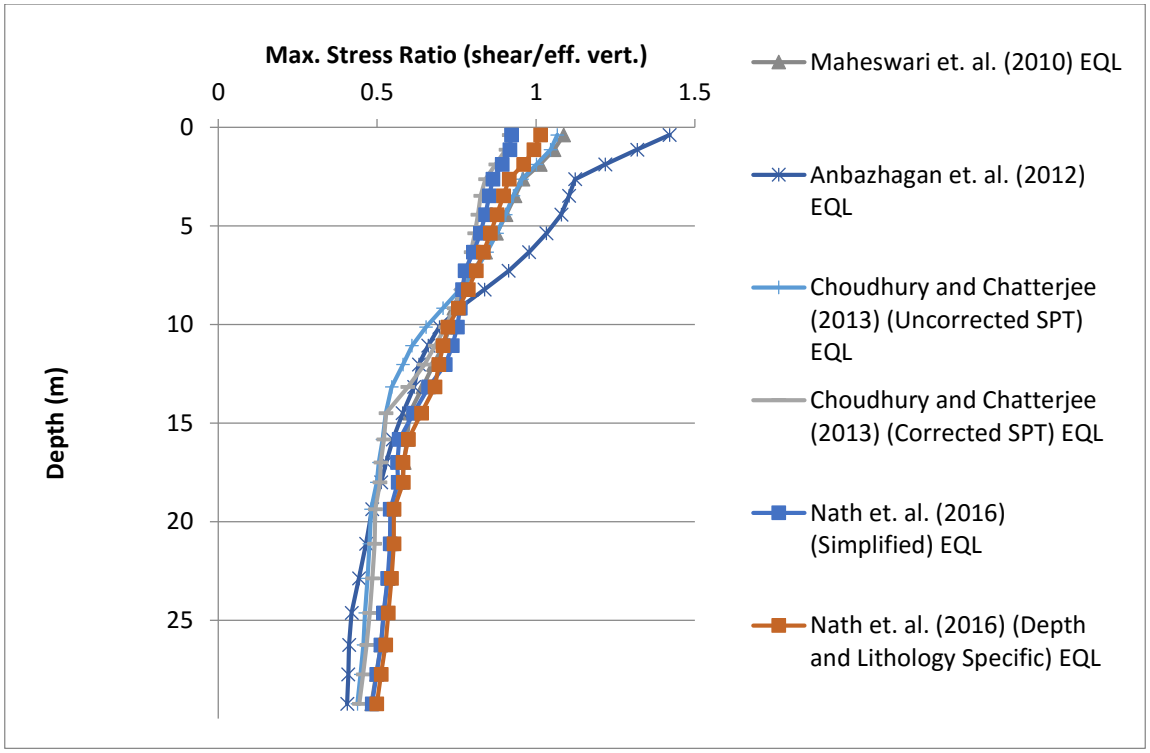

Figure 4.26: Maximum Stress Ratio Profiles for Equivalent Linear Analysis for Normal Kolkata Soil Deposit using Spectrally Matched San Fernando Earthquake and various N-Vs correlations

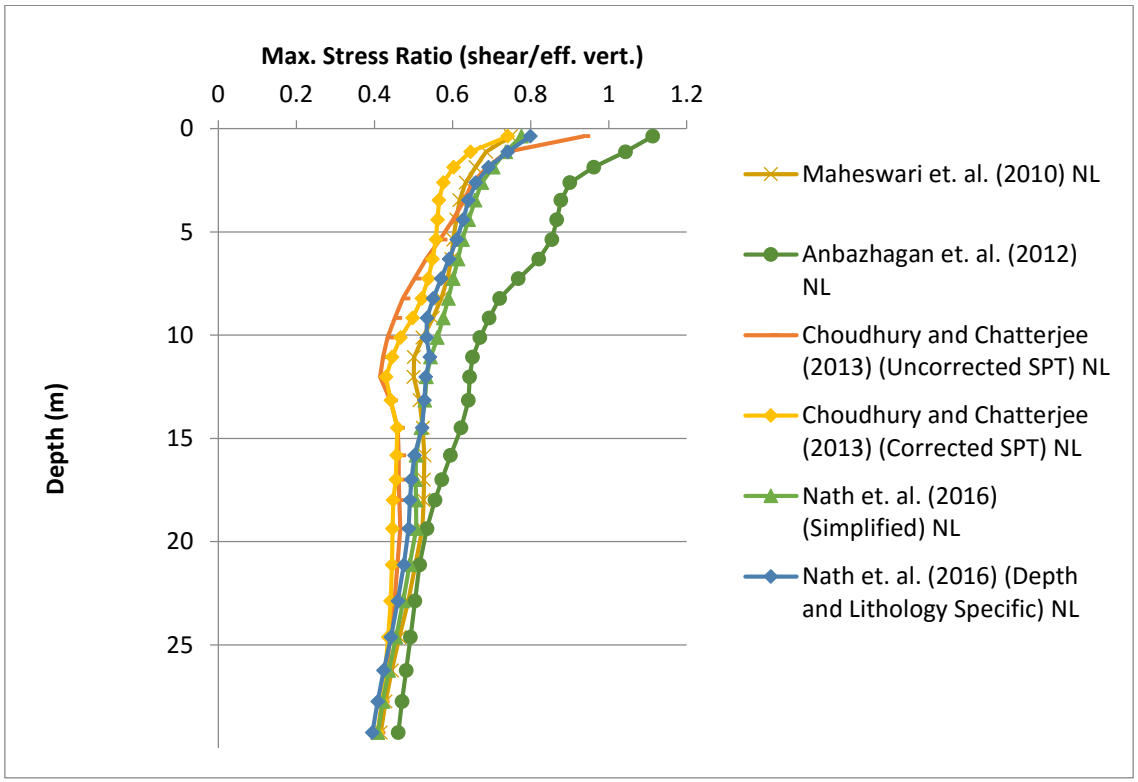

Figure 4.27: Maximum Stress Ratio Profiles for Nonlinear Analysis for Normal Kolkata Soil Deposit using Spectrally Matched San Fernando Earthquake and various N-Vs correlations

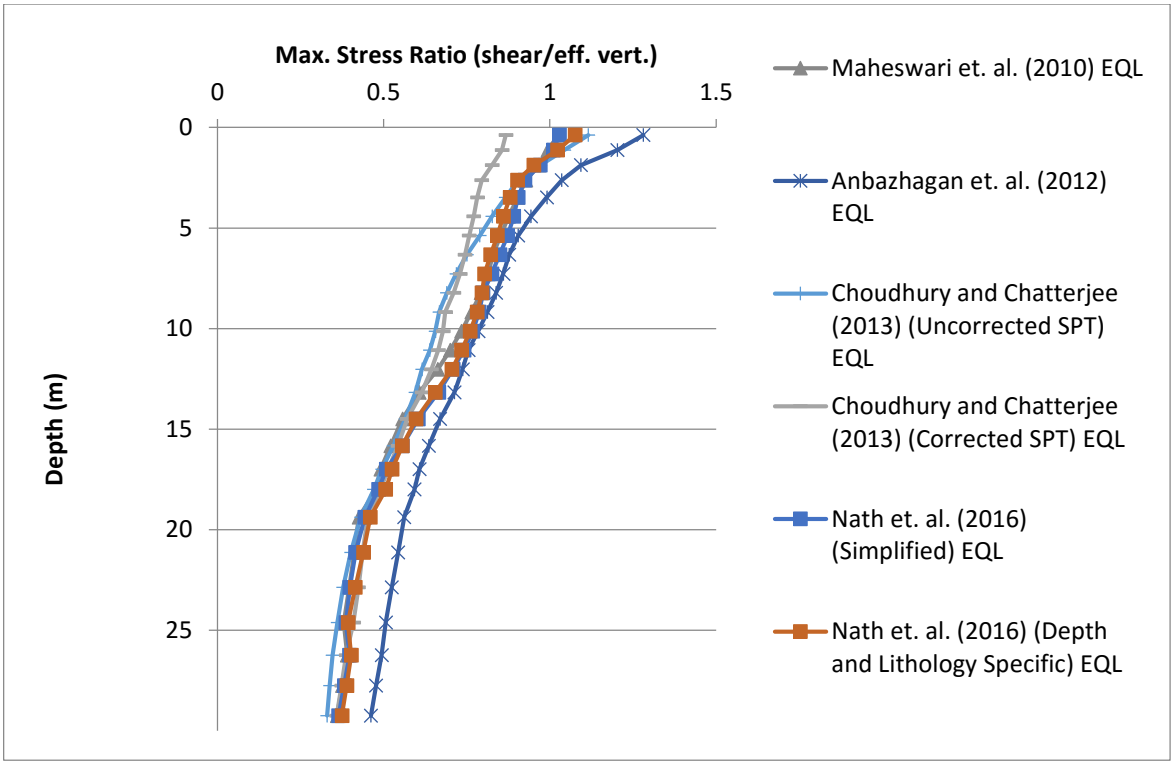

Figure 4.28: Maximum Stress Ratio Profiles for Equivalent Linear Analysis for Normal Kolkata Soil Deposit using Spectrally Matched Northridge Earthquake and various N-Vs correlations

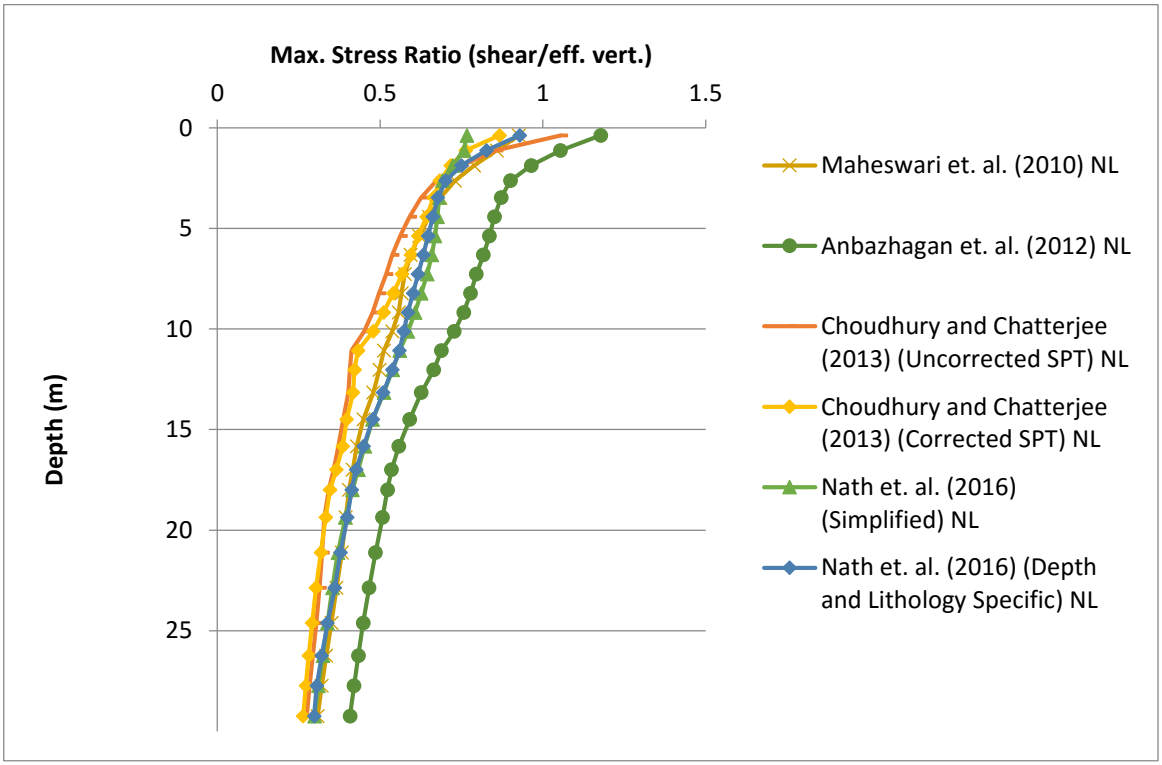

Figure 4.29: Maximum Stress Ratio Profiles for Nonlinear Analysis for Normal Kolkata Soil Deposit using Spectrally Matched Northridge Earthquake and various N-Vs correlations

From the figures 4.26 to4.29, it is observed that, maximum shear stresses induced in the surface layer may be slightly greater than effective stresses with some SPT-Vs correlations down to a depth of about 3m. However, it is in general, less than vertical effective stress and also shows a decreasing trend for all correlations.

4.2.6.Maximum Pore Pressure Ratio

The maximum pore pressure ratio is defined as excess pore pressure generated in the soil due to strong motion shaking normalised by initial vertical effective stress at any depth in the soil profile. In effective stress based nonlinear analysis pore pressure profile can be generated. Comparative analysis of maximum pore pressure variation for various SPT-Vs correlations are shown in figures 4.30 to 4.31.

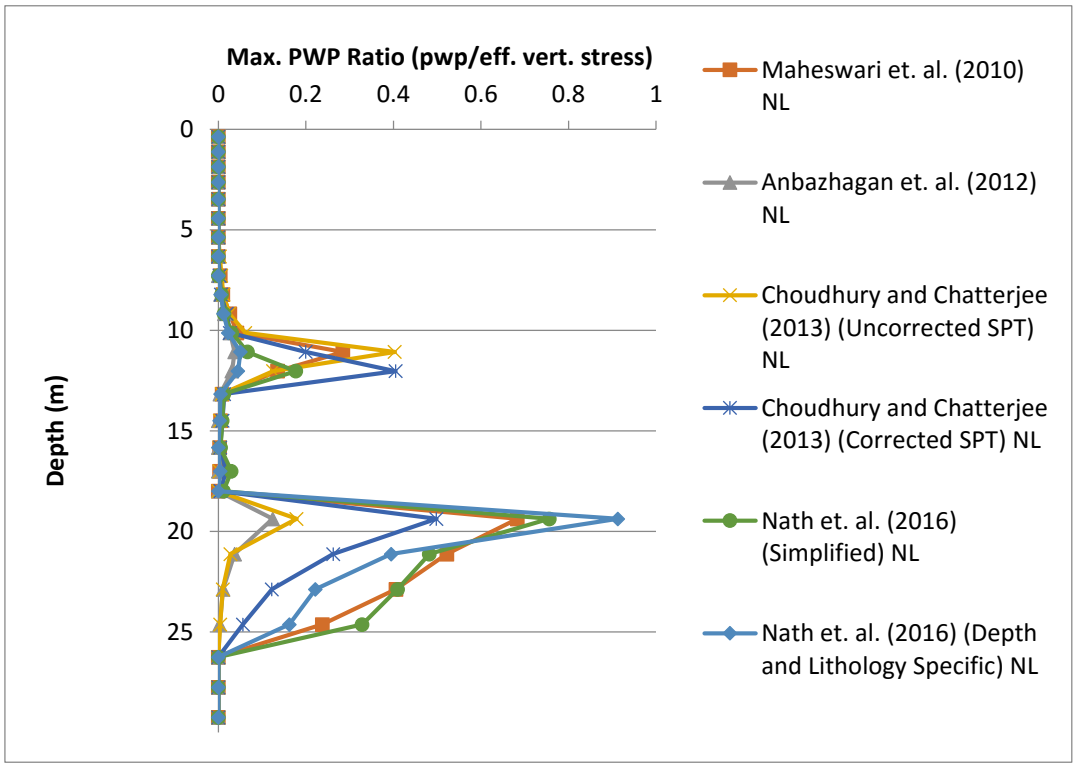

Figure 4.30: Maximum Pore Pressure Ratio Profiles for Nonlinear Analysis for Normal Kolkata Soil Deposit using Spectrally Matched San Fernando Earthquake and various N-Vs correlations

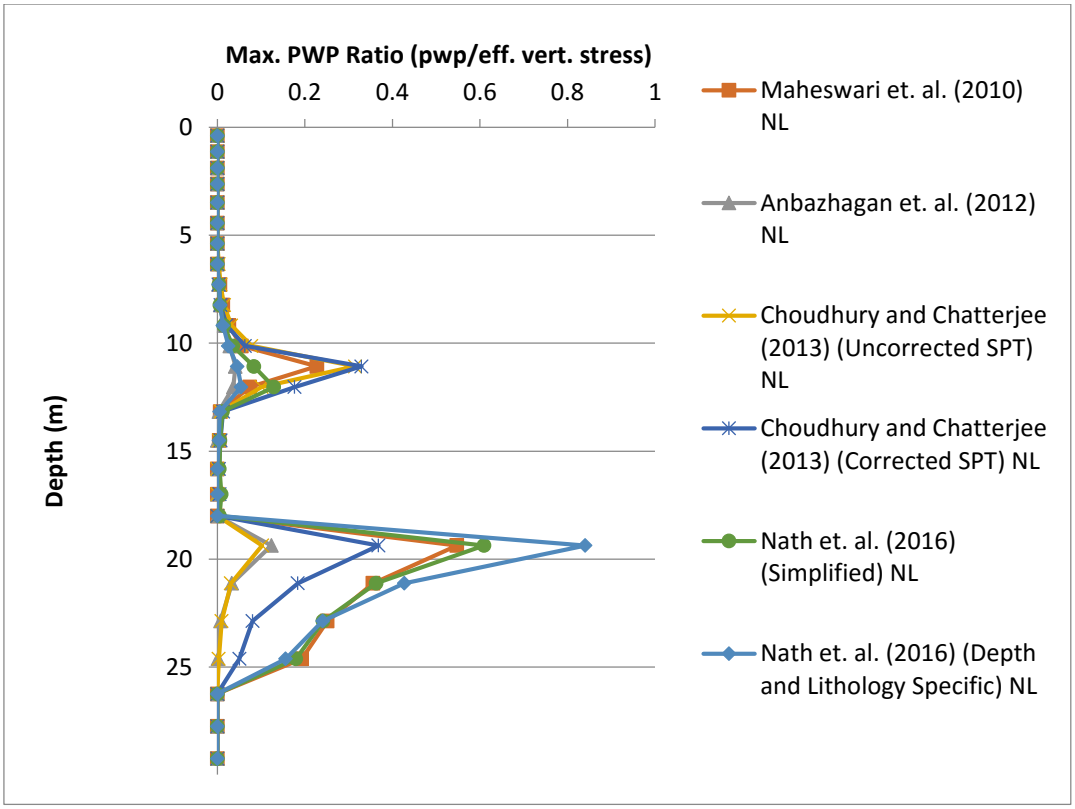

Figure 4.31: Maximum Pore Pressure Ratio Profiles for Nonlinear Analysis for Normal Kolkata Soil Deposit using Spectrally Matched Northridge Earthquake and various N-Vs correlations

From the figures 4.30 and 4.31, it is observed that maximum pore pressure ratio is in the range of 0.1~0.4 at depth 10-12m and 0.1~0.8 at depth about 19~20m. The former is due to high shear strain developed the depth 10-12m and due to presence of sand layer at depth of 18.5-25.5m. The maximum pore pressure ratio as observed in clay layer (at a depth of about 12m) and in the sand layer (at a depth of about 20m) as shown the figures 4.30 and 4.31 are presented in Table 4.2 and 4.3. for various SPT N and Vs correlations.

Table 4.2. Maximum Pore Pressure Ratio in Clay and Sand Layer for San Fernando Earthquake

Correlation	San Fernando			
	Depth (m)	Maximum Pore Pressure Ratio in clay layer	Depth (m)	Maximum Pore Pressure Ratio in sand layer
Maheswari et. al. (2010)	11.1	0.28	19.4	0.68
Anbazhagan et. al. (2012)	11.1	0.04	19.4	0.12

Choudhury and Chatterjee (2013) (Uncorrected SPT)	11.1	0.4	19.4	0.18
Choudhury and Chatterjee (2013) (Corrected SPT)	12.0	0.4	19.4	0.5
Nath et. al. (2016) (Simplified)	12.0	0.18	19.4	0.76
Nath et. al. (2016) (Depth and Lithology Specific)	11.1	0.05	19.4	0.91

Table 4.3. Maximum Pore Pressure Ratio in Clay and Sand Layer for Northridge Earthquake

Correlation	Northridge			
	Depth (m)	Maximum Pore Pressure Ratio in clay layer	Depth (m)	Maximum Pore Pressure Ratio in sand layer
Maheswari et. al. (2010)	11.1	0.23	19.4	0.55
Anbazhagan et. al. (2012)	11.1	0.04	19.4	0.12
Choudhury and Chatterjee (2013) (Uncorrected SPT)	11.1	0.31	19.4	0.10
Choudhury and Chatterjee (2013) (Corrected SPT)	11.1	0.33	19.4	0.37

Nath et. al. (2016) (Simplified)	12.0	0.13	19.4	0.61
Nath et. al. (2016) (Depth and Lithology Specific)	12.0	0.05	19.4	0.84

4.2.7.Fourier Amplification Ratio

Fourier amplification ratio is the ratio of Fourier amplitude of the surface acceleration time history to the Fourier amplitude of the input acceleration time history. It indicates the transfer of the bedrock response to the ground surface at various frequencies. Fourier amplification ratio variation with different frequencies for two strong motions are shown in figures 4.32 to 4.33.

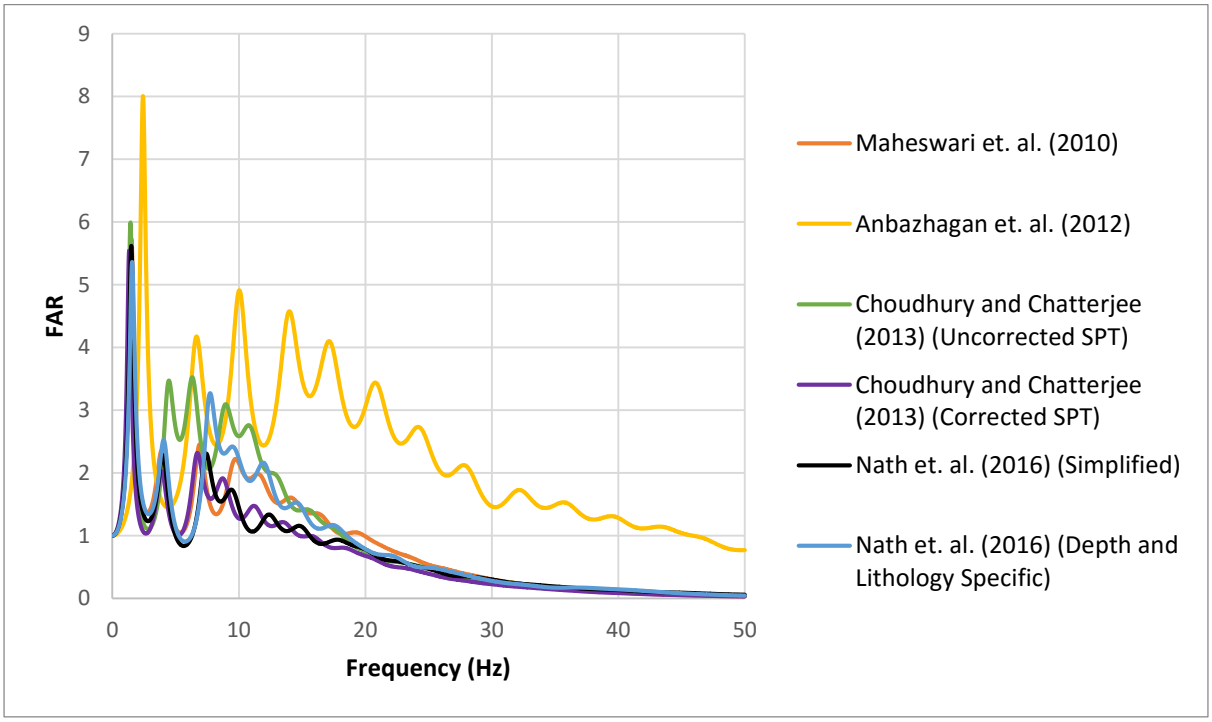

Figure 4.32: Fourier Amplification Ratio for Equivalent Linear Analysis for Normal Kolkata Soil Deposit using Spectrally Matched San Fernando Earthquake and various N-Vs correlations

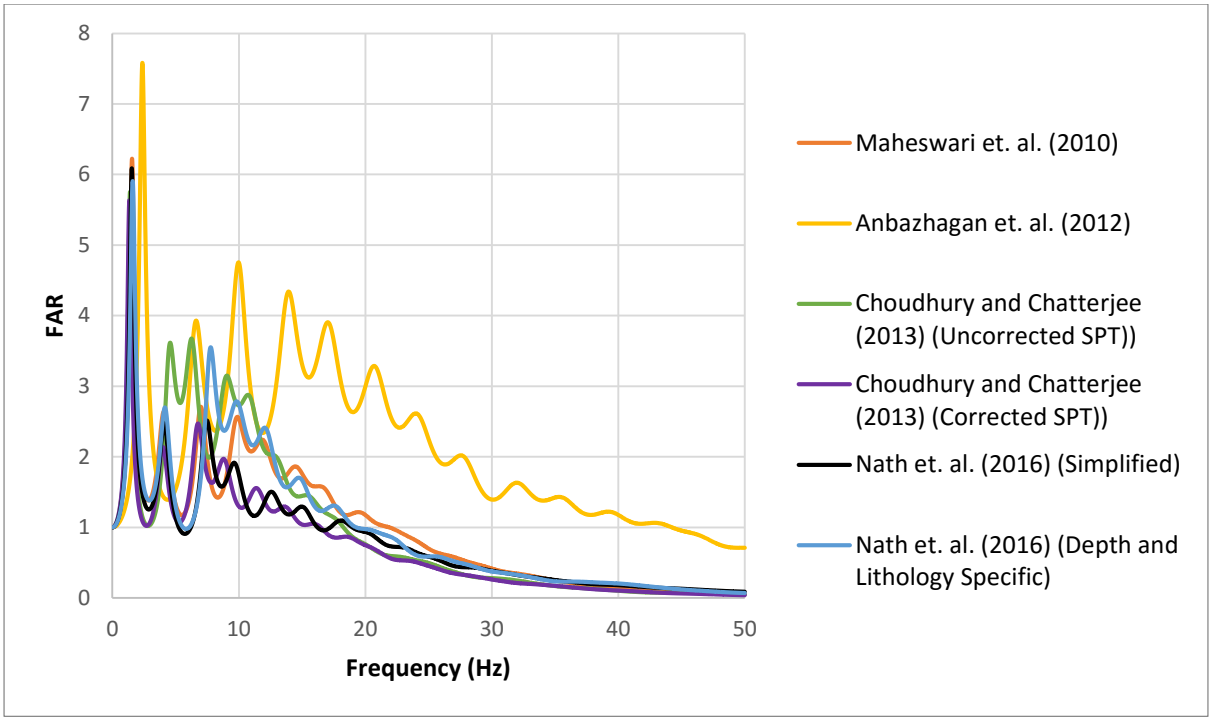

Figure 4.33: Fourier Amplification Ratio for Equivalent Linear Analysis for Normal Kolkata Soil Deposit using Spectrally Matched Northridge Earthquake and various N-Vs correlations

From figures 4.32 to 4.33, the maximum FAR and corresponding frequencies are shown in Table 4.4.

Table 4.4: FAR and Corresponding Frequencies

SPT-Vs Correlations	Natural Frequency of the Soil Profile (Hz)	San Fernando		Northridge	
		Maximum FAR	Corresponding Frequency (Hz)	Maximum FAR	Corresponding Frequency (Hz)
Maheswari et. al. (2010)	1.6	5.69	1.53	6.15	1.53
Anbazhagan et. al. (2012)	2.12	7.9	2.45	7.46	2.41
Choudhury and Chatterjee (2013) (Uncorrected SPT)	1.56	5.97	1.42	5.67	1.42

Choudhury and Chatterjee (2013) (Corrected SPT)	1.58	5.48	1.35	5.51	1.37
Nath et. al. (2016) (Simplified)	1.66	5.57	1.52	6	1.56
Nath et. al. (2016) (Depth and Lithology Specific)	1.65	5.32	1.59	5.8	1.64
Average	1.695	6	1.643	6.1	1.655
Range	1.56 - 2.12	5.32 - 7.9	1.35 – 2.45	5.51 – 7.46	1.37 – 2.41

It is observed that, soil profile gets amplified at frequencies close to the natural frequency of the soil column but due to hysteretic damping and bedrock elasticity, resonance never occurs. FAR for Normal Kolkata Deposit soil subjected to spectral compatible strong motions can be in the range of 5~8 and the corresponding frequency range is 1.35 – 2.45Hz which is close to natural frequency of soil column. It is also observed that normal Kolkata soil deposit will get amplified in the frequency range of 0.4-15 Hz.

4.2.8. Acceleration Response Spectra

The IS:1893 (Part 1)-2002 has prescribed acceleration response spectra for different types of soil namely, soft soil, medium to dense soil and hard soil. But site specific acceleration response spectra is necessary due to local site effects. If the soil column can be assumed be a single degree of freedom system (SDOF), the acceleration response spectra shows the peak acceleration response of soil column for different time periods. The acceleration response spectra calculated for equivalent linear and nonlinear analyses for two different strong motions are shown in figures 4.34 to 4.37.

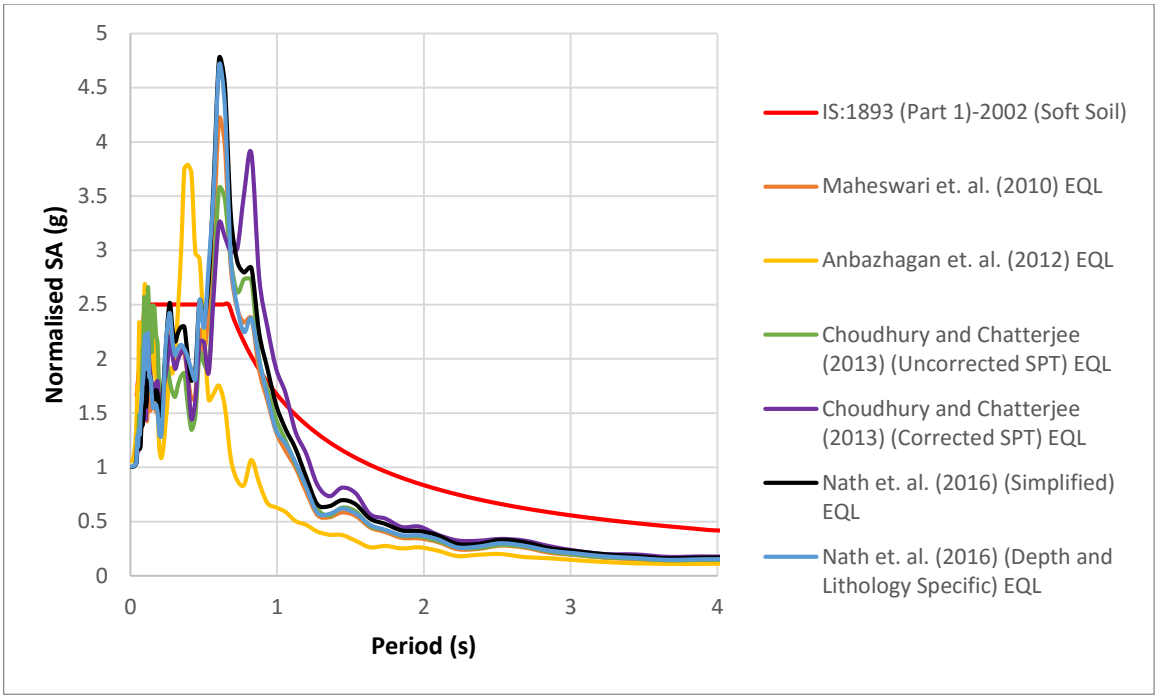

Figure 4.34: Normalised Spectral Acceleration for Equivalent Linear Analysis for Normal Kolkata Soil Deposit using Spectrally Matched San Fernando Earthquake and various N-Vs correlations

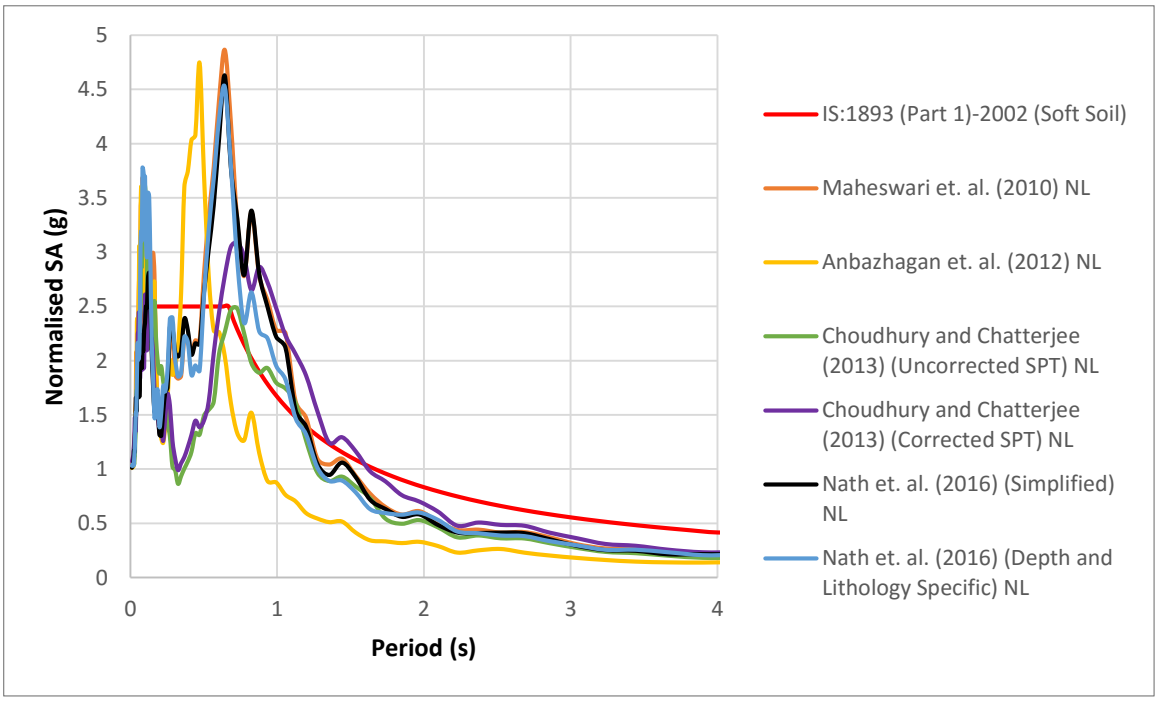

Figure 4.35: Normalised Spectral Acceleration for Nonlinear Analysis for Normal Kolkata Soil Deposit using Spectrally Matched San Fernando Earthquake and various N-Vs correlations

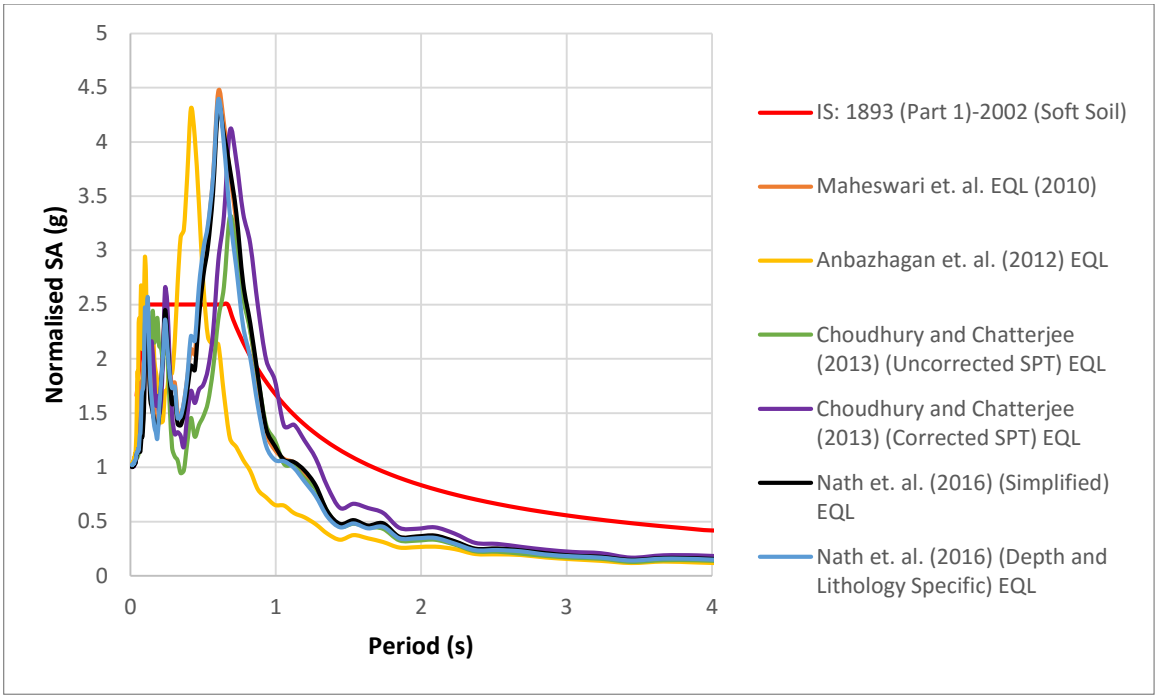

Figure 4.36: Normalised Spectral Acceleration for Equivalent Linear Analysis for Normal Kolkata Soil Deposit using Spectrally Matched Northridge Earthquake and various N-Vs correlations

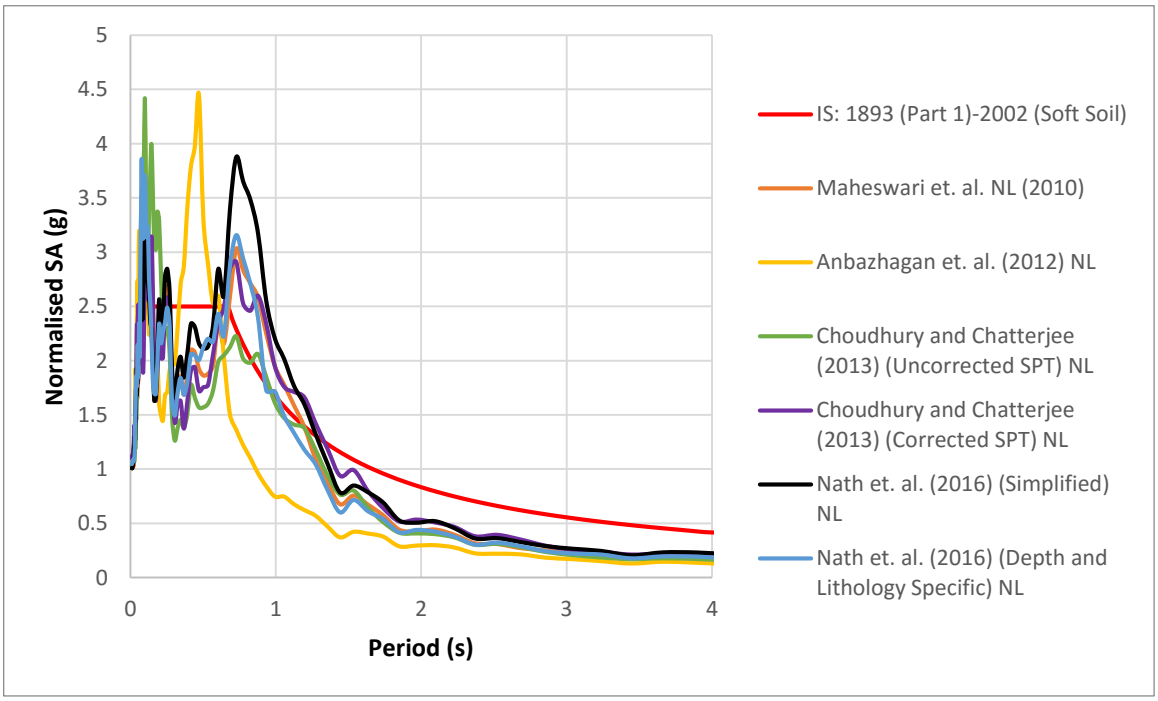

Figure 4.37: Normalised Spectral Acceleration for Nonlinear Analysis for Normal Kolkata Soil Deposit using Spectrally Matched Northridge Earthquake and various N-Vs correlations

The calculated acceleration response spectra are compared with IS:1893 (Part 1)-2002 (Soft Soil) and considerable variations are found in the calculated response spectra and the IS code prescribed response spectra. The results of peak spectral acceleration obtained from equivalent linear and nonlinear analyses and their corresponding time periods for two different ground motions are presented in the Table 4.5 and 4.6.

Table 4.5. Peak Acceleration Response and Corresponding Time Periods for Spectrum Compatible San Fernando Earthquake

Correlations	San Fernando Earthquake			
	Equivalent Linear		Nonlinear	
	Peak Spectral Acceleration (g)	Corresponding Time Period (s)	Peak Spectral Acceleration (g)	Corresponding Time Period (s)
Maheswari et. al. (2010)	4.2	0.6	4.9	0.64
Anbazhagan et. al. (2012)	3.8	0.4	4.7	0.47
Choudhury and Chatterjee (2013) (Uncorrected SPT)	3.5	0.6	3.6	0.1
Choudhury and Chatterjee (2013) (Corrected SPT)	3.9	0.8	3.1	0.73
Nath et. al. (2016) (Simplified)	4.8	0.6	4.6	0.64
Nath et. al. (2016) (Depth and Lithology Specific)	4.8	0.6	4.5	0.64
Average	4.17	0.6	4.23	0.54
Range	3.5-4.8	0.4-0.8	3.1-4.9	0.1-.73

Table 4.6. Peak Acceleration Response and Corresponding Time Periods for Spectrum Compatible Northridge Earthquake

Correlations	Northridge Earthquake			
	Equivalent Linear		Nonlinear	
	Peak Spectral Acceleration (g)	Corresponding Time Period (s)	Peak Spectral Acceleration (g)	Corresponding Time Period (s)
Maheswari et. al. (2010)	4.5	0.6	3.6	0.1
Anbazhagan et. al. (2012)	4.3	0.4	4.5	0.47
Choudhury and Chatterjee (2013) (Uncorrected SPT)	3.3	0.68	4.4	0.1
Choudhury and Chatterjee (2013) (Corrected SPT)	3.8	0.73	2.8	0.1
Nath et. al. (2016) (Simplified)	4.3	0.6	3.9	0.7
Nath et. al. (2016) (Depth and Lithology Specific)	4.4	0.6	3.9	0.1
Average	4.1	0.6	3.85	0.26
Range	3.3-4.5	0.4-0.73	2.8-4.5	0.1-0.7

4.3. EQUIVALENT LINEAR AND NONLINEAR ANALYSES FOR RIVER CHANNEL DEPOSIT USING DEEPSOIL

The two input motions spectrum compatible with the response spectra of IS:1893 (Part 1)-2002 Zone 4 medium dense soil as mentioned in Chapter 3 are presented in figures 4.38 and 4.39. PGA of these two input motions are 0.255g and 0.211g respectively. In this context, it is worthwhile to mention that Peak

Bed Rock Acceleration of Kolkata region as reported by various researchers are in the range of 0.1g to 0.34g (Roy and Sahu, 2012; Akhila et. al., 2012; Govindaraju and Bhattacharya, 2012).

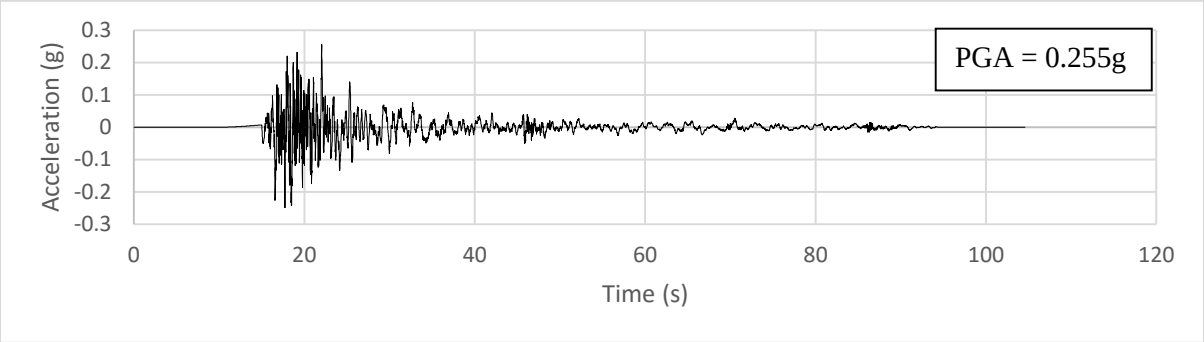

Figure 4.38: Matched San Fernando Earthquake Acceleration Time History

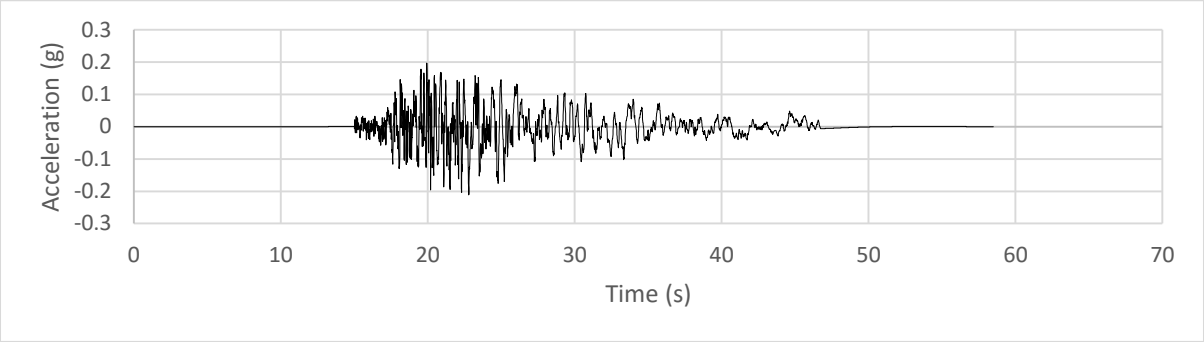

Figure 4.39: Matched Northridge Earthquake Acceleration Time History

4.3.1.Peak Ground Acceleration (PGA)

The variation of PGA with depth for different N-Vs correlations for equivalent linear and nonlinear analyses are separately presented in figures 4.40 to 4.47 for comparison. In figures 4.48 to 4.51, PGA for different N-Vs correlations as obtained from equivalent linear and nonlinear analyses are presented sseparately.

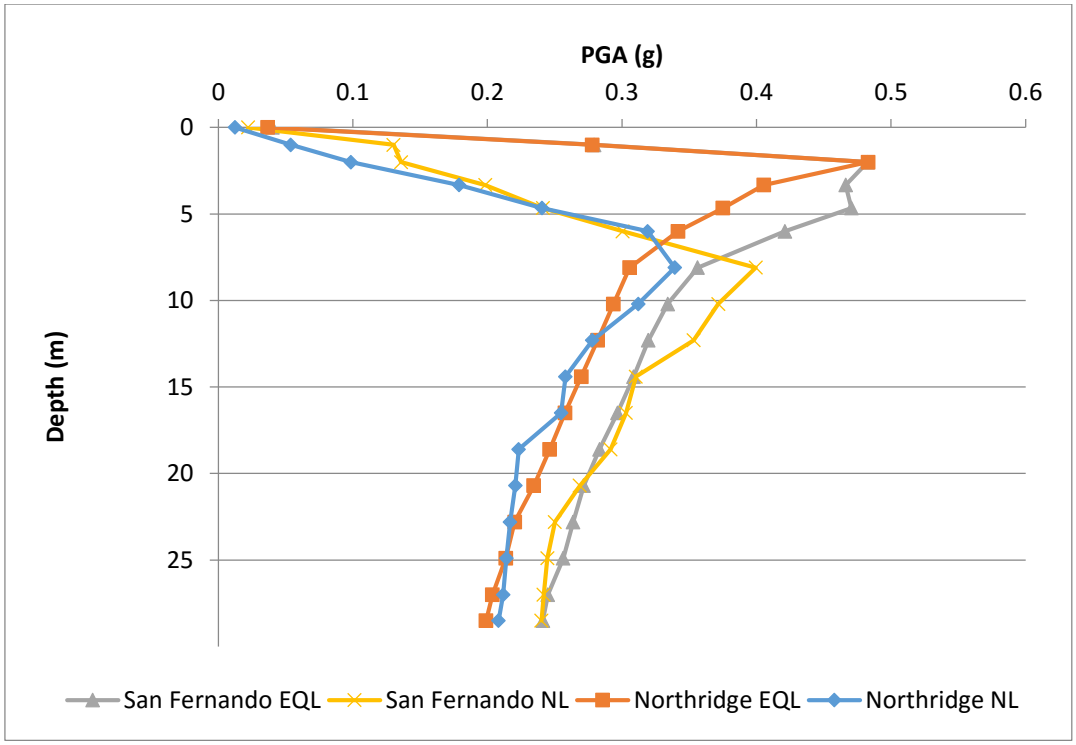

Figure 4.40: PGA Profiles for Equivalent Linear and Nonlinear Analysis using N-Vs correlations given by Jafari et. al. (2010)

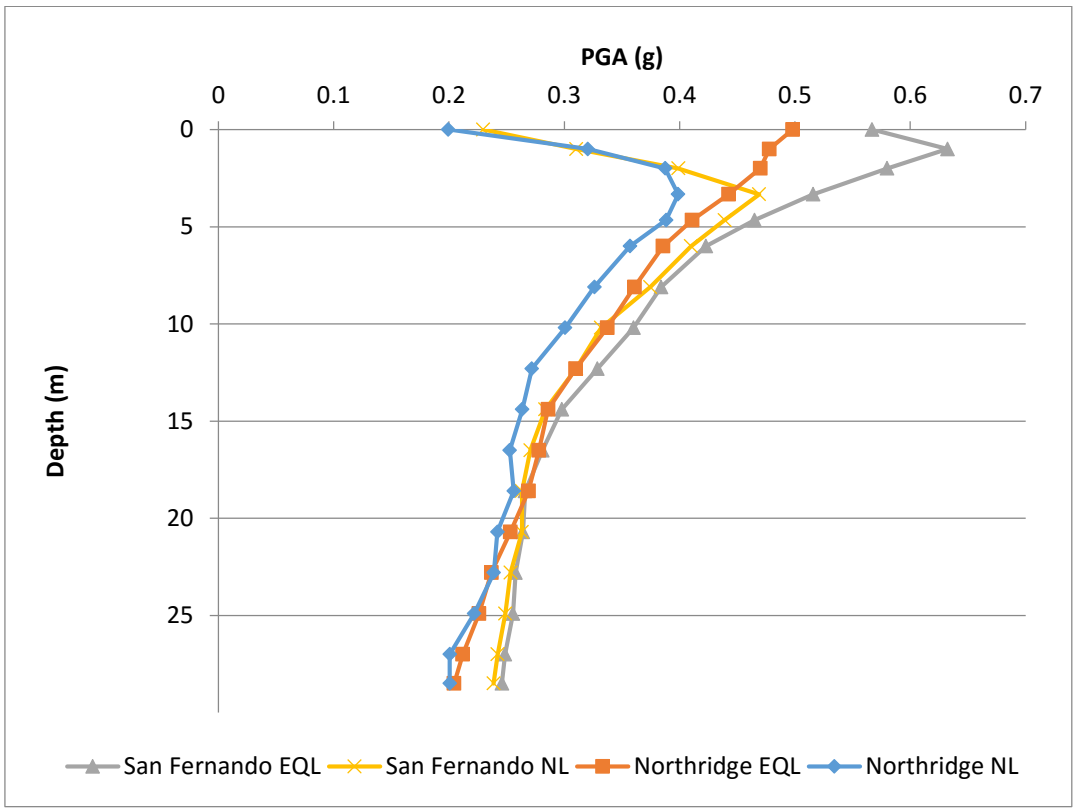

Figure 4.41: PGA Profiles for Equivalent Linear and Nonlinear Analysis using N-Vs correlations given by Hanumantharao and Ramana (2008)

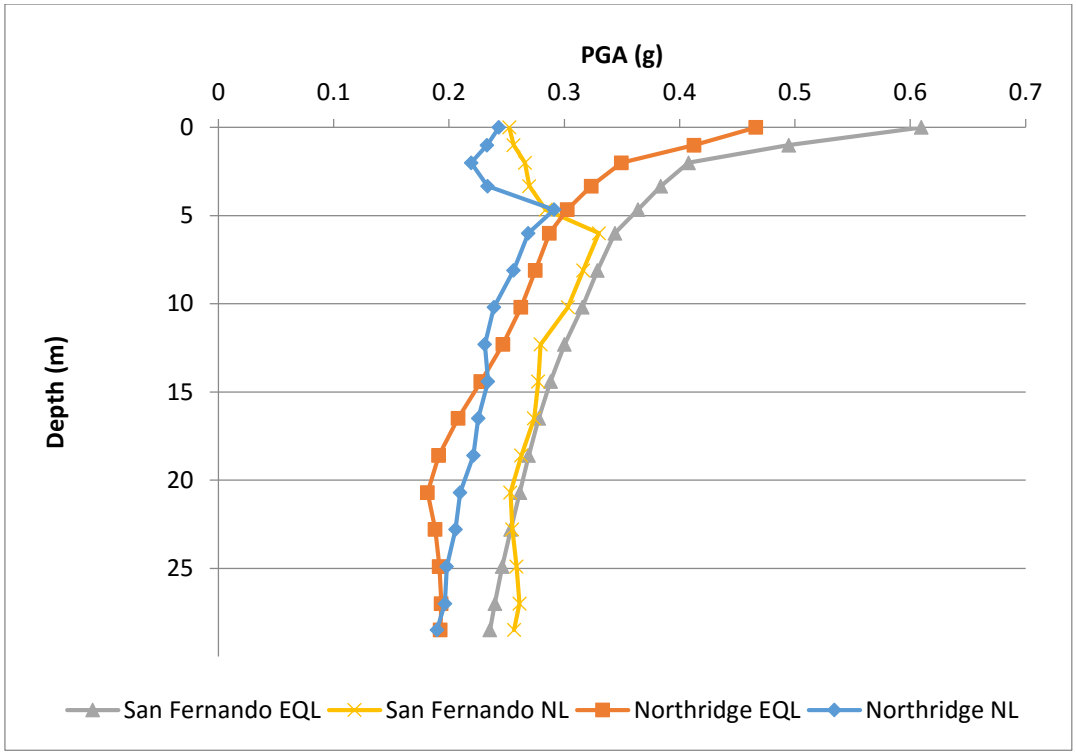

Figure 4.42: PGA Profiles for Equivalent Linear and Nonlinear Analysis using N-Vs correlations given by Maheswari et. al. (2010)

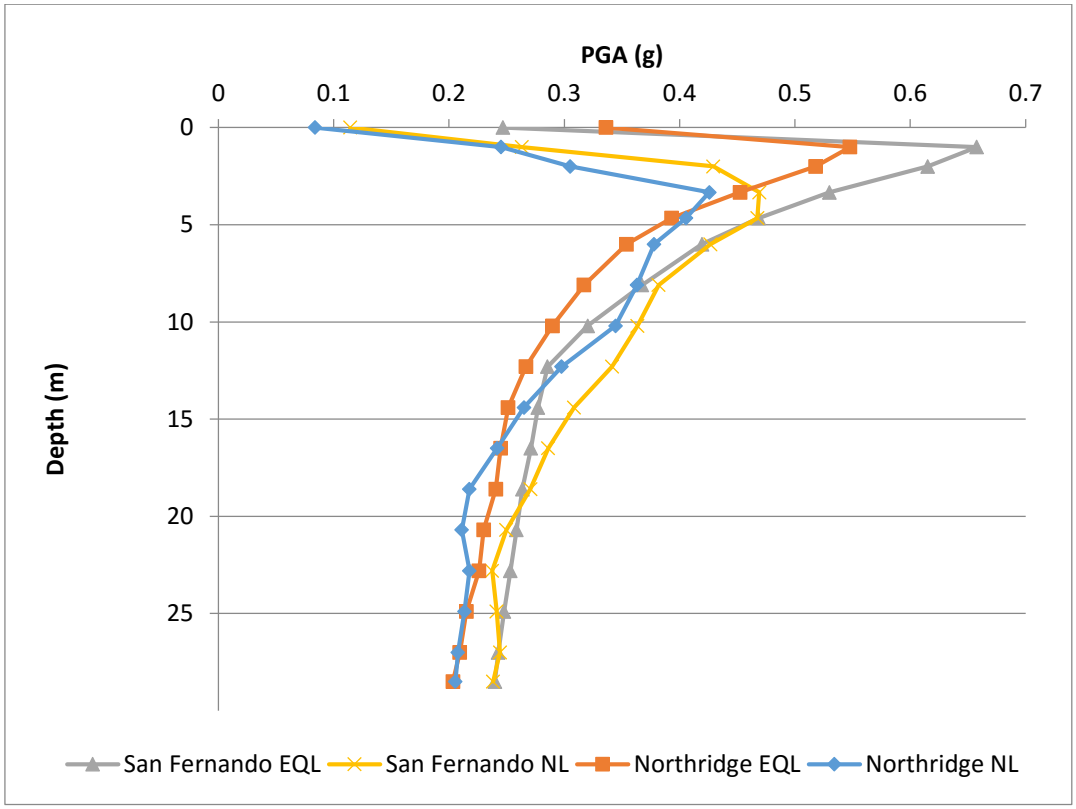

Figure 4.43: PGA Profiles for Equivalent Linear and Nonlinear Analysis using N-Vs correlations given by Anbazhagan et. al. (2012)

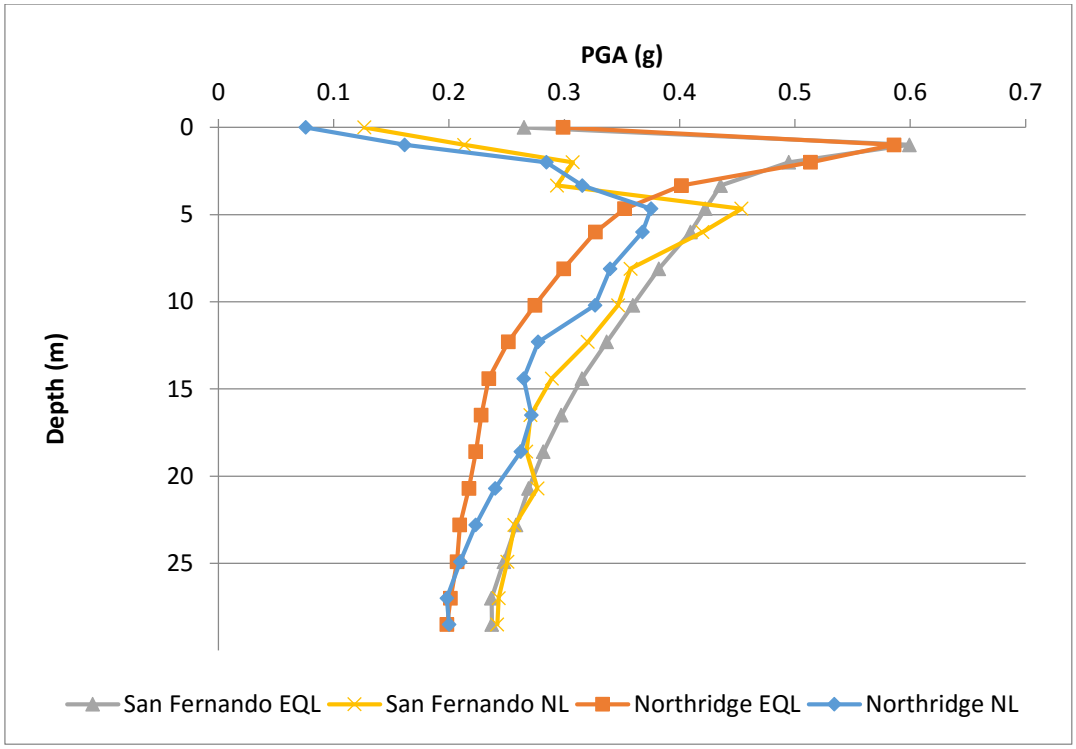

Figure 4.44: PGA Profiles for Equivalent Linear and Nonlinear Analysis using N-Vs correlations given by Choudhury and Chatterjee (2013) (Uncorrected SPT)

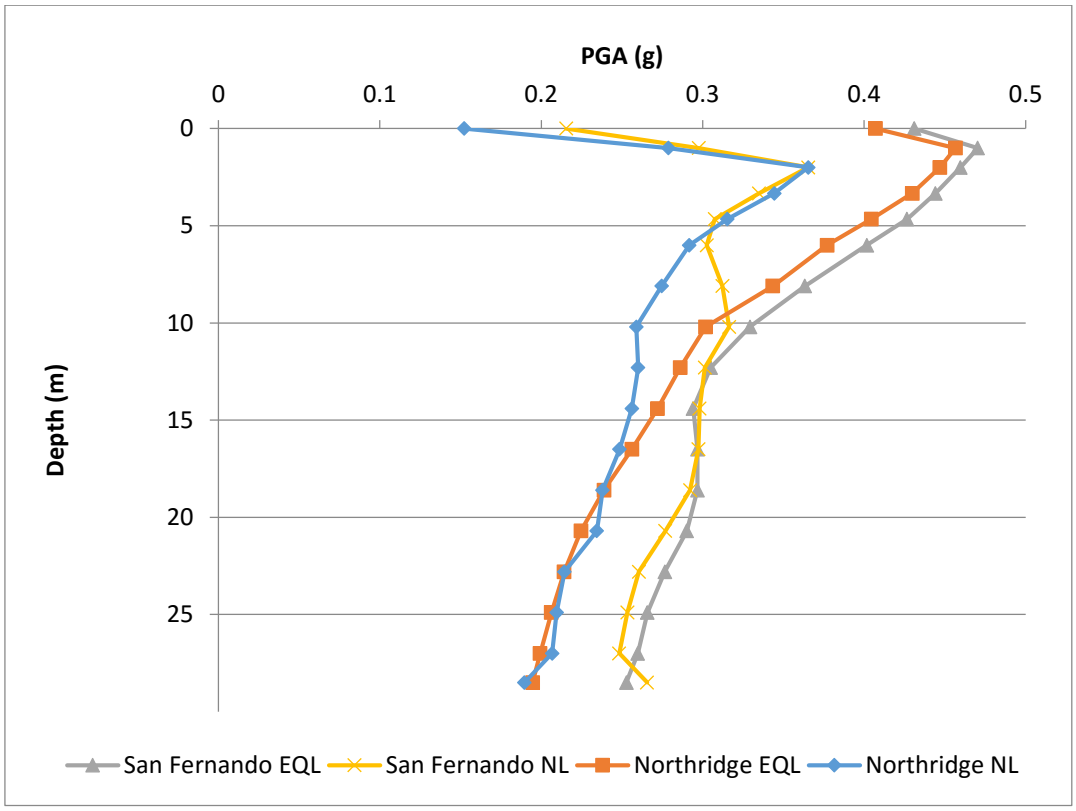

Figure 4.45: PGA Profiles for Equivalent Linear and Nonlinear Analysis using N-Vs correlations given by Choudhury and Chatterjee (2013) (Corrected SPT)

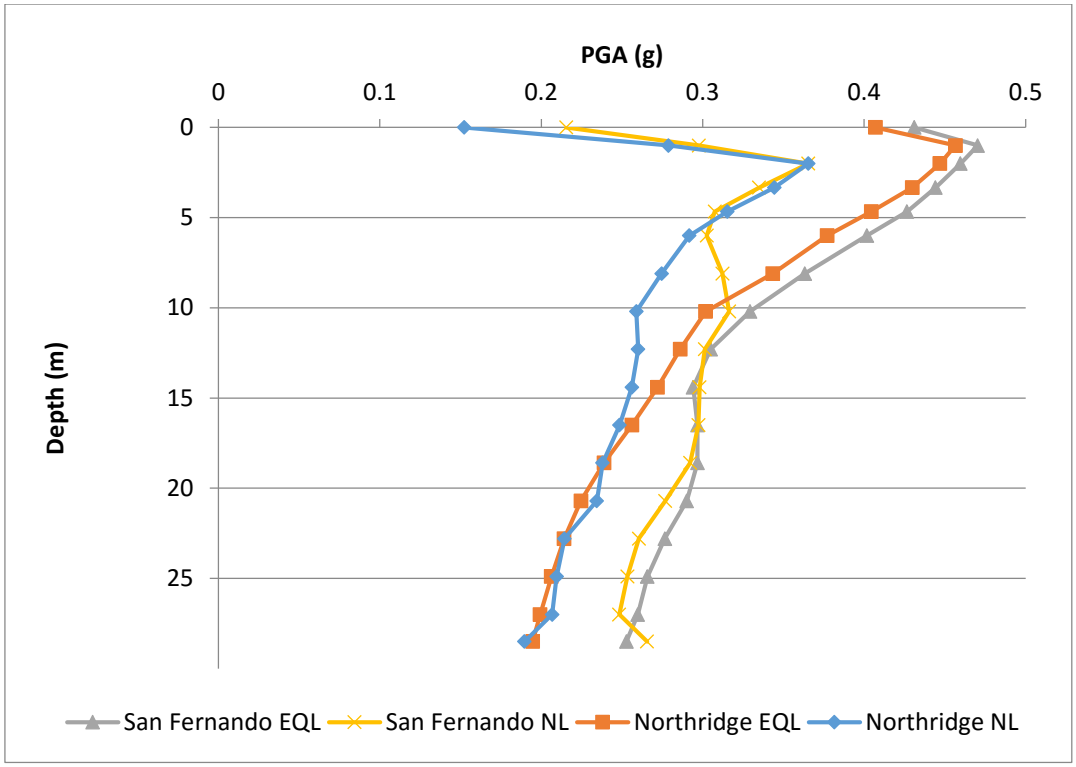

Figure 4.46: PGA Profiles for Equivalent Linear and Nonlinear Analysis using N-Vs correlations given by Nath et. al. (2016) (Simplified)

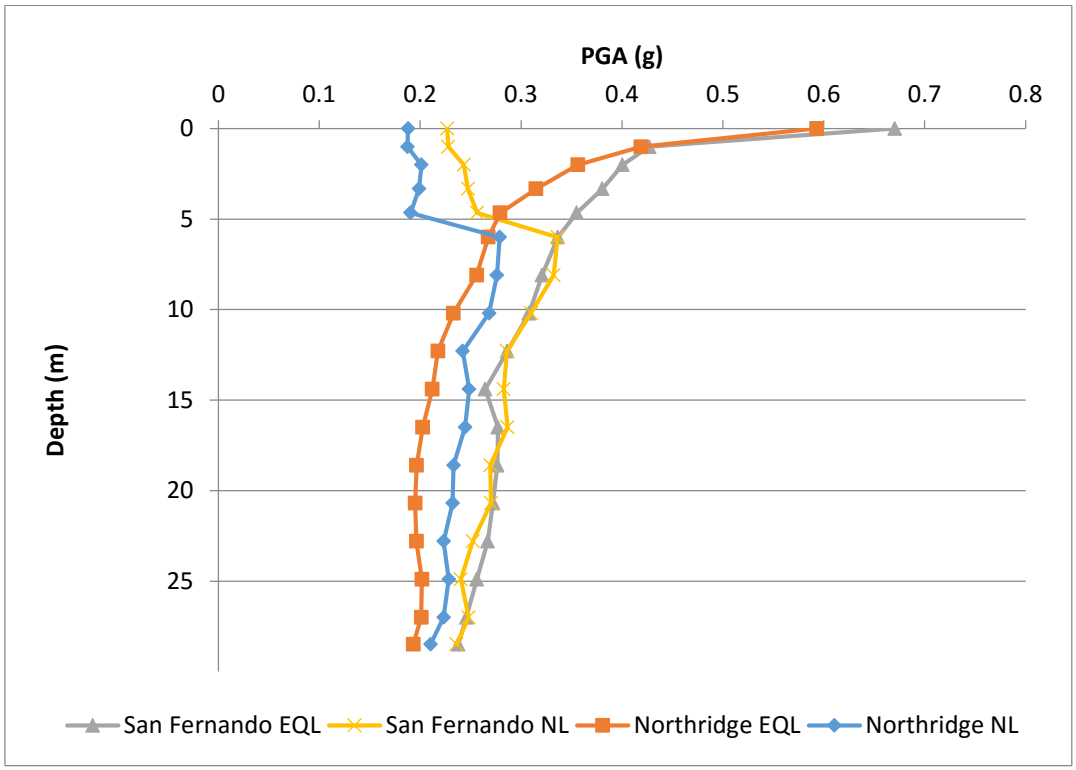

Figure 4.47: PGA Profiles for Equivalent Linear and Nonlinear Analysis using N-Vs correlations given by Nath et. al. (2016) (Depth and Lithology Specific)

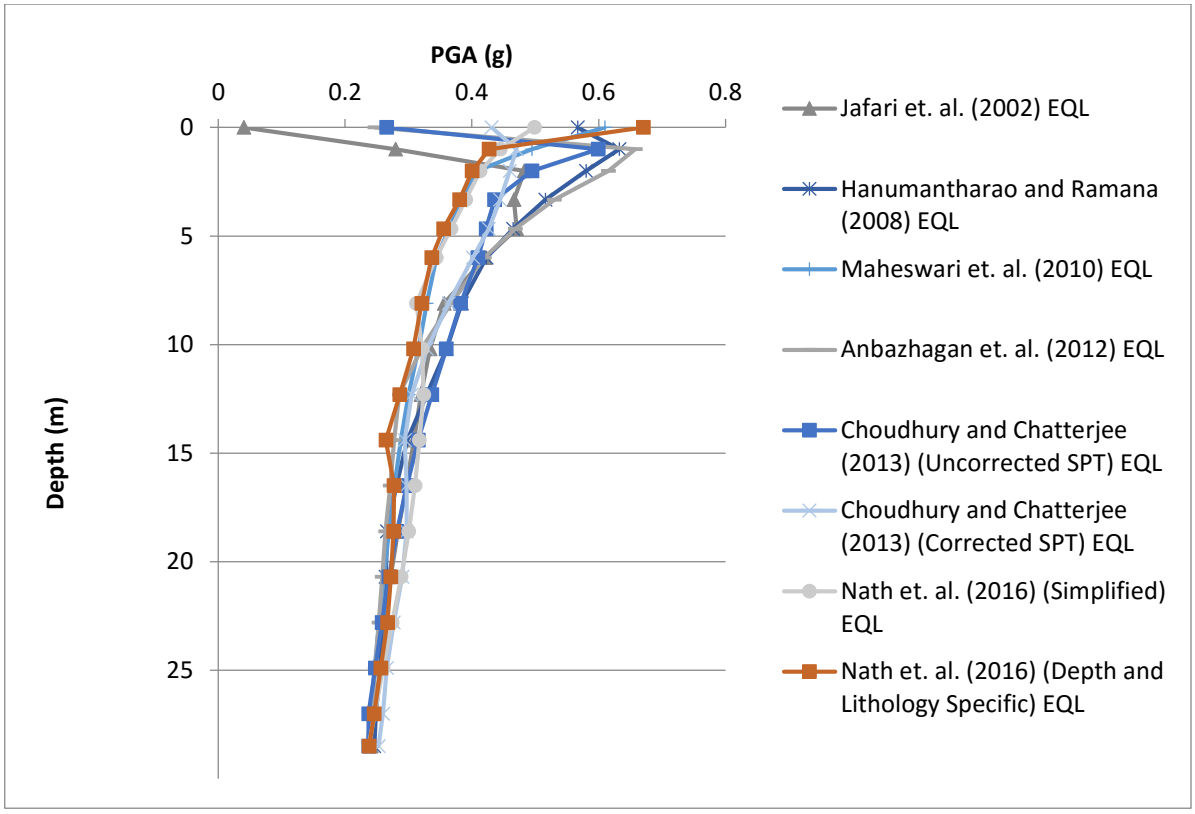

Figure 4.48: PGA Profiles for Equivalent Linear Analysis for River Channel Soil Deposit using Spectrally Matched San Fernando Earthquake and various N-Vs correlations

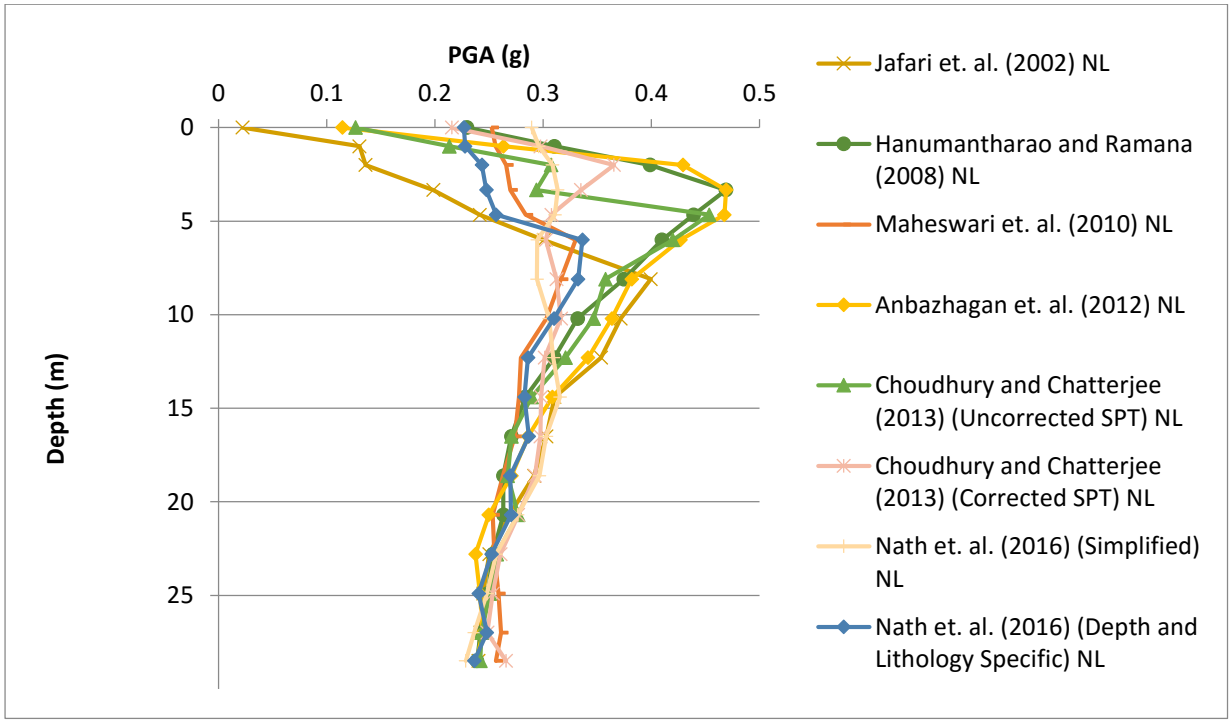

Figure 4.49: PGA Profiles for Nonlinear Analysis for River Channel Soil Deposit using Spectrally Matched San Fernando Earthquake and various N-Vs correlations

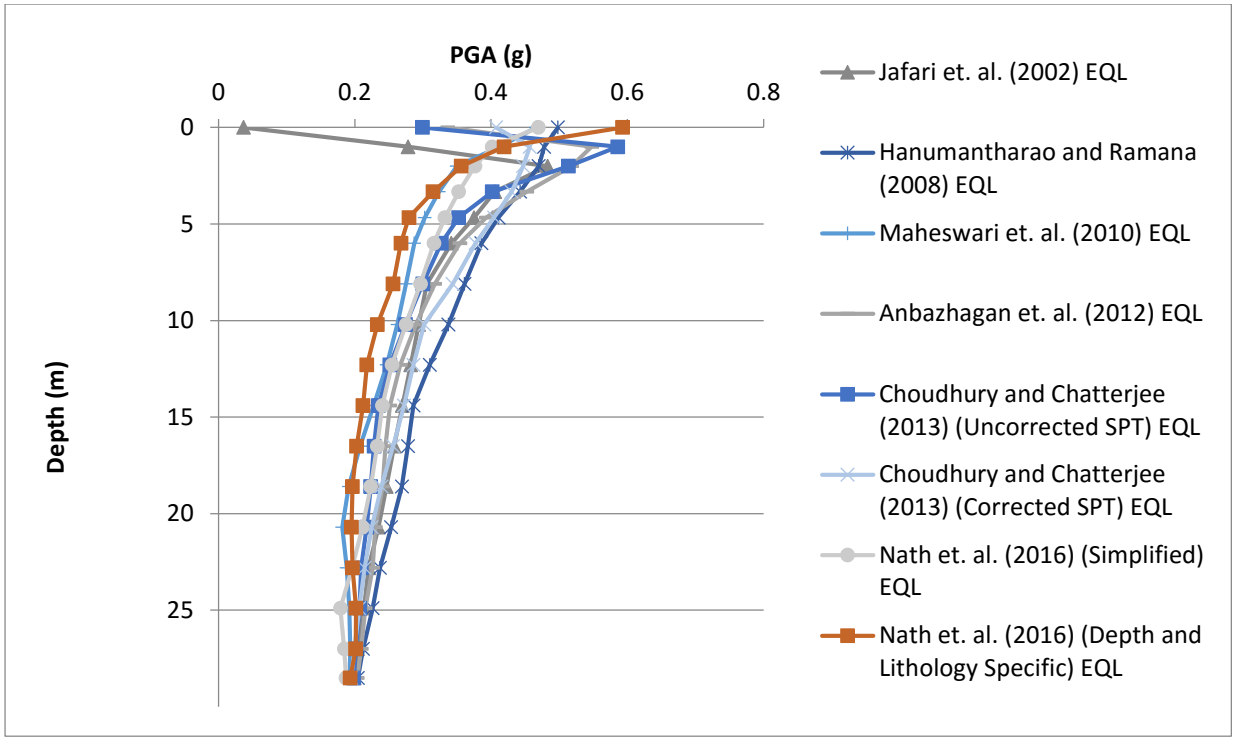

Figure 4.50: PGA Profiles for Equivalent Linear Analysis for River Channel Soil Deposit using Spectrally Matched Northridge Earthquake and various N-Vs correlations

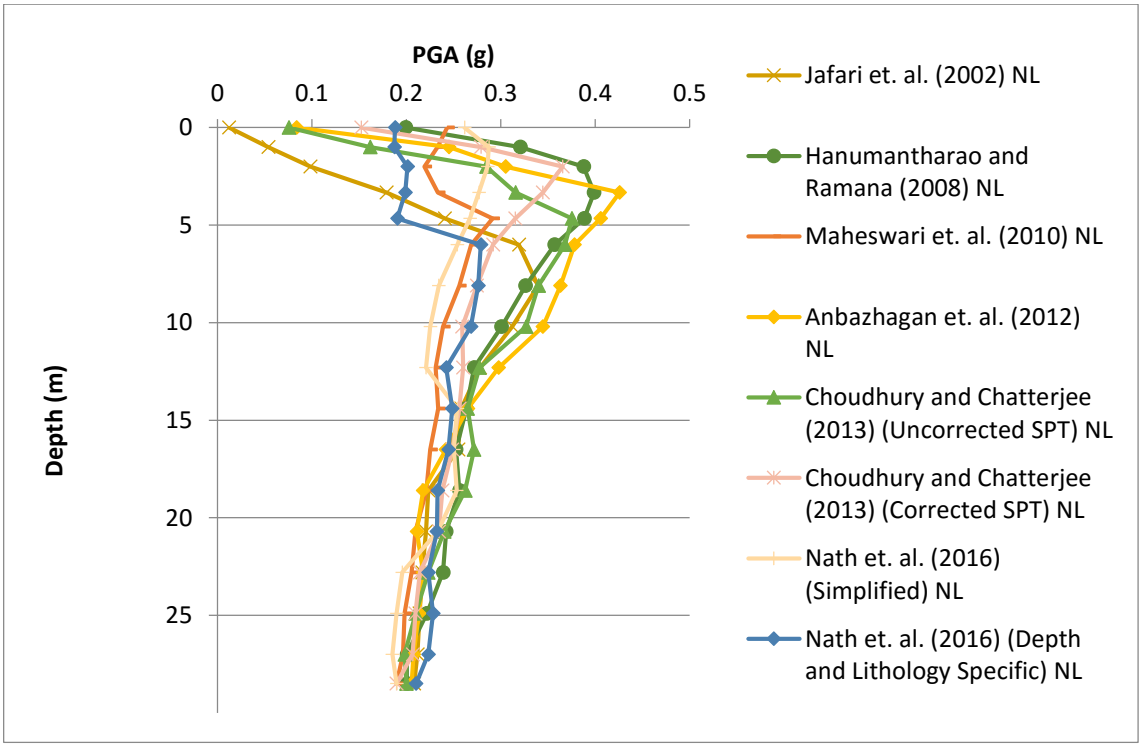

Figure 4.51: PGA Profiles for Nonlinear Analysis for River Channel Soil Deposit using Spectrally Matched Northridge Earthquake and various N-Vs correlations

From the figures 4.40 to 4.51, it may be observed that for both equivalent linear and nonlinear analyses, PGA from bedrock in general increases up to a depth of 5m below ground surface. Above this it further increases for equivalent linear analysis while reduces substantially for nonlinear analysis. The differences in PGA variation for different N – Vs correlations in both equivalent linear and nonlinear analyses are not significant from bedrock to 5m below ground surface but above this the PGA values are found to be scattered. The maximum value of PGA at the ground surface as obtained in equivalent linear analysis is in the range of 0.4 – 0.6g. For nonlinear analysis the maximum value found at a depth of about 5m is in the range of 0.3 – 0.5g while at the ground surface it is 0.1 – 0.2g. The reduction in PGA values above 5m may be due to low consistency (N value = 5-11/ 30 cm) which induces comparatively higher strain resulting higher damping in the top loose sand layer.

4.3.2.PGA Amplification Ratio

PGA amplification ratio at any depth is the PGA at that corresponding depth normalised by peak bedrock amplification (PBRA). PGA amplification ratio depicts the amount of amplification or attenuation of ground motion at any depth. The PGA amplification ratio calculated with equivalent linear and nonlinear analysis with two different spectrum compatible strong motions are shown in figures 4.52 to 4.55.

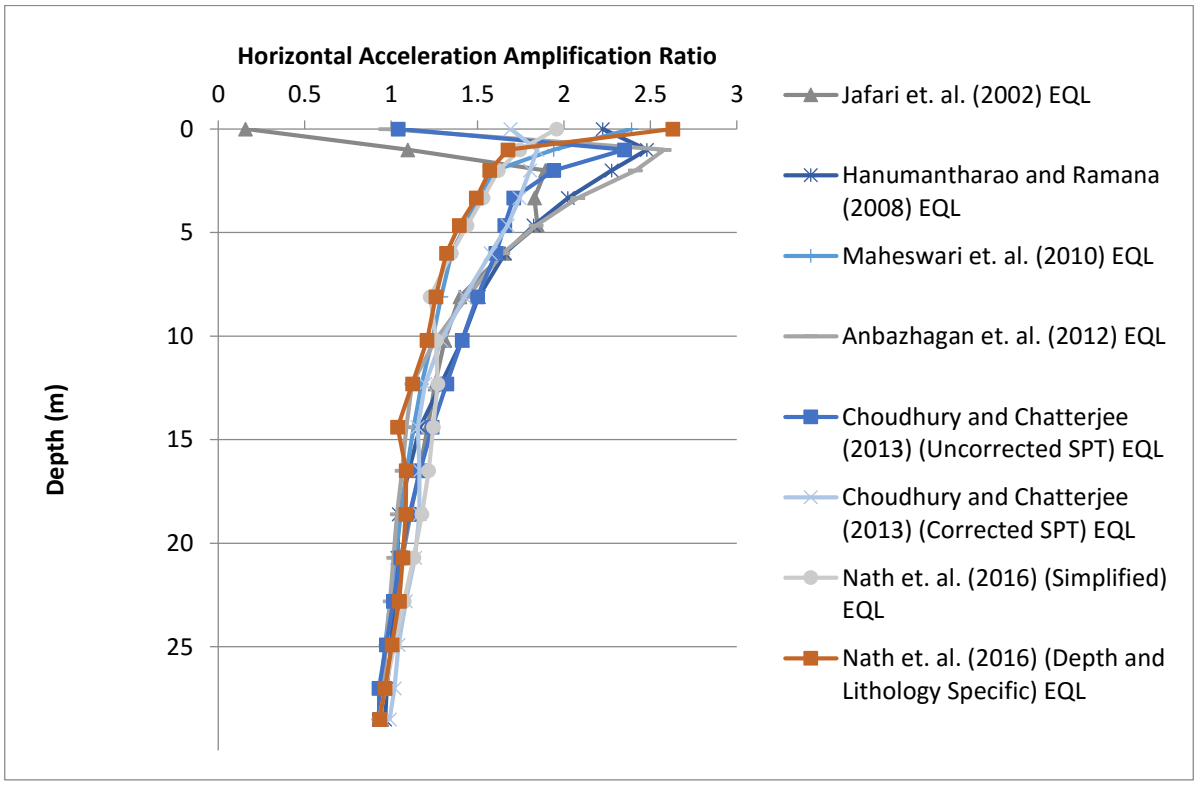

Figure 4.52: PGA Amplification Ratio Profiles for Equivalent Linear Analysis for River Channel Soil Deposit using Spectrally Matched San Fernando Earthquake and various N-Vs correlations

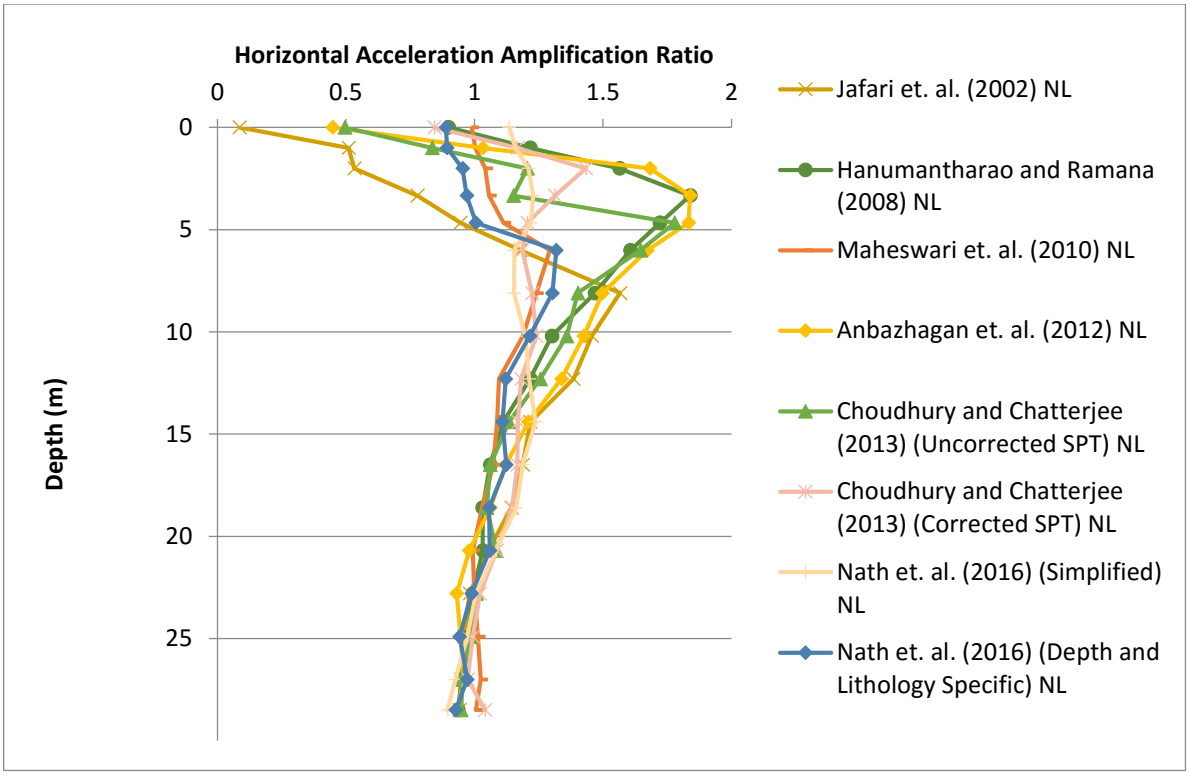

Figure 4.53: PGA Amplification Ratio Profiles for Nonlinear Analysis for River Channel Soil Deposit using Spectrally Matched San Fernando Earthquake and various N-Vs correlations

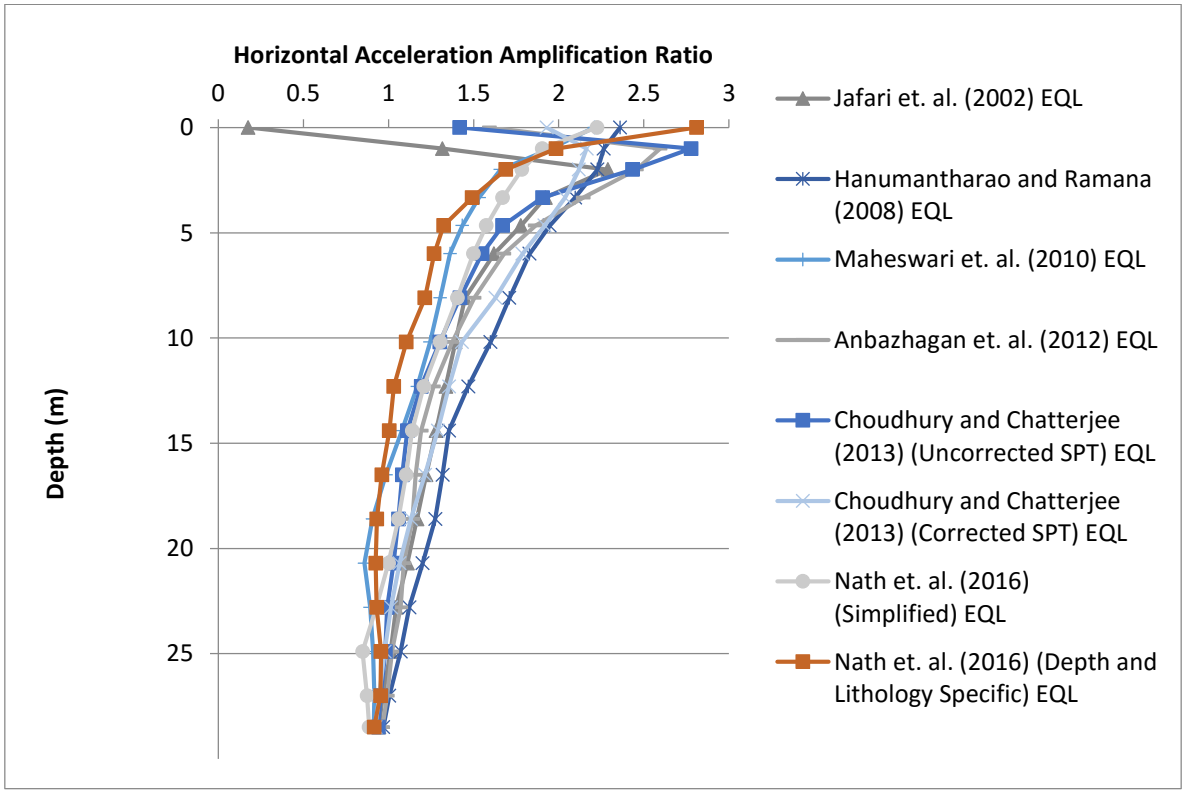

Figure 4.54: PGA Amplification Ratio Profiles for Equivalent Linear Analysis for River Channel Soil Deposit using Spectrally Matched Northridge Earthquake and various N-Vs correlations

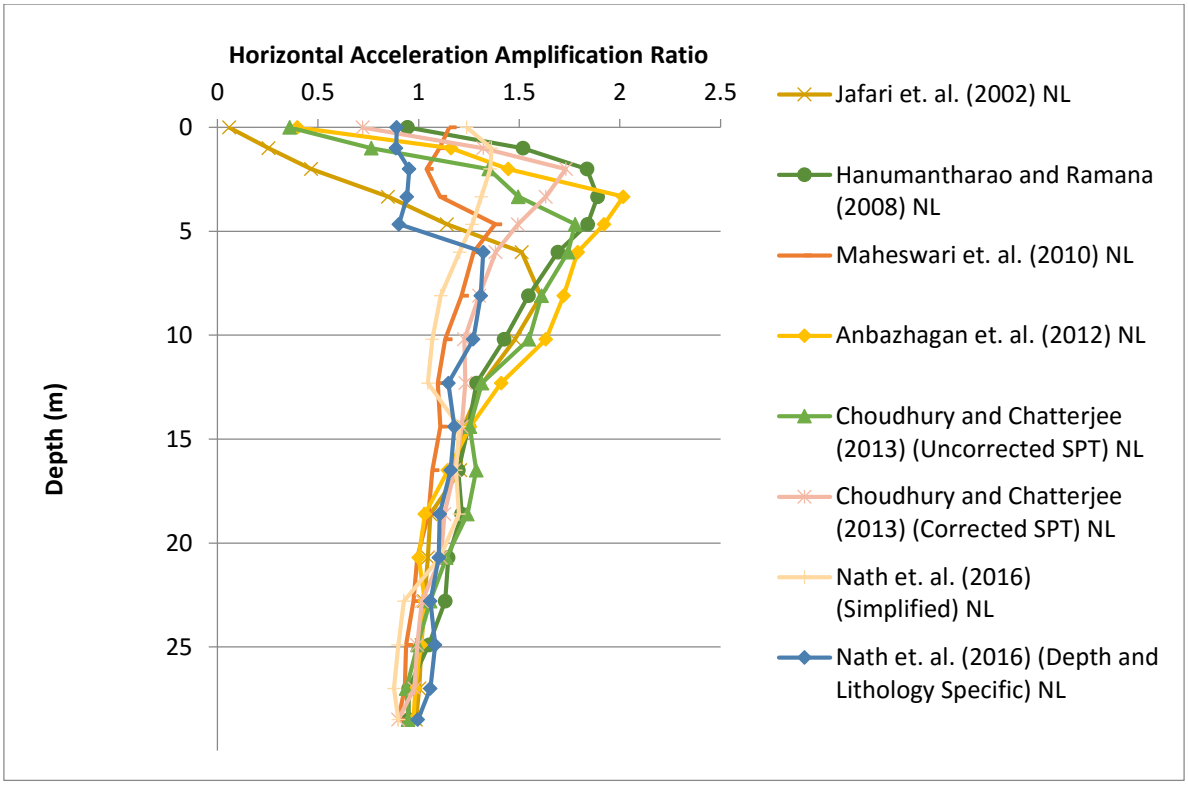

Figure 4.55: PGA Amplification Ratio Profiles for Nonlinear Analysis for River Channel Soil Deposit using Spectrally Matched Northridge Earthquake and various N-Vs correlations

From figures 4.52 to 4.55, it is noted that maximum ground amplification occurs nearly at the ground surface for equivalent linear analysis and at a depth of 4-6 m for nonlinear analysis and then sudden attenuation occurs and becomes insignificant at the ground surface. In some cases, (e.g. Nath et. al., 2016) PGA attenuation does not occur for equivalent linear analysis even at the ground surface. This may be due to higher values of shear wave velocity obtained from these correlations, thus top layers are stiffer in terms of shear wave velocity than that in other correlations and amplifies the incoming waves. It is also to be noted that ground amplification for equivalent linear analysis is observed to be more than that from nonlinear analysis.

4.3.3.Relative Displacement

The relative displacement of each layers calculated with equivalent linear and nonlinear analysis with two different spectrum compatible strong motions are shown in Figures 4.56 to 4.59.

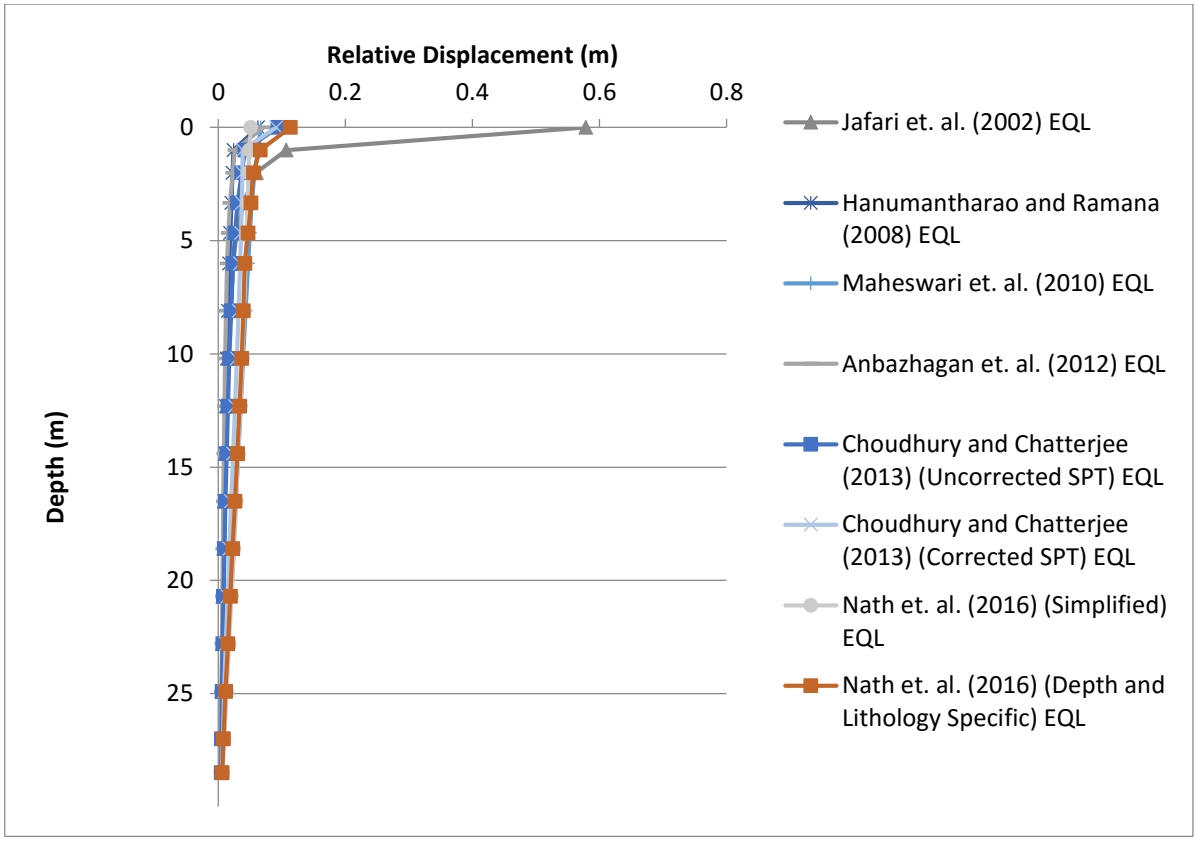

Figure 4.56: Relative Displacement Profiles for Equivalent Linear Analysis for River Channel Soil Deposit using Spectrally Matched San Fernando Earthquake and various N-Vs correlations

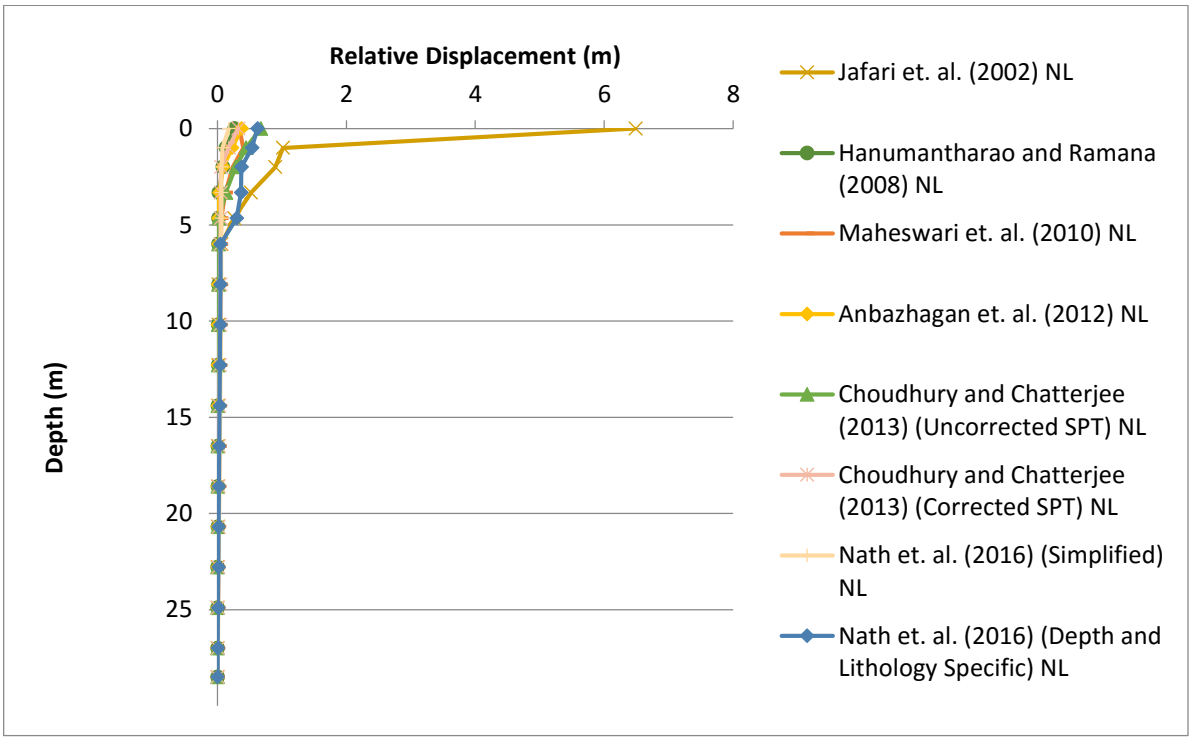

Figure 4.57: Relative Displacement Profiles for Nonlinear Analysis for River Channel Soil Deposit using Spectrally Matched San Fernando Earthquake and various N-Vs correlations

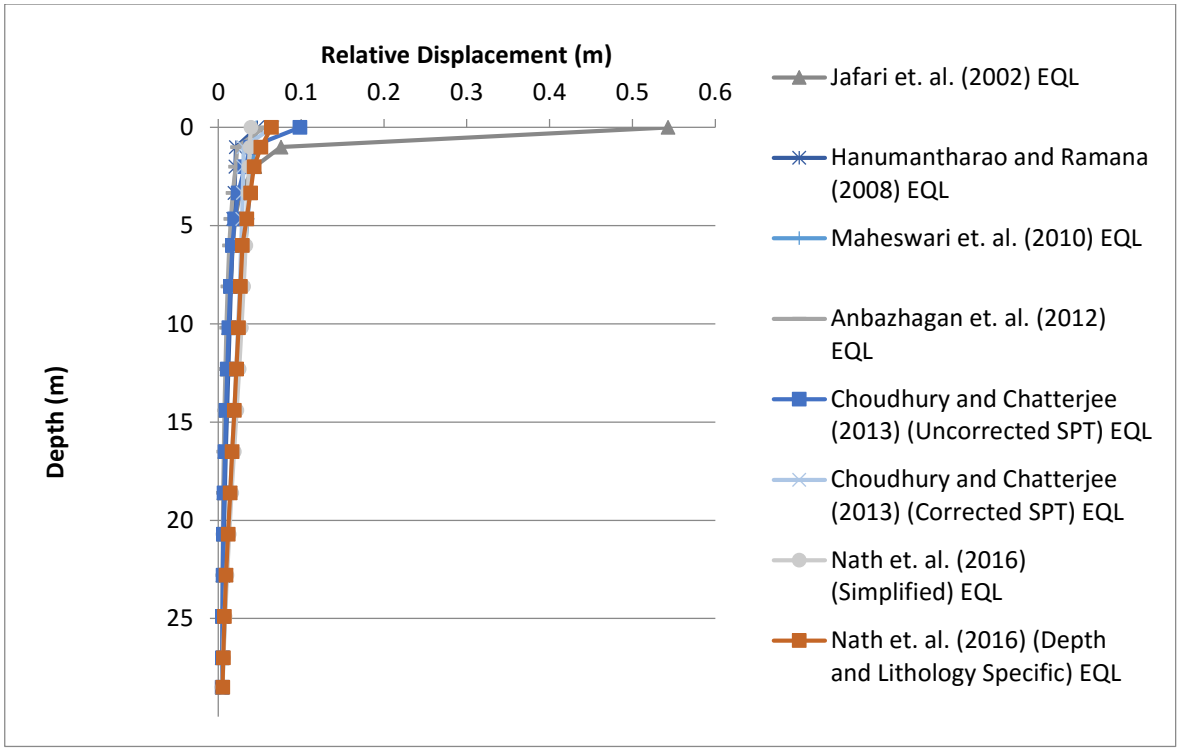

Figure 4.58: Relative Displacement Profiles for Equivalent Linear Analysis for River Channel Soil Deposit using Spectrally Matched Northridge Earthquake and various N-Vs correlations

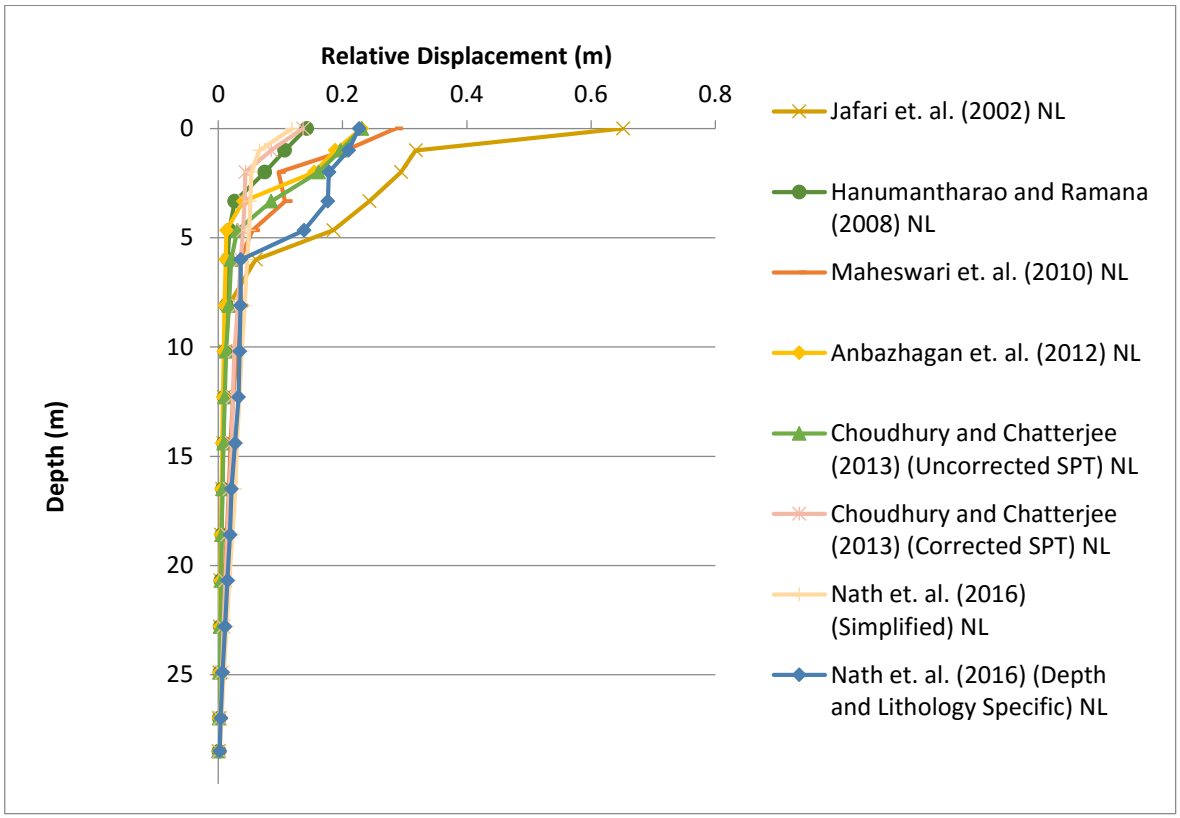

Figure 4.59: Relative Displacement Profiles for Nonlinear Analysis for River Channel Soil Deposit using Spectrally Matched Northridge Earthquake and various N-Vs correlations

From the figures 4.56 to 4.59 it is observed that in equivalent linear analysis, ground deformation is very less upto a depth of 2-3 m and then suddenly increases from that depth upto ground surface. It may be due to the presence of loose fill layer in the top 2m depth of the soil profile. In case of nonlinear analysis, ground deformation occurs in the top 5-6m depth. Below these depths, ground deformation is negligible. It is also to be noted that for the N-Vs correlation given by Jafari et. al. (2002), significant ground displacement occurs at the surface. It may be due to very low stiffness of the layer due to very small shear wave velocity as prescribed by Jafari et. al. (2002). Ground deformation for various N-Vs correlations are presented in Table 4.7.

Table 4.7. Surface Displacement (m) for Various Correlations

N-Vs correlation	San Fernando Earthquake		Northridge Earthquake	
	Equivalent Linear	Nonlinear	Equivalent Linear	Nonlinear
Jafari et. al. (2002)	0.58	6.5	0.55	0.65
Hanumantharao and Ramana (2008)	0.062	0.27	0.047	0.15
Maheswari et. al. (2010)	0.065	0.35	0.045	0.28
Anbazhagan et. al. (2012)	0.07	0.38	0.055	0.22
Choudhury and Chatterjee (2013) (Uncorrected SPT)	0.092	0.65	0.1	0.23
Choudhury and Chatterjee (2013) (Corrected SPT)	0.09	0.33	0.065	0.14
Nath et. al. (2016) (Simplified)	0.05	0.17	0.04	0.12
Nath et. al. (2016) (Depth and Lithology Specific)	0.11	0.6	0.06	0.22

4.3.4.Maximum Shear Strain

Variation of maximum shear strain is obtained from equivalent linear and nonlinear analysis for a typical N-Vs correlation (Choudhury and Chatterjee, 2013 (Uncorrected SPT)) has been presented in

figure 4.60. Further comparative presentations of maximum shear strains are shown in figures 4.61 to 4.64.

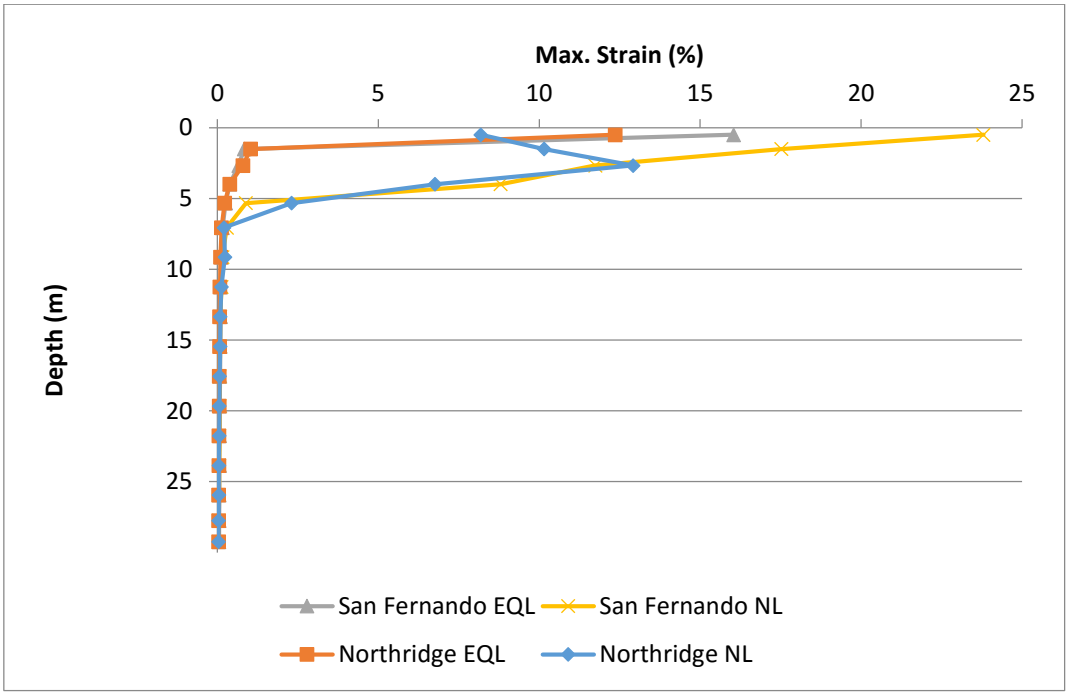

Figure 4.60: Maximum Shear Strain Profiles for Equivalent Linear and Nonlinear Analysis given by Choudhury and Chatterjee (2013) (Uncorrected SPT)

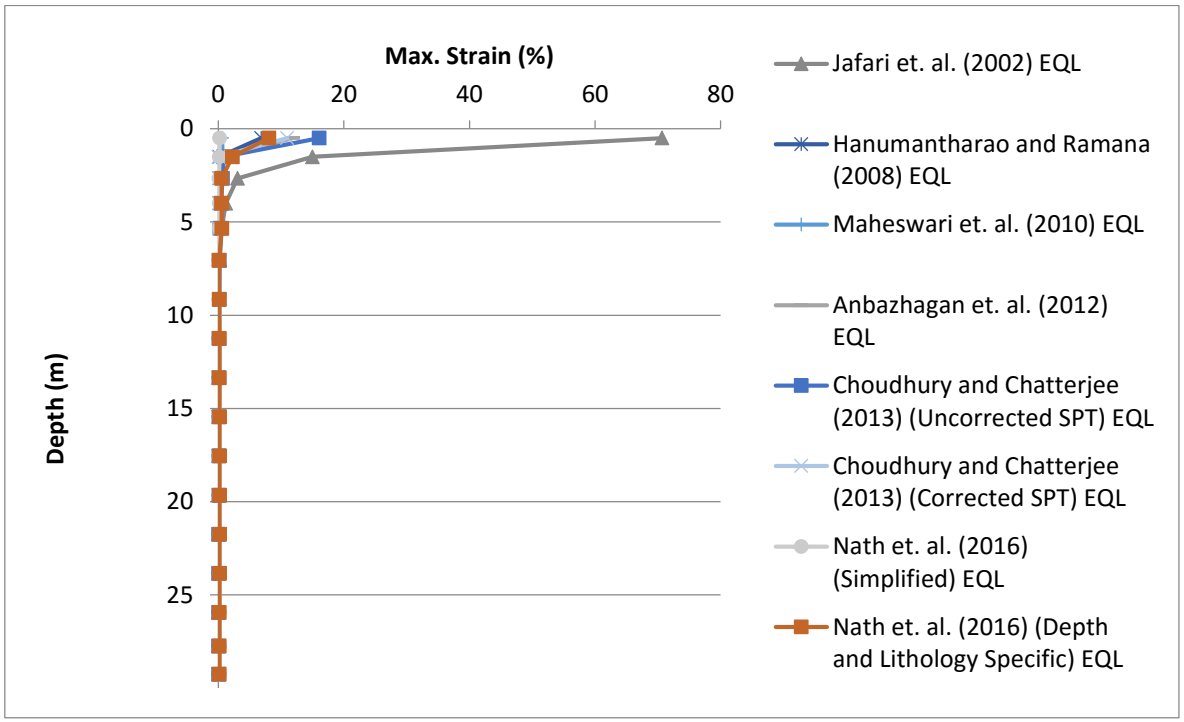

Figure 4.61: Maximum Shear Strain Profiles for Equivalent Linear Analysis for River Channel Soil Deposit using Spectrally Matched San Fernando Earthquake and various N-Vs correlations

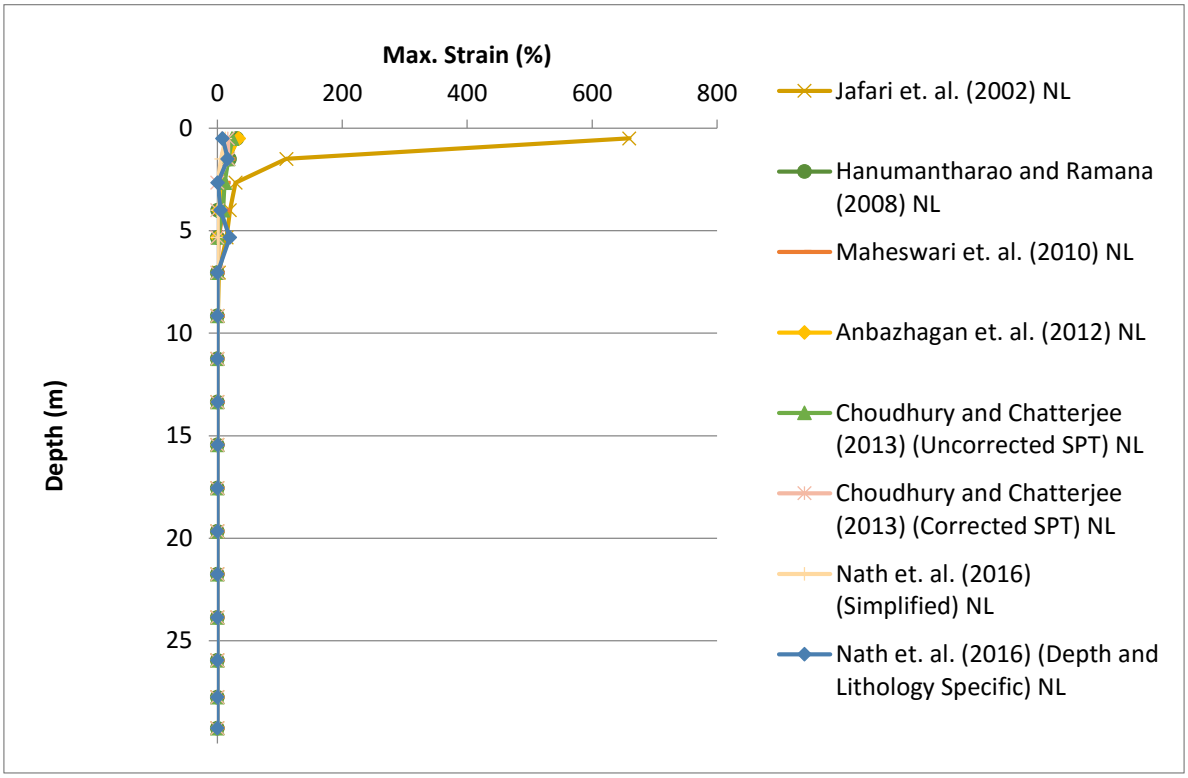

Figure 4.62: Maximum Shear Strain Profiles for Nonlinear Analysis for River Channel Soil Deposit using Spectrally Matched San Fernando Earthquake and various N-Vs correlations

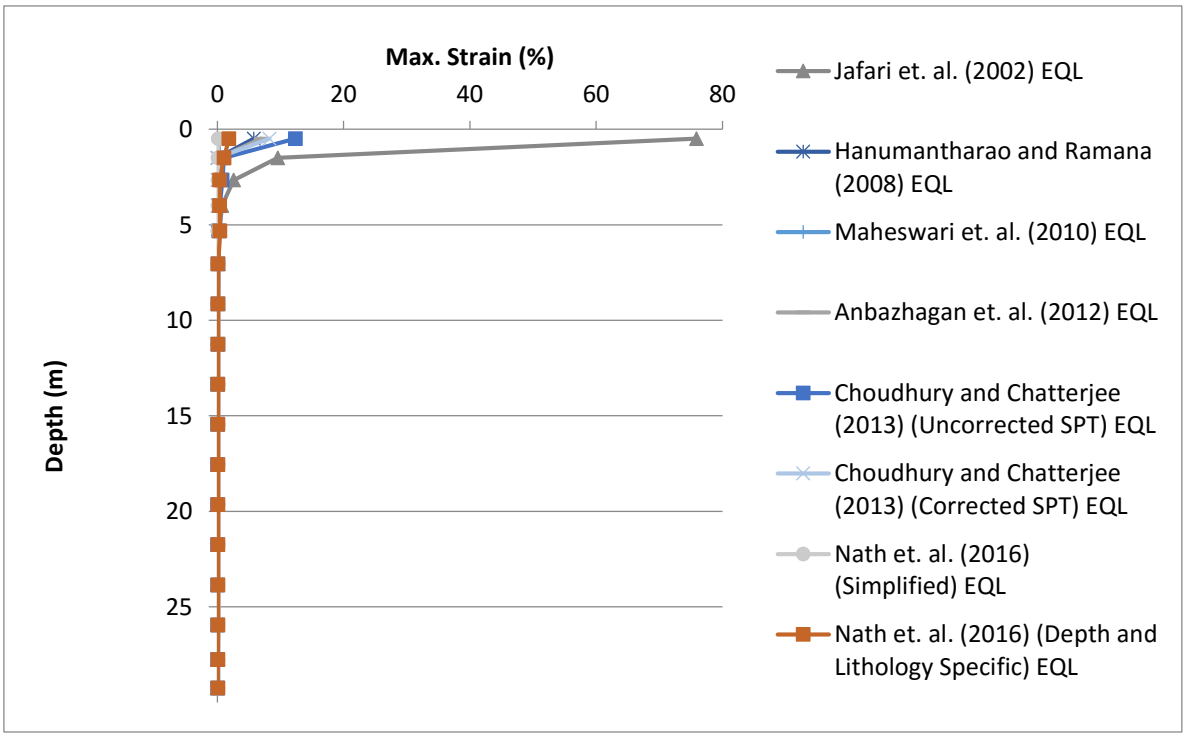

Figure 4.63: Maximum Shear Strain Profiles for Equivalent Linear Analysis for River Channel Soil Deposit using Spectrally Matched Northridge Earthquake and various N-Vs correlations

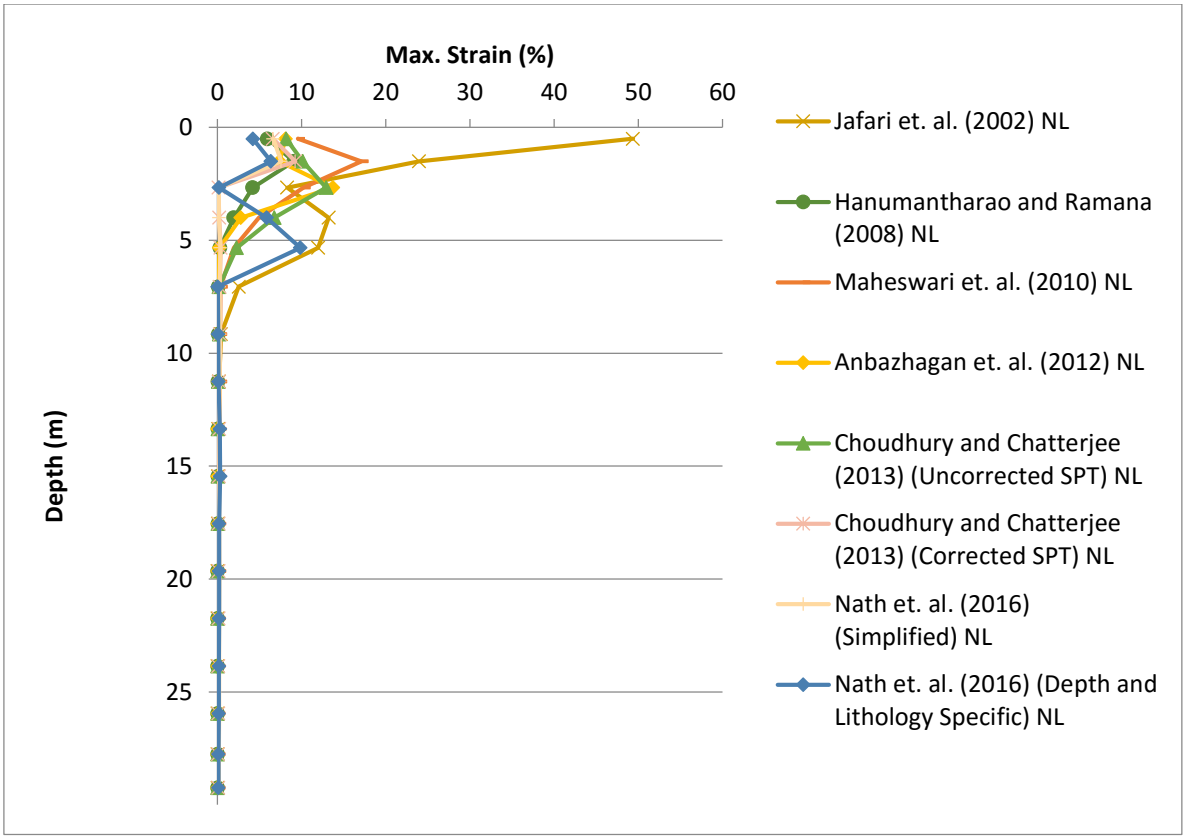

Figure 4.64: Maximum Shear Strain Profiles for Nonlinear Analysis for River Channel Soil Deposit using Spectrally Matched Northridge Earthquake and various N-Vs correlations

From figures 4.61 to 4.64, it is seen that top soil layers upto a depth of 5-6m experiences high shear strain as it is loose type of soil. High ground deformation due to strong motions occurs in that layer which results in high strain.

4.3.5.Maximum Stress Ratio

Maximum stress ratio is defined as induced shear stress normalised by effective vertical stress in soil. The comparative representation of maximum stress ratio profiles in equivalent linear and nonlinear analyses for various SPT-Vs correlations are shown in figures 4.65 to 4.68

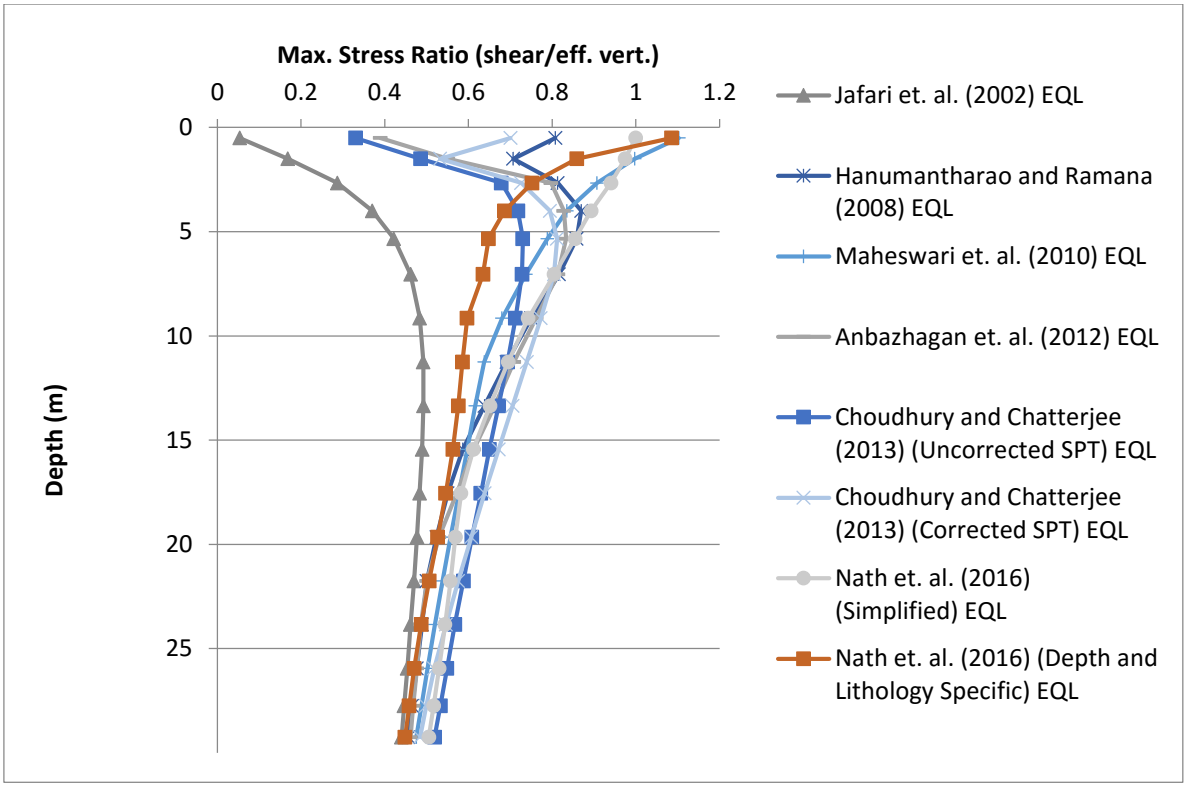

Figure 4.65: Maximum Stress Ratio Profiles for Equivalent Linear Analysis for River Channel Soil Deposit using Spectrally Matched San Fernando Earthquake and various N-Vs correlations

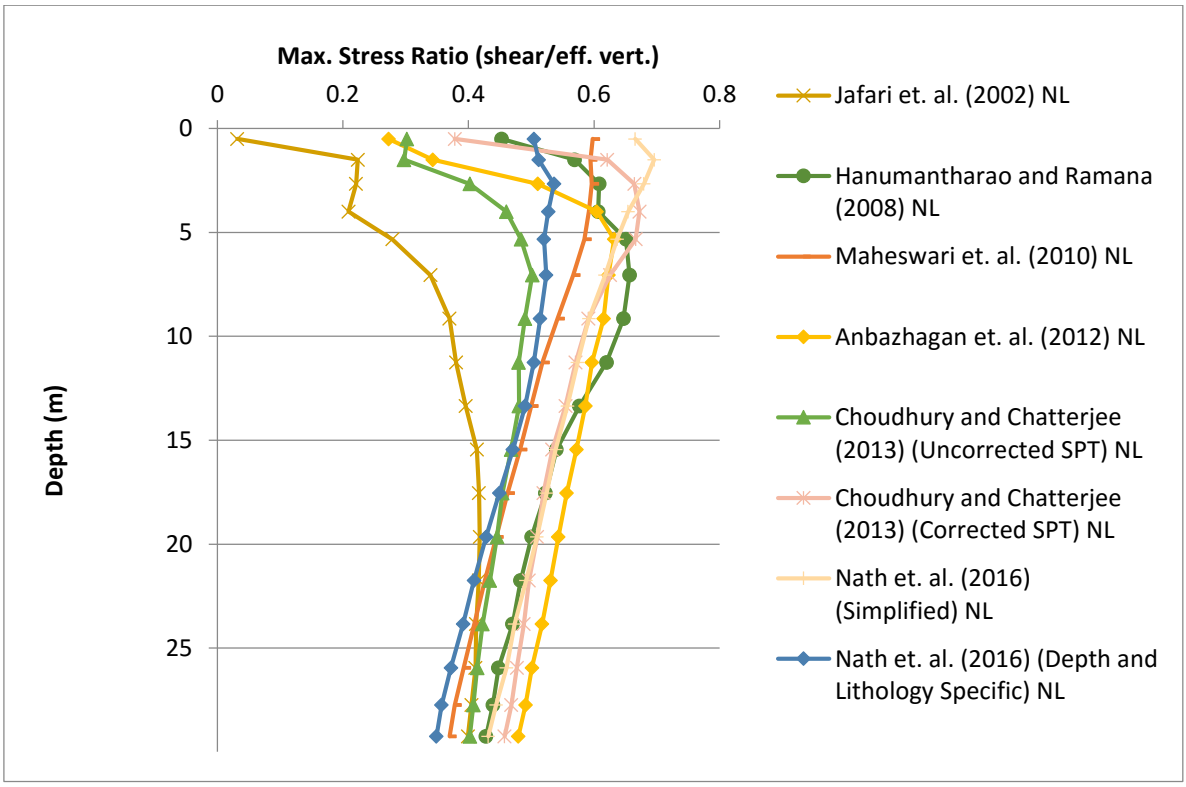

Figure 4.66: Maximum Stress Ratio Profiles for Nonlinear Analysis for River Channel Soil Deposit using Spectrally Matched San Fernando Earthquake and various N-Vs correlations

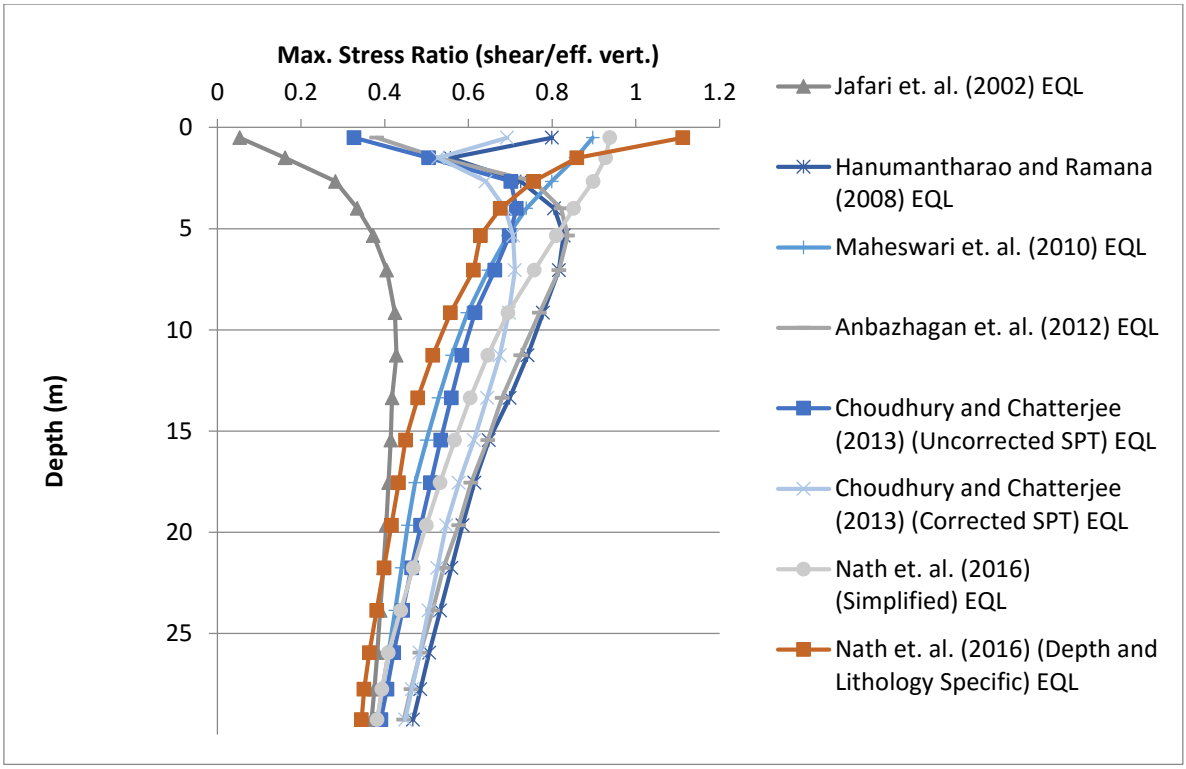

Figure 4.67: Maximum Stress Ratio Profiles for Equivalent Linear Analysis for River Channel Soil Deposit using Spectrally Matched Northridge Earthquake and various N-Vs correlations

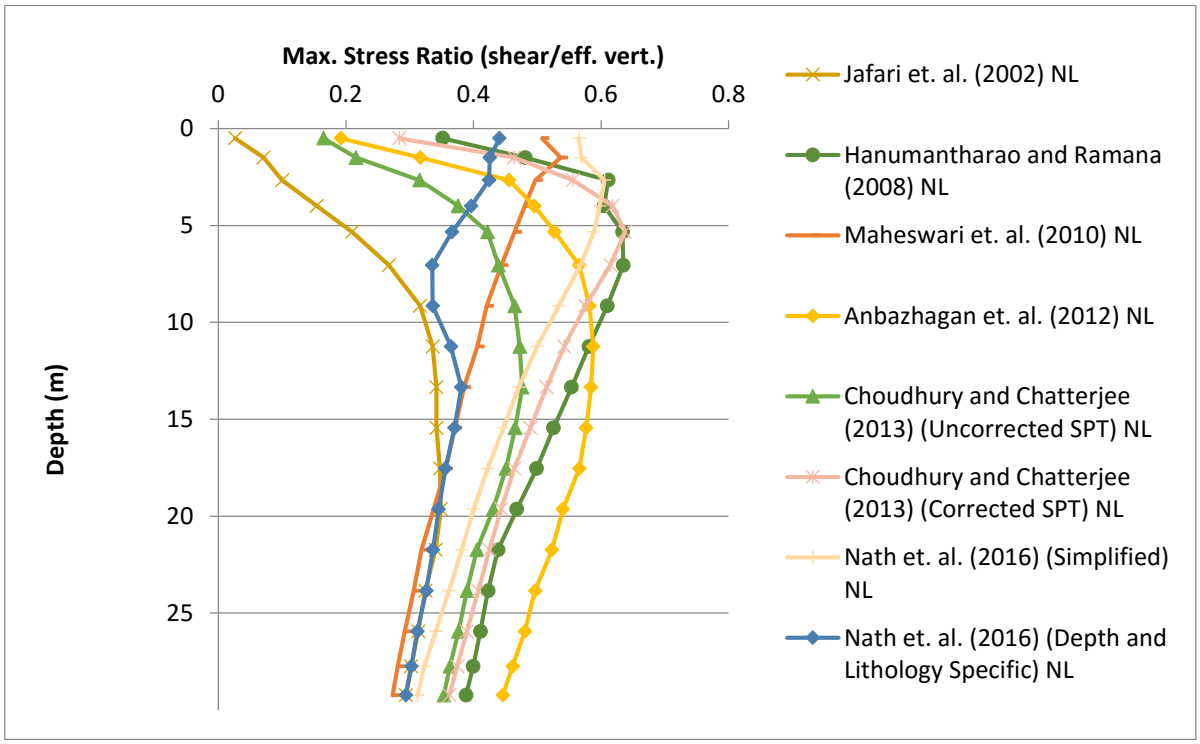

Figure 4.68: Maximum Stress Ratio Profiles for Nonlinear Analysis for River Channel Soil Deposit using Spectrally Matched Northridge Earthquake and various N-Vs correlations

From figures 4.65 to 4.68, it is found that shear stress ratio remains constant from bedrock upto a depth of 8-10m and from that depth upto surface, it diverges for different N-Vs correlations in both equivalent linear and nonlinear analyses.

4.3.6.Maximum Pore Pressure Ratio

The maximum pore pressure ratio is defined as excess pore pressure generated in the soil due to strong motion shaking normalised by initial effective stress at any depth in the soil profile. In effective stress based nonlinear analysis pore pressure profile can be generated. Comparative analysis of maximum pore pressure variation for various SPT-Vs correlations is shown in figures 4.69) to (4.74).

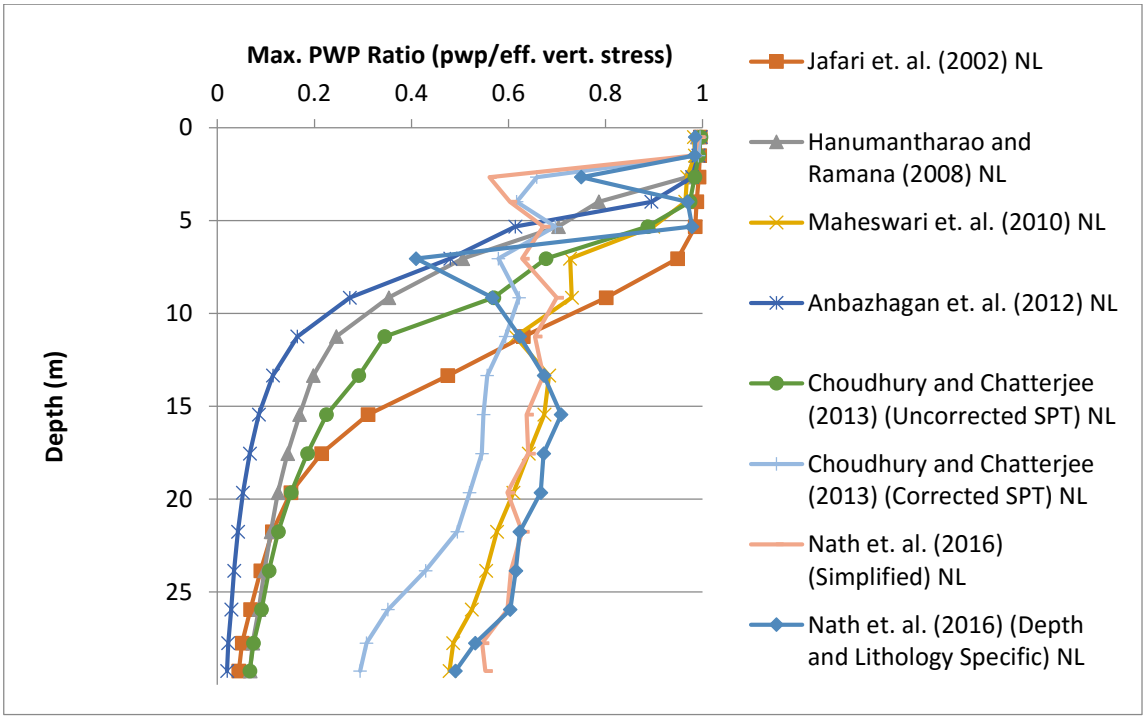

Figure 4.69: Maximum Pore Pressure Profiles for Nonlinear Analysis for River Channel Soil Deposit using Spectrally Matched San Fernando Earthquake and various N-Vs correlations

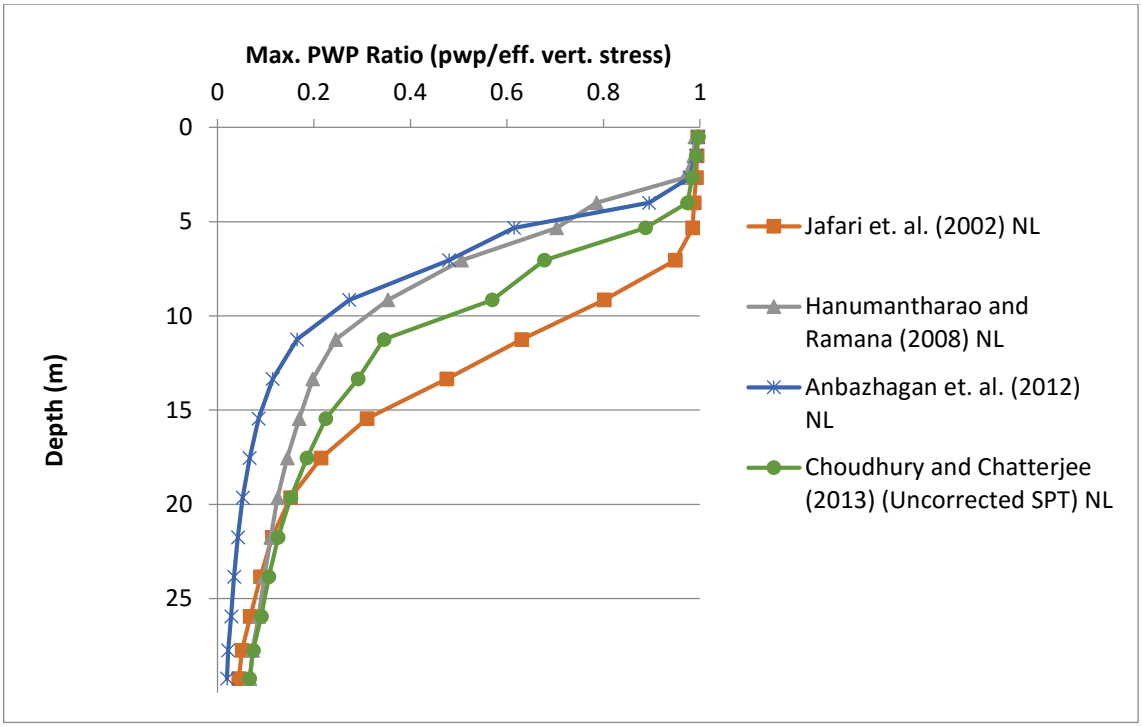

Figure 4.70: Maximum Pore Pressure Profiles for Nonlinear Analysis for River Channel Soil Deposit using Spectrally Matched San Fernando Earthquake and various N-Vs correlations

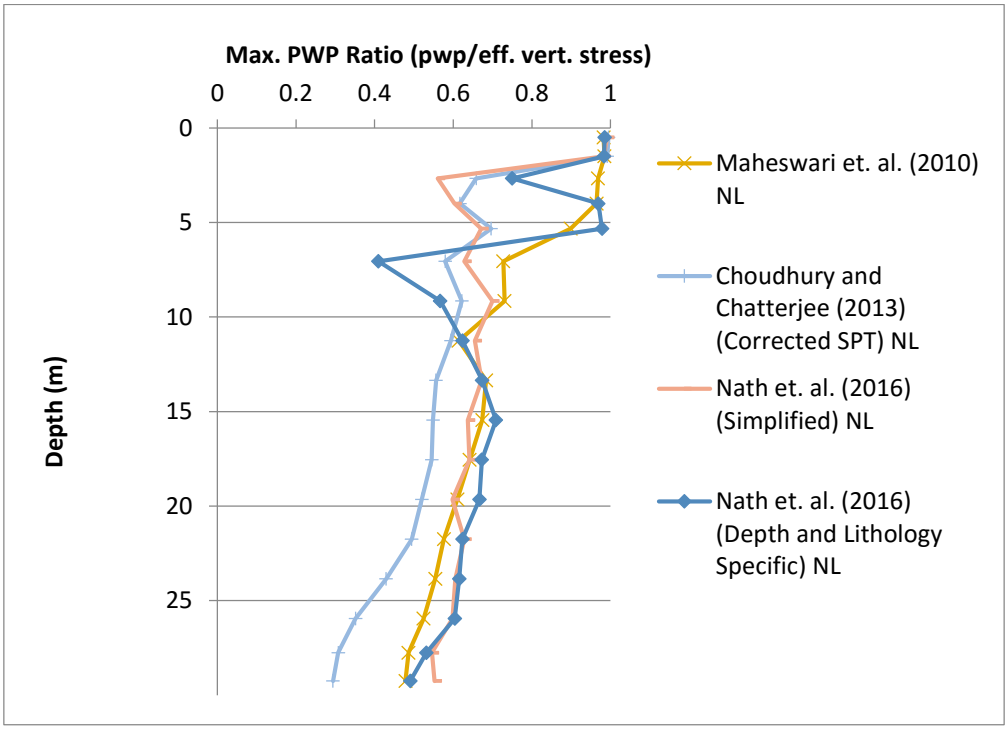

Figure 4.71: Maximum Pore Pressure Profiles for Nonlinear Analysis for River Channel Soil Deposit using Spectrally Matched San Fernando Earthquake and various N-Vs correlations

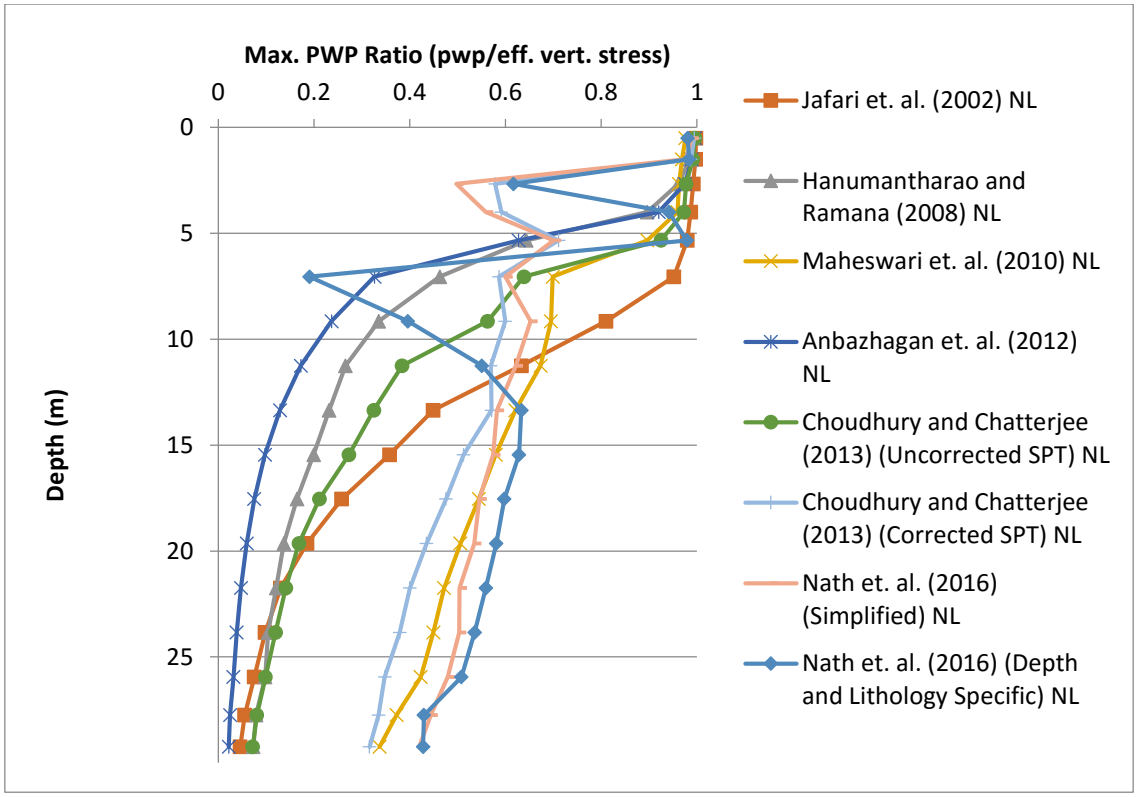

Figure 4.72: Maximum Pore Pressure Profiles for Nonlinear Analysis for River Channel Soil Deposit using Spectrally Matched Northridge Earthquake and various N-Vs correlations

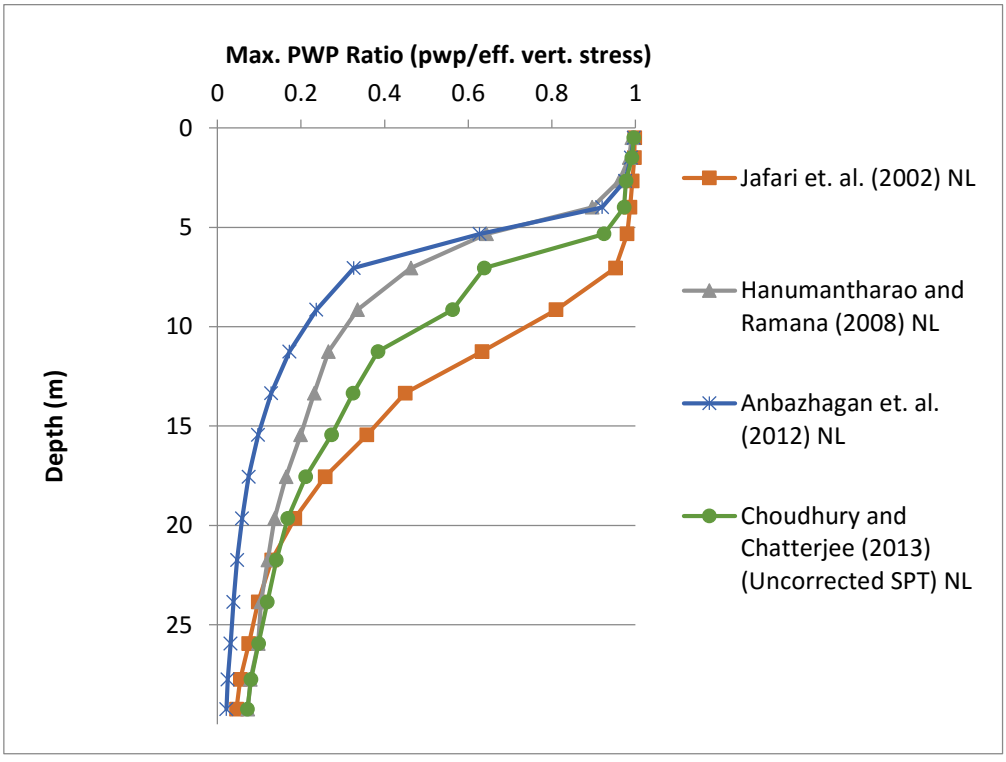

Figure 4.73: Maximum Pore Pressure Profiles for Nonlinear Analysis for River Channel Soil Deposit using Spectrally Matched Northridge Earthquake and various N-Vs correlations

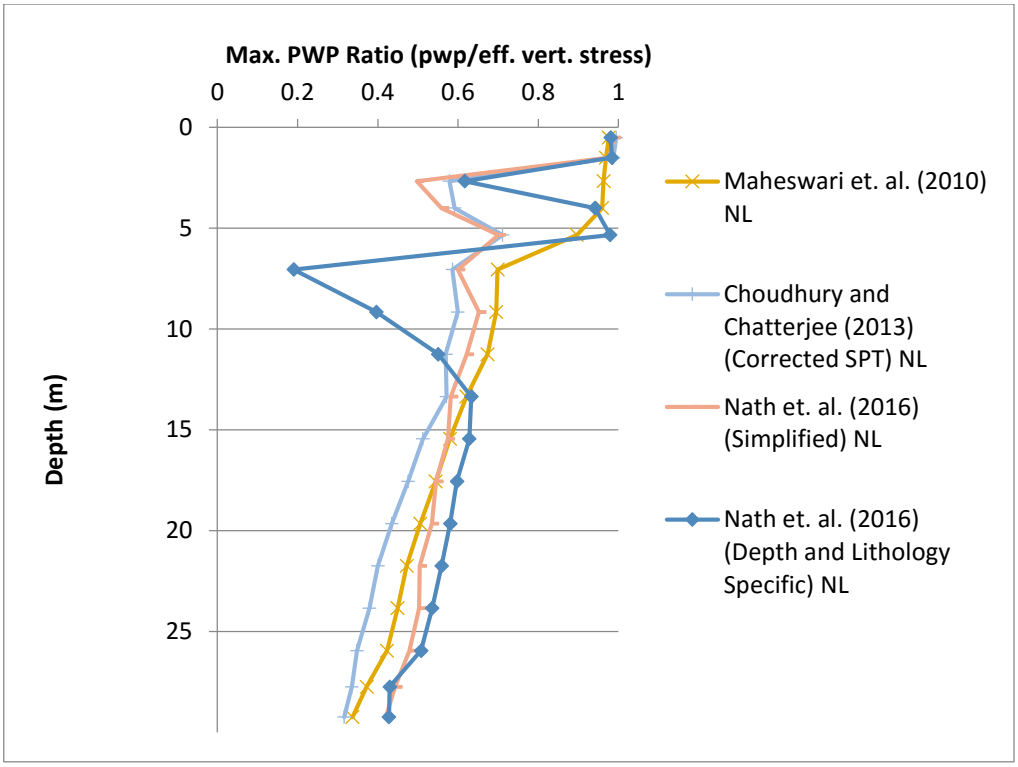

Figure 4.74: Maximum Pore Pressure Profiles for Nonlinear Analysis for River Channel Soil Deposit using Spectrally Matched Northridge Earthquake and various N-Vs correlations

From figures 4.69 and 4.72, it is observed that pore pressure becomes unity in the top 5m for both strong motions. Thus the top 5-6m soil layer liquefies in presence of the input strong motions. It is also found that there are two distinct patterns of pore pressure variation with depth. It has been plotted in figures 4.70, 4.71, 4.73 and 4.74. Figure 4.70 and 4.73 show that pore water pressure is about unity down to a depth of 4-6m below the ground surface, below which it reduces quickly and becomes 0.2 at about 20m depth. However, figures 4.71 and 4.74 indicate that pore water pressure is close to unity near ground surface and reduces to about 0.6 at a depth of 4-5 m and then decreases gradually with about 0.5 at a depth of 20m. It implies that pore pressure variation depends on N-Vs correlations used in the analysis.

4.3.7.Fourier Amplification Ratio

Fourier amplification ratio is the ratio of Fourier amplitude of the surface acceleration time history to the Fourier amplitude of the input acceleration time history. It indicates the transfer of the bedrock response to the ground surface at various frequencies. Fourier amplification ratio variation with different frequencies for two strong motions are shown in figures 4.75 to 4.76.

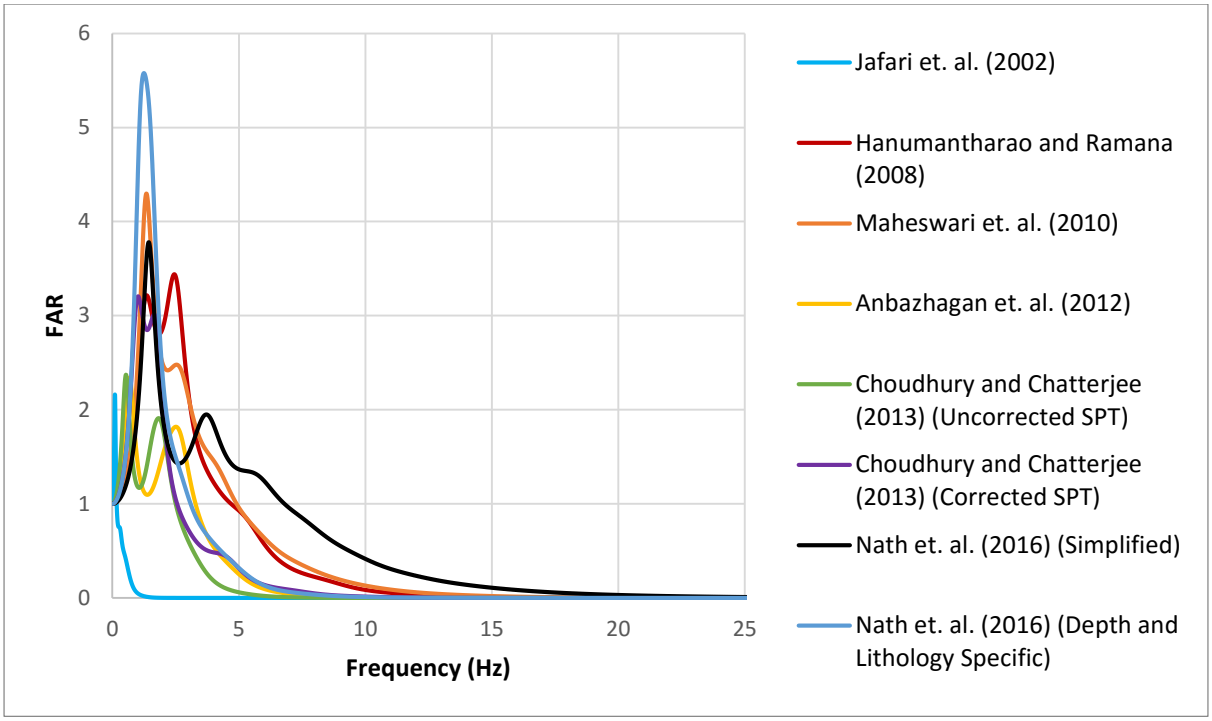

Figure 4.75: Fourier Amplification Ratio for Equivalent Linear Analysis for River Channel Soil Deposit using Spectrally Matched San Fernando Earthquake and various N-Vs correlations

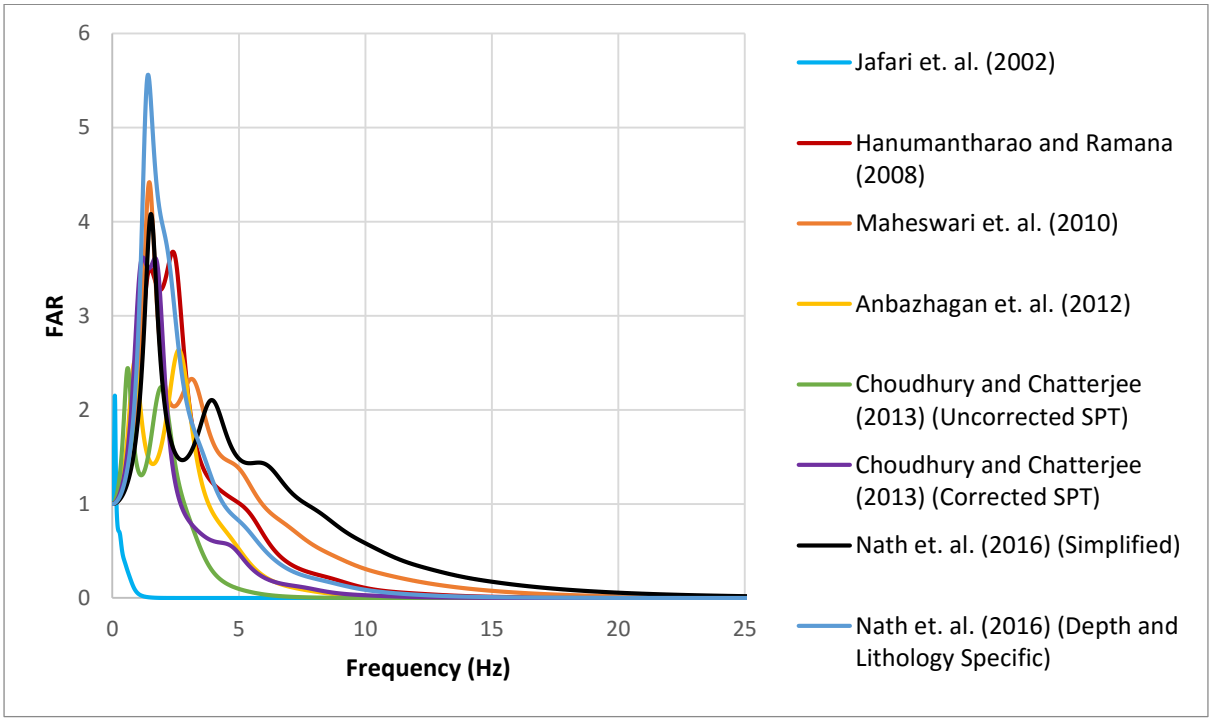

Figure 4.76: Fourier Amplification Ratio for Nonlinear Analysis for River Channel Soil Deposit using Spectrally Matched Northridge Earthquake and various N-Vs correlations

From figures 4.75 and 4.76, the maximum FAR and corresponding frequencies are shown in Table 4.8.

Table 4.8: FAR and Corresponding Frequencies

SPT-Vs Correlations	Natural Frequency of the Soil Profile (Hz)	San Fernando		Northridge	
		FAR	Corresponding Frequency (Hz)	FAR	Corresponding Frequency (Hz)
Jafari et. al. (2002)	1.23	2.16	0.098	2.12	0.104
Hanumantharao and Ramana (2008)	2.25	3.42	2.5	3.66	2.45
Maheswari et. al. (2010)	1.77	4.27	1.31	4.4	1.44
Anbazhagan et. al. (2012)	2.19	2.33	0.7	2.63	2.6
Choudhury and Chatterjee (2013) (Uncorrected SPT)	1.86	2.3	0.58	2.43	0.63
Choudhury and Chatterjee (2013) (Corrected SPT)	1.96	3.2	0.99	3.61	1.22
Nath et. al. (2016) (Simplified)	1.90	3.77	1.42	4.08	1.53
Nath et. al. (2016) (Depth and Lithology Specific)	1.70	5.49	1.35	5.56	1.4
Average	1.88	3.77	1.12	3.57	1.42
Range	1.23-2.25	2.16-5.49	0.098-2.5	2.12-5.56	0.104-2.6

It is observed that, soil profile gets amplified at frequencies close to the natural frequency of the soil column but due to hysteretic damping and bedrock elasticity, resonance never occurs. FAR for River Channel Deposit soil subjected to spectral compatible strong motions can be in the range of 2~6 with corresponding frequency range of 0.098-2.6Hz which is very close to the natural frequency range of soil. It is also observed that river channel soil deposit will be amplified in the frequency range of 0.1-0.7Hz. From Table 4.4, it was observed that normal Kolkata soil deposit would be amplified in the frequency range of 0.4-15Hz.

4.3.8. Acceleration Response Spectra

If the soil column can be assumed be a single degree of freedom system (SDOF), the acceleration response spectra shows the peak acceleration response of soil column for different natural time periods. The acceleration response spectra calculated for equivalent linear and nonlinear analyses for two different strong motions are shown in figures (4.77) to (4.80).

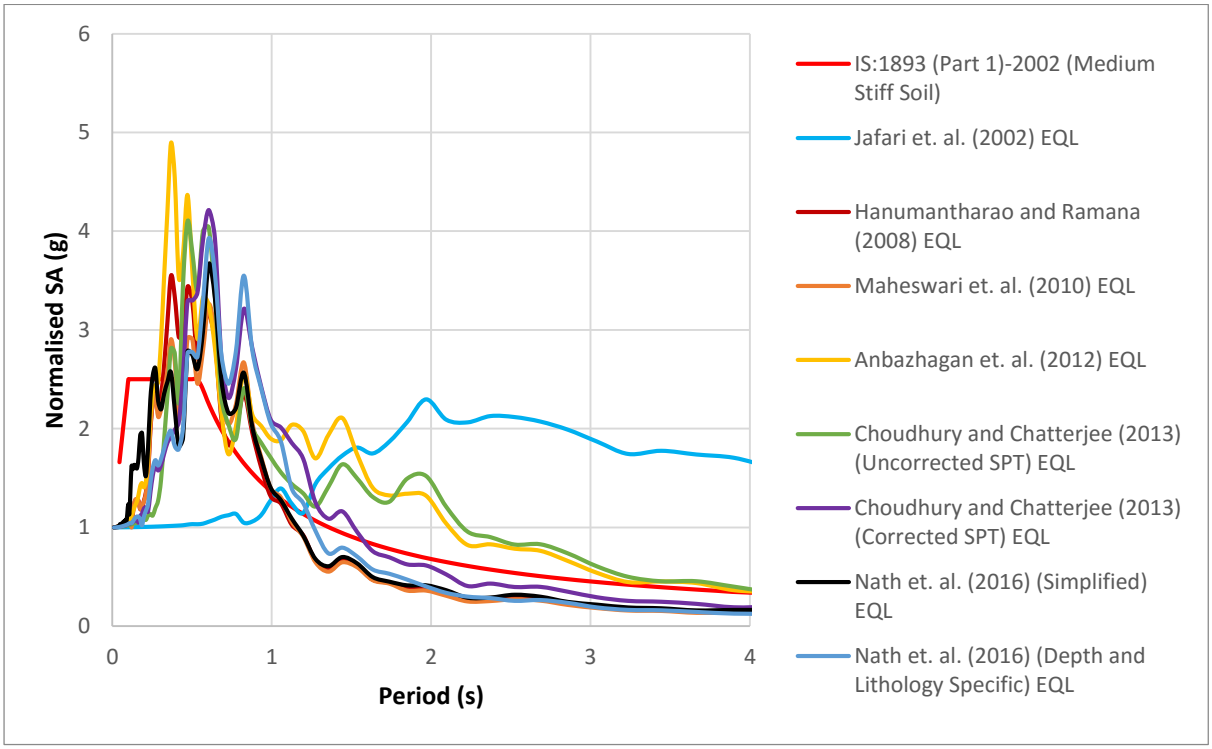

Figure 4.77: Spectral Acceleration for Equivalent Linear Analysis for River Channel Soil Deposit using Spectrally Matched San Fernando Earthquake and various N-Vs correlations

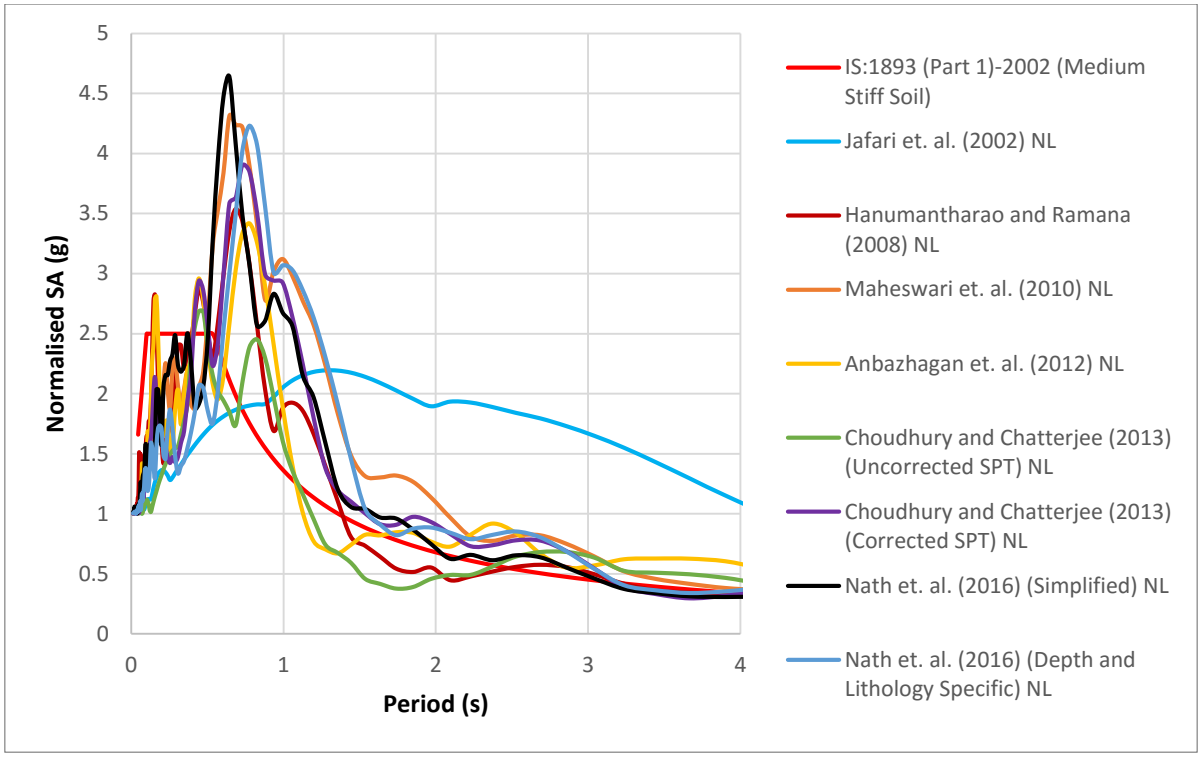

Figure 4.78: Spectral Acceleration for Nonlinear Analysis for River Channel Soil Deposit using Spectrally Matched San Fernando Earthquake and various N-Vs correlations

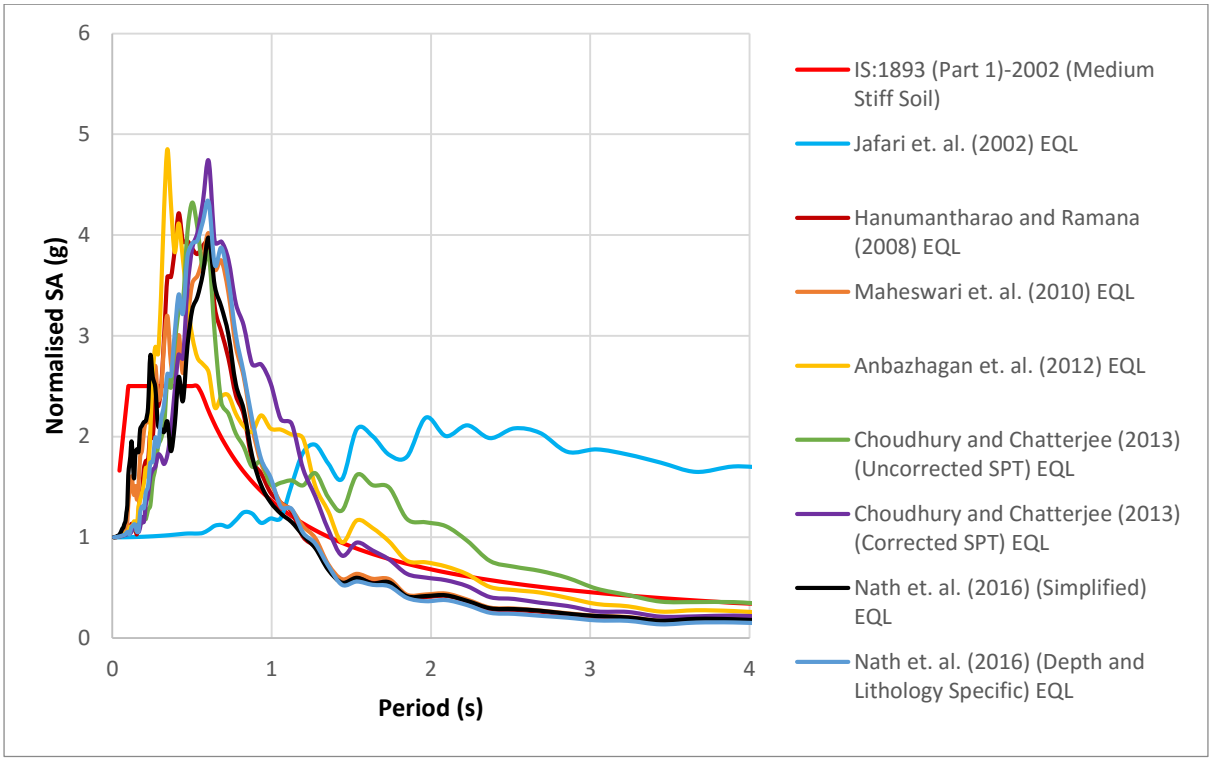

Figure 4.79: Spectral Acceleration for Equivalent Linear Analysis for River Channel Soil Deposit using Spectrally Matched Northridge Earthquake and various N-Vs correlations

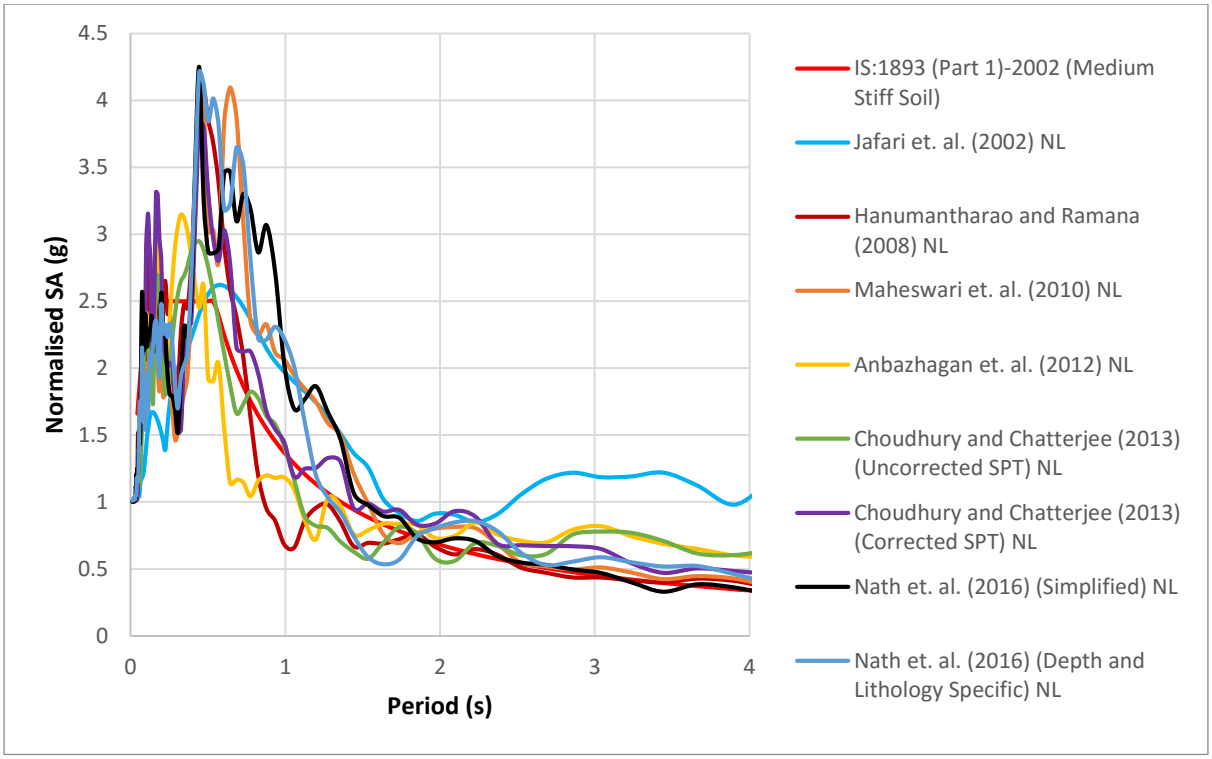

Figure 4.80: Spectral Acceleration for Nonlinear Analysis for River Channel Soil Deposit using Spectrally Matched Northridge Earthquake and various N-Vs correlations

Except for correlations given by Jafari et. al. (2002), the acceleration response spectra almost follows a similar trend. The calculated acceleration response spectra are compared with IS:1893 (Part 1)-2002 (Medium Dense Soil) and it is found that there are variations in the calculated response spectra and the IS code prescribed response spectra. The results of peak spectral acceleration obtained from equivalent linear and nonlinear analyses and their corresponding time periods for two different ground motions are presented in the Table 4.9 and 4.10. In this context it may be worthwhile to mention that the displacement obtained using the SPT N-Vs correlation given by Jafari et. al. (2002) is showing abnormal trend and thus has not been included in Table 4.9 and 4.10.

Table 4.9. Peak Acceleration Response and Corresponding Time Periods for Spectrum Compatible San Fernando Earthquake

Correlations	San Fernando Earthquake			
	Equivalent Linear		Nonlinear	
	Peak Spectral Acceleration (g)	Corresponding Time Period (s)	Peak Spectral Acceleration (g)	Corresponding Time Period (s)
Hanumantharao and Ramana (2008)	3.55	0.37	3.54	0.68
Maheswari et. al. (2010)	3.26	0.6	4.3	0.64
Anbazhagan et. al. (2012)	4.9	0.37	3.42	0.77
Choudhury and Chatterjee (2013) (Uncorrected SPT)	4.1	0.47	2.68	0.47
Choudhury and Chatterjee (2013) (Corrected SPT)	4.2	0.6	3.85	0.77
Nath et. al. (2016) (Simplified)	3.67	0.6	4.64	0.64
Nath et. al. (2016) (Depth and Lithology Specific)	3.93	0.6	4.23	0.77
Average	3.94	0.52	3.81	0.68
Range	3.26-4.9	0.37-0.6	2.68-4.64	0.47-0.77

Table 4.10. Peak Acceleration Response and Corresponding Time Periods for Spectrum Compatible Northridge Earthquake

Correlations	Northridge Earthquake			
	Equivalent Linear		Nonlinear	
	Peak Spectral Acceleration (g)	Corresponding Time Period (s)	Peak Spectral Acceleration (g)	Corresponding Time Period (s)
Hanumantharao and Ramana (2008)	4.2	0.42	4.1	0.47
Maheswari et. al. (2010)	4.0	0.6	4.2	0.44
Anbazhagan et. al. (2012)	4.85	0.35	3.15	0.32
Choudhury and Chatterjee (2013) (Uncorrected SPT)	4.32	0.5	2.95	0.44
Choudhury and Chatterjee (2013) (Corrected SPT)	4.74	0.6	3.83	0.44
Nath et. al. (2016) (Simplified)	3.98	0.6	4.25	0.44
Nath et. al. (2016) (Depth and Lithology Specific)	4.33	0.6	4.21	0.44
Average	4.35	0.52	3.81	0.43
Range	3.98-4.85	0.35-0.6	2.95-4.25	0.32-0.44

4.4.NONLINEAR ANALYSIS IN NORMAL KOLKATA SOIL AND RIVER CHANNEL SOIL USING OPENSEES

The results in section 4.2 are obtained by performing equivalent linear and nonlinear ground response analysis in the software DEEPSOIL for various N-Vs correlations. One specific correlation prescribed by Choudhury and Chatterjee (2013) (Uncorrected SPT) is now used for nonlinear analysis with OPENSEES software. The input parameters for OPENSEES are shown in Table 3.7 in the Chapter 3. The input parameters are selected on the basis of Pressure Independent Multi Yield (PIMY) and Pressure Dependent Multi Yield (PDMY) soil model. The PIMY and PDMY soil models are applicable for plastic soils and non-plastic soils respectively. The PIMY and PDMY soil models are presented in section 2.8 in Chapter 2. The output parameters (i.e. PGA, PGA Amplification, Relative Displacement, Maximum Shear Strain, Maximum Stress Ratio and Maximum Pore Pressure Ratio) as obtained from OPENSEES are now presented along with those obtained from DEEPSOIL already given in section 4.2 and 4.3 and plotted in this section for comparison.

4.4.1.Peak Ground Acceleration (PGA)

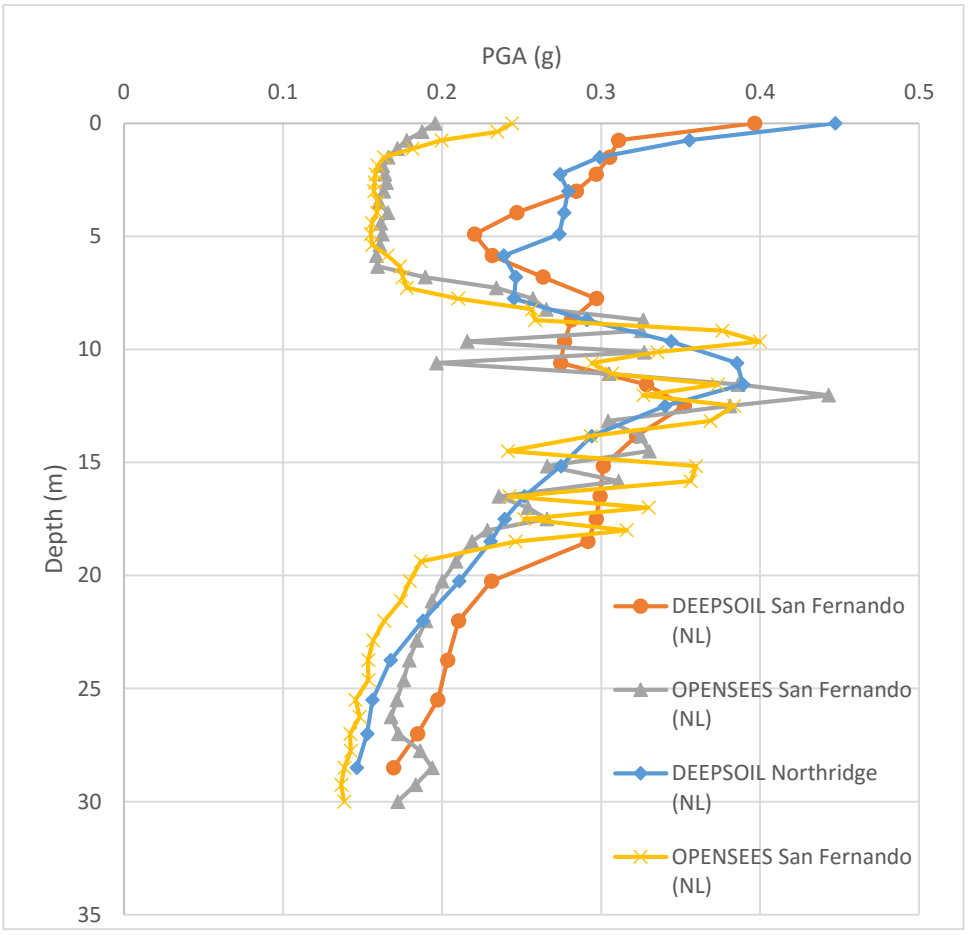

Figure 4.81: PGA Profiles for Normal Kolkata Soil using Nonlinear Analysis with DEEPSOIL and OPENSEES with N-Vs correlations given by Choudhury and Chatterjee (2013) (Uncorrected SPT)

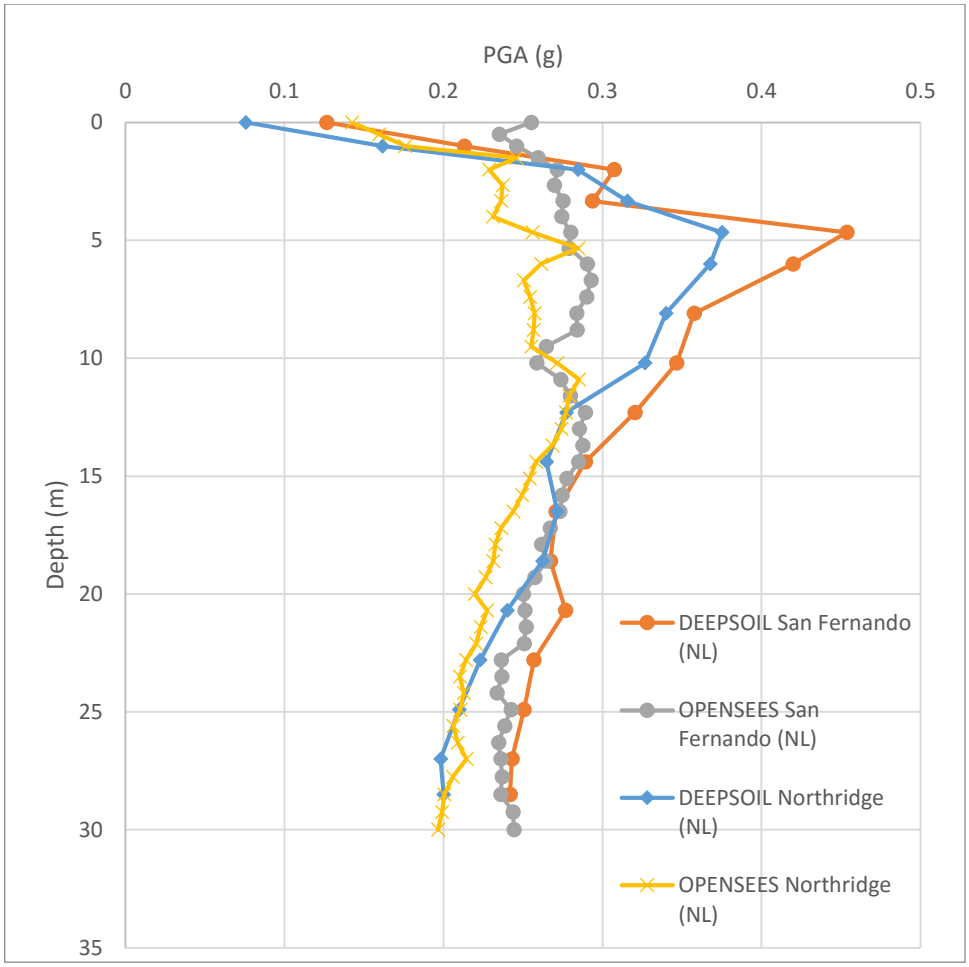

Figure 4.82: PGA Profiles for River Channel Soil using Nonlinear Analysis with DEEPSOIL and OPENSEES with N-Vs correlations given by Choudhury and Chatterjee (2013) (Uncorrected SPT)

From the figure 4.81, it is observed that the PGA values as obtained from both DEEPSOIL and OPENSEES amplifies from bedrock (PGA = 0.158g and 0.18g for Northridge and San Fernando earthquake respectively) up to a depth of 12m (0.3-0.5g). After that, it attenuates and finally near the ground surface, PGA increases slightly. In case of DEEPSOIL analysis, surface PGA is around 0.4-0.45g while for OPENSEES analysis, surface PGA comes out to be 0.2-0.25g. The PGA attenuation is generally due to presence of soft clay layer at the depth of 5-12m which results in low SPT value. From figure 4.82, it can be stated that for river channel deposit, the PGA values obtained from both DEEPSOIL and OPENSEES software follow similar trend from bedrock to a depth of about 15m. Then the PGA values as obtained from OPENSEES remains almost constant while in DEEPSOIL, PGA values keeps amplifying up to a depth of 5m. Beyond that level up to ground surface, there is a sudden reduction in PGA values. At surface, PGA values as obtained from OPENSEES and DEEPSOIL analyses are about 0.15-0.25g and 0.08-0.12g respectively.

4.4.2.PGA Amplification Ratio

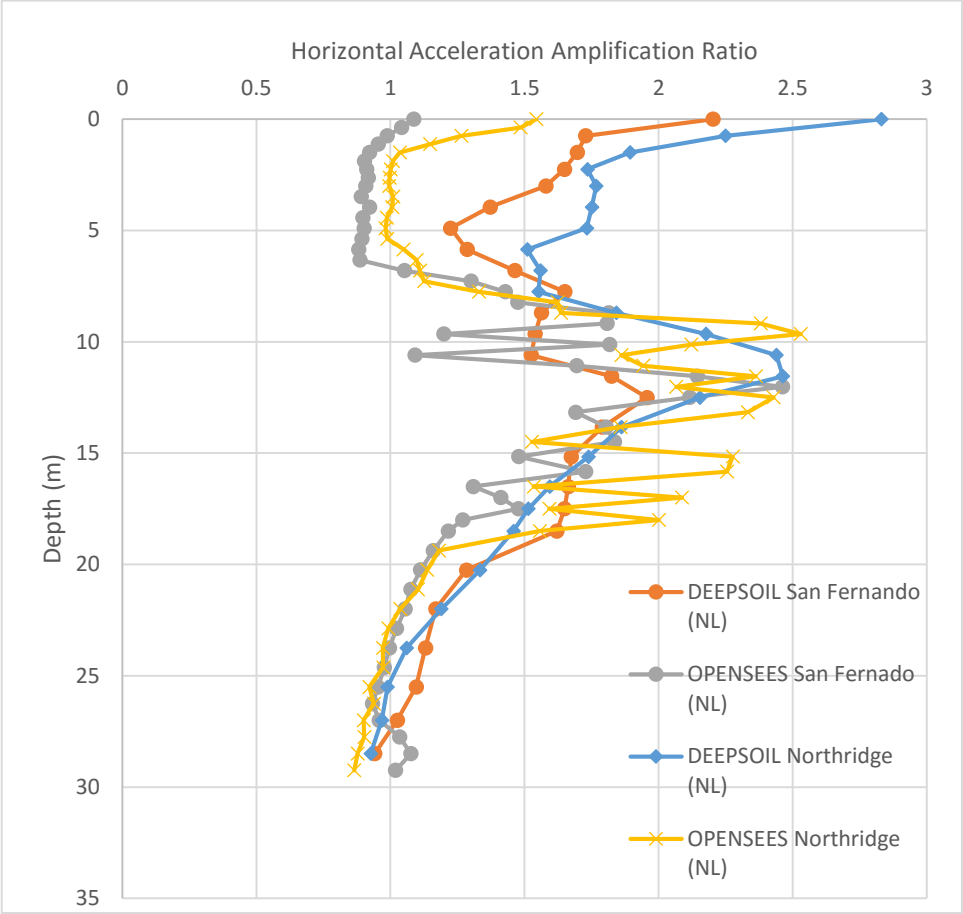

Figure 4.83: PGA Amplification Factor Profiles for Normal Kolkata Deposit using Nonlinear Analysis with DEEPSOIL and OPENSEES using N-Vs correlations given by Choudhury and Chatterjee (2013) (Uncorrected SPT)

In figure 4.83, similar trend is seen in case of PGA amplification ratio as that in figure 4.81. At depth of around 10-12m, PGA amplification is around 1.2-2.5 times. Then in the soft clay layer PGA deamplification occurs and above 5m depth, again PGA amplification takes place. At surface PGA amplification is about 2.2-2.8 times in DEEPSOIL software and 1.1-1.5 times in OPENSEES software.

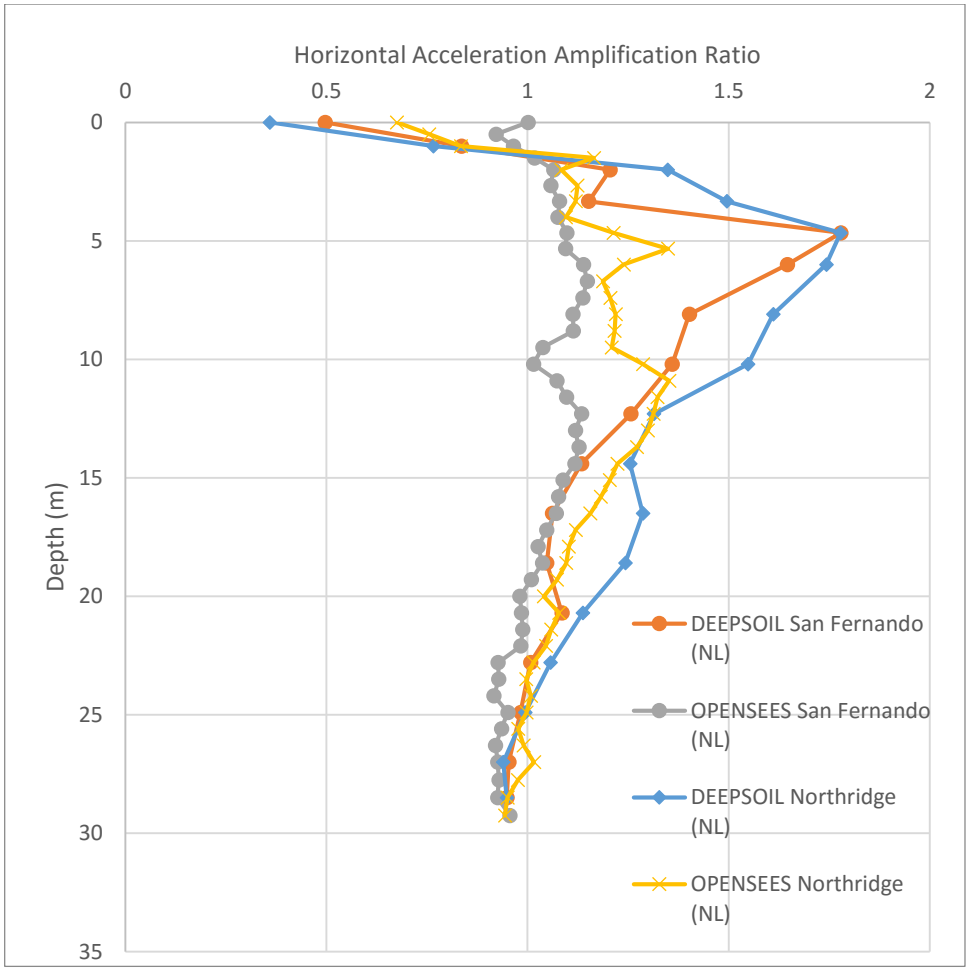

Figure 4.84: PGA Amplification Factor Profiles for River Channel Deposit using Nonlinear Analysis with DEEPSOIL and OPENSEES using N-Vs correlations given by Choudhury and Chatterjee (2013) (Uncorrected SPT)

From figure 4.84, it can be stated that the PGA amplification occurs from bedrock upto a depth of 15m. Then for OPENSEES analysis, it almost remains constant up to a depth of 2-3 m. Beyond that depth small deamplification occurs. However, in case of DEEPSOIL software, amplification of around 1.8 times occurs at depth of around 4-5m. Then sudden attenuation takes place. At surface PGA amplification is around 0.5 times for both strong motions. In OPENSEES, surface PGA amplification is around 0.8-1 times. Thus From both software, it can be observed that PGA attenuation occurs in River Channel soil at surface.

4.4.3.Relative Displacement

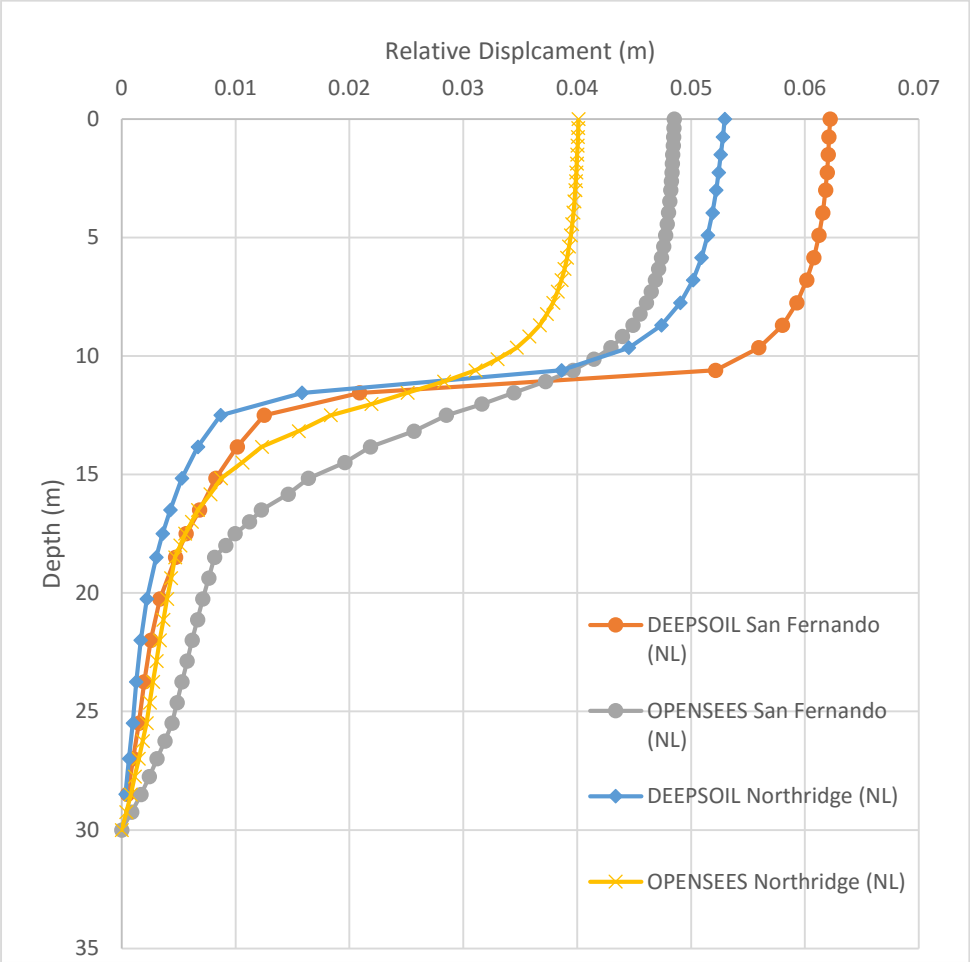

Figure 4.85: Relative Displacement Profiles for Normal Kolkata Soil using Nonlinear Analysis with DEEPSOIL and OPENSEES using N-Vs correlations given by Choudhury and Chatterjee (2013) (Uncorrected SPT)

From the figure 4.85, it is to be noted that from bedrock up to a depth of 12m, negligible displacement occurs. But in 10-15m depth, significant displacement takes place which results in high shear strain. Above 8m depth up to surface, again ground displacement is negligible. Also it can be observed that surface displacement produced in DEEPSOIL (0.053-0.062m) is more than that in OPENSEES (0.04-0.048m).

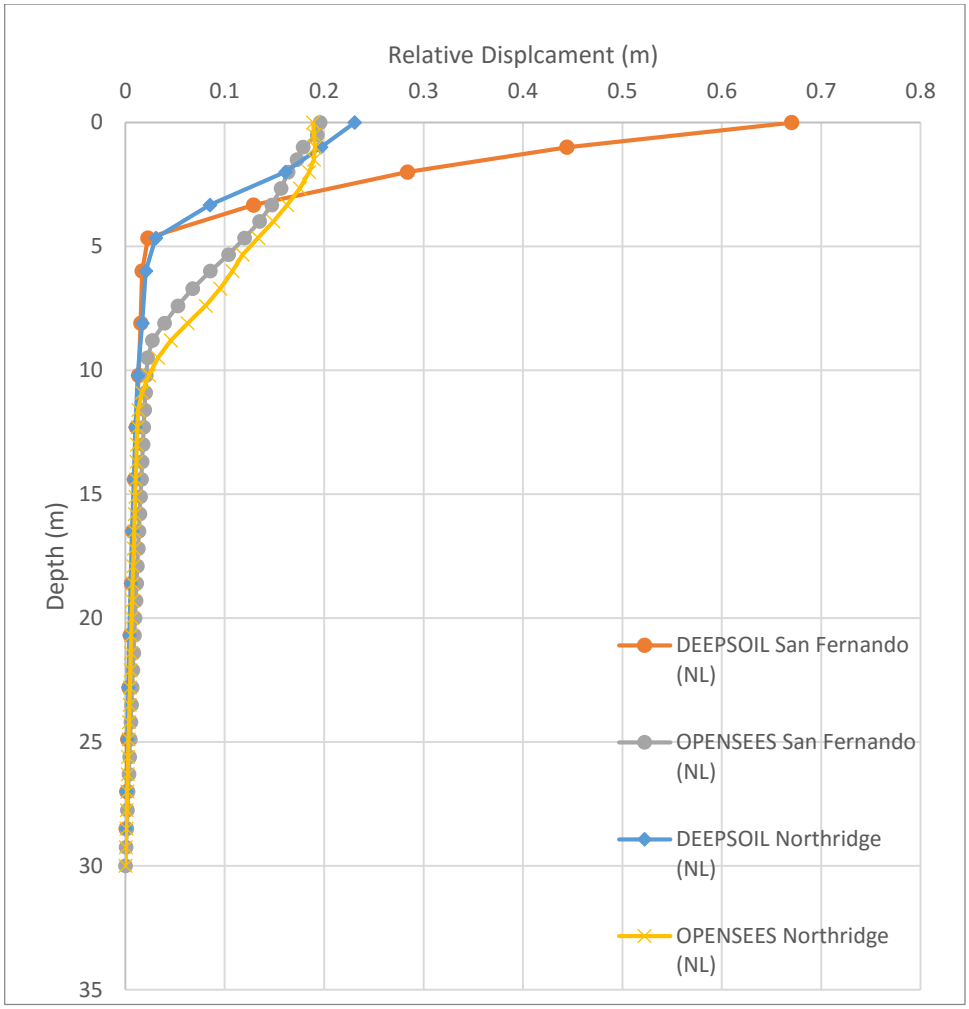

Figure 4.86: Relative Displacement Profiles for River Channel Soil using Nonlinear Analysis with DEEPSOIL and OPENSEES using N-Vs correlations given by Choudhury and Chatterjee (2013) (Uncorrected SPT)

As shown in figure 4.86, the relative displacement of soil layers is almost negligible i bedrock up to a depth of 10m. Beyond that sudden increase in ground displacement occurs. At surface, ground displacement is about 0.22-0.68m and 0.2m in case of DEEPSOIL and OPENSEES analyses respectively. Thus variability in surface displacement is less in case of OPENSEES than that in DEEPSOIL.

4.4.4.Maximum Shear Strain

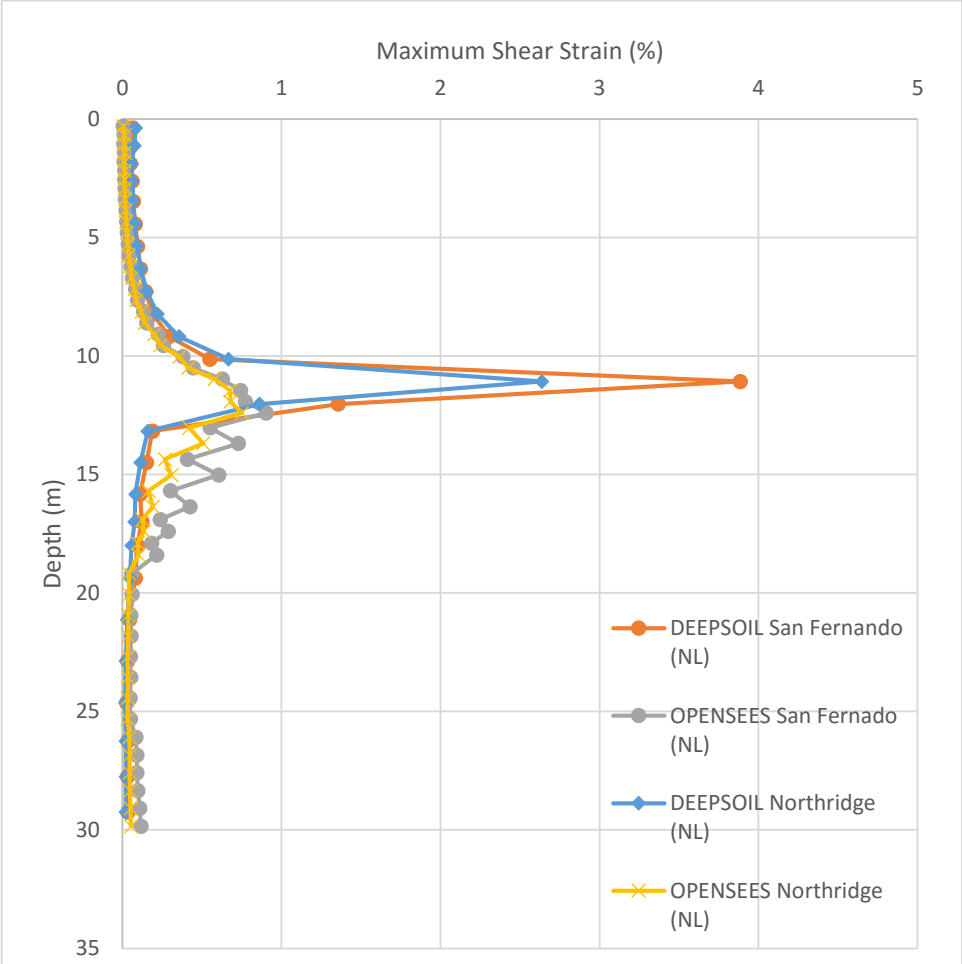

Figure 4.87: Maximum Shear Strain Profiles for Normal Kolkata Soil using Nonlinear Analysis with DEEPSOIL and OPENSEES using N-Vs correlations given by Choudhury and Chatterjee (2013) (Uncorrected SPT)

From figure 4.87, it can be stated that due to high ground displacement (figure 4.85) between 10-15m, high strain gets induced. DEEPSOIL predicts maximum shear strain of about 2.5- 4% at around 12m depth while OPENSEES predicts maximum shear strain of 0.8% in that depth. Since, relative displacement is rather uniform at every other depth in figure 4.85, the shear strain is thus negligible.

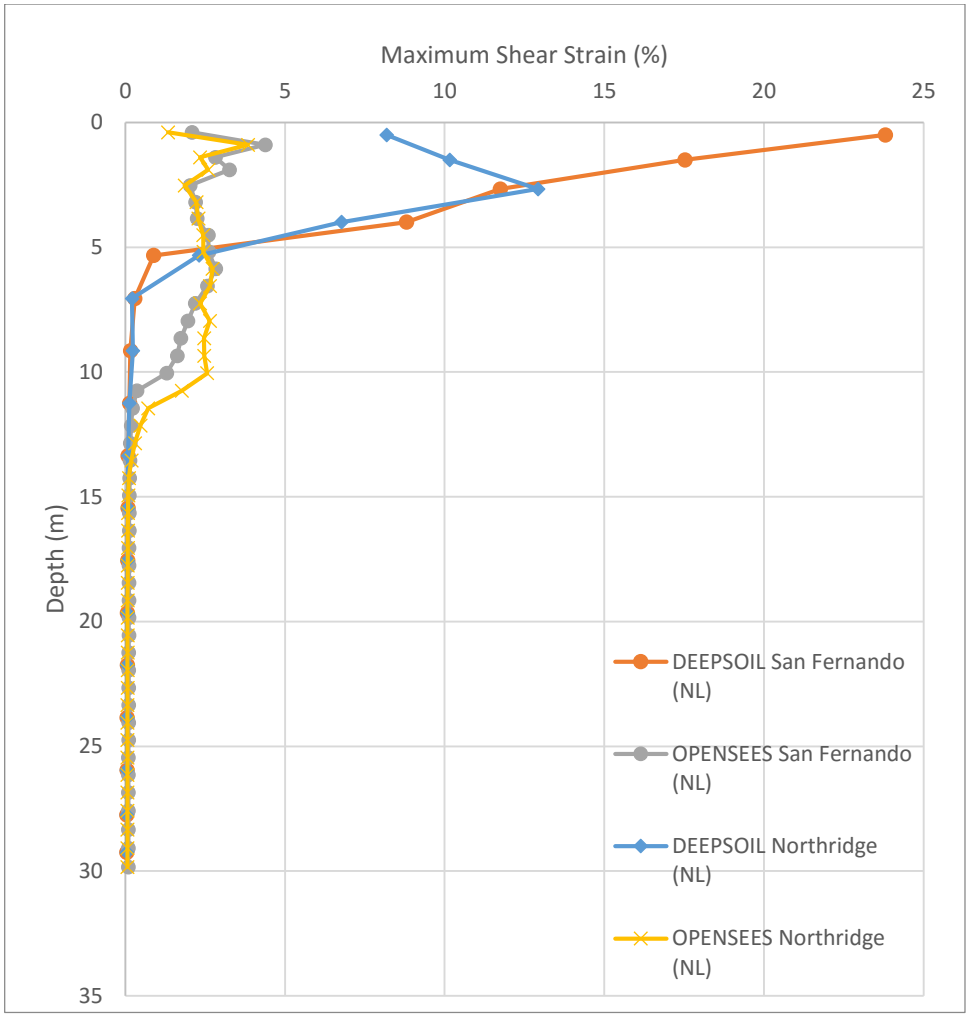

Figure 4.88: Maximum Shear Strain Profiles for River Channel Soil using Nonlinear Analysis with DEEPSOIL and OPENSEES using N-Vs correlations given by Choudhury and Chatterjee (2013) (Uncorrected SPT)

From figure 4.88, it is observed that due to sudden increase in ground displacement above 5m depth (figure 4.86), maximum shear strain is negligible below 5m depth in but beyond 5m depth, it suddenly increases to 8-24% in case of DEEPSOIL. Since in figure 4.86, gradual displacement starts to take place from around 10m depth, the shear strain also starts to induce from that depth but due to gradual deformation, shear strain almost remains constant beyond that depth upto surface level. At surface, shear strain is around 1-1.5% in OPENSEES analysis.

4.4.5.Maximum Stress Ratio

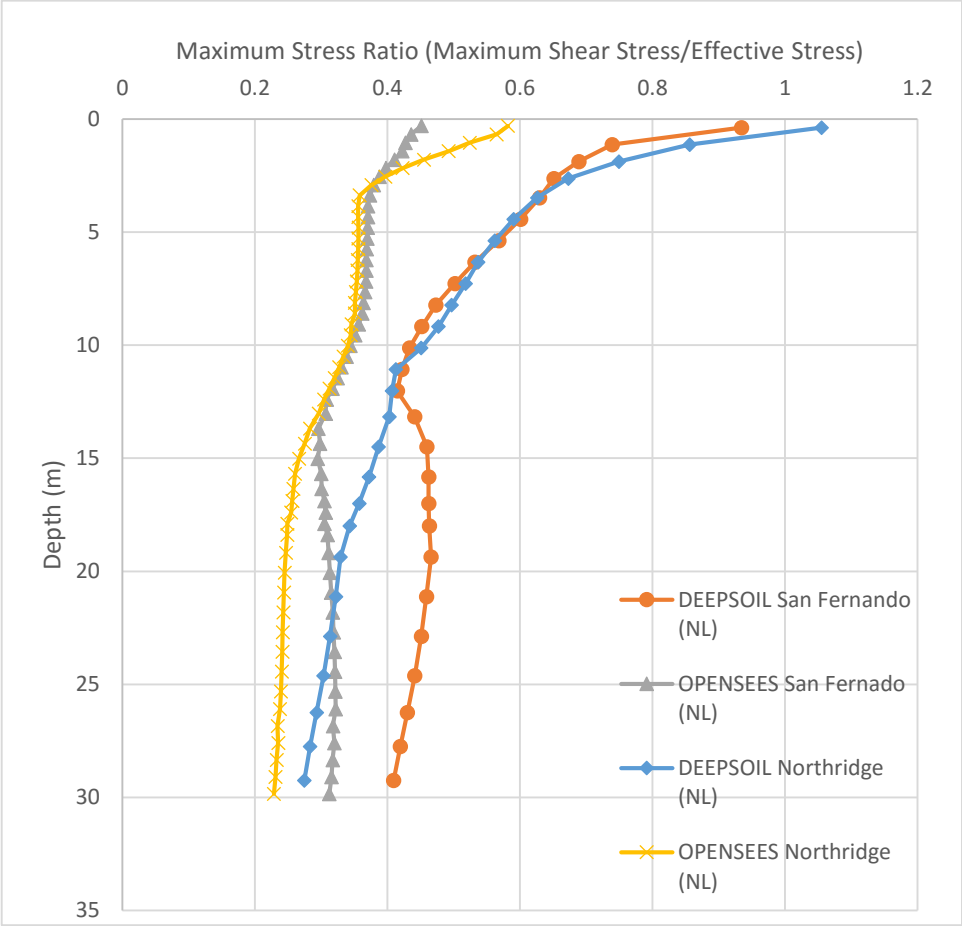

Figure 4.89: Maximum Stress Ratio Profiles for Normal Kolkata Soil using Nonlinear Analysis with DEEPSOIL and OPENSEES using N-Vs correlations given by Choudhury and Chatterjee (2013) (Uncorrected SPT)

From figure 4.89, it can be stated that maximum stress ratio keeps decreasing from surface to about 12m depth and then almost remains almost constant. The maximum stress ratio at surface ranges from 0.4-0.6 in case of OPENSEES analysis and 0.9-1.1 in case of DEEPSOIL analysis.

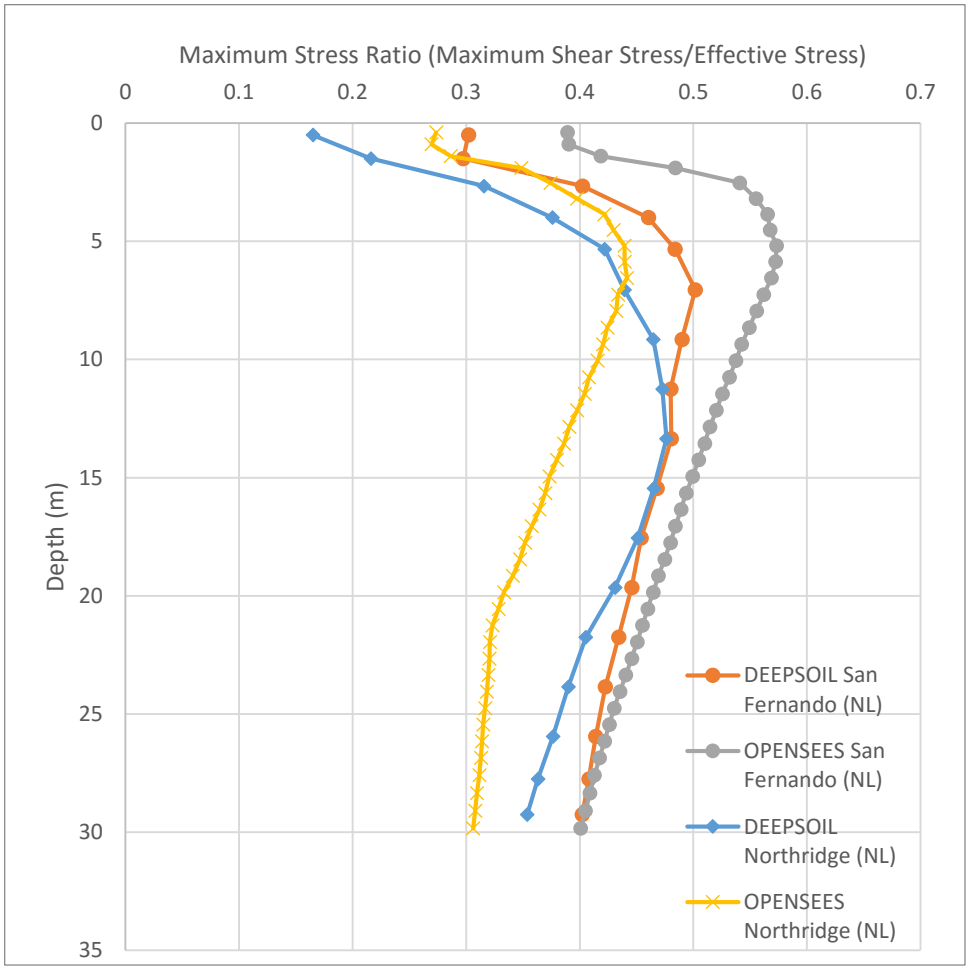

Figure 4.90: Maximum Stress Ratio Profiles for River Channel Soil using Nonlinear Analysis with DEEPSOIL and OPENSEES using N-Vs correlations given by Choudhury and Chatterjee (2013) (Uncorrected SPT)

From figure 4.90, it is observed that maximum stress ratio increases from bedrock to a depth of 5-12 m and then it decreases towards surface. The maximum stress ratio at surface ranges from 0.15-0.4.

4.4.6.Maximum Pore Pressure Ratio

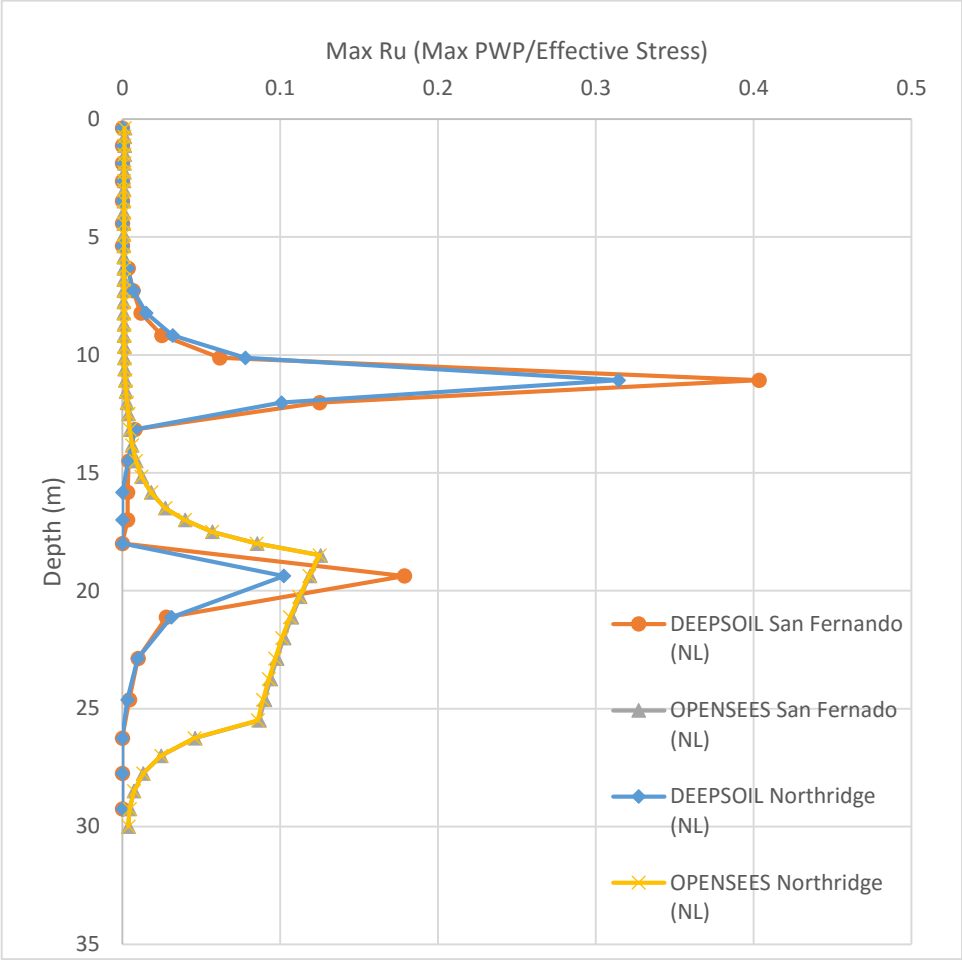

Figure 4.91: Maximum Pore Pressure Ratio Profiles for Normal Kolkata Soil using Nonlinear Analysis with DEEPSOIL and OPENSEES using N-Vs correlations given by Choudhury and Chatterjee (2013) (Uncorrected SPT)

From figure 4.91, it is observed that DEEPSOIL and OPENSEES both predict excess pore pressure ratio at 19-20m depth in the sand layer as 0.1-0.18 and 0.12 respectively. But it is also observed that DEEPSOIL though predicts excess pore pressure generation in the soft clay layer at 12m depth (excess pore pressure ratio = 0.3-0.4), OPENSEES overlooks this phenomenon.

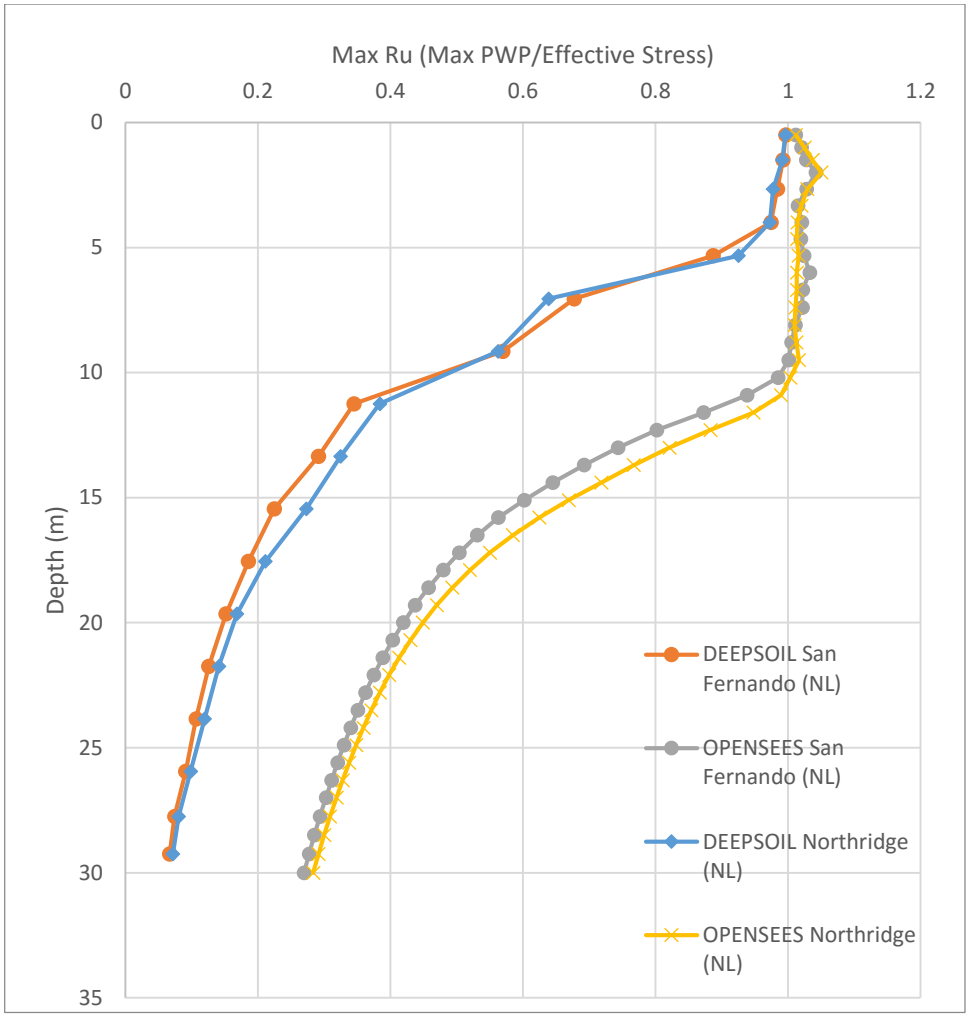

Figure 4.92: Maximum Pore Pressure Ratio Profiles for River Channel Soil using Nonlinear Analysis with DEEPSOIL and OPENSEES using N-Vs correlations given by Choudhury and Chatterjee (2013) (Uncorrected SPT)

From figure 4.92, it is observed that DEEPSOIL and OPENSEES both predict excess pore pressure ratio equal to unity at the top 5m. DEEPSOIL predicts that the pore pressure ratio decreases from unity at 5m depth to almost 0.1 at around 30m depth while OPENSEES predicts that pore pressure ratio remains unity down to a depth of 10m. Then it decreases gradually as depth increases and equals 0.25 at 30 m depth. It is to be noted that as pore pressure ratio becomes almost unity, liquefaction triggering takes place. Thus due to the strong motion applied at the bedrock of river channel soil, the top 5m might liquefy.

4.5. SIMPLIFIED PROCEDURE OF LIQUEFACTION ANALYSIS IN RIVER CHANNEL SOIL DEPOSIT

As observed in section (4.3) and (4.4), the river channel soil deposit will experience liquefaction if the spectrum compatible strong motions used in the analysis occur in the region. The simplified Seed and Idriss (1971) (modified by Idriss and Boulanger (2014)) liquefaction potential evaluation procedure is used in this case to verify the result from ground response analysis. The moment magnitude of the earthquake used in this case is 6.2 for Eocene Hinge Zone vulnerable source as reported by Roy and Sahu (2012). The maximum surface PGA used is the average surface PGA obtained from section (4.4.1) for spectrum compatible San Fernando earthquake Northridge earthquake. The results are presented in the form of Cyclic Resistance Ratio (CRR) and Cyclic Stress Ratio (CSR) and Factor of Safety against Liquefaction [FS (liq)] variation with depth.

4.5.1. CRR & CSR

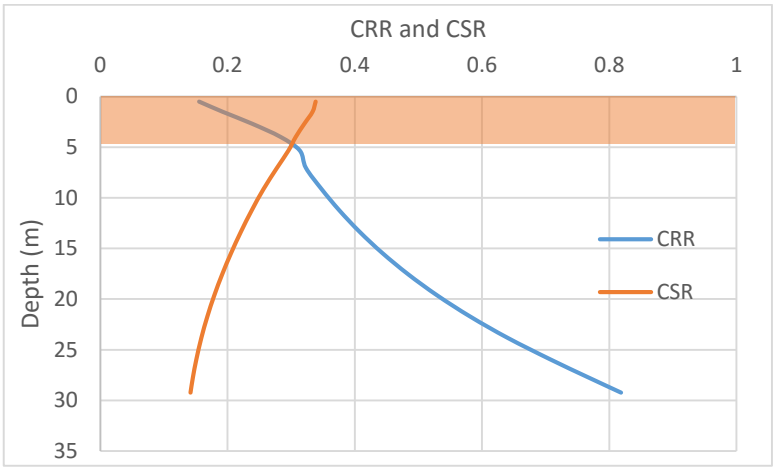

Figure 4.93: CRR and CSR Profiles for River Channel Deposit for San Fernando Earthquake

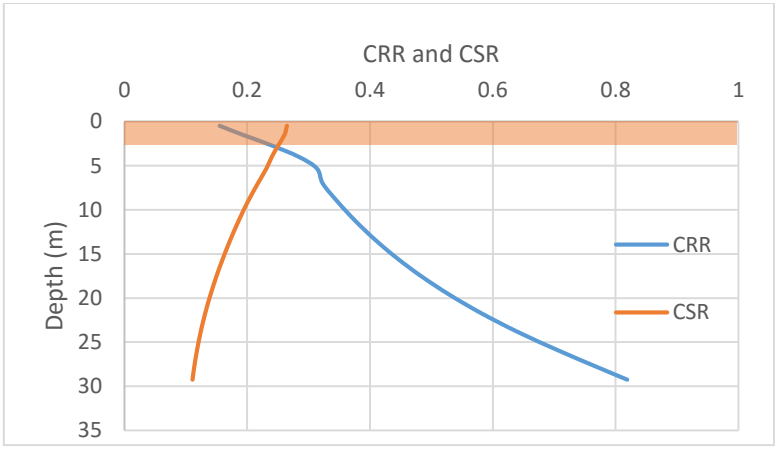

Figure 4.94: CRR and CSR Profiles for River Channel Deposit for Northridge Earthquake

From figure 4.94 and 4.95, it is observed that CSR decreases gradually from around 0.32-0.36 at surface to 0.15-0.17 at 30m depth. While, CRR increases from 0.15 at ground surface to 0.82 at 30m depth. The two curves intersect at 5m and 3m depth in figures 4.94 and 4.95 respectively. So the top 3-5m deep soil layer may experience liquefaction if a strong motion earthquake similar to that used in the study occurs in the region.

4.5.2.FACTOR OF SAFETY AGAINST LIQUEFACTION

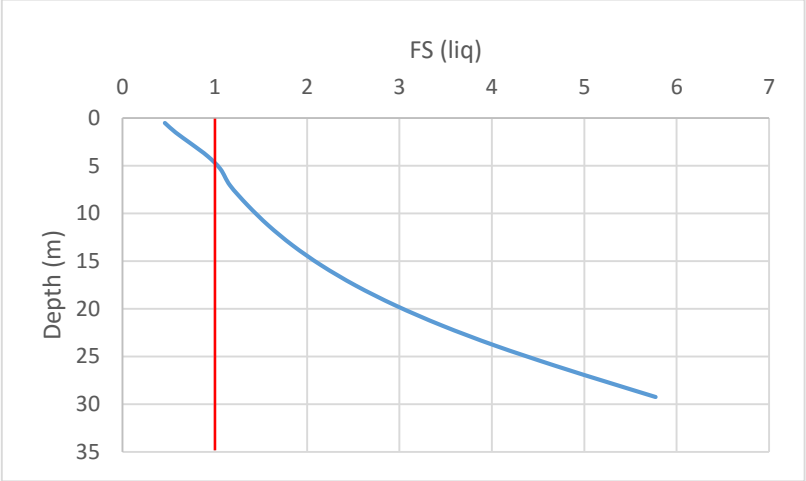

Figure 4.95: Factor of Safety Profiles for River Channel Deposit for San Fernando Earthquake

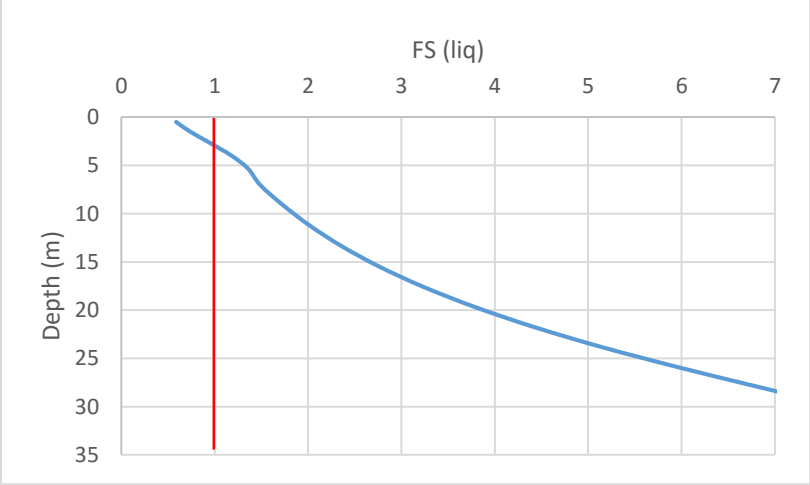

Figure 4.96: Factor of Safety Profiles for River Channel Deposit for Northridge Earthquake

It is observed from figure 4.95 and 4.96 that Factor of Safety against liquefaction increases with depth. Factor of Safety is less than unity for soil depth less than around 5m. In that zone, CSR is more than CRR. Thus the top fill layer and loose sandy silt is susceptible to liquefaction for the spectrum

compatible strong motion used in this case. It also shows similarity with the result obtained from ground response analysis with DEEPSOIL and OPENSEES where in the top 5m, the pore pressure ratio is almost equal to unity. Hence it is quite safe to say that the analyses used in the study produces quite similar results for the strong motion used in each case.

4.6.POST LIQUEFACTION SETTLEMENT CALCULATION IN RIVER CHANNEL SOIL DEPOSIT

Since river channel deposit soil undergoes liquefaction under the two strong motions used in the study, post liquefaction settlement is calculated in the river channel deposit for the two spectrum compatible time histories used [figures 4.38 and 4.39]. Two approaches for calculation of post-liquefaction settlement are followed namely, Tokimatsu and Seed (1987) approach and Ishihara and Yoshemine (1992) approach. Tokimatsu and Seed (1987) approach is a graphical approach where volumetric strain is calculated from figure 3.22 in Chapter 3 from CSR and $(N_1)_{60}$ values. On the other hand, approximation of Ishihara and Yoshemine (1992) method is performed analytically with the help of Idriss and Boulanger (2008). Then a depth correction factor is introduced in each case (Cetin et. al., 2009). The calculations for Tokimatsu and Seed (1987) and Ishihara and Yoshemine (1992) approaches for two strong motions are provided in Table 4.12 – 4.15. The final settlements are shown in tabulated form in Table 4.16.

Table 4.11. Calculation for Post-liquefaction Settlement using Tokimatsu and Seed (1987) Approach for San Fernando Earthquake

Layer #	Thickness (m)	Depth (m)	N1,60	CSR (M=7.5)	ε(v) (%)	DF	ε(v) x t x DF	t x DF
1	1	0.5	1.766323125	0.218742337	10	0.972222222	0.097222222	0.972222222
2	1	1.5	5.283109125	0.215633131	4.5	0.916666667	0.04125	0.916666667
3	1.33	2.665041146	9.353639322	0.207418388	2.8	0.851942159	0.031726326	1.133083071
4	1.33	3.995123438	12.5919769	0.198495102	2.2	0.778048698	0.022765705	1.034804768
5	1.34	5.330082292	14.36910521	0.191144176	2	0.703884317	0.0188641	0.943204985
6	2.1	7.049984761	16.11797961	0.183256231	1.8	0.60833418	0.022995032	1.277501778
7	2.1	9.149954282	17.85590291	0.175616155	1	0.491669207	0.010325053	1.032505334
8	2.1	11.2499238	19.41662038	0.168419581	0.1	0.375004233	0.000787509	0.78750889
9	2.1	13.34989333	20.83107598	0.161448139	0	0.25833926	0	0.542512445
10	2.1	15.44986285	22.12400317	0.15480699	0	0.141674286	0	0.297516001
11	2.1	17.54983237	23.31424489	0.14868187	0	0.025009313	0	0.052519557
12	2.1	19.64980189	24.41633582	0.143265534	0	0	0	0
13	2.1	21.74977141	25.44148342	0.138733556	0	0	0	0
14	2.1	23.84974093	26.39871102	0.135242026	0	0	0	0
15	2.1	25.94971045	27.29523454	0.132931808	0	0	0	0
16	1.5	27.74961902	27.99954084	0.131914488	0	0	0	0
17	1.5	29.24946663	28.53649408	0.131780924	0	0	0	0
Σ=	30					Σ=	0.245935947	8.990045718

						ε_v(equivalent)=	0.027356473	
						S (calibrated) (m)=	**1.190006595**	

Table 4.12. Calculation for Post-liquefaction Settlement using Ishihara and Yoshemine (1992) Approach for San Fernando Earthquake

Layer #	Thickness (m)	Depth (m)	N1,60,cs	FS, liq	F(α)	ϒ(lim)	ϒ(max)	ε(v)	DF	ε(v) x t x DF	t x DF
1	1	0.5	7.342167426	0.458794591	0.94717219	0.63896295	0.63896295	0.044151784	0.972222222	0.042925345	0.972222222
2	1	1.5	10.85895343	0.575643148	0.89408796	0.430598221	0.430598221	0.035570931	0.916666667	0.032606687	0.916666667
3	1.33	2.665041146	14.71627484	0.741247119	0.765848277	0.283690629	0.283690629	0.029135036	0.851942159	0.033012416	1.133083071
4	1.33	3.995123438	17.95461242	0.923116955	0.621629335	0.199542119	0.009611644	0.003018865	0.778048698	0.003123936	1.034804768
5	1.34	5.330082292	19.73174073	1.060125283	0.531882965	0.163879664	-0.003744225	-0.001090423	0.703884317	-0.001028493	0.943204985
6	2.1	7.049984761	20.59418197	1.16395011	0.486032447	0.148729813	-0.007076769	-0.001989196	0.60833418	-0.002541201	1.277501778
7	2.1	9.149954282	22.33210527	1.356540673	0.389549443	0.12188666	-0.008303777	-0.002177979	0.491669207	-0.002248775	1.032505334
8	2.1	11.2499238	23.89282274	1.579401403	0.298672717	0.101443973	-0.006659755	-0.001645206	0.375004233	-0.001295614	0.78750889
9	2.1	13.34989333	25.30727834	1.842507157	0.213191269	0.085491589	-0.002850343	-0.000668045	0.25833926	-0.000362423	0.542512445
10	2.1	15.44986285	26.60020553	2.154579996	0.13267499	0.07278438	0	0	0.141674286	0	0.297516001
11	2.1	17.54983237	27.79044725	2.523593234	0.056690405	0.062491286	0	0	0.025009313	0	0.052519557
12	2.1	19.64980189	28.89253818	2.956536302	-0.015157166	0.054038264	0	0	0	0	0
13	2.1	21.74977141	29.91768578	3.45870986	-0.083201882	0.047017844	0	0	0	0	0
14	2.1	23.84974093	30.87491338	4.032862947	-0.147740009	0.041131349	0	0	0	0	0
15	2.1	25.94971045	31.77143691	4.678073613	-0.209021943	0.036155924	0	0	0	0	0
16	1.5	27.74961902	32.4757432	5.269190273	-0.257709622	0.032585366	0	0	0	0	0
17	1.5	29.24946663	33.01269644	5.771651938	-0.295139877	0.030050764	0	0	0	0	0
Σ=	30								Σ=	0.104191877	8.990045718
									ε(v,equivalent)=	0.011589694	
									S (calibrated) (m)=	**0.312921734**	

Table 4.13. Calculation for Post-liquefaction Settlement using Tokimatsu and Seed (1987) Approach for Northridge Earthquake

Layer #	Thickness (m)	Depth (m)	N1,60	CSR (M=7.5)	ε(v) (%)	DF	ε(v) x t x DF	t x DF
1	1	0.5	1.766323125	0.171016736	10	0.972222222	0.097222222	0.972222222
2	1	1.5	5.283109125	0.168585902	4	0.916666667	0.036666667	0.916666667
3	1.33	2.665041146	9.353639322	0.162163467	3	0.851942159	0.033992492	1.133083071
4	1.33	3.995123438	12.5919769	0.155187079	2.4	0.778048698	0.024835314	1.034804768
5	1.34	5.330082292	14.36910521	0.149439992	2.2	0.703884317	0.02075051	0.943204985
6	2.1	7.049984761	16.11797961	0.143273053	0.2	0.60833418	0.002555004	1.277501778
7	2.1	9.149954282	17.85590291	0.137299903	0	0.491669207	0	1.032505334
8	2.1	11.2499238	19.41662038	0.131673491	0	0.375004233	0	0.78750889
9	2.1	13.34989333	20.83107598	0.12622309	0	0.25833926	0	0.542512445
10	2.1	15.44986285	22.12400317	0.12103092	0	0.141674286	0	0.297516001
11	2.1	17.54983237	23.31424489	0.116242189	0	0.025009313	0	0.052519557

12	2.1	19.64980189	24.41633582	0.1120076	0	0	0	0
13	2.1	21.74977141	25.44148342	0.108464416	0	0	0	0
14	2.1	23.84974093	26.39871102	0.105734675	0	0	0	0
15	2.1	25.94971045	27.29523454	0.103928504	0	0	0	0
16	1.5	27.74961902	27.99954084	0.103133146	0	0	0	0
17	1.5	29.24946663	28.53649408	0.103028723	0	0	0	0
Σ=	30					Σ=	0.216022209	8.990045718
						ε(v,equivalent)=	0.024029045	
						S (calibrated) (m)=	**1.045263436**	

Table 4.14. Calculation for Post-liquefaction Settlement using Ishihara and Yoshemine (1992) Approach for Northridge Earthquake

Layer #	Thickness (m)	Depth (m)	N1,60,cs	FS, liq	F(α)	ϒ(lim)	ϒ(max)	ε(v)	DF	ε(v) x t x DF	t x DF
1	1	0.5	7.342167426	0.586830291	0.94717219	0.63896295	0.63896295	0.044151784	0.972222222	0.042925345	0.972222222
2	1	1.5	10.85895343	0.736287747	0.89408796	0.430598221	0.430598221	0.035570931	0.916666667	0.032606687	0.916666667
3	1.33	2.665041146	14.71627484	0.94810678	0.765848277	0.283690629	0.010482443	0.003817579	0.851942159	0.004325635	1.133083071
4	1.33	3.995123438	17.95461242	1.180730989	0.621629335	0.199542119	-0.009269076	-0.00291127	0.778048698	-0.003012596	1.034804768
5	1.34	5.330082292	19.73174073	1.355974199	0.531882965	0.163879664	-0.009736762	-0.002835618	0.703884317	-0.002674569	0.943204985
6	2.1	7.049984761	20.59418197	1.488773397	0.486032447	0.148729813	-0.008721683	-0.002451562	0.60833418	-0.003131875	1.277501778
7	2.1	9.149954282	22.33210527	1.735110163	0.389549443	0.12188666	-0.005065035	-0.001328497	0.491669207	-0.00137168	1.032505334
8	2.1	11.2499238	23.89282274	2.020164586	0.298672717	0.101443973	0	0	0.375004233	0	0.78750889
9	2.1	13.34989333	25.30727834	2.356695201	0.213191269	0.085491589	0	0	0.25833926	0	0.542512445
10	2.1	15.44986285	26.60020553	2.755858134	0.13267499	0.07278438	0	0	0.141674286	0	0.297516001
11	2.1	17.54983237	27.79044725	3.227851811	0.056690405	0.062491286	0	0	0.025009313	0	0.052519557
12	2.1	19.64980189	28.89253818	3.7816162	-0.015157166	0.054038264	0	0	0	0	0
13	2.1	21.74977141	29.91768578	4.423931216	-0.083201882	0.047017844	0	0	0	0	0
14	2.1	23.84974093	30.87491338	5.158313072	-0.147740009	0.041131349	0	0	0	0	0
15	2.1	25.94971045	31.77143691	5.983582529	-0.209021943	0.036155924	0	0	0	0	0
16	1.5	27.74961902	32.4757432	6.739661978	-0.257709622	0.032585366	0	0	0	0	0
17	1.5	29.24946663	33.01269644	7.382345502	-0.295139877	0.030050764	0	0	0	0	0
Σ=	30								Σ=	0.069666947	8.990045718
									ε(v,equivalent)=	0.007749343	
									S (calibrated) (m)=	**0.209232257**	

Table 4.16. Result for Post Liquefaction Settlement in River Channel Soil Deposit

Earthquake (Spectrum Compatible):		**San Fernando**	**Northridge**
PGA (g):		0.255	0.211
Liquefaction up to depth (m):		5	3
Settlement (cm):	**Tokimatsu and Seed (1987)**	119	105
	Ishihara and Yoshemine (1992)	31	21

From Table 4.16, it is found that Tokimatsu and Seed (1987) approach results in more settlement than that in Ishihara and Yoshemine (1992). But the difference of settlements in each approach are quite similar for both strong motions. However, contribution of top 5-6m is about 85-90% of the total predicted settlement.

CHAPTER 5

SUMMARY AND CONCLUSION

5.1. SUMMARY

This thesis paper is about the study of nonlinear ground response analysis of Kolkata soil. The two soil profiles examined for ground response analysis were the Normal Kolkata soil deposit and River Channel soil deposit. According to NEHRP (2003) and IBC (2009), the Normal Kolkata Deposit and River Channel Deposit can be classified as Site Class 'D' and 'E' though they provided contradicting site classes with respect to average 30m N value and V_s value. The software mainly used for the study was DEEPSOIL. In case of lack of strong motion data, spectrum compatible strong motion can be artificially generated. Thus, two strong motions used in the analysis were generated artificially by spectrum compatibility method of respective zones and types of soil of the two sites. Dynamic soil properties were estimated for plastic and non-plastic soils from Ishibashi and Zhang (1993) method as laboratory test data were not available. Both equivalent linear analysis and nonlinear analyses were performed with various SPT-N and V_s correlations to predict the PGA variation, PGA amplification ratio variation, relative displacement of soil profile, maximum shear strains variation and maximum pore pressure variation with depth. Additionally, Fourier amplification ratio variation with frequency and surface response spectra were also presented. One specific V_s-N correlation was used in OPENSEES software to compare the output with that of DEEPSOIL. It was noted that soil stiffness is heavily dependent on shear wave velocity. So if in-situ values of shear wave velocity is not available, a proper site, depth and lithology specific V_s-N correlation should be used for ground response analysis. At last, simplified liquefaction potential analysis was performed for river channel deposit with the average PGA obtained from equivalent linear analysis and nonlinear analysis and post-liquefaction settlement was calculated thereafter.

5.2. CONCLUSIONS

The observations from the study are summarized below:

1. PGA and response spectral acceleration calculated from equivalent linear analysis is more than that from nonlinear analysis because in case of nonlinear analysis, due to soil nonlinearity, large hysteretic damping is induced which attenuates the surface PGA.
2. Low PBRA motion amplifies more than that in high PBRA motion as high PBRA motion induces high strain which results in higher damping.
3. Maximum shear strain generated in soil due to strong motion shaking is more in case of nonlinear analysis whereas, equivalent linear analysis underestimates it.

4. Nonlinear analysis coupled with effective stress approach presents pore pressure variation in soil which is useful to predict liquefaction initiation.
5. Excess pore pressure generated in soil due to strong motion shaking is correlated with shear strain. High induced strain in soil generates higher excess pore pressure.
6. In River Channel Deposit, pore pressure ratio becomes unity in the top 5-10m depth which signified the initiation of liquefaction. Liquefaction is also found to observe in the evaluation of liquefaction potential by simplified procedure and nonlinear analysis performed with OPENSEES.
7. Post liquefaction settlement in River Channel Deposit is calculated with two approaches proposed by Tokimatsu and Seed (1987) and Ishihara and Yoshemine (1992). In the former approach, the settlement is found to be higher than that in the latter one. The probable reason for this might be the use of $N_{1,60}$ in case of Tokimatsu and Seed (1987) method and use of $(N_1)_{60,CS}$ in the Ishihara and Yoshemine (1992) method. $(N_1)_{60,CS}$ considers the fines content which might decrease the liquefaction potential and thus results in lower settlement.
8. The response spectra obtained from the current study can be used for site specific design of engineering structures.
9. The response spectra obtained from the study is observed to be varied from that prescribed by IS:1893 (Part 1)-2002. This necessitates the need for the estimation of site specific response spectra from seismic hazard study of that particular region.
10. Response spectra obtained from equivalent linear and nonlinear analysis is found to vary substantially for different adopted V_s-N correlations. This may affect the outcome of hazard study significantly. So, it is recommended to use the site specific shear wave velocity values as input in ground response analysis.

5.3. FUTURE SCOPE OF WORK

This thesis work may be considered as a basic work as far as nonlinear ground response analysis is considered. The findings of this thesis may serve as the basis of various future investigations.

The future scope of works may be as under:

1. Various correlations of SPT and shear wave velocity have been used. The in-situ testing of shear wave velocity and maximum shear modulus can be used to predict more reliable data.
2. OPENSEES software is used for only one specific SPT-Vs correlation. It can be used for other correlations too.
3. In case of strong motion occurrence in Kolkata, actual rock outcrop acceleration time history obtained from recording stations can be used rather than using spectrum compatible strong motion data.

4. Laboratory testing of dynamic soil properties along with pore pressure parameters can be done instead of relying on empirical relationships.
5. DEEPSOIL has recently incorporated a new constitutive soil model known as General Quadratic/Hyperbolic (GQ/H) Strength-Controlled Constitutive Model (Groholski et. al. 2015). It can be used for comparative study with MKZ soil model used in the study.
6. Strain-based pore pressure generation model was used in the study. Energy based pore pressure generation model (Green et. al., 2000) can be used to testify the validity of the strain-based model.

REFERENCES

Akhila Manne, Chandan Ghosh and Neelima Satyam D (2012) "Detailed Ground Response Analysis for Kolkata City, India" 15th World conference on Earthquake Engineering (15 WCEE), Sep 24-28, 2012, Lisbon, Portugal, Paper No:5158

Ashford SA, Jakrapyanun W and Lukkanaprasit P (2000), "Amplification of earthquake ground motions in 401 Bangkok," Proceedings of the 12th World Conference on Earthquake Engineering, Auckland, New Zealand, 402 pp.1-7. 403

Boominathan A., Dodagoudar G.R., Suganthi, A. and Uma Maheswari, R. (2008). "Seismic hazard assessment of Chennai city considering local site effects", Journal of Earth System Science, 117(S2), 853-863.

Boulanger, Ross & Idriss, I. (2014). CPT and SPT based liquefaction triggering procedures. Report No. UCD/CGM-14/01, Center for Geotechnical Modeling, University of California, Davis.

Carlton, Brian. (2014). An Improved Description of the Seismic Response of Sites with High Plasticity Soils, Organic Clays, and Deep Soft Soil Deposits.

Cetin K, Bile H, Wu J, AM K, RB S 2009: J. Geotech. and Geoenv. Engrg., 135, 387–398

Chappidi, Hanumantharao & Gunturi, R. (2007). SITE SPECIFIC GROUND RESPONSE ANALYSES AT DELHI, INDIA.

Chatterjee, K. and Choudhury, D. (2016) Influences of Local Soil Conditions for Ground Response in Kolkata City During Earthquakes. In: Proc. National Acad. Sci., India Section A: Physical Sciences. Springer India.

Desai, S.S. and Choudhury, D. (2015) Site-Specific Seismic Ground Response Study for Nuclear Power Plants and Ports in Mumbai. Nat. Hazards Rev., v.16(4), pp.1–13.

Dobry, R & Ladd, R.S. & Yokel, F.Y. & Chung, R.H. & Powell, D. (1982). Prediction of Pore Water Pressure Buildup and Liquefaction of Sand by the Cyclic Strain Method. National Bureau of Standards Building Science Series 138, Washington, D.C.

GovindaRaju, L & Gunturi, R & Chappidi, Hanumantharao & Thallak, Sitharam. (2004). Site-specific ground response analysis. Current science. 87. 1354-1362.
Govindaraju, L. and Bhattacharya, S. (2012) Site-specific earthquake response study for hazard assessment in Kolkata city, India. Natural Hazards, v.61(3), pp.943–965.

GSI (2000), "Seismotectonic atlas of India and its environs," Geological Survey of India, Calcutta, India. 427

Hanumantharao C, Ramana GV (2008) Dynamics soil properties for microzonation of Delhi, India. J Earth Syst Sci 117(S2):719–730

Hardin BO and Drnevich VP (1972), "Shear modulus and damping soils: Design equations and curves," 428 Journal of Soil Mechanics and Foundations Division, ASCE, 98:289-324.429.

Hashash YMA and Park D (2001), "Nonlinear one-dimensional seismic ground motion propagation in the 433 Mississippi embayment," Engineering Geology, 62(1-2):185-206. 434

Hashash, Y.M.A., Musgrove, M.I., Harmon, J.A., Groholski, D.R., Phillips, C.A., and Park, D. (2016) "DEEPSOIL 6.1, User Manual"

Housner GW and Jennings PC (1972), "The San Fernando California earthquake," Earthquake Engineering 438 and Structural Dynamics, 1(1):5-31. 439

IBC (2009), "International building code," International Code Council. 440

IS: 1893-Part 1 (2002), "Criteria for earthquake resistant design of structures," Bureau of Indian Standards. 443

Ishibashi I and Zhang X (1993), "Unified dynamic shear moduli and damping ratios of sand and clay," Soils 444 and Foundations, 33(1):182-191. 445

Ishihara K, Yoshimine M 1992: Soils and Foundations, 32, No. 1, 173–188.

Jafari, M.K. Shafiee, A. and Ramshaw, A. (2002). "Dynamic properties of the fine grained soils in south of Tehran," J. Seismol. Earthq. Eng. 4 25–35

Jishnu, R.B & Naik, Sambit & Patra, N.R. & Malik, Javed. (2013). Ground response analysis of Kanpur soil along Indo-Gangetic Plains. Soil Dynamics and Earthquake Engineering. 51. 47–57. 10.1016/j.soildyn.2013.04.001.

Kaustav Chatterjee and Deepankar Choudhury (2013); "Variations in shear wave velocity and soil site class in Kolkata city using regression and sensitivity analysis", Natural Hazards, (ISSN: 0921-030X, Impact Factor: 1.639/2012) Springer, Netherlands, Vol. 69, No. 3, pp. 2057-2082, doi: 10.1007/s11069-013-0795-7

Kondner RL and Zelasko JS (1963), "A hyperbolic stress-strain formulation of sands," Proceedings of the 2nd 453 Pan American Conference on Soil Mechanics and Foundation Engineering, Sao Paulo, Brasil, pp.289-324. 454

Kramer SL (1996), Geotechnical earthquake engineering, Prentice Hall, Upper Saddle River, New Jersey. 455

Kumar A, Harinarayan NH and Baro O (2015), "High Amplification factor for Low Amplitude Ground 456 Motion: Assessment for Delhi," Disaster Advances, 8(12):1-11. 457

Kumar dammala, Pradeep & Kumar, Shiv & Murali Krishna, A & Bhattacharya, Subhamoy. (2019). Dynamic soil properties and liquefaction potential of northeast Indian soil for non-linear effective stress analysis. Bulletin of Earthquake Engineering. 1-35. 10.1007/s10518-019-00592-6.

Kumar SS and Murali Krishna A (2013), "Seismic ground response analysis of some typical sites of Guwahati 458 city," International Journal of Geotechnical Earthquake Engineering, 4(1):83-101. 459

Kumar, Shiv & Murali Krishna, A. (2013). Seismic Ground Response Analysis of Some Typical Sites of Guwahati City. International Journal of Geotechnical Earthquake Engineering. 4. 83-101. 10.4018/jgee.2013010106.

Kwok AOL, Stewart JP and Hashash YMA (2008), "Nonlinear ground response analysis of Turkey Flat 460 shallow stiff-soil site to strong ground motions," Bulletin of the Seismological Society of America, 98(1):331-461 343. 462

Masing G (1926), "Eignespannungen und verfestigung beim messing," In: 2nd International Congress on 470 Applied Mechanics, Zurich, Switzerland, pp.332-335. 471

Matasovic N and Vucetic M (1993), "Cyclic characterization of liquefiable sands," Journal of Geotechnical 472 and Geoenvironmental Engineering, ASCE, 119(11):1805-1822. 473

Matasovic, Neven & Vucetic, Mladen. (1992). Pore pressure model for cyclic straining of clay. SOILS AND FOUNDATIONS. 32. 156-173. 10.3208/sandf1972.32.3_156.

McKenna, F. and Fenves, G. (2001). "The OpenSees Command Language Manual: version 1.2," Pacific Earthquake Engineering Center, Univ. of Calif., Berkeley.

Mei, Xuan & Olson, Scott M. & Hashash, Youssef M.A. (2018). Empirical porewater pressure generation model parameters in 1-D seismic site response analysis. 10. 1016/ j.soildyn.2018.07.011

Mukherjee, Sushovan and Vinay Kumar Gupta. "Wavelet-based generation of spectrum-compatible time-histories." (2002).

Nath, S. K., M. D. Adhikari, S. K. Maiti, N. Devaraj, N. Srivastava, and L. D. Mohapatra (2014). Earthquake scenario in West Bengal with emphasis on seismic hazard microzonation of the city of Kolkata, India, Nat. Hazards Earth Syst. Sci. 14, 2549–2575, doi:10.5194/nhess-14-2549-2014, 2014.

NEHRP Part 1: Provisions (2003), "NEHRP recommended provisions for seismic regulations for new 474 buildings and other structures (FEMA 450)," Building Seismic Safety Council, National Institute of Building 475 Sciences, Washington, pp.338. 476

Newmark NM (1959), "A method of computation for structural dynamics," Journal of Engineering Mechanics 477 Division, 85:67-94. 478

Newmark NM and Hall WJ (1982), "Earthquake Spectra and Design," EERI Monograph, Earthquake 479 Engineering Research Institute, Berkeley, California, pp.103. 480

Panjamani, Anbazhagan & Parihar, Aditya & N. Rashmi, H. (2012). Review of correlations between SPT N and shear modulus: A new correlation applicable to any region. Soil Dynamics and Earthquake Engineering. 36. 52–69. 10.1016/j.soildyn.2012.01.005.

Panjamani, Anbazhagan & Thallak, Sitharam. (2008). Site Characterization and Site Response Studies Using Shear Wave Velocity. Journal of Seismology and Earthquake Engineering. 10. 53-67.

Phillips C and Hashash YMA (2009), "Damping formulation for non-linear 1D site response analyses," Soil 489 Dynamics and Earthquake Engineering, 29:1143-1158. 490

Puri, Nitish & Jain, Ashwani & Mohanty, Piyush & Bhattacharya, Subhamoy. (2018). Earthquake Response Analysis of Sites in State of Haryana using DEEPSOIL Software. Procedia Computer Science. 125. 357-366. 10.1016/j.procs.2017.12.047.

Raju, Uma Maheswari & Boominathan, A & Dodagoudar, G. (2010). DEVELOPMENT OF EMPIRICAL CORRELATION BETWEEN SHEAR WAVE VELOCITY AND STANDARD PENETRATION RESISTANCE IN SOILS OF CHENNAI CITY.

Rathje EM, Kottke AR and Trent WL (2010), "Influence of input motion and site property variabilities on 496 seismic site response analysis," Journal of Geotechnical and Geoenvironmental Engineering, ASCE, 136(4): 497 607-619. 498

Roy, Narayan & Sahu, Ramendu. (2012). Site specific ground motion simulation and seismic response analysis for microzonation of Kolkata,. Geomechanics and Engineering. Vol. 4,. 1-18.. 10.12989/gae.2012.4.1.001.

Seed, B & Idriss, I. (1971). 'Simplified procedure for evaluating soil liquefaction potential'. PROC. JSME. 97. 1249-1273.

Stewart JP, Kwok AO, Hashash YMA, Matasovic N, Pyke R, Wang Z and Yang (2008), "Benchmarking of 517 nonlinear geotechnical ground response analysis procedures," PEER Report 2008/04, Pacific Earthquake 518 Engineering Research Center, College of Engineering, University of California, Berkeley. 519

Stewart, J. P. Kwok, A.O.L. Hashash, Y.M.A. Matasovic, N. Pyke, R. Wang, Z. and Yang Z. August 2008: Benchmarking of Nonlinear Geotechnical Ground Response Analysis Procedures

Terzaghi K (1925), "Principles of Soil mechanics. IV. Settlement and consolidation of clay," Engineering 520 News-Record, 95:874-878. 521

Tokimatsu K, Seed H 1987: J. Geotech. Engrg., 113, 861–878.

Vucetic, Mladen. (1986). Pore pressure buildup and liquefaction at level sand sites during earthquakes.

Warnitchai P and Lisantono A (1996), "Probabilistic seismic risk mapping for Thailand," Proceedings of the 524 11th World Conference on Earthquake Engineering, Acapulco, Mexico. 525

Yang, Zhaohui & Elgamal, Ahmed-Waeil. (2003). Computational Model for Cyclic Mobility and Associated Shear Deformation. Journal of Geotechnical and Geoenvironmental Engineering - J GEOTECH GEOENVIRON ENG. 129. 10.1061/(ASCE)1090-0241(2003)129:12(1119).